

**UNCLASSIFIED**

**AD 411438**

**DEFENSE DOCUMENTATION CENTER**

**FOR**

**SCIENTIFIC AND TECHNICAL INFORMATION**

**CAMERON STATION, ALEXANDRIA, VIRGINIA**



**UNCLASSIFIED**

NOTICE: When government or other drawings, specifications or other data are used for any purpose other than in connection with a definitely related government procurement operation, the U. S. Government thereby incurs no responsibility, nor any obligation whatsoever; and the fact that the Government may have formulated, furnished, or in any way supplied the said drawings, specifications, or other data is not to be regarded by implication or otherwise as in any manner licensing the holder or any other person or corporation, or conveying any rights or permission to manufacture, use or sell any patented invention that may in any way be related thereto.

501 500

N-63-4-3

7  
File 2

411438



Interim Report

I-A2321-1

AN ANALYTICAL STUDY OF BEARING NOISE  
AND VIBRATION GENERATION AND TRANSMISSION

by

— Harry C. Rippel  
John S. Tawresey

June 1961

Prepared for

DEPARTMENT OF THE NAVY  
Bureau of Ships  
Code 644 Propeller, Shafting and Bearing Branch  
Washington 25, D.C.

Contract No. N0bs-77184

DDC  
AUG 2 1963  
TISA 8

411438

FILE COPY

AD No.

**THE FRANKLIN INSTITUTE**  
LABORATORIES FOR RESEARCH AND DEVELOPMENT  
PHILADELPHIA PENNSYLVANIA

\$19.75

(5) 501 500  
(4) \$ 19.75

THE FRANKLIN INSTITUTE · Laboratories for Research and Development

Interim Report

(14) Rpt. no.  
I-A2321-1  
I I

(6) AN ANALYTICAL STUDY OF BEARING NOISE  
AND VIBRATION GENERATION AND TRANSMISSION,

(10)

by

Harry C. Rippel and  
John S. Tawresey,

June, 1961

(7) NA

(8) NA

(9) NA

(11) June 61,

(12) 1v

(13) NA

Prepared for

DEPARTMENT OF THE NAVY  
BUREAU OF SHIPS

Code 644 Propeller, Shafting and Bearing Branch  
Washington 25, D. C.

(15) Contract No. NObS-77184

16-19 NA

(20) U

(21) VA



THE FRANKLIN INSTITUTE . *Laboratories for Research and Development*

I-A2321-1

PREFACE

The personnel responsible for the work performed under this contract and their technical qualifications as related to the specific tasks assigned are as follows:

Mr. John S. Tawresey, Principal Engineer, Friction and Lubrication Branch, Franklin Institute, guided the technical progress of the work.

Professor Dudley D. Fuller, Mechanical Engineering Department of Columbia University and Principal Engineer, Friction and Lubrication Branch, Franklin Institute, contributed to the sliding surface bearing sections.

Mr. Vittorio Castelli, Instructor in the Mechanical Engineering Department of Columbia University and Research Engineer, Friction and Lubrication Branch, Franklin Institute, contributed to the sliding surface bearing sections.

Mr. Daniel Mullen, Research Engineer, Applied Mechanics Branch, Franklin Institute, contributed to the rolling element bearing sections.

Mr. Stanley Malanoski, Research Engineer, Friction and Lubrication Branch, Franklin Institute, contributed to the section on load-deflection characteristics of rolling element bearings.

Mr. Vincent Bressi, Senior Analyst, Computing Center, Franklin Institute, programmed and ran all computer work.

Mr. James Hinkle, Research Engineer, Friction and Lubrication Branch, Franklin Institute, assisted in the computational work.

Mr. Harry C. Rippel, Senior Staff Engineer, Friction and Lubrication Branch, Franklin Institute, and Project Engineer on this program was responsible for accomplishing the work and preparing this report.

THE FRANKLIN INSTITUTE • *Laboratories for Research and Development*

I-A2321-1

ABSTRACT

~~The objective of this~~ study was, <sup>made</sup> to determine the characteristics of both rolling contact and sliding surface bearings that contribute to noise and vibration generation and transmission and the corrective steps and specifications necessary to reduce such troublesome noise and vibration. Both the single-row, radial deep-groove ball bearing and the full-film lubricated journal bearing are considered. ~~Within this report,~~ the frequencies and magnitudes of vibration producing disturbing forces are determined for both types of bearing as associated with the inherent operating characteristics, the geometrical imperfections of bearing components, the design, and the use in the particular application. It has been concluded that rolling contact bearings generate vibrations over a very broad frequency range (15 cps to 15,000 cps). Geometrical errors, particularly waviness of the inner and outer raceway and balls, are believed to be the chief sources of rolling contact bearing noise and vibration generation. Well designed, well lubricated and correctly applied sliding surface bearings generate a minimum level of vibration, being restricted to once-per-revolution occurrences and higher harmonics thereof. The transmission of periodic disturbing forces by a rolling contact bearing will be equal to or greater than unity depending upon frequency. Changes in rolling contact bearing design, manufacturing tolerances and mounting to introduce damping are possible. Due to the high damping qualities associated with full-film lubricated journal bearings, vibrational amplitudes are minimized and the transmission of periodic disturbing forces is essentially unity regardless of frequency. The apparent advantages of sliding surface bearings with regard to vibration generation and transmission must be weighed in light of the practical problems associated with their use. Means of improving (but not eliminating) the vibration levels of rolling contact bearings, and thereby taking advantage of their desirable properties not found in other types of bearings, are suggested.

TABLE OF CONTENTS

	<u>Page</u>
PREFACE. . . . .	i
ABSTRACT . . . . .	ii
1. INTRODUCTION . . . . .	1
1.1 Definition of Noise and Vibration . . . . .	2
1.2 Objective of Study. . . . .	2
1.3 Approach to the Problem . . . . .	2
2. SUMMARY OF ANALYSIS AND CONCLUSIONS. . . . .	7
3. ANALYSIS . . . . .	10
3.1 Noise and Vibration Generation. . . . .	10
3.1.1 Rolling Contact Bearings . . . . .	10
3.1.2 Sliding Surface Bearings . . . . .	45
3.2 Vibrational Response and Resonand Frequencies and Their Relationship to Disturbing Forces . . . . .	55
3.2.1 Rolling Contact Bearings . . . . .	55
3.2.2 Sliding Surface Bearings . . . . .	148
3.3 Transmission of Vibration Forces. . . . .	173
3.3.1 Rolling Contact Bearings . . . . .	174
3.3.2 Sliding Surface Bearing Vibration Force Transmission. . . . .	179
3.3.3 Summary of Vibration Force Transmissibility. . . . .	195
4. CONCLUSIONS . . . . .	196
4.1 Rolling Element Bearings. . . . .	196
4.1.1 Vibration Generation . . . . .	196
4.1.2 Vibrational Response . . . . .	197
4.1.3 Transmission of Vibration Forces Through the Bearing . . . . .	202
4.2 Sliding Surface Bearings. . . . .	203
4.2.1 Vibration Generation . . . . .	203
4.2.2 Vibrational Response . . . . .	204
4.2.3 Transmission of Disturbing Forces. . . . .	205

THE FRANKLIN INSTITUTE • *Laboratories for Research and Development*

I-A2321-1

TABLE OF CONTENTS (Cont.)

	<u>Page</u>
4.3 Comparisor of Rolling Contact and Sliding Surface Bearings . . . . .	205
4.4 Means for Improving the Vibrational Quality of Ball Bearings . . . . .	206
5. ACKNOWLEDGEMENTS . . . . .	209
APPENDICES	
A. DEEP GROOVE BALL BEARING DIMENSIONS. . . . .	A
A.1 Deep Groove Ball Bearing Dimensions . . . . .	A1
A.2 Fundamental Frequency Factors . . . . .	A3
A.3 Ball-Pass Frequency Factors . . . . .	A5
B. DETERMINATION OF Q FOR USE IN EQUATIONS (17) AND (18). . . . .	B
B.1 Determination of Q for Use in Equations (17) and (18) . .	B1
B.2 Development of an Expression for Outer Waviness Sub-Frequency Factor. . . . .	B4
B.3 Development of an Expression for Inner Waviness Sub-Frequency Factor. . . . .	B8
C. GENERALIZED EQUATIONS FOR THE GEOMETRY OF BALL BEARING COMPONENTS . . . . .	C
C.1 Generalized Equations for the Geometry of Ball Bearing Components. . . . .	C1
C.2 Normal Approach of Inner and Outer Faces (Ball Deformation). . . . .	C5
C.3 Ball Deformation - Load Relationships . . . . .	C8
C.4 Zero Clearance Bearing. . . . .	C12
C.5 Values of $k_N$ and $k_N^{3/2}$ . . . . .	C16
C.6 Locus of Shaft Due to Rotating Load . . . . .	C17
C.7 Bearings with Internal Clearance. . . . .	C21
D. COMPUTER DATA FOR CLEARANCE BEARING. . . . .	D
E. COMPUTER DATA FOR INTERFERENCE BEARING . . . . .	E
F. FREQUENCY OF FREE VIBRATIONS - OUTER RING. . . . .	F
G. COMBINED SPRING RATE OF LOADED BALL. . . . .	G
H. ELECTRIC MOTOR MECHANICAL UNBALANCE. . . . .	H
J. FREQUENCY RESPONSE AND TRANSMISSIBILITY CHARACTERISTICS OF A JOURNAL BEARING DUE TO PURE UNBALANCE LOAD . . . . .	J
K. PRELOADING OF ELECTRIC MOTOR BALL BEARINGS . . . . .	K
L. LIST OF REFERENCES . . . . .	L

THE FRANKLIN INSTITUTE • *Laboratories for Research and Development*

I-A2321-1

1. INTRODUCTION

Over the years, the number of electric motors for submarine auxiliary equipment has steadily increased while the allowable noise and vibration levels for the same have decreased. To meet this situation, electric motor manufacturers have been forced to continually improve their product both electrically and mechanically. Recently there has been some evidence that a fruitful area for further noise and vibration reduction effort is the bearings for these motors. Since the noise and vibration level requirements for new construction are quite stringent, smoother running bearings than those currently being procured for these applications under specification MIL-B-17931A (Ships), 16 September 1959, are a necessity. Although the contribution of just the bearings to the overall noise and vibration level of electric motors has never been assessed, it has been demonstrated, by such methods as changing or replacing bearings and observing the changes in vibration and noise spectrum, that they do contribute. In July of 1959, the Friction and Lubrication Branch of The Franklin Institute Laboratories undertook for the Bearings Branch of the Bureau of Ships a research program dealing with an investigation of bearing noise and vibration. The entire program consists of the following three phases.

1. Analytical Study of Bearing Noise and Vibration Generation and Transmission.
2. Design and Construction of a Test Device to Evaluate Bearing Noise and Vibration.
3. Experimental Evaluation of Bearing Noise and Vibration.

This interim report summarizes all of the work accomplished on the first phase.

THE FRANKLIN INSTITUTE • *Laboratories for Research and Development*

I-A2321-1

1.1 Definition of Noise and Vibration

"Noise" and "Vibration" are used synonymously in this work and taken to mean both structural borne vibration and sound (air vibration). Noise may originate within the bearing, and in this case the bearing is a noise generator. Hence, noise generation implies the vibration, or periodic motion about a position of equilibrium, which is initiated and sustained by the bearing. The disturbing forces either generated in the bearing or present in the rotating mass being supported (such as rotor unbalance, magnetic unbalance, slot disturbances, etc.) must be transmitted through the bearing. Noise transmission (or transmissibility) is defined in this work as the ratio of the magnitude of the force transmitted by the bearing to its support (housing) and the magnitude of the disturbing force.

1.2 Objective of Study

The objective of this analytical study is to determine the characteristics of both rolling contact and sliding surface bearings that contribute to noise and vibration generation and transmission and the corrective steps and specifications necessary to reduce such troublesome noise and vibration. The results will serve to guide the assignment of relative importance among the complex system of interrelated variables involved.

1.3 Approach to the Problem

From the beginning it was realized that a complete theoretical synthesis of the noise generating and transmitting characteristics of rolling contact and sliding surface bearings would not be practical,

THE FRANKLIN INSTITUTE • *Laboratories for Research and Development*

I-A2321-1

let alone possible, for our purpose in the overall program. The concept adopted in our approach to the problem is that the principal source of noise in a bearing is that due to forced vibrations of the outer race as produced by varying periodic forces at the ball contact areas (rolling contact bearings) or pressurized fluid film (sleeve bearings). The outer ring of a rolling contact bearing and the sleeve in a sliding surface bearing as used in electric motor applications are continually subjected to periodic forces due to such considerations as one or more of the following:

1. Varying applied load
2. External vibration
3. Rotor disturbances such as mechanical and electrical unbalances and slot forces
4. Inherent bearing operating characteristics
5. Imperfections in bearing component geometry giving rise to rotor and bearing component inertia effects.

Such disturbing forces may be broadly classified into two groups: those generated within the bearing and those to which the bearing is subjected from some external source. The first group of vibration producing forces are of primary concern because they may be attributed directly to the bearing. Also, both groups of disturbing periodic forces must ultimately be transmitted by the bearing to the housing or to the rotor. The spring rates and damping afforded by the bearing in combination with the masses being vibrated and the frequencies of the periodic disturbing forces become of interest in determining whether the bearing amplifies or suppresses these disturbing forces. Hence, our

THE FRANKLIN INSTITUTE • *Laboratories for Research and Development*

I-A2321-1

efforts were directed toward determining how bearings of the rolling contact and sliding surface types as used in electric motors:

- a. contribute to vibration generation,
- b. respond to periodic disturbing forces, and
- c. transmit periodic disturbing forces.

Each of these three separate, but dependent, parts of the total problem are given individual consideration in the analysis which follows. Due to the bulk of material contained in this report it is important to point out its arrangement and content so as to prepare the reader for what follows and thereby allow him to more readily follow and better understand our approach to the problem and the development of the technical conclusions.

Both types of bearing considered in this work contribute to vibration generation by virtue of (a) the inherent operating characteristics, (b) the geometrical imperfections of bearing components, (c) the design and (d) the use in the particular application. Hence, in our study of bearing vibration generation we first evaluated the frequencies associated with each of these considerations. In order to not lose sight of the parameters involved in producing these generated disturbing frequencies and thereby possibly make use of the variables involved to control said frequencies, dimensionless frequency factors were determined for a multitude of possible generated frequencies in both rolling contact and sliding surface bearings. The second aspect of vibration generation, namely, the magnitude of the disturbing periodic forces



THE FRANKLIN INSTITUTE • *Laboratories for Research and Development*

I-A2321-1

generated within the bearing, presents an extremely difficult analytical problem from which to obtain a rigorous solution, if indeed it is at all possible. Thus, instead of attacking this problem directly, the relationship between bearing component imperfections (and bearing inherent operating characteristics) and generated forces was investigated using a very simplified approach which led to a relative ranking of bearing imperfection magnitudes and other force producing vibrations.

Once having some insight into the frequencies of disturbing forces generated within the bearing and taking into account that the bearing is subjected to other disturbing forces external to the bearing, the next part of the problem is to determine how the bearing responds to such excitation. The primary considerations in determining the response of a system to forced vibration are spring rates, masses vibrated, damping involved and imposed constraints or boundary conditions. The first effort in this direction was to investigate the load-displacement characteristics of rolling contact and sliding surface bearings and develop therefrom their associated spring rates. Once again, this was done in a non-dimensional manner which preserves the relationship of the variables which constitute the spring rate and also allows for the ready computation of magnitude for varying conditions. With regard to damping, it was found necessary to neglect it in the case of ball bearings, but it was included in the sliding surface bearing study. Various spring-mass systems afforded within the bearing and by the bearing with different imposed constraints were evaluated for resonant

THE FRANKLIN INSTITUTE • *Laboratories for Research and Development*

I-A2321-1

frequencies which were then compared with the frequencies of disturbing forces. Also, the natural frequencies of bearing components were investigated to establish their contribution if any.

The final part of the analysis is devoted to the determination of the force transmission qualities of the bearings; that is, whether vibratory forces to which the bearing is subjected are suppressed or amplified in being transmitted through the bearing. In this effort, use is again made of the spring rates and damping qualities of the bearings to determine possible troublesome frequency ranges.

## 2. SUMMARY OF ANALYSIS AND CONCLUSIONS

The objective of this analytical study is to determine the characteristics of both rolling contact and sliding surface bearings that contribute to the generation and transmission of noise and vibration and the corrective steps and specifications necessary to reduce such troublesome noise and vibration. In this work both single row radial, deep-groove ball bearings and full-film lubricated journal bearings as used in electric motors were considered. The concept adopted in our approach to the problem is that the principal source of noise in a bearing is that due to forced vibrations of the outer ring as produced by varying periodic forces at the ball-race contact areas (rolling contact bearings) or pressurized fluid film (journal bearings).

Consideration was first given to the determination of the frequencies and forces of periodic disturbances generated within both types of bearings as due to their inherent operating characteristics, geometrical imperfections of bearing components, design, and how used in the particular application. Dimensionless frequency factors were determined for a multitude of possible generated frequencies due to such considerations. In addition, numerical results have been obtained using a typical size bearing (50 mm bore, 120 mm O.D. ball bearing and a two-inch diameter by two-inch long journal bearing). It has been concluded that rolling contact bearings generate vibrations over a very broad frequency range (15 cps to 15,000 cps or approximately one-half of shaft frequency to 1000 times shaft frequency). The very low

THE FRANKLIN INSTITUTE • *Laboratories for Research and Development*

I-A2321-1

frequencies are attributed to cage phenomena and rotational effects. Frequencies from shaft frequency to 10 times shaft frequency are attributed to inner and outer ball-pass, ball rotation, and low order ball and raceway waviness. The sources of high frequency vibrations are associated with high order ball and raceway waviness. Also, another potential source of vibration in a perfectly made bearing is that due to ball-pass instability (periodic oscillation of the shaft due to varying ball position). Ways and means of suppressing this phenomena are discussed herein. Properly designed, well lubricated, and correctly applied sliding surface bearings operating on a full-film of lubricant generate a minimum level of vibration being restricted to once-per-revolution phenomena and higher harmonics. Such vibration is attributed to low order waviness. Oil-whip and oil-whirl are not normally present in electric motor applications.

The components of rolling contact bearings are continually subjected to highly concentrated forces of varying magnitude and direction at the ball-race contacts. Investigation of the spring-mass systems of rolling contact bearing supported rotors in electric motors indicated resonant frequencies to lie between 300 and 1000 cps depending upon the bearing spring rates and rotor masses. To assist in this work, dimensionless bearing spring rates for rolling contact bearings having clearance and interference were developed and proved to be useful in determining resonant frequencies and judging the effect of bearing design and application changes on spring rates. Various other spring-mass systems

THE FRANKLIN INSTITUTE • *Laboratories for Research and Development*

I-A2321-1

established within the bearing were also investigated and found to exhibit resonant frequencies in the range from 1000 to 20,000 cps. In addition it was found that the natural frequency of flexural vibration of the outer ring and its higher harmonics are in the range of 2000 cps and above, and thereby can account for the high levels of vibration observed in the high frequency range. Comparison of all of these resonant frequencies attributable to the rolling contact bearing with the generated disturbing force frequencies indicated that excessive vibrations in the general frequency range from 300 to 20,000 cps may be experienced. Due to the high damping associated with oil-lubricated journal bearings, vibrational amplitudes due to the low frequency disturbing forces generated within such bearings are minimized, and resonant conditions should not be experienced.

The transmission of periodic disturbing forces, whether generated within the bearing or from some external source, was investigated. For rolling contact bearings the transmission will be unity or greater depending upon excitation frequency. For journal bearings, the transmission is unity regardless of excitation frequency. The apparent advantages of sliding surface bearings with regard to limited, low frequency noise generation, absence of resonant frequencies and unity transmission of disturbing forces at all frequencies must be weighed in the light of the practical problems associated with their use. Also, changes in the design, specifications, and application of rolling contact bearings are suggested herein to improve their vibration and transmission characteristics. By such means it should be possible to take advantage of their desirable properties not found in any other type of bearing.

### 3. ANALYSIS

#### 3.1 Noise and Vibration Generation

As discussed in Section 1, noise generation in bearings is vibration as produced by the varying periodic forces initiated within and sustained by the bearing. Both the frequency and the amplitude of such forces are of interest for both rolling contact and sliding surface bearings.

##### 3.1.1 Rolling Contact Bearings

The rolling contact bearings primarily used for electric motors are of the single row radial, deep-groove, non-filling slot type, medium series. The size range of interest is from 25 mm bore to 90 mm bore, and of ABEC Class 3 tolerances. Pertinent dimensions for this type of bearing are given in Appendix A for the medium, light and extra light series.

In this section use is made of the velocity relationships in rolling contact bearings to establish dimensionless frequency factors which allow the expedient computation of the disturbing force frequencies associated with the inherent operating characteristics of the bearing, the geometrical imperfections of the bearing components, the design, and the use in the particular application. A possible typical frequency spectrum is prepared for a 310 bearing which demonstrates the range of disturbing force frequencies generated. Consideration is then given to the relationship between vibration sources and generated forces.

3.1.1.1 Frequency Factors

In this work it has been found expedient to express the frequency of particular events within the bearing in terms of dimensionless frequency factors where the frequency factor is the ratio of the frequency in question divided by the inner ring rotational frequency. By this means, the frequency may be readily computed regardless of the operating speed.

The velocity relationships for the components of the single row, deep groove type radial bearing, illustrated in Figure 1 may be determined as follows.

I-A2321-1

SINGLE ROW DEEP GROOVE  
RADIAL BEARING GEOMETRY

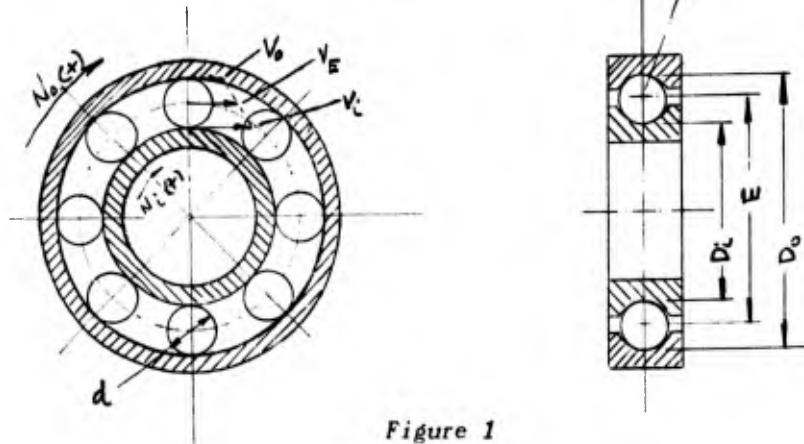


Figure 1

NOMENCLATURE

- $n$  = Total Number of Balls
- $N_i$  = RPM (inner ring)
- $N_o$  = RPM (outer ring)
- $N_e$  = RPM (Rolling Elements and Cage)
- $N_b$  = RPM (Rolling Element about its own Center)
- $N_{ei}$  = RPM (Set of Rolling Elements Relative to Inner Ring)
- $N_{oe}$  = RPM (Set of Rolling Elements Relative to Outer Ring)
- $V_i$  = Circumferential Speed Inner Ring Raceway,
- $V_o$  = Circumferential Speed Outer Ring Raceway,
- $V_e$  = Circumferential Speed Rolling Element Centers and Cage
- $D_i$  = Diameter of Inner Ring Raceway
- $D_o$  = Diameter of Outer Ring Raceway
- $E$  = Bearing Pitch Diameter
- $d$  = Diameter of Rolling Element
- $\beta$  = Contact Angle
- Clockwise Rotation = Positive



$$V_e = \frac{V_i + V_o}{2} \quad \text{in/sec}$$

$$V_i = \frac{\pi D_i N_i}{60} \quad \text{in/sec}$$

$$V_o = \frac{\pi D_o N_o}{60} \quad \text{in/sec}$$

Assume Contact Angle  $\beta = 0$

$$D_i = E - d$$

$$D_o = E + d$$

$$\therefore V_e = \frac{\pi}{120} N_i (E - d) + \frac{\pi}{120} N_o (E + d) \quad \text{in/sec}$$

$$V_e = \frac{\pi}{120} N_i E \left(1 - \frac{d}{E}\right) + \frac{\pi}{120} N_o E \left(1 + \frac{d}{E}\right) \quad \text{in/sec}$$

$$V_e = \frac{\pi}{2} N_i E \left(1 - \frac{d}{E}\right) + \frac{\pi}{2} N_o E \left(1 + \frac{d}{E}\right) \quad \text{in/min}$$

Since there are  $\pi E$  in/REV of rolling element then

$$N_e = \frac{N_i}{2} \left(1 - \frac{d}{E}\right) + \frac{N_o}{2} \left(1 + \frac{d}{E}\right) \quad \text{RPM} \quad (1)$$

$$N_{ei} = N_e - N_i = \frac{1}{2} (N_o - N_i) \left(1 + \frac{d}{E}\right) \quad \text{RPM} \quad (2)$$

$$N_{oe} = N_o - N_e = \frac{1}{2} (N_o - N_i) \left(1 - \frac{d}{E}\right) \quad \text{RPM} \quad (3)$$

$$N_B = \frac{D_i}{d} N_{ei} \quad \text{or} \quad N_B = \frac{D_o}{d} N_{oe}$$

$$N_B = \frac{1}{2} \frac{E}{d} (N_o - N_i) \left(1 - \frac{d}{E}\right) \left(1 + \frac{d}{E}\right) \quad \text{RPM} \quad (4)$$

THE FRANKLIN INSTITUTE • *Laboratories for Research and Development*

I-A2321-1

3.1.1.1.1 Fundamental Frequency Factors

Assuming a stationary outer race ( $N_o = 0$ ),

Then from Equations (1), (2), (3), and (4),

$$\text{Cage Speed} = N_E = \frac{N}{2} \left(1 - \frac{d}{E}\right), \text{ RPM}$$

$$\text{Ball Rotational Speed} = N_B = -\frac{N}{2} \frac{E}{d} \left(1 - \frac{d}{E}\right) \left(1 + \frac{d}{E}\right), \text{ RPM}$$

$$\text{Cage to inner ring speed} = N_{Ei} = -\frac{N}{2} \left(1 + \frac{d}{E}\right), \text{ RPM}$$

Converting to frequency gives,

$$\text{Cage Frequency} = f_E = \frac{1}{2} \left(1 - \frac{d}{E}\right) \times f_i, \text{ cps}$$

$$\text{Ball Rotational Frequency} = f_B = \frac{1}{2} \frac{E}{d} \left(1 - \frac{d}{E}\right) \left(1 + \frac{d}{E}\right) \times f_i, \text{ cps}$$

$$\text{Cage to inner ring frequency} = f_{Ei} = \frac{1}{2} \left(1 + \frac{d}{E}\right) \times f_i, \text{ cps}$$

The fundamental frequency factors become:

$$\text{Cage Frequency Factor} = \frac{f_E}{f_i} = \frac{1}{2} \left(1 - \frac{d}{E}\right) \quad (5)$$

$$\text{Ball Rotational Frequency Factor} = \frac{f_B}{f_i} = \frac{1}{2} \frac{E}{d} \left(1 - \frac{d}{E}\right) \left(1 + \frac{d}{E}\right) \quad (6)$$

$$\text{Cage to inner ring frequency factor} = \frac{f_{Ei}}{f_i} = \frac{1}{2} \left(1 + \frac{d}{E}\right) \quad (7)$$

THE FRANKLIN INSTITUTE • *Laboratories for Research and Development*

I-A2321-1

Fundamental frequency factors were calculated for the 100, 200 and 300 series bearings using the data of Appendix A.1 and are shown plotted in Figure 2, and tabled in Appendix A.2. Multiplying these frequency factors by the inner ring frequency,  $f_i$ , (or rotational speed,  $N_i$ ), gives the cage, cage to inner, and ball rotational frequencies (or speeds).

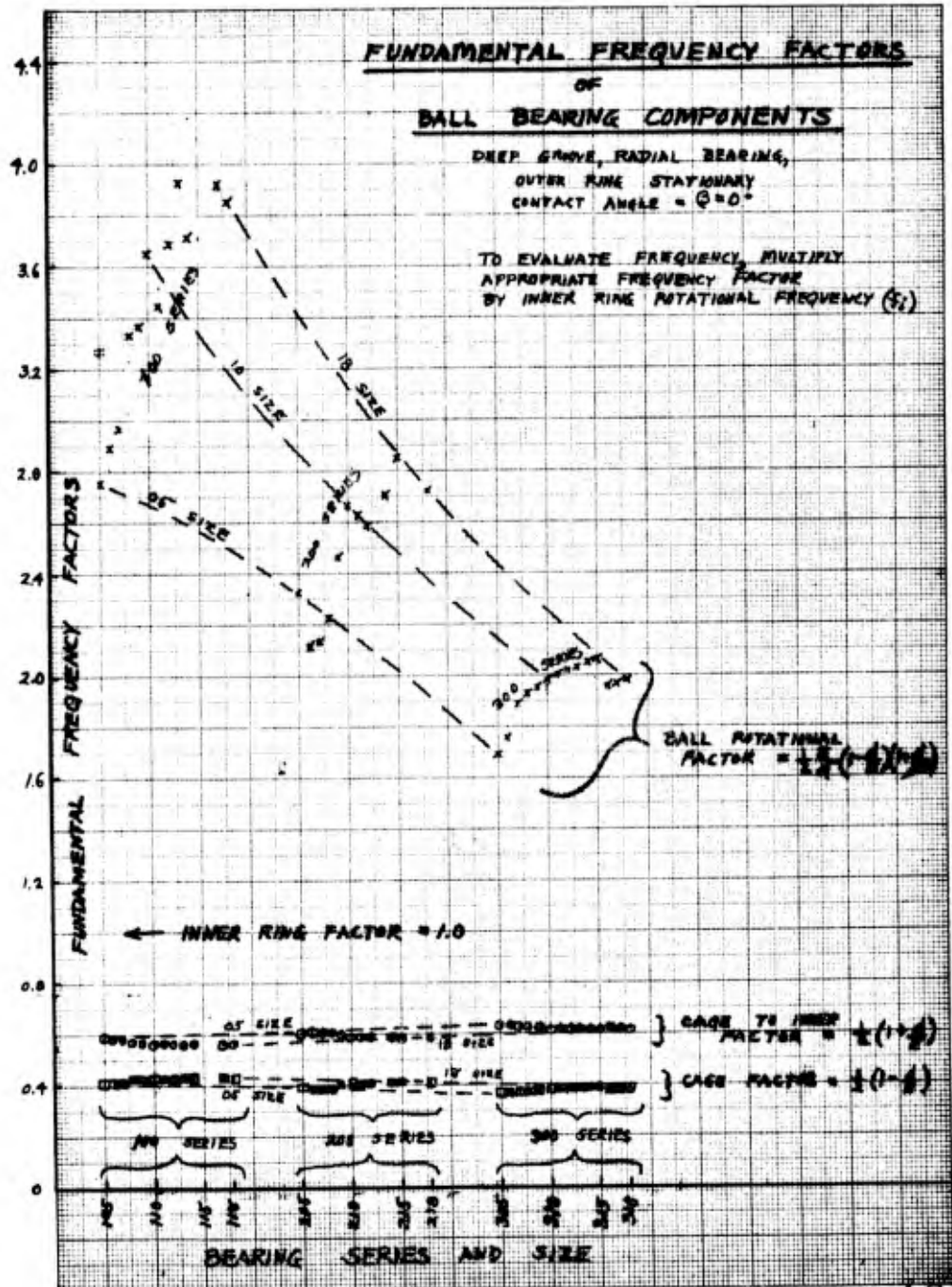


Figure 2

THE FRANKLIN INSTITUTE • *Laboratories for Research and Development*

I-A2321-1

The following observations may be made from Figure 2..

1. Cage Frequency Factors  $\square$ 
  - a. Decrease slightly with increasing series for the same size.
  - b. Increase slightly with increasing size for the same series.
  - c. Average value  $\approx 0.4$ .
2. Cage to Inner Frequency Factors  $\odot$ 
  - a. Increase slightly with increasing series for the same size.
  - b. Decrease slightly with increasing size for the same series.
  - c. Average value  $\approx 0.6$ .
3. Ball Rotational Frequency Factors X
  - a. Decrease rapidly with increasing series for the same size.
  - b. Increase rapidly (general trend but there are exceptions) with increasing size.
4. Ball Rotational Frequency Factors are 5 to 10 times higher than Cage Frequency Factors
5. Ball Rotational Frequency Factors are 3 to 7 times higher than Cage to Inner Frequency Factors
6. Cage to Inner Frequency Factors are 50% greater than Cage Frequency Factors

### 3.1.1.1.2 Ball-Pass Frequency Factors

The frequency of occurrence of the balls passing any particular point on the outer race is of interest. This frequency is the product of cage frequency and the number of balls.

$$\text{Outer Ball-Pass Frequency} = f_{Bo} = n \times f_E.$$

From Equation (5),

$$\text{Outer Ball-Pass Frequency Factor} = \frac{f_{Bo}}{f_i} = n \times \frac{1}{2} \left(1 - \frac{d}{E}\right) \quad (8)$$

Likewise, the frequency of occurrence of the balls passing any particular point on the inner race is,

$$\text{Inner Ball-Pass Frequency} = f_{Bi} = n \times f_{Ei}$$

From Equation (7),

$$\text{Inner Ball-Pass Frequency Factor} = \frac{f_{Bi}}{f_i} = n \times \frac{1}{2} \left(1 + \frac{d}{E}\right) \quad (9)$$

Ball-pass frequency factors were calculated for the 100, 200 and 300 series bearings using the data of Appendix A.1 and are shown plotted in Figure 3 and are tabled in Appendix A.3. Multiplying these frequency factors by the inner ring frequency,  $f_i$ , gives the inner and outer ball-pass frequencies.

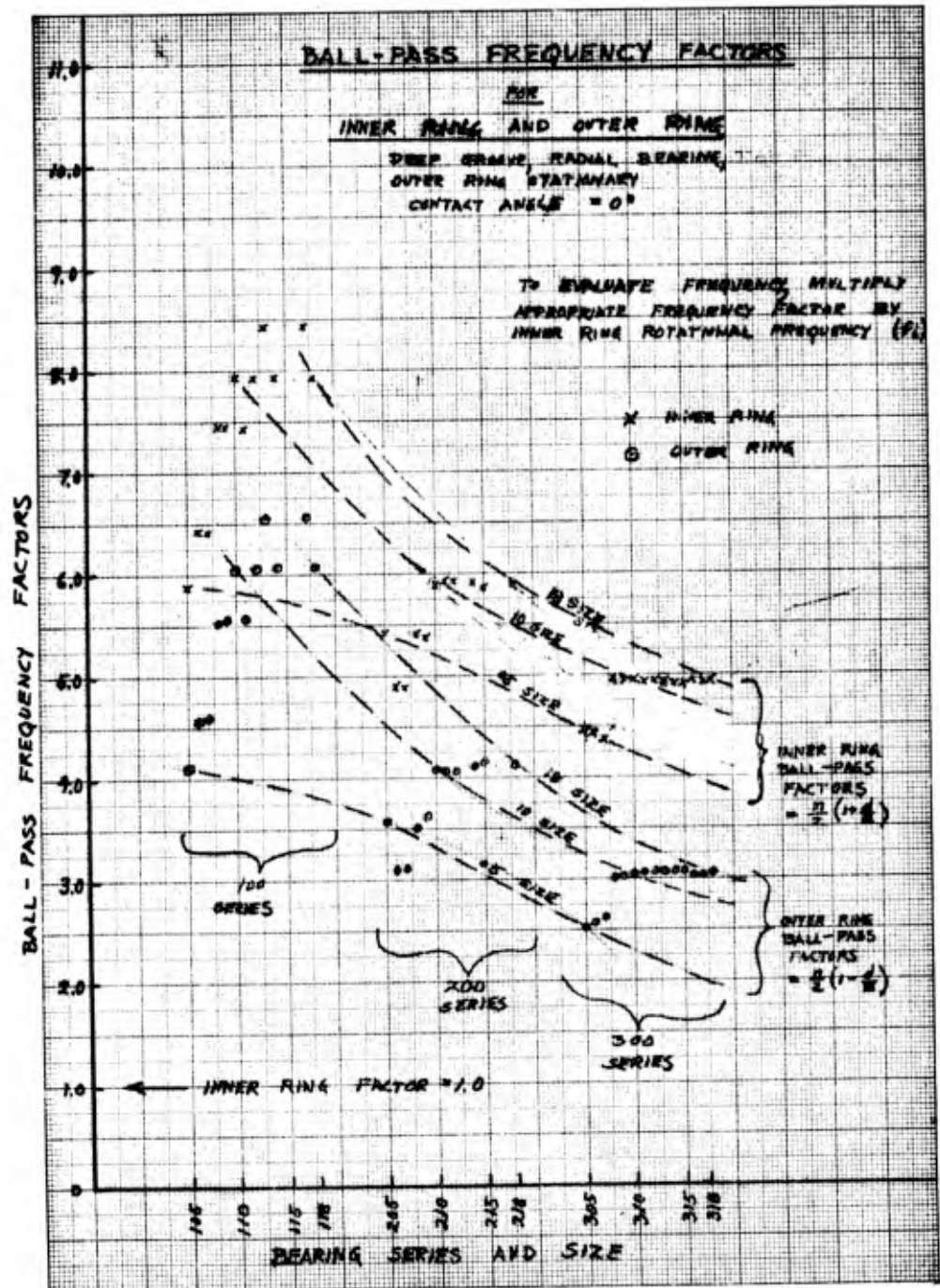


Figure 3

THE FRANKLIN INSTITUTE • *Laboratories for Research and Development*

I-A2321-1

The following observations may be made from Figure 3.

1. Inner Ring Ball-Pass Frequency Factors
  - a. Decrease rapidly with increasing series for the same size
  - b. Increase rapidly with increasing size for small series and only slightly for larger series. This is the general trend but there are exceptions.
2. Outer Ring Ball-Pass Frequency Factors

Same as for inner ring
3. Inner Ball Pass Frequency Factors are approximately 50% greater than Outer Ball Pass Frequency Factors.



### 3.1.1.1.3 Ball-Defect Frequency Factors

The frequency of occurrence of a particular spot on one ball contacting the outer ring is equal to the rotational frequency of the ball. The same is true for contact with the inner ring. For every 180° rotation of the ball, the same spot will contact either the outer ring or the inner at a frequency equal to twice the ball rotational frequency. We shall call these the "Ball-Defect" frequencies.

$$\begin{array}{l} \text{Outer ball-defect frequency} = f_{BDo} = f_B \\ \text{From (6)} \end{array}$$

$$\text{Outer ball defect frequency factor} = \frac{f_{BDo}}{f_i} = \frac{1}{2} \frac{E}{d} (1 - \frac{d}{E}) (1 + \frac{d}{E}) \quad (10)$$

$$\begin{array}{l} \text{Inner ball-defect frequency} = f_{BDi} = f_B \\ \text{From (6)} \end{array}$$

$$\text{Inner ball-defect frequency factor} = \frac{f_{BDi}}{f_i} = \frac{1}{2} \frac{E}{d} (1 - \frac{d}{E}) (1 + \frac{d}{E}) \quad (11)$$

$$\begin{array}{l} \text{Outer-inner ball-defect frequency} = f_{BDoi} = 2 \times f_B \\ \text{From (6)} \end{array}$$

$$\text{Outer-inner ball-defect frequency factor} = \frac{f_{BDoi}}{f_i} = \frac{E}{d} (1 - \frac{d}{E}) (1 + \frac{d}{E}) \quad (12)$$

Ball-defect frequency factors were calculated for the 100, 200 and 300 series bearings using the data of Appendix A and are shown plotted in Figure 4. Multiplying these frequency factors by the inner ring rotational frequency,  $f_i$ , gives the ball-defect frequencies.

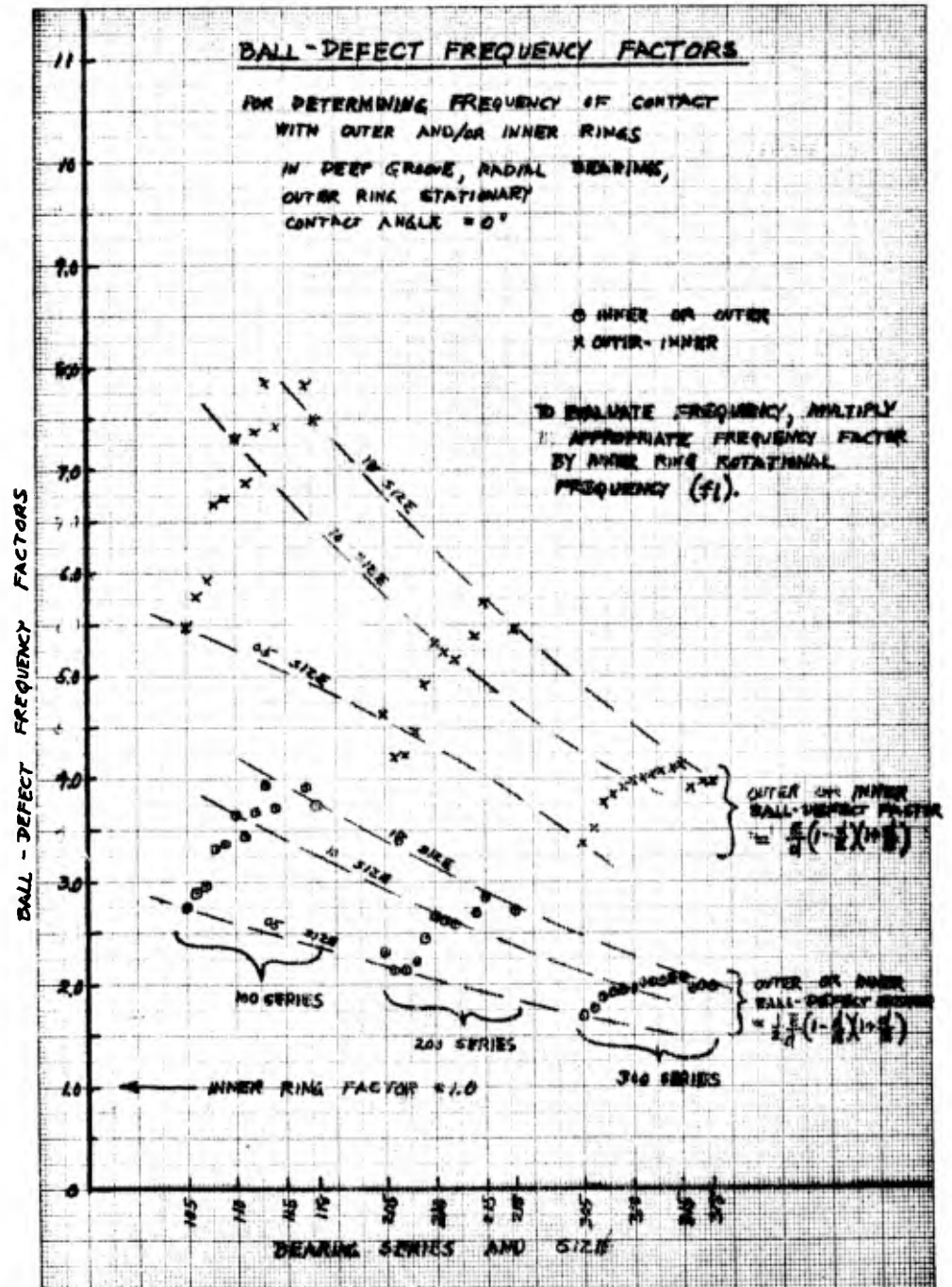


Figure 4

THE FRANKLIN INSTITUTE • *Laboratories for Research and Development*

I-A2321-1

The following observations may be made from Figure 4:

1. Outer - Inner Ball Defect Factors
  - a. Decrease rapidly with increasing series for the same size
  - b. Increase rapidly with increasing size for small series and less rapidly for larger series. This is the general trend but there are exceptions.
2. Outer or Inner Ball Defect Factors
  - a. Same as for outer - inner ball defect factors.

#### 3.1.1.1.4 Ball-Waviness Frequency Factors

More often than not, balls have more than one defect (waviness, scratches, dents, etc.) over a given circumference. If such defects are uniformly spaced on the circumference then the frequency of contact with the inner or outer ring is the product of the number of defects and the ball rotational frequency. For simplicity, we shall call multiple defects "waves" and denote the number of such waves as " $w_B$ ".

$$\begin{array}{l} \text{Outer ball-wave frequency} = f_{Bwo} = w_B \times f_B \\ \text{From (6)} \end{array}$$

$$\text{Outer ball-wave frequency factor} = \frac{f_{Bwo}}{f_i} = \frac{1}{2} \frac{E}{d} \left(1 - \frac{d}{E}\right) \left(1 + \frac{d}{E}\right) \times w_B \quad (13)$$

$$\begin{array}{l} \text{Inner ball-wave frequency} = f_{Bwi} = w_B \times f_B \\ \text{From (6)} \end{array}$$

$$\text{Inner ball-wave frequency factor} = \frac{f_{Bwi}}{f_i} = \frac{1}{2} \frac{E}{d} \left(1 - \frac{d}{E}\right) \left(1 + \frac{d}{E}\right) \times w_B \quad (14)$$

Inner - outer ball-wave frequency

$$\begin{array}{l} \text{Odd No. of waves } f_{Bwio} = 2w_B \times f_B \\ \text{From (6)} \end{array}$$

$$\text{Inner-outer Ball-wave frequency factor} = \frac{f_{Bwio}}{f_i} = \frac{E}{d} \left(1 - \frac{d}{E}\right) \left(1 + \frac{d}{E}\right) \times w_B \quad (15 \text{ Odd})$$

$$\begin{array}{l} \text{Even No. of Waves } f_{Bwio} = w_B \times f_B \\ \text{From (6)} \end{array}$$

$$\text{Inner-outer ball-wave frequency factor} = \frac{f_{Bwio}}{f_i} = \frac{1}{2} \frac{E}{d} \left(1 - \frac{d}{E}\right) \left(1 + \frac{d}{E}\right) \times w_B \quad (15 \text{ Even})$$

THE FRANKLIN INSTITUTE • *Laboratories for Research and Development*

I-A2321-1

Ball-wave frequency factors were calculated for the 100, 200 and 300 series bearings using the data of Appendix A and are shown plotted in Figure 5. Multiplying these ball wave frequency factors by the product of the number of waves on the ball and the inner ring frequency,  $(w_B \times f_i)$ , gives the ball-wave frequencies. Numerically, these ball-wave frequency factors (plotted in Figure 5) are the same as for the ball-defect frequencies (plotted in Figure 4). Separate figures are used to avoid multiple and, perhaps, confusing labelling for odd and/or even waviness or defects.

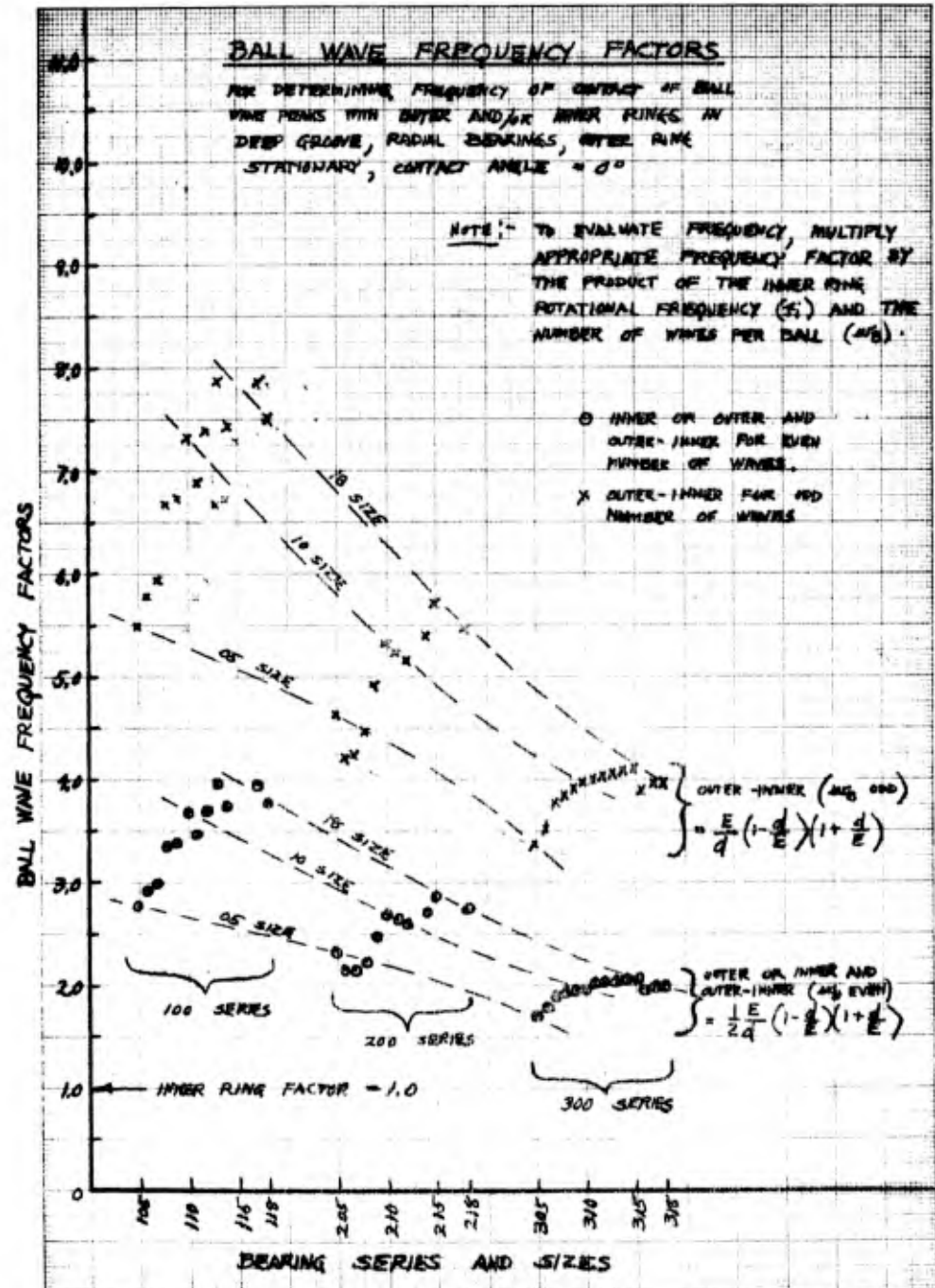


Figure 5

3.1.1.1.5 Raceway-Waviness Frequency Factors

When the outer (or inner) race has a finite number of periodic waves per circumference, the frequency of occurrence of any ball(s) touching any wave peak(s) somewhere in the bearing is dependent upon the number of waves per circumference, the total number of balls in the bearing and the cage frequency. Depending upon the particular combination of the number of waves and the total number of balls,  $n$ , one,  $n$ , or some other intermediate number of balls,  $Q$ , will be touching wave peaks at the same instant of time somewhere in the bearing. Some finite time later, the same number of balls,  $Q$ , (but different balls) will touch different wave peaks. This process is continually repeated giving rise to a particular frequency of ball-peak contact. It should be pointed out, that although the resulting frequency,  $f_{wo}$ , and the number of simultaneous contacts,  $Q$ , are constant, the angular location of contact will, in general, vary in still another periodic fashion giving rise to another lower frequency. This will be discussed later.

THE FRANKLIN INSTITUTE • *Laboratories for Research and Development*

I-A2321-1

The usual equation used to determine the resulting frequency of ball-peak contact for outer ring waviness is

$$f_{wo} = w_o \times f_E, \text{ cps} \quad 16$$

This equation is not strictly correct. It is only valid when the number of waves is equal to, or a multiple of, the total number of balls.

To illustrate, consider a bearing with 6 balls. (Shown unwrapped in Fig. 6). If  $w_o = 1$  wave, each ball hits the peak as the ball train moves to the right at a frequency equal to  $n \times w_o \times f_E$  or,  $f_{wo} = 6 f_E$  (Eq. 16 yields  $f_{wo} = f_E$ )

If  $w_o = 2$  waves, balls 3 and 6 are touching peaks. As the train moves, balls 2 and 5 will touch next. The frequency will be equal to  $\frac{n}{Q} \times w_o \times f_E$ , or  $f_{wo} = 6 f_E$  (Eq. 16 yields  $f_{wo} = 2 f_E$ ) If  $w_o = 3$  waves, balls 2, 4 and 6 are touching. As the train moves, balls 1, 3 and 5 will touch next. The frequency will be equal to  $\frac{n}{Q} \times w_o \times f_E$ , or  $f_{wo} = 6 f_E$  (Eq. 16 yields  $f_{wo} = 3 f_E$ ) If  $w_o = 4$  waves, balls 3 and 6 are touching. As the train moves, balls 1 and 4 touch next (at different peaks). The frequency will be equal to  $\frac{n}{Q} \times w_o \times f_E$ , or  $f_{wo} = 12 f_E$  (Eq. 16 yields  $f_{wo} = 4 f_E$ ) It is apparent that Eq. (16) must be modified by the factor  $(\frac{n}{Q})$  to make it valid for all cases.



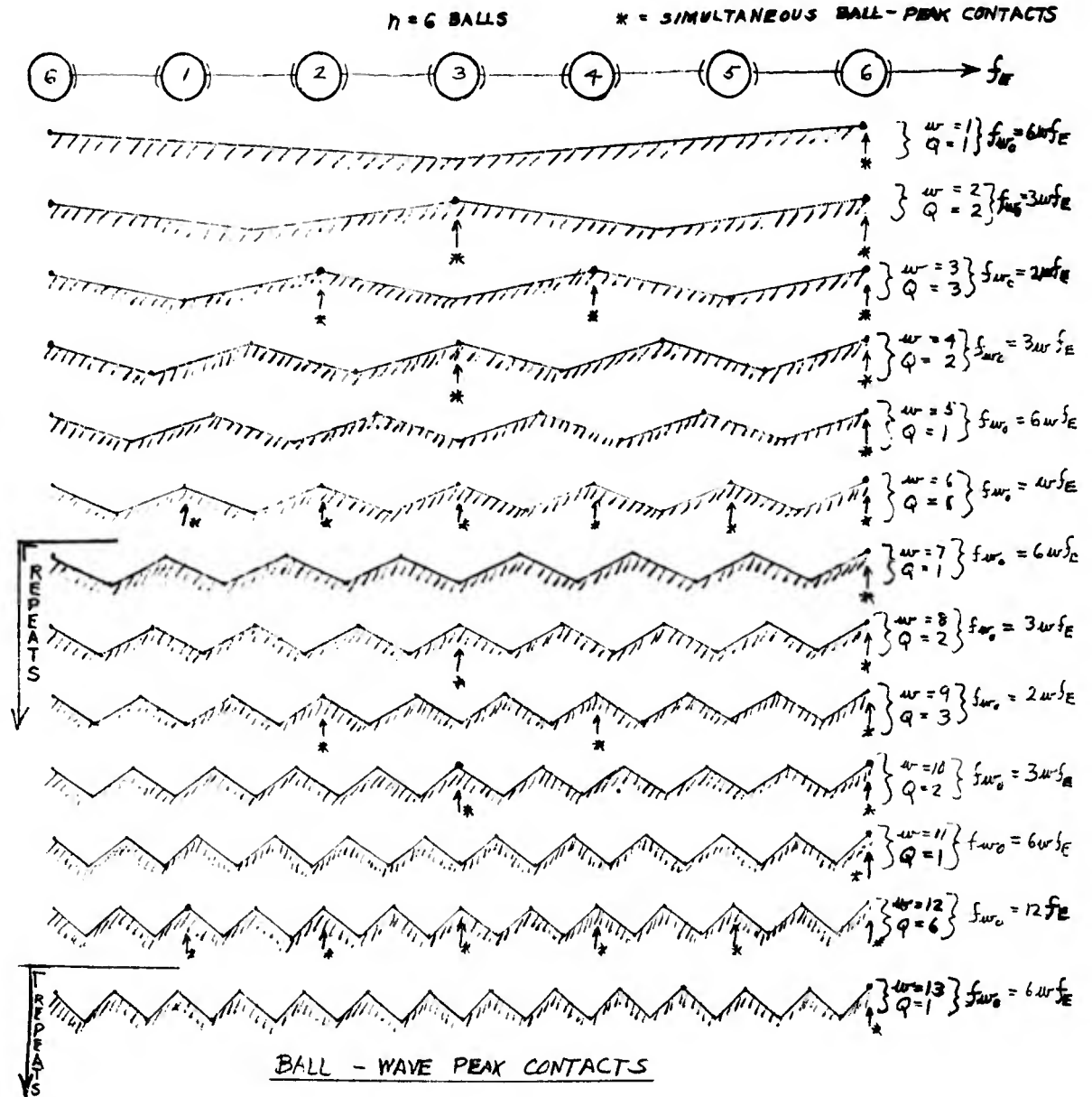


Figure 6

Therefore, we may write;

$$\text{Outer waviness frequency factor} = \frac{f_{w_o}}{f_i} = \frac{n}{Q} w_o \frac{1}{2} \left(1 - \frac{d}{E}\right) \quad (17)$$

Similarly,

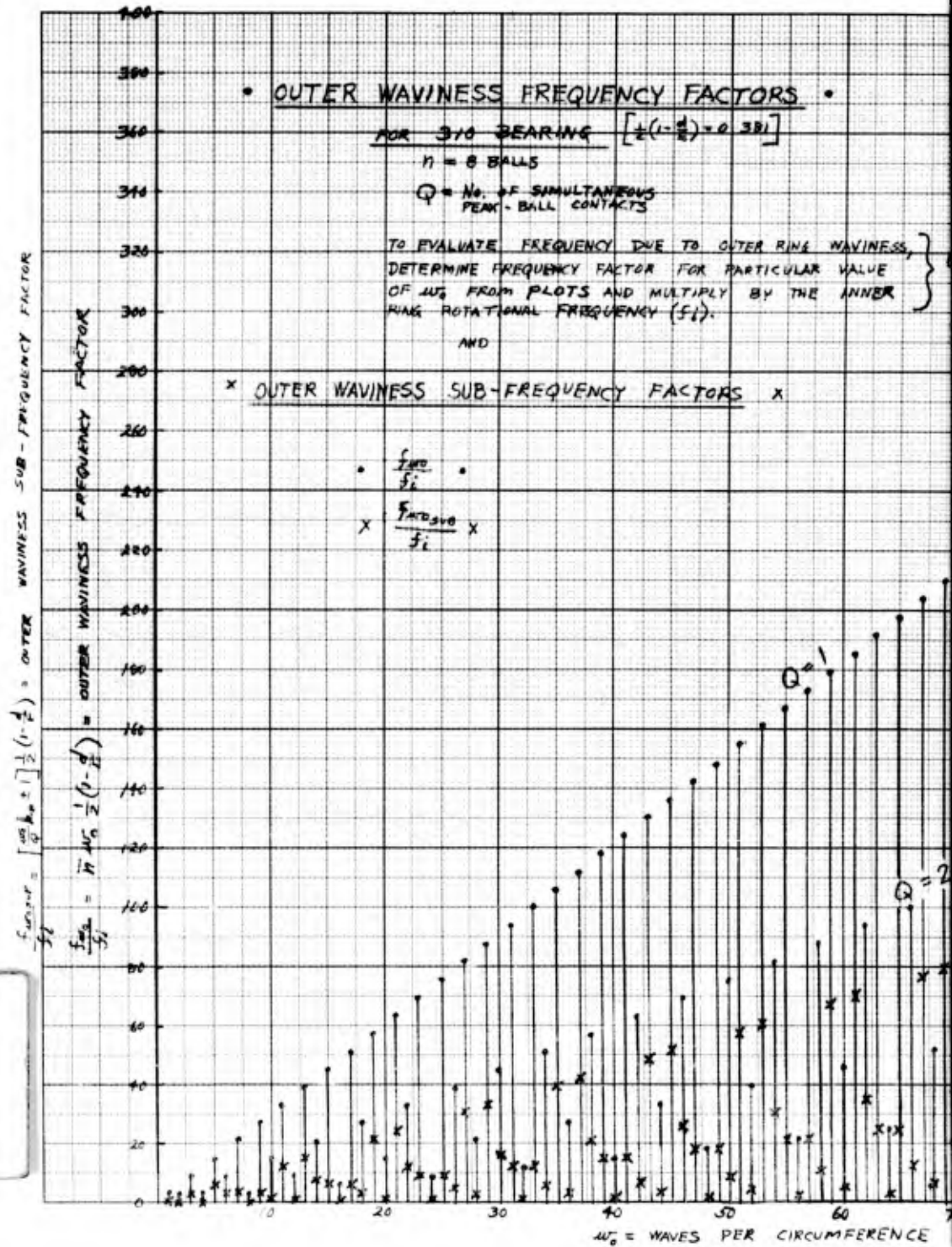
$$\text{Inner waviness frequency factor} = \frac{f_{w_i}}{f_i} = \frac{n}{Q} w_i \frac{1}{2} \left(1 + \frac{d}{E}\right) \quad (18)$$

$n$ ,  $w_i$ ,  $w_o$ ,  $d$ , and  $E$  are known values, but  $Q$  is a function of  $n$  and  $w$ , hence must be determined. The method of determining  $Q$  for a particular combination of  $n$  and  $w$  is discussed in Appendix B.1. For convenience, a table of values of  $Q$  for many combinations of  $n$  and  $w$  is also presented in Appendix B.1. Notice that the pattern of  $Q$  repeats every  $n^{\text{th}}$  wave. That is,

$$Q_w = Q_{w \pm n} = Q_{w \pm 2n} = Q_{w \pm in}$$

Summarizing briefly, the frequency factors for the occurrence of ball-peak contact somewhere in the bearing may be determined by the use of equations (17) and (18) and the data presented in Appendix B for  $Q$ . Outer and inner waviness frequency factors are plotted for the 310 bearing in Figures 7 and 8.

1



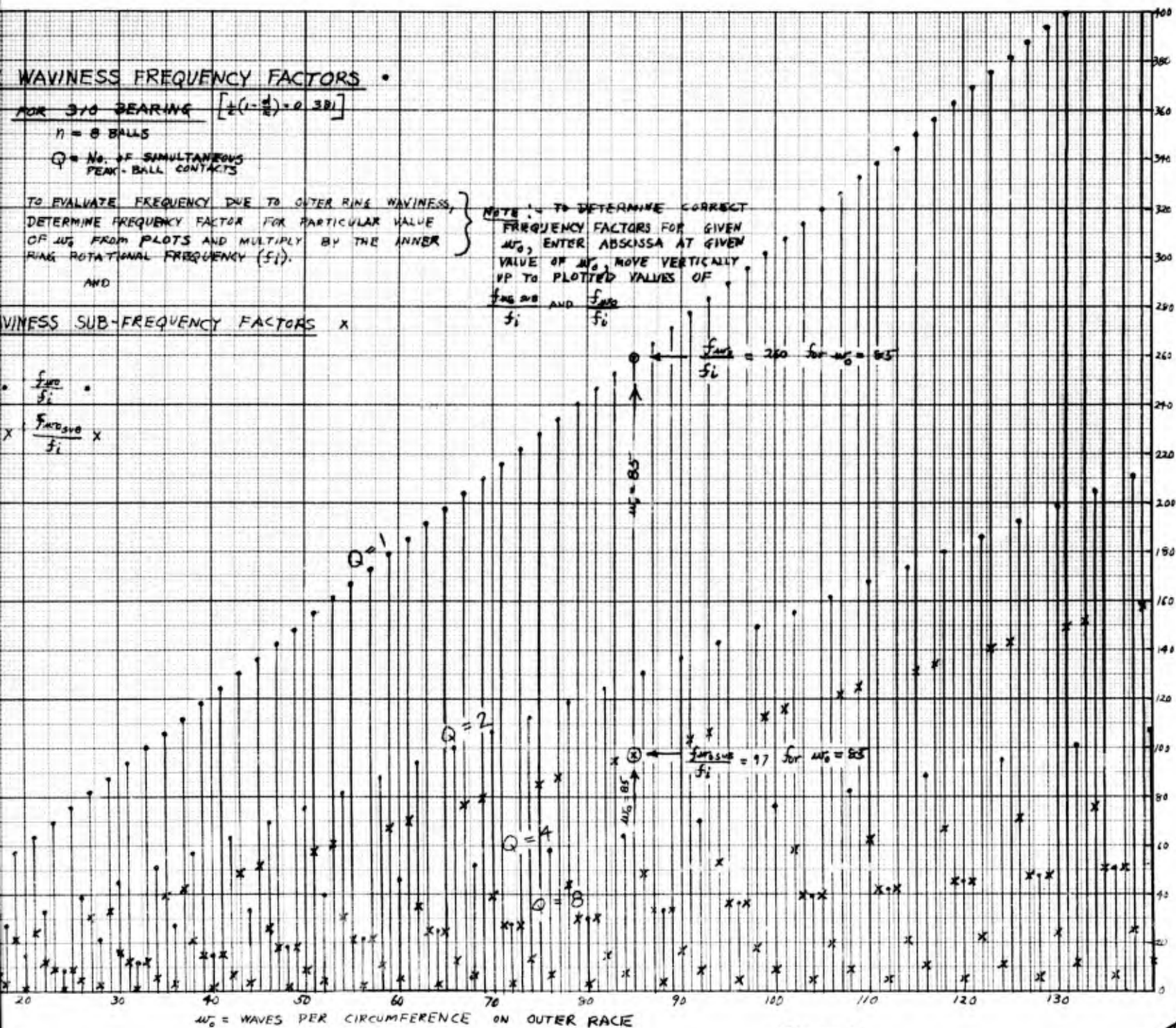


Figure 7

2

$$\frac{f_{wv,sub}}{f_i} = \text{INNER WAVINESS SUB-FREQUENCY FACTOR} = \left[ \frac{wv_i}{Q} \cdot b_o \cdot \frac{1}{2} \left( 1 + \frac{Q}{E} \right) \right]$$

$$\frac{f_{wv}}{f_i} = \text{INNER WAVINESS FREQUENCY FACTOR} = \frac{1}{2} \left( 1 + \frac{Q}{E} \right)$$

• INNER WAVINESS FREQUENCY FACTORS •

FOR 316 BEARING  $\left[ \frac{1}{2} \left( 1 + \frac{Q}{E} \right) = 0.619 \right]$

$N = 8$  BALLS

$Q =$  NO. OF SIMULTANEOUS PEAK-BALL CONTACTS

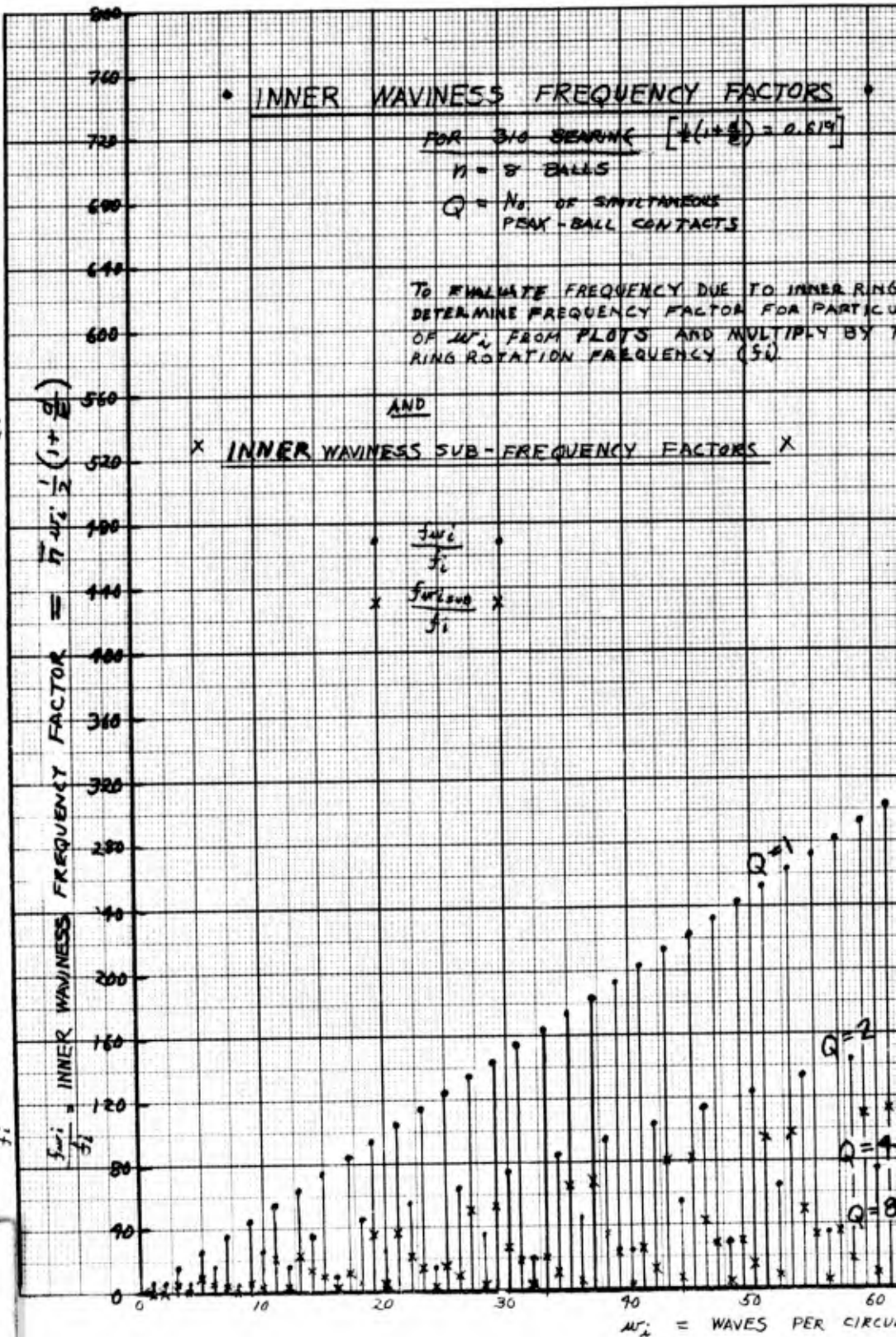
TO EVALUATE FREQUENCY DUE TO INNER RING DETERMINE FREQUENCY FACTOR FOR PARTICULAR  $wv_i$  FROM PLOTS AND MULTIPLY BY RING ROTATION FREQUENCY (50)

AND

x INNER WAVINESS SUB-FREQUENCY FACTORS x

$$\frac{f_{wv}}{f_i}$$

$$\frac{f_{wv,sub}}{f_i}$$



$wv_i =$  WAVES PER CIRCUMFERENCE

1



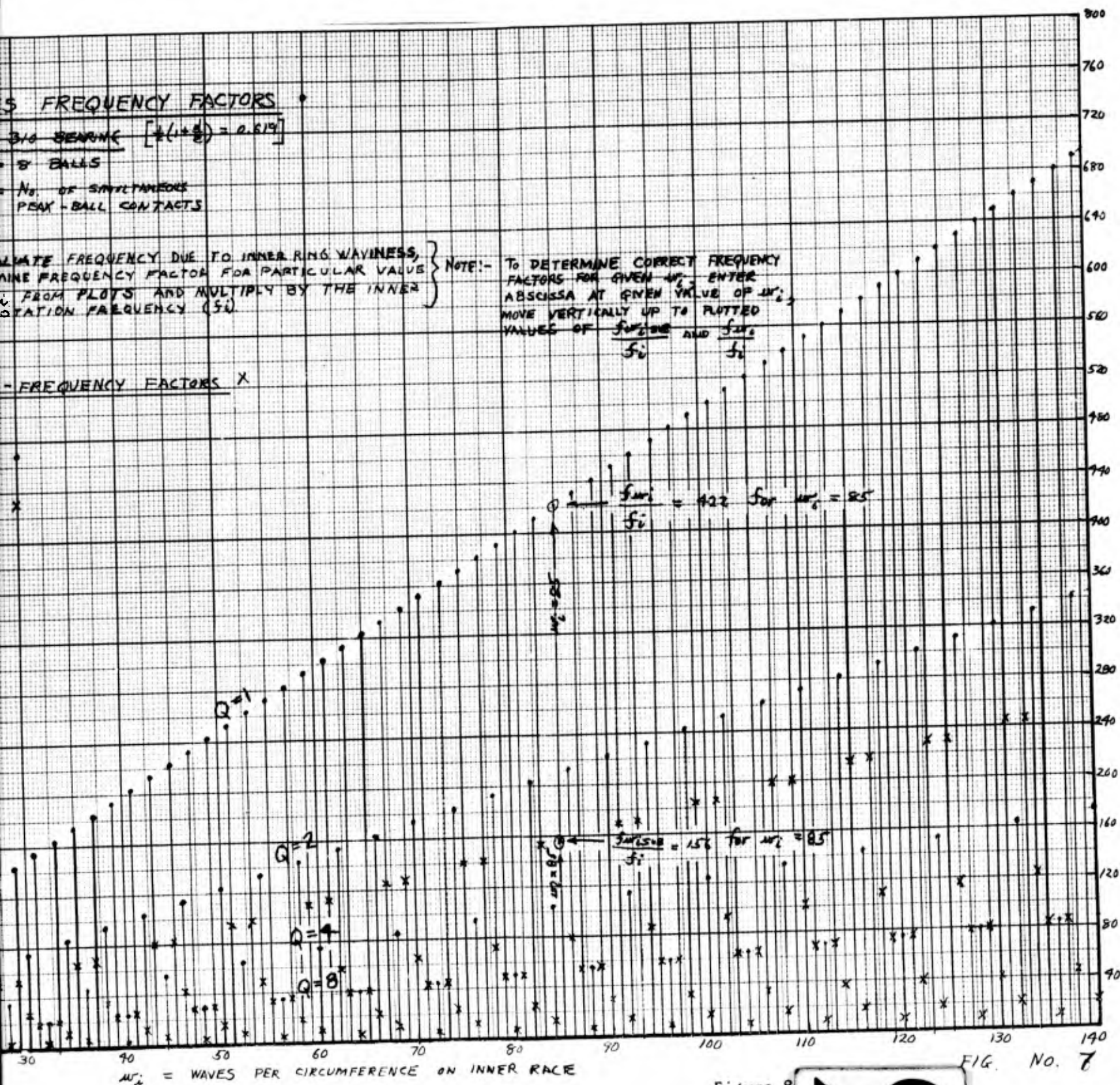


Figure 8

FIG. No. 7



THE FRANKLIN INSTITUTE • *Laboratories for Research and Development*

I-A2321-1

From Figures 7 and 8 the effect on frequency due to small changes in the number of waves is immediately apparent. Consider a 310 bearing with 48 waves on the outer race. At 1800 RPM, the resulting frequency would be from (17);

$$f_{w_o} = \frac{n}{Q} w_o \frac{1}{2} \left( 1 - \frac{d}{E} \right) f_1 = [18.5] \left[ \frac{1800}{60} \right]$$

[where  $\frac{n}{Q} w_o \frac{1}{2} \left( 1 - \frac{d}{E} \right) = 18.5$  as determined from Figure 7 for  $w_o = 48$ ]

$$\therefore f_{w_o} = 555 \text{ cps}$$

49 waves would yield a frequency of,

$$f_{w_o} = (148) \left( \frac{1800}{60} \right)$$

$$f_{w_o} = 4440 \text{ cps}$$

50 waves gives

$$f_{w_o} = (75.5) \left( \frac{1800}{60} \right)$$

$$f_{w_o} = 2265 \text{ cps}$$

Thus the absolute number of waves plays an important role in the vibration frequency generated.

### 3.1.1.1.6 Raceway-Waviness Sub-Frequency Factors

Outer and inner ring waviness also generate other frequencies which are lower than those determined by (17) and (18). To illustrate, consider a 310 bearing with

$$n = 8$$

$$w_o = 15$$

From Appendix B,

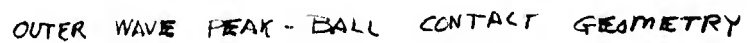
$$Q = 1$$

The outer waviness frequency as predicted by Equation (17) is

$$\begin{aligned} f_{wo} &= \frac{n}{Q} \times w_o f_E \\ &= \frac{8}{1} \times 15 f_E \\ f_{wo} &= 120 \times f_E \end{aligned}$$

This tells us that once every  $\left(\frac{1}{120 f_E}\right)$  seconds, one of the balls will be contacting one of the peaks somewhere in the bearing. Referring to Figure 9, at time zero, assume that ball No. 8 is touching wave peak No. 15 at 0°. The first contact is ball 1 with wave 2 at  $t = \frac{1}{120 f_E}$ . Ball 2 makes the next contact with wave 4 at  $t = \frac{2}{120 f_E}$  followed by ball 3 contacting wave 6 at  $t = \frac{3}{120 f_E}$  and so forth around the bearing. As determined above, the frequency of contact is  $120 \times f_E$ , but notice that the angular location of the impact is rotating clockwise at a frequency equal to  $\frac{48^\circ}{3^\circ} \times f_E = 16 f_E$  which is considerably less than  $120 \times f_E$ .





- 35 -

THE FRANKLIN INSTITUTE • Laboratories for Research and Development

I-A2321-1

If now the number of waves were 17 instead of 15, ball No. 7 would make the first contact (with wave 15) followed by ball 6 with wave 13.

The frequency of contact would be

$$f_{wo} = \frac{w}{Q} \times n f_E = \frac{17}{1} \times 8 f_E$$

$$f_{wo} = 136 f_E,$$

but the location of contact would rotate counter-clockwise at a frequency

$$\text{of } \frac{42 \frac{6}{17}}{2 \frac{11}{17}} \times f_E = 16 f_E$$

For 19 waves, ball 5 would make the first contact with wave 12 @ -  $132 \frac{12}{19}$  followed by ball 2 with wave 5 @ -  $265 \frac{5}{19}$ . The frequency of contact would be

$$f_{wo} = \frac{w}{Q} \times n f_E = \frac{19}{1} \times 8 f_E$$

$$f_{wo} = 152 f_E,$$

but the location of contact would rotate counter clockwise at a frequency

$$\begin{aligned} &= \frac{132 \frac{12}{19}}{2 \frac{7}{19}} \times f_E \\ &= 56 f_E \end{aligned}$$

THE FRANKLIN INSTITUTE • Laboratories for Research and Development

I-A2321-1

The equation for outer waviness sub-frequency factor is;

$$\text{Outer waviness sub-frequency factor} = \frac{f_{w_o \text{ sub}}}{f_i}$$

$$\frac{f_{w_o \text{ sub}}}{f_i} = \left[ \frac{w_o}{Q} k_B \pm 1 \right] \frac{1}{2} \left( 1 - \frac{d}{E} \right) \quad (19)$$

where  $k_B$  = smallest number of ball spaces between successive balls  
contacting peaks

(+ sign used if 2nd ball is closer in direction of cage  
movement)

(- sign used if 2nd ball is closer in opposite direction)

The development of equation (19) is given in Appendix B.2.

Values of  $\left[ \frac{w_o}{Q} k_B \pm 1 \right]$  for an 8-ball bearing are also tabulated in Table B-2.  
Once again, a definite pattern exists for  $\left[ \frac{w_o}{Q} k_B \pm 1 \right]$  which repeats every  
n<sup>th</sup> ball. Outer waviness sub-frequency factors are plotted in Figure 7  
for the 310 bearing.

The sub-frequencies generated by inner race waviness are more  
difficult to determine because the inner race rotates in addition to the  
balls. The frequency factor for inner race waviness sub-frequency is  
developed in Appendix B.3 and may be written as:

$$\text{Inner waviness sub-frequency factor} = \frac{f_{w_i \text{ sub}}}{f_i}$$

$$\frac{f_{w_i \text{ sub}}}{f_i} = \left[ \frac{w_i}{Q} k_B \pm \frac{(1 - \frac{d}{E})}{(1 + \frac{d}{E})} \right] \frac{1}{2} \left( 1 + \frac{d}{E} \right) \quad (20)$$

where  $k_B$  = smallest number of ball spaces from ball in contact to next ball to touch

(+ sign used if 2nd ball is closer in direction of cage rotation)

(- sign used if 2nd ball is in opposite direction)

These inner waviness frequency factors for the 310 bearing are plotted in Figure 8, and values of  $\left[ \frac{w_i}{2} k_B \pm \frac{(1 - \frac{d}{E})}{(1 + \frac{d}{E})} \right]$  are tabulated in Table

No. B-3 to show its repetitive nature for every  $n^{\text{th}}$  ball.

### 3.1.1.1.7 Raceway Eccentricity Frequency Factors

Outer race eccentricity does not generate vibration. However, if the inner race is eccentric with respect to its bore, the center of mass of the rotor will not coincide with the center of rotation, and an unbalance force will be generated which rotates around the bearing at a frequency equal to  $f_i$ .

$$\text{Outer eccentricity frequency factor} = \frac{f_{eo}}{f_i} = 0 \quad (21)$$

and

$$\text{Inner eccentricity frequency factor} = \frac{f_{ei}}{f_i} = 1 \quad (22)$$

Notice that these frequencies agree with those for outer and inner waviness sub-frequencies for  $w_o = 1$  and  $w_i = 1$  (See Appendix B).

### 3.1.1.1.8 Unbalance Force Frequency Factor

The frequency generated by a rotating mechanical or electrical unbalance is equal to the frequency of rotor rotation. Hence, the frequency factor associated with this disturbance is

$$\frac{f_u}{f_1} = 1 \quad (23)$$

Also, in the presence of a rotating unbalance force and in an application of a rolling contact bearing having no other applied radial or axial loads, another higher frequency will be generated which is equal to the inner ball-pass frequency. This is discussed further in the following section on ball-pass instability frequency factors.

### 3.1.1.1.9 Ball-Pass Instability Frequency Factors

In an operating ball bearing, the balls are continually changing their angular positions within the bearing. As a result, even in a bearing with perfect geometry of all bearing components the rotor will be forced to exhibit a periodic oscillation. When the applied load is of constant magnitude and fixed direction, the frequency of oscillation will be equal to the outer ball-pass frequency. For a pure rotating load, rotating with the shaft (such as due to unbalance), an inner ball-pass frequency disturbing force will be generated in addition to the once-per-revolution disturbing force. Within this work, we choose to call this generated disturbance "ball-pass instability." It is discussed in considerably more detail in the section devoted to load-displacement characteristics of rolling contact bearings. Thus, the frequency factors associated with this phenomena are equal to the inner and outer ball-pass frequency factors (Equations (8) and (9) and Figure 3.)

### 3.1.1.1.10 Cage Defect Frequency Factors

The frequencies of disturbing forces generated by cage defects such as cage unbalance, or cage asymmetries will, in general, be a fractional part of the rotational frequency of the inner ring as dictated by ball diameter and ball pitch line diameter. Hence,

$$\text{Cage defect - outer ring frequency factor} = \frac{f_{co}}{f_i} = \frac{1}{2} \left( 1 - \frac{d}{E} \right) \quad (24)$$

and

$$\text{Cage defect - inner ring frequency factor} = \frac{f_{ci}}{f_i} = \frac{1}{2} \left( 1 + \frac{d}{E} \right) \quad (25)$$

### 3.1.1.2 Summary Of Possible Disturbing Force Frequencies

The purpose of this study was to determine the frequencies of occurrence of particular events within the rolling contact bearing which, associated with bearing imperfections, operating characteristics and design, generate varying periodic forces within the bearing; hence, generate vibration. Within this study, dimensionless frequency factors have been determined for various bearing series and sizes to allow the ready evaluation of frequencies due to

Ball defects

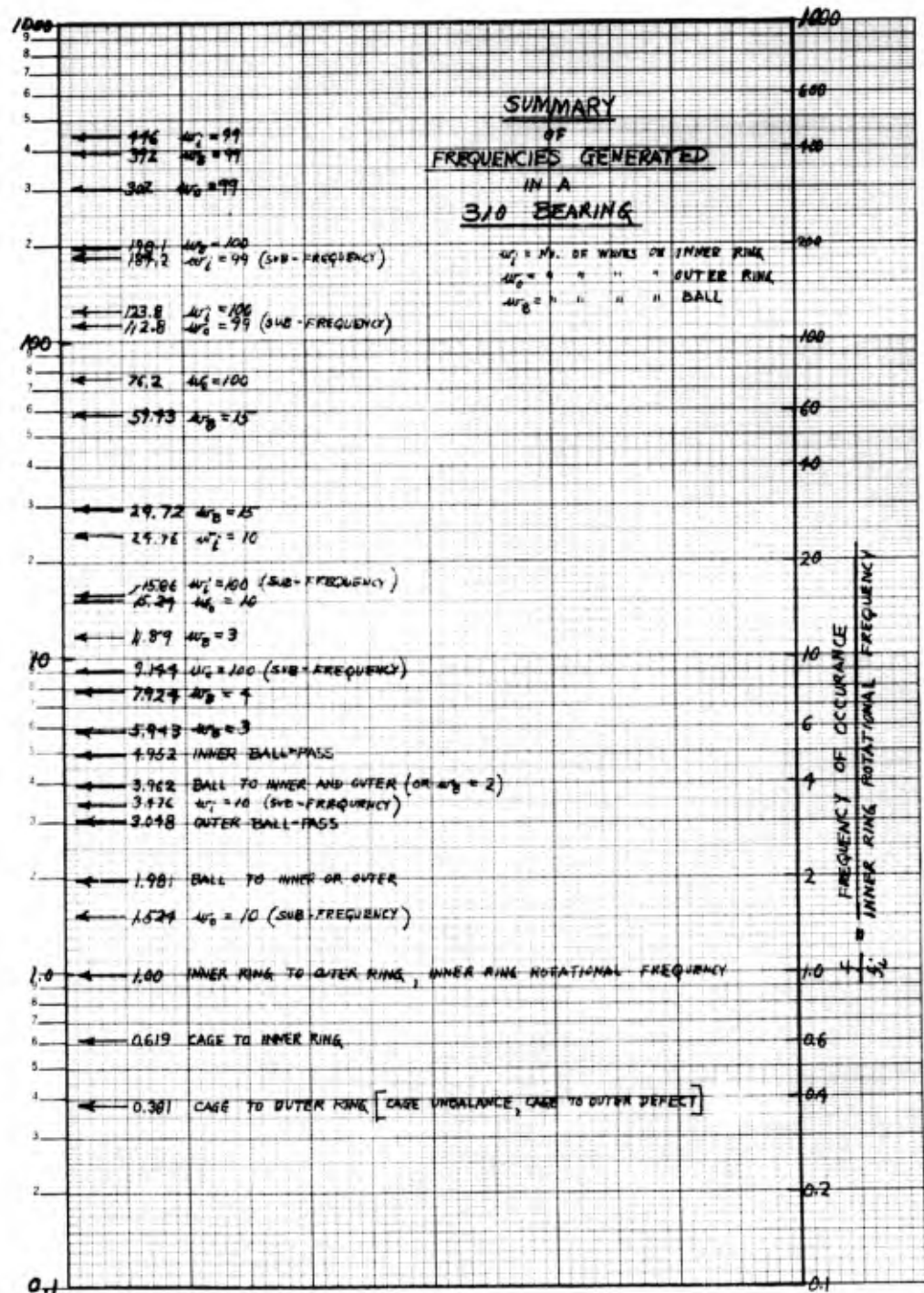
Inner and outer race defects

Cage defects

Ball pass

Eccentricity and unbalance

Figure 10 summarizes these factors on a dimensionless frequency spectrum for a 310 bearing. Observation of this figure reveals:



THE FRANKLIN INSTITUTE • *Laboratories for Research and Development*

I-A2321-1

1. (  $\frac{f}{f_1} < 1.0$  ) Primarily due to cage and its ball train
2. (  $\frac{f}{f_1} = 1.0$  ) Due to rotational frequency of inner ring
3. (  $1.0 < \frac{f}{f_1} < 10$  ) Due to inner - outer ball-pass, ball rotation, low order ball and ring waviness
4. (  $\frac{f}{f_1} > 10$  ) Due to higher order ball and ring waviness

Similar results would be obtained with bearings of other series and sizes, hence the same general conclusions may be applied to all ball bearings of this type. If one considers the possibility of higher harmonics, gross changes in contact angle, varying raceway path, variation of ball rotational axis, surface finish and ball skidding, it becomes immediately apparent that rolling contact bearings can generate disturbing forces in the frequency range from a fraction of the inner ring rotational frequency to a thousand times rotational frequency. A bearing of perfect geometry of all its members and ideally loaded so as to produce constant and equal loading of all the balls will, of necessity, still generate varying periodic forces on its races and balls due to ball-pass instability.



## 3.1.1.3 Relationship Between Vibration Sources and Generated Forces

In this section we shall determine the relative magnitudes of bearing component imperfections and operating characteristics which with their respective frequencies will produce equal maximum periodic forces. As a first simplified approach we have neglected deformation at the ball race contacts and assumed that the resulting vibration is sinusoidal and that the same mass is being vibrated which yields the following expression for the maximum force;

$$F_{\max} = (2\pi)^2 m A f^2$$

where A is the one-half peak-to-peak vibration distance of the mass m vibrating at a frequency of f. The generated disturbing force due to radial runout of the inner race would be

$$F_{\max} = (2\pi)^2 m A_r f_1^2$$

where  $A_r$  is one-half of the inner race runout error.

Equating the two above equations yields

$$\frac{A}{A_r} = \frac{1}{(f/f_1)^2} \quad (26)$$

which states that the ratio of vibration source amplitude to the radial runout amplitude required to produce equal peak forces is inversely proportional to the square of frequency factor associated with the source. On this basis then, the high frequency vibration sources must necessarily be of small amplitude compared to low frequency sources to produce equal peak forces. In Table No. 3-1, several vibration sources in a 310 bearing were considered. Their associated frequency factors were obtained from the

THE FRANKLIN INSTITUTE • *Laboratories for Research and Development*

I-A2321-1

previous work. The ratio of  $\frac{A}{A_r}$  as given in equation (26) was then determined, and the results are shown in Table 3-1. For those considerations having relatively high frequency factors, the ratio  $\frac{A}{A_r}$  becomes extremely small. This is better illustrated by examining the results for A, the source amplitude, when the total inner race runout is  $2 \times 10^{-4}$  inch ( $A_r = 1.0 \times 10^{-4}$  inch) also shown in Table 3-1. This comparison assumes that deformations at the ball-race contacts do not occur which is, of course, not true. This is to say, larger errors than those computed for the higher frequency sources would be required to generate the same peak forces because the bearing can "swallow" small errors. The magnitude of ball load will also influence the amplitude of vibration for a given error. The vibration level will decrease with increasing level of load. However, it can be said with some assurance that ball size variation (ball-to-ball), ball waviness and inner and outer raceway waviness geometry errors on the order of  $10 \times 10^{-6}$  inch will produce vibratory peak forces of the same magnitude as the once per revolution force generated by an inner race runout of  $2 \times 10^{-4}$  inch.

Table No. 3-1

COMPARISON OF VIBRATION SOURCE AMPLITUDES WHICH  
YIELD FORCES OF AMPLITUDE EQUAL TO THAT OF  
INNER RACE RADIAL RUNOUT (310 BEARING)

$$\frac{A}{A_r} = \frac{1}{(f/f_1)^2}$$

<u>Vibration Source</u>	$\left(\frac{f}{f_1}\right)$	$\frac{A}{A_r}$ (Eq. (28))	$\frac{A}{A_r}$ (For $A_r = 1 \times 10^{-4}$ in.) (in.)
Inner race radial runout	1	1	$1 \times 10^{-4}$
Outer " " "	0	$\infty$	$\infty$
Single defect on outer race	3.048	0.1080	$10.8 \times 10^{-6}$
" " " inner "	4.952	0.0408	$4.08 \times 10^{-6}$
" " " ball	3.962	0.0639	$6.39 \times 10^{-6}$
Variation in ball dimensions or ball-pass instability			
Fixed load	3.048	0.1080	$10.8 \times 10^{-6}$
Rotating load	4.952	0.0408	$4.08 \times 10^{-6}$
Waviness			
$w_o = 10$ (sub-frequency)	1.524	0.430	$43 \times 10^{-6}$
$w_o = 10$	15.24	0.0043	$0.43 \times 10^{-6}$
$w_o = 100$ (sub-frequency)	9.144	0.0120	$1.2 \times 10^{-6}$
$w_o = 100$	76.2	0.000172	$0.0172 \times 10^{-6}$
$w_i = 10$ (sub-frequency)	3.476	0.0835	$8.35 \times 10^{-6}$
$w_i = 10$	24.76	0.00157	$0.157 \times 10^{-6}$
$w_i = 100$ (sub-frequency)	15.86	0.00397	$0.397 \times 10^{-6}$
$w_i = 100$	123.8	0.000066	$0.0066 \times 10^{-6}$
$w_B = 3$	5.493	.033	$3.3 \times 10^{-6}$
$w_B = 10$	19.81	.00255	$0.255 \times 10^{-6}$

### 3.1.2 Sliding Surface Bearings

In this work we shall deal only with full, 360° journal bearings. In addition, we shall limit the discussion to only full-film, hydrodynamic operation implying no metal-to-metal contact. That is, the journal never touches the sleeve bearing. The two other modes of sleeve bearing operation, namely, mixed-film and boundary lubricated, both implying

THE FRANKLIN INSTITUTE • *Laboratories for Research and Development*

I-A2321-1

some degree of metal-to-metal contact, are not considered for noise-critical applications.\*

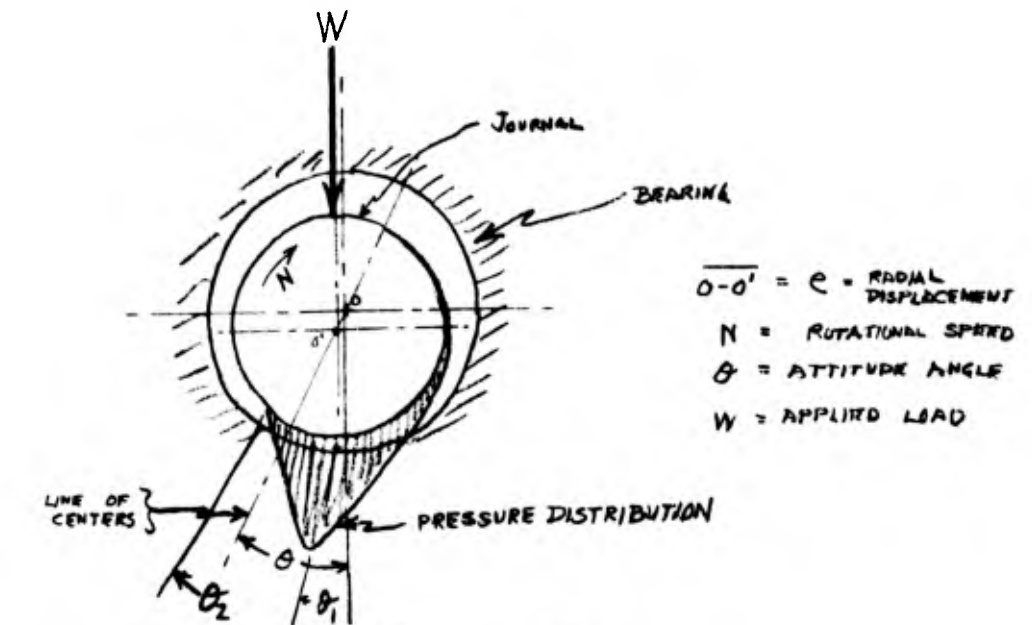
In this section we shall investigate those factors inherent in the sleeve bearing that promote and sustain forces of a periodic nature which generate vibration within the bearing. In general, such generated forces are due to

1. Inherent instabilities (oil whirl, oil whip)
2. Geometry errors (bearing and journal waviness)
3. Improper design for particular application

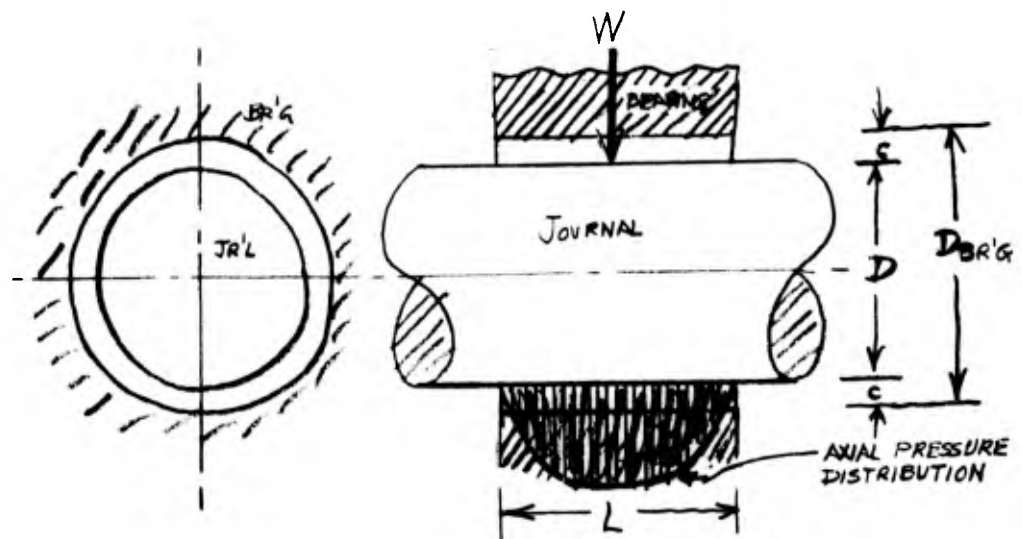
Before embarking upon the determination of the frequencies and magnitudes of generated periodic forces in the sleeve bearing, it should be pointed out that such forces are the result of a variation with time of the oil-film pressure distribution. Hence, any phenomenon or geometry and design consideration (or requirement) which promotes varying fluid film pressures must be considered as contributing to noise and vibration generation in fluid film bearings. A typical pressure distribution for a sleeve bearing operating on a full film of lubricant is illustrated in Fig. No. 11(a). Other geometry and nomenclature are indicated in Fig. No. 11(b). For a steady unidirectional load the pressure distribution remains fixed with respect to the bearing. For a rotating load, the pressure distribution rotates with the load. Notice that, of necessity, the journal becomes eccentric with respect to the center of the bearing. Increasing load requires more eccentric operation. Notice also that the load carrying pressure distribution covers quite a large

---

\*It is conceivable that a boundary or mixed-film operated sleeve bearing operating under favorable conditions can be relatively quiet.



(a) TYPICAL PRESSURE DISTRIBUTION



(b) GEOMETRY OF SLEEVE BEARING

Figure 11

area (circumferentially and axially). This is a decided advantage for the sleeve bearing in that varying forces are distributed over appreciable area as opposed to the local, concentrated forces in a ball bearing at the ball-race contacts. Common design practice is to provide a diametral clearance on the order of 0.0010 inch per inch of diameter. Since the normal lubricants used (oil) resist being forced out of the small clearance volume, appreciable shock load capacity and damping are inherent qualities of full film lubricated sliding surface bearings.

#### 3.1.2.1 Frequency Factors

In this section we shall give consideration to the frequencies of periodic forces generated within a full film lubricated, 360° plain journal bearing.

##### 3.1.2.1.1 Inherent Instabilities

Full film lubricated sleeve bearings are susceptible to two types of instability commonly referred to as half-frequency whirl and resonant whip. There currently exists a great deal of confusion as to which type of instability is present when extreme vibrations of a sleeve bearing rotor are encountered. However, general agreement among investigators indicates that instabilities, if present, at rotational speeds less than twice the shaft critical speed will exhibit a frequency equal to one-half of the rotational speed of the shaft. Hence, the term "half-frequency" whirl. At speeds greater than twice the shaft critical speed, resonant whip occurs and persists. The frequency of resonant whip is equal to the critical speed frequency of the shaft.

This is illustrated in Figure 11A below.

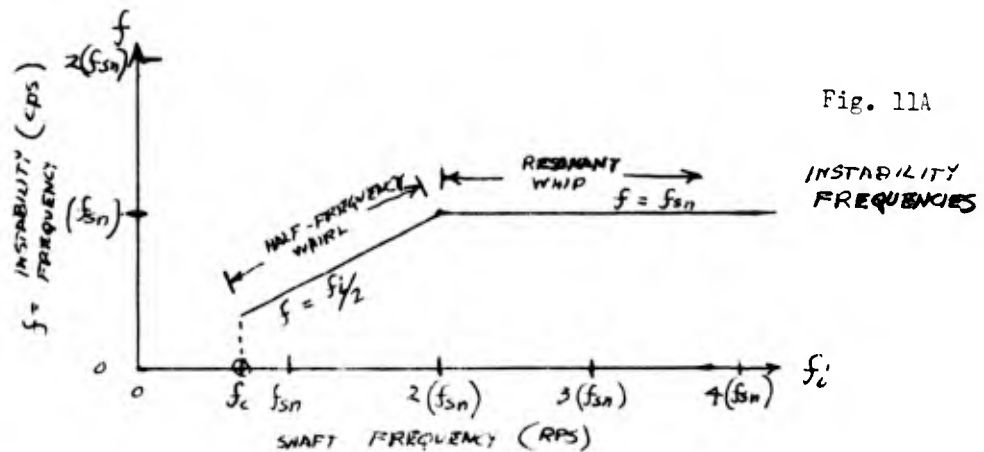


Fig. 11A

Half-frequency whirl is a self-exciting phenomenon and may be attributed to the instability of the oil film. It is sometimes experienced with light load, high speed operation. Techniques are available for predicting the onset of half frequency whirl (marked  $f_c$  in the above Figure).<sup>1\*</sup> As an example for a 60 pound rotor supported on two, 2-inch diameter x 2-inch long bearings lubricated with an SAE 20 motor oil @ 130°F,  $f_c \approx 50,000$  RPM ( $f_c = 830$  cps), which is more than a factor of ten greater than normal motor speeds. This would indicate that half-frequency whirl should not be a problem in electric motors. Since this is true, resonant whip will not occur (at normal motor speeds) since it is dependent upon resonance of half-frequency whirl with the shaft critical speed. If, as in some isolated cases,

\*Numbers refer to references listed in Appendix L.

such as vertical shaft applications or high frequency generators and alternators of large size, whirl and whip is a serious problem, they can usually be suppressed by proper design.

In any case, the frequency factors are

Half-frequency whirl ( $0 < f_i < 2f_{sn}$ )

$$\frac{f_{wh}}{f_i} = 0.5 \quad (27)$$

Resonant Whip ( $2f_{sn} < f_i < \infty$ )

$$\frac{f_{wh}}{f_i} = \frac{f_{sn}}{f_i} = \frac{\text{Shaft (rotor) critical speed}}{\text{Shaft rotational speed}} \quad (28)$$

### 3.1.2.1.2 Geometry Errors

Any departure from true cylinders of the journal and bearing geometries may produce variations of a periodic nature of the fluid film pressure distribution. Some possible errors and their associated frequency factors are discussed below.

#### 3.1.2.1.2.1 Journal Waviness

An out of round journal in a sleeve bearing operating under the influence of a unidirectional load will cause periodic variations in the fluid film pressure distribution due to varying film clearance geometry in the load area. The frequency factor associated with journal waviness would be

$$\frac{f_{wj}}{f_i} = w_j = \text{No. of waves per circumference} \quad (29)$$



For a pure rotating load, journal waviness does not produce a varying pressure distribution. Instead, a fixed pressure distribution rotates around the bearing at a frequency equal to shaft speed.

#### 3.1.2.1.2.2 Bearing Waviness

An out of round bearing supporting a unidirectional load will not cause periodic variations in the fluid film pressure distribution. Disturbing frequencies will be generated, however, if the load rotates. The frequency factor for bearing waviness and a rotating load is,

$$\frac{f_{WB}}{f_i} = w_B = \text{No. of waves per circumference} \quad (30)$$

#### 3.1.2.1.3 Improper Design

Improper design of sleeve bearings can generate noise and vibration. The primary offenders are:

1. Misplaced and over-zealous oil-grooving
2. Overloading
3. Misalignment
4. Insufficient supply of lubricant

Such factors can promote periodic metal-to-metal contact with resulting severe noise and vibration generation, hence cannot be tolerated. Improper grooving while still providing full film lubrication with no metal-to-metal contact can produce a varying pressure distribution. As an example, a bearing supporting a unidirectional load and supplied with lubricant from a groove or hole in the journal will produce a once per revolution vibration. The reverse situation, rotating load with groove in bearing, will likewise generate once per revolution vibration.

It must be emphasized that the design of the journal bearing must be tailored to the particular application to insure proper full film operation.

### 3.1.2.2 Relationship Between Vibration Sources and Generated Forces

As was indicated previously load carrying capacity in a sleeve bearing is a result of the fluid film pressure distribution generated within the clearance volume. The main bulk of this pressure distribution is from approximately  $\theta_2$  (Fig. 11 (a)) to  $-\frac{1}{2} \theta_2$  which, for a lightly loaded bearing, encompasses approximately  $180^\circ$  and condenses to about  $45^\circ$  for a highly loaded bearing. Sleeve bearings, as used in electric motors, are relatively lightly loaded. As an example, for a 60 pound rotor supported on two, 2-inch diameter by 2-inch long bearings lubricated with an SAE 20 motor oil @  $130^\circ\text{F}$  and running at 1800 RPM, the journal will be displaced only  $30 \times 10^{-6}$  inch from center for a bearing having a radial clearance of  $1500 \times 10^{-6}$  inch. For a 300 pound load (belt pull), the heavily loaded bearing will operate with the journal displaced from the center by only  $270 \times 10^{-6}$  inch. For a maximum load (max belt pull) of 1500 pounds the journal displacement is approximately  $825 \times 10^{-6}$  inch. For this last condition, the oil film pressure distribution still encompasses approximately  $120^\circ$  of arc. Amplitudes of rotor vibration equal to the waviness amplitude could possibly be realized when the waviness wave lengths are greater than the load supporting fluid film arc length (approximately  $120^\circ$ ). For shorter waviness wave lengths ( $w_j > 3$ ) wherein more than one wave lies within the pressure film, the amplitude of rotor vibration will be less

THE FRANKLIN INSTITUTE • *Laboratories for Research and Development*

I-A2321-1

than the waviness amplitude due to the averaging effect afforded by the large area containing the load  $\left\{ \begin{array}{l} \text{carrying} \\ \text{pressure} \\ \text{distribution} \end{array} \right.$ . How much less is, of course, impossible to practically predict. The greater the number of waves, the smaller will be the ratio of rotor vibration amplitude to waviness amplitude. The simplest imaginable relationship would be

$$\frac{A}{\delta} = \frac{1}{w_j} \quad (31)$$

where  $A$  = vibration amplitude

$\delta$  = waviness amplitude

$w_j$  = No. of waves on journal circumference

Resorting again to the assumption that the magnitude of the force generated is

$$F = m A \omega^2$$

$$F = m \frac{\delta_r}{w_j} (2\pi)^2 f_{w_j}^2$$

Again, as before, equating this force to the once per revolution runout force,  $F = m \frac{\delta_r}{1} (2\pi)^2 f_1^2$

$$\frac{\delta_r}{\delta} = \frac{w_j}{\frac{f_{w_j}}{f_1}}$$

where  $\delta_r = \frac{1}{2}$  of journal runout

Since  $\frac{f_{w_j}}{f_1} = w_j$

$$\boxed{\frac{\delta_r}{\delta} = \frac{1}{w_j} = \frac{1}{(f_{w_j}/f_1)}} \quad (32)$$

THE FRANKLIN INSTITUTE • *Laboratories for Research and Development*

I-A2321-1

Equation 32 indicates that the waviness amplitude which would generate peak forces of the same magnitude as those generated by the radial runout error  $\delta_r$  varies inversely as the number of waves. For a ball bearing it was found (Section 3.1.1.3) that the waviness error varied inversely as the square of waviness frequency factor when applying the same criteria. It would, therefore, appear that higher amplitudes of waviness may be allowable in a sleeve bearing than in a ball bearing.

Taking the other approach and assuming that the rotor does not vibrate (which is more valid for higher frequency waviness), the pressure distribution will have "ripples" superimposed upon it and, more or less, synchronized with the moving waviness pattern on the rotating journal. The local variation of film pressure at a particular spot on the bearing in the loaded zone will depend upon such considerations as:

1. Amplitude of waviness
2. Lubricant film thickness
3. Extent of load-carrying pressure distribution
4. Frequency of waves

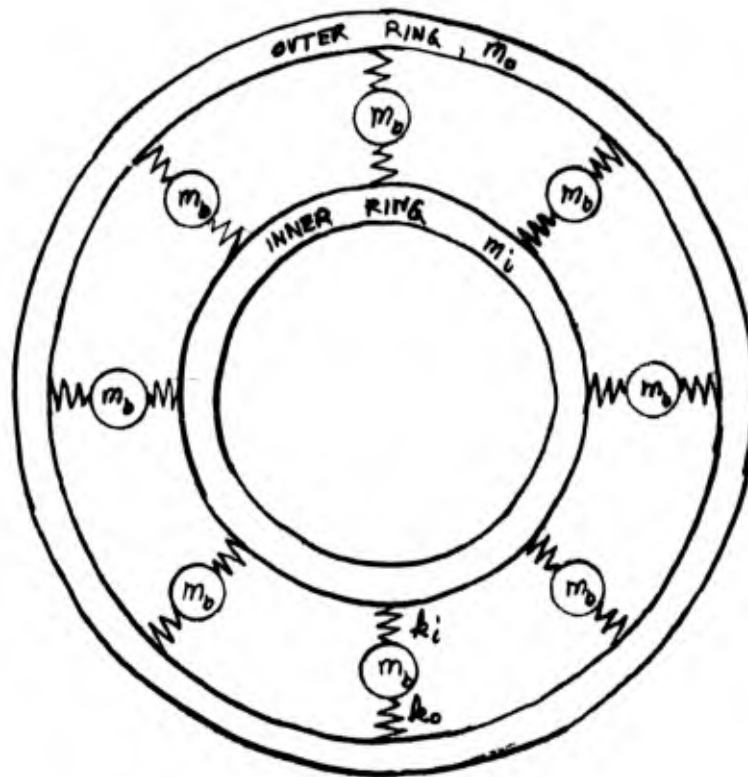
Lubricant film thicknesses in sleeve bearings are on the order of  $1000 \times 10^{-6}$  inch. Thus, waviness, in order to generate local magnitude variations in the fluid film pressure distribution, should be on the order of  $100 \times 10^{-6}$  inch. Relatively high frequency waviness ( $w_j > 10$ ) of this amplitude would be considered poor workmanship by almost any standard for a precision journal.

### 3.2 Vibrational Response and Resonant Frequencies and Their Relationship to Disturbing Forces

Some insight has now been gained into the frequencies of periodic disturbing forces generated within the bearing. Taking into account that the bearing is also subjected to other disturbing forces external to the bearing, the next part of the problem is to determine how the bearing responds to such excitation. The primary considerations in determining the response of a system to forced vibration are spring rates, masses vibrated, damping involved, and imposed constraints or boundary conditions. Hence, in what follows hereafter, the load-displacement characteristics of rolling contact and sliding surface bearings were investigated to resolve the parameters involved with their spring rates. With regard to damping, it was found necessary to neglect it for rolling contact bearings, but damping was considered in the sliding surface bearing study. Various spring-mass systems afforded within the bearing and by the bearing with different imposed constraints were evaluated for resonant frequencies which were then compared to possible frequencies of disturbing forces. Also, the natural frequencies of bearing components were investigated to determine their contribution, if any.

#### 3.2.1 Rolling Contact Bearings

A loaded rolling contact bearing presents an extremely complex, multi-degree of freedom system containing many non-linear springs, masses and unknown damping. Figure 12 shows, schematically, a rolling contact bearing with no constraints on its inner and outer races other than the "springs" at the inner and outer race contacts with the balls. In an



SCHEMATIC DIAGRAM OF UN-CONSTRAINED BALL-BEARING

Figure 12

THE FRANKLIN INSTITUTE • *Laboratories for Research and Development*

I-A2321-1

electric motor, the inner ring becomes, effectively, a part of the rotor and the outer ring is constrained in a close clearance housing. As such, several spring-mass systems are established and it becomes of interest to determine how these systems respond to bearing-generated or bearing-transmitted periodic disturbing forces. Since practically all bearing vibration and noise work is conducted using rolling contact bearings having a close clearance fit of their inner rings on a rotating spindle and an essentially free outer ring, the vibrational response of the spring-mass systems established by these conditions is also of interest. Our approach to this problem is to determine the resonant frequencies of such spring-mass systems and then compare the same with possible disturbing force frequencies. To make even the simplest analysis possible, it is expedient to assume zero damping. This was felt to be somewhat justified since it requires more damping than is probably present to appreciably alter the frequency of resonance.

### 3.2.1.1 Load-Displacement Characteristics

Since the vibrational response and transmission of vibratory forces whether generated within the bearing or the rotor it supports is dependent to a great extent upon the numerous "springs" formed within the bearing at ball-race contacts, an analytical investigation of the load-displacement characteristics of deep-groove ball bearings was undertaken. Also, radial deep-groove ball bearings with internal radial clearance exhibit an inherent instability, or relative motion (radial and circumferential) between inner and outer races, for a constant load applied in a given direction as the inner ring rotates. The same statement may be made about pre-loaded (radial interference) ball bearings and zero clearance bearings except that the relative motion is considerably suppressed. It is important to note that these statements apply even though the bearing components are of perfect geometry, perfectly mounted, clean and adequately lubricated. Relative periodic motion of the inner and outer rings result in periodic forces (due to the inertia of the rotor) at frequencies equal to outer or inner ball-pass frequency depending upon whether the load is fixed or rotating with the shaft. Hence, there would appear to be a finite minimum level of vibration always generated in a ball bearing. What follows hereafter is an analytical study to determine the magnitude and nature of this unstable motion so as to evaluate its contribution to the vibration picture and to determine what particular bearing design parameters are involved in producing it, and what must be done to minimize or suppress it.



THE FRANKLIN INSTITUTE • *Laboratories for Research and Development*

I-A2321-1

Since electric motors use the medium series bearings from 05 to 18 bore code and since these bearings have 7 or 8 balls (8 for code 308 to 318), we concentrated our efforts in this study on a bearing with eight balls. The work was carried out in a non-dimensional manner (the only restriction being that the bearing have 8 balls) so as to be able to apply the results to any size or series of bearings.

Since the load applied to the inner race is supported by many balls acting as springs (non-linear), one cannot readily determine the deflection of the center of the shaft under the influence of a given load because the problem is indeterminate. The problem is further compounded if the balls move with respect to the load line. However, what one can do is purposely displace the shaft a given amount in a given direction, compute the individual deformations at ball-race contacts, compute the individual reactions at these contacts and, finally, take the vector addition of all the reactions to determine the magnitude and direction of the resultant load, which, if applied to the bearing, would yield the originally imposed displacement angle and magnitude. If this procedure is repeated for many combinations of displacement angle and magnitude, sufficient data on resultant load magnitude and direction can be obtained to determine the location of the displaced shaft for any given load (magnitude and angle) with respect to ball position. Since quite a bit of computational effort is involved to determine the resultant load for a given location of the shaft with respect to the balls, and since the procedure must be repeated many, many times to

THE FRANKLIN INSTITUTE • *Laboratories for Research and Development*

I-A2321-1

provide sufficient data, it was decided to derive the necessary equations and program the same for solution on the UNIVAC computer available to us at The Franklin Institute. This was done for bearings with radial clearance, radial interference and zero clearance. This provided a wealth of information from which we were able to determine the locus (path of motion) of the center of the shaft as the inner ring rotates under the influence of any given magnitude and angle of load as a function of time. Likewise, we were able to determine the shaft center locus due to a rotating unbalance load. Another important result of this study of ball bearing load-displacement characteristics was the compilation of non-dimensional bearing spring rates.

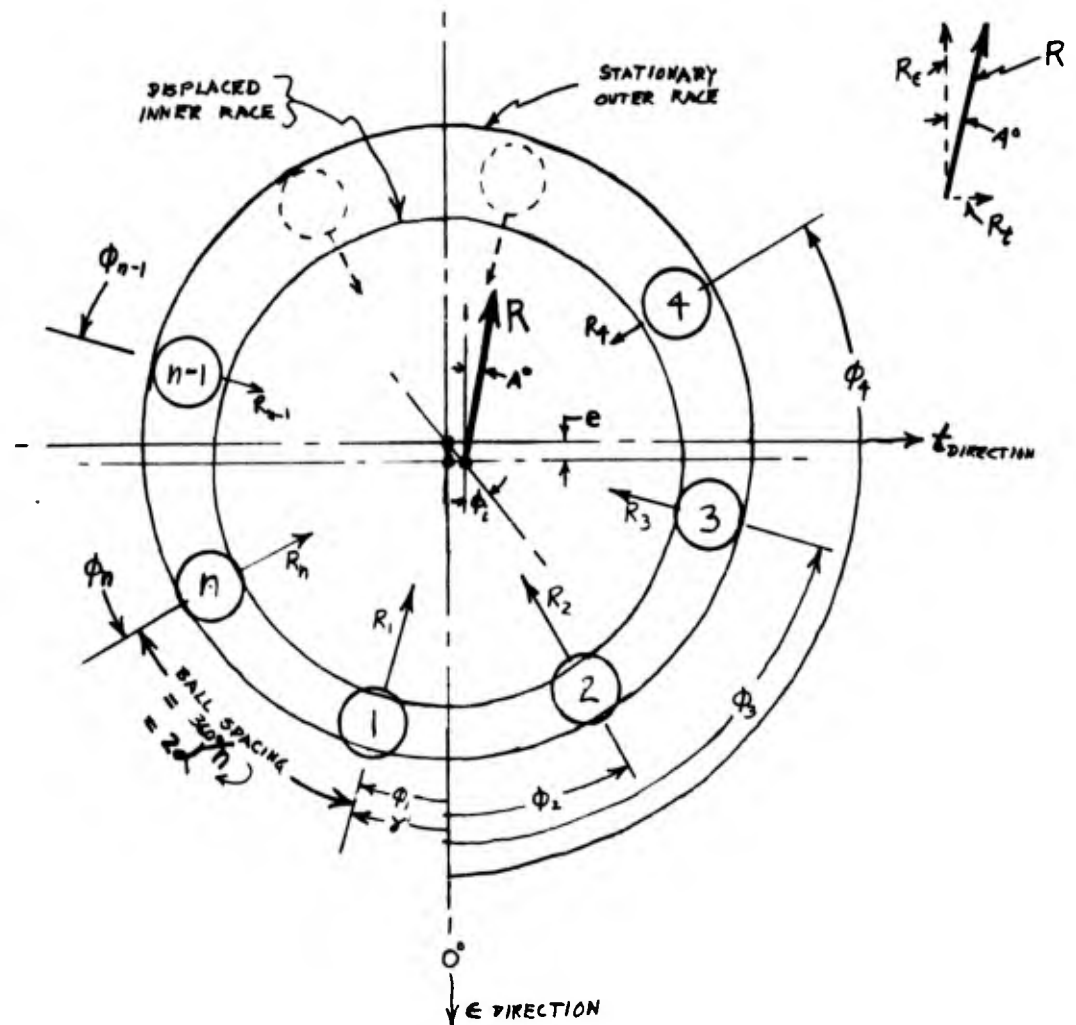
The important equations and results of this investigation follow hereafter. In addition, the derivation, solution of equations and most of the computer data obtained are included in Appendices C and D. The complete derivation is included herein to offer a guide for similar studies of ball bearing load-displacement characteristics.

### 3.2.1.1.1. Governing Equations

Consider a ball bearing with  $n$  equally spaced balls as shown schematically in Figure 13. The radial load required to move the inner race to the radially displaced position  $(e, \phi_1)$  will have some magnitude  $R$  and some attitude angle  $\lambda$  with respect to the  $\varepsilon$ -axis when one of the balls is at a position angle  $\gamma$  from the  $\varepsilon$ -axis. For a given bearing with its inner ring center displaced from the outer ring center an amount  $e$  at an angle  $\phi_1$ , containing  $n$  balls equally spaced at  $2\alpha$  degrees, and one of the balls is at an angle  $\gamma$  from the direction of displacement of the inner ring, it is possible to determine the normal approach of the inner race to the outer race at each ball location. From Appendix C.1 and C.2, the normal approach of the races at the  $n^{\text{th}}$  ball may be written as;

$$\delta_{Nn} = \cos(\phi_1 - \phi_n) - c + 1 \quad (33)$$

where  $\delta_{Nn}$  = normal approach of the races at the  $n^{\text{th}}$  ball, (in.)  
 $e$  = displacement of inner race center from outer race center, (in.)  
 $\phi_1$  = angle of displaced inner race with respect to  $\varepsilon$ -axis, (deg.)  
 $\phi_n$  = angle of center  $n^{\text{th}}$  ball with respect to  $\varepsilon$ -axis, (deg.)



# GEOMETRY OF LOADED BALL BEARING

Figure 13

I-A2321-I

$c$  = radial clearance (if any) = 1/2 of radial play, (in.)

$i$  = radial interference (if any) = 1/2 of total interference, (in.)

All of the balls yielding positive results in equation (33) contribute to the support of the applied load. The normal load contributed by each ball due to the normal approach of the races at the particular ball location then becomes (See Appendix C.3),

$$R_n = k_N \left[ e \cos(\phi_i - \phi_n) - c + i \right]^{3/2} \quad (34)$$

where  $R_n$  = normal ball load, (lbs)

$k_N$  = constant of proportionality between load and normal approach,  
(lbs/in<sup>3/2</sup>)

The total load (magnitude and direction) supported by the bearing is the vector summation of each normal ball load.

$$\vec{R} = \vec{R}_c + \vec{R}_t = k_N \left\{ \begin{aligned} \sum_{n=1}^{n=n} & \left[ e \cos(\phi_i - \phi_n) - c + i \right]^{3/2} \cos \phi_n + \\ \sum_{n=1}^{n=n} & \left[ e \cos(\phi_i - \phi_n) - c + i \right]^{3/2} \sin \phi_n \end{aligned} \right\} \quad (35)$$

The total load magnitude is

$$R = \left[ R_c^2 + R_t^2 \right]^{1/2} \quad (36)$$

The total load angle with respect to the  $\epsilon$ -axis is,

$$A^\circ = \tan^{-1} \left( \frac{R_t}{R_c} \right) \quad (37)$$

If now, as in an operating bearing, the balls assume different angular locations and if the center of the inner ring remains at the same position, the resulting load magnitude and direction will assume slightly different values. The reverse is also true: if the load magnitude and direction remain constant while the balls change position, then the center of the inner ring will assume different positions. Since, the bearing presents an indeterminent problem, that is, we cannot, for a given load, directly solve for  $e$  and  $\phi_i$ , we must work the problem backwards. We must, using equation (35), assign values to  $c$  or  $i$ ,  $e$ , and  $\phi_i$  for various values of  $\gamma$  (hence  $\phi_n$ ) and solve for  $R$  and  $A^\circ$  for each operating condition. This process must be repeated a sufficient number of times to obtain sufficient data from which to obtain  $e$  and  $\phi_i$  for any combination of  $R$  and  $A^\circ$  as a function of  $\gamma$  and  $\alpha$  in a bearing with clearance  $[c = 1/2(D_o - D_i - 2d)]$ , a bearing with interference  $[i = -1/2(D_o - D_i - 2d)]$  and a bearing with zero clearance  $[c = i = 0]$ .

For the clearance bearing letting  $c = \frac{e}{c}$  and  $\phi_i = 0^\circ$ ,

Equation (35) becomes

$$\vec{R} = \vec{R}_c + \vec{R}_t = k_N^{3/2} \left\{ \sum_{n=1}^{n=n} \left[ \frac{c \cos \phi_n - 1}{\sin \phi_n} \right]^{3/2} \cos \phi_n + \sum_{n=1}^{n=n} \left[ \frac{c \cos \phi_n - 1}{\sin \phi_n} \right]^{3/2} \sin \phi_n \right\}$$

I-A2321-I

$$\frac{\vec{R}}{k_N c^{3/2}} = \sum_{n=1}^{n=n} \left[ \epsilon \cos \phi_n - 1 \right]^{3/2} \cos \phi_n + \sum_{n=1}^{n=n} \left[ \epsilon \cos \phi_n - 1 \right]^{3/2} \sin \phi_n \quad (38)$$

We shall call  $\frac{R}{k_N c^{3/2}}$  the "clearance bearing parameter".

For the zero clearance bearing, ( $\epsilon = c = 0$ )

$$\begin{aligned} \text{"Zero clearance bearing parameter"} &= -\frac{R}{k_N e^{3/2}} \\ \frac{\vec{R}}{k_N e^{3/2}} &= \sum_{n=1}^{n=n} \left[ \cos \phi_n \right]^{3/2} \cos \phi_n + \sum_{n=1}^{n=n} \left[ \cos \phi_n \right]^{3/2} \sin \phi_n \end{aligned} \quad (39)$$

For a bearing with interference,

$$\begin{aligned} \text{Interference Bearing Parameter} &= \frac{R}{k_N i^{3/2}} \\ \frac{R}{k_N i^{3/2}} &= \sum_{n=1}^{n=n} \left[ \epsilon \cos \phi_n + 1 \right]^{3/2} \cos \phi_n + \sum_{n=1}^{n=n} \left[ \epsilon \cos \phi_n + 1 \right]^{3/2} \sin \phi_n \end{aligned} \quad (40)$$

All important equations for the three types of rolling contact bearings considered are summarized in Table C - 1.

### 3.2.1.1.2. Zero Clearance Bearing

This is the easiest case to consider. Equations (37) and (39) were solved for  $n = 6, 8$  and  $12$  balls as a function of ball position angle  $\gamma$ . The details of the computations are given in Appendix C.4. and the results are plotted in figures 14, 15 and 16. Figure 14 shows the

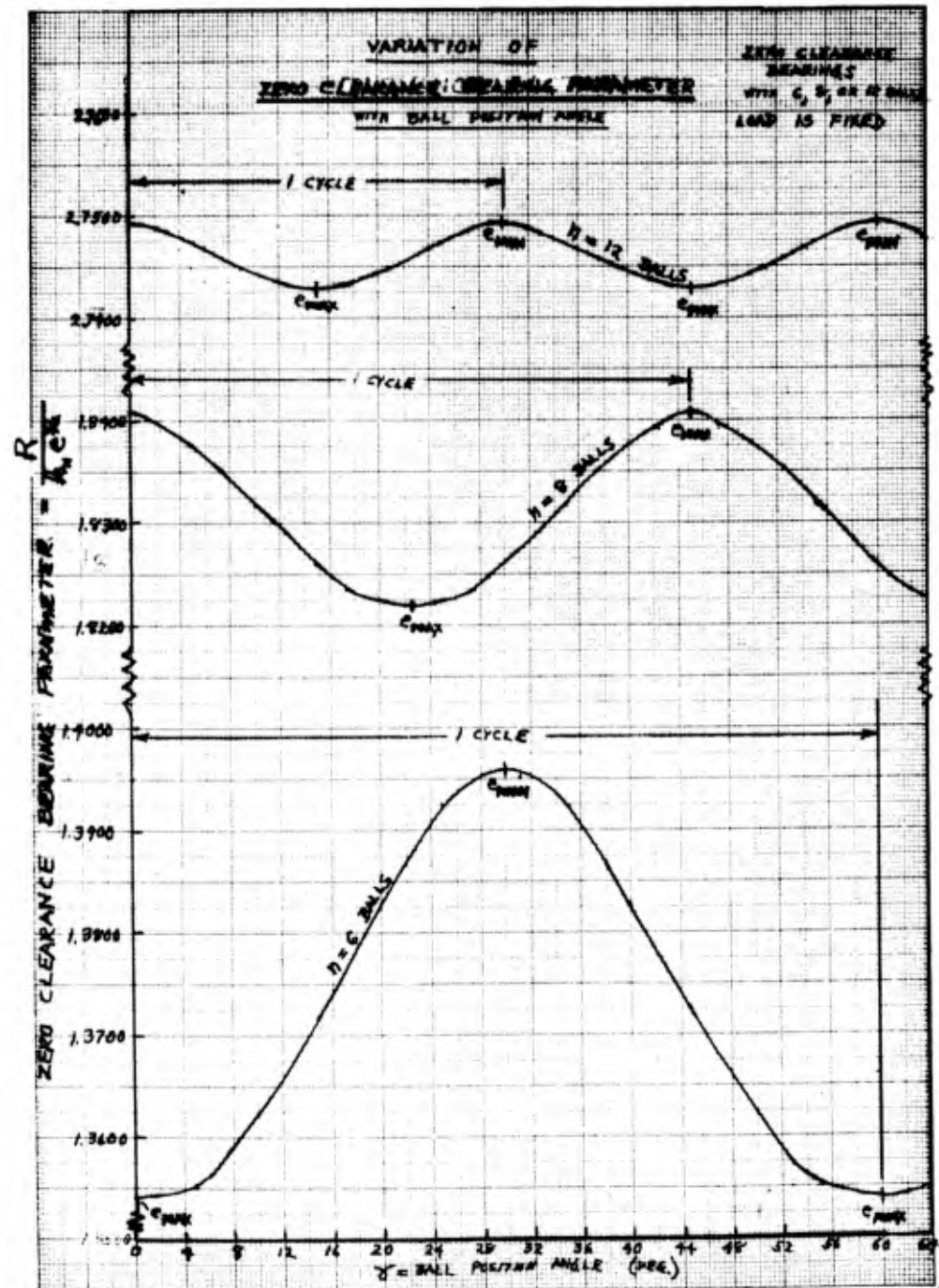


Figure 14



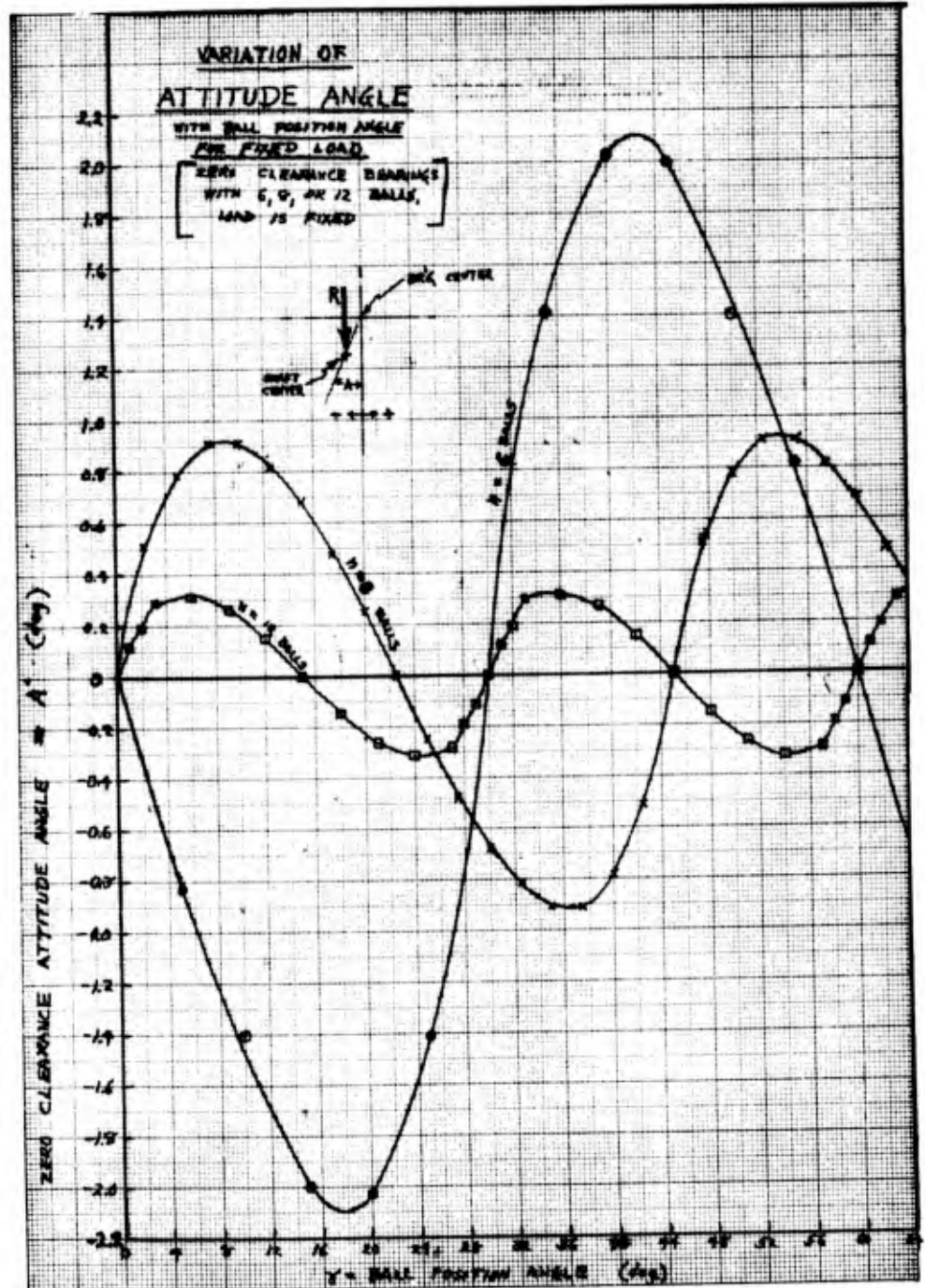


Figure 15

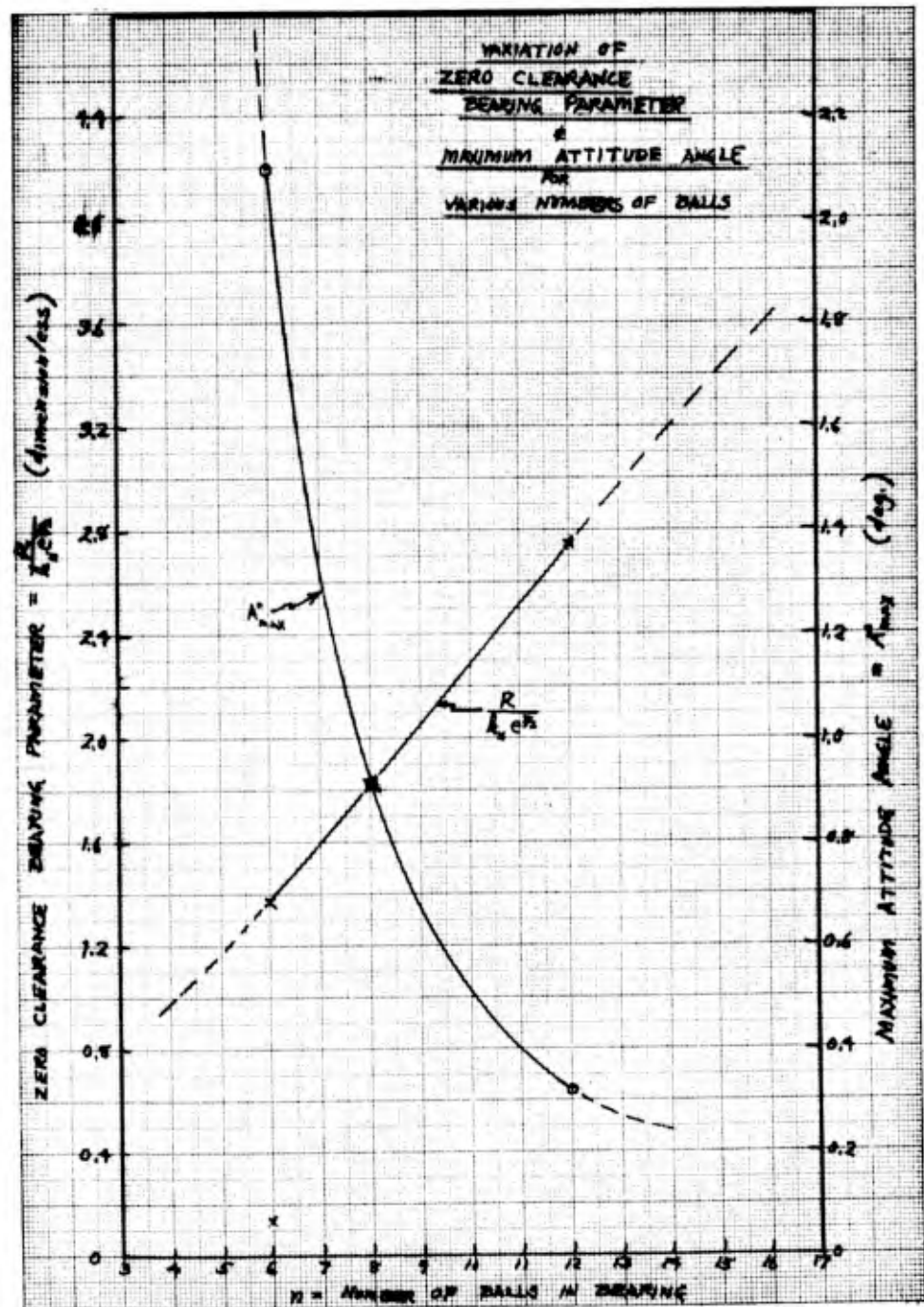


Figure 16

I-A2321-1

variation of  $R/k_N e^{3/2}$  with ball position angle indicating that if  $R$  is a constant then  $e$  varies. That is, for a fixed load, the center of the inner ring moves inward and outward as the balls move. The amplitude of this motion decreases but the frequency increases with increased number of balls. Figure 15 shows the variation of attitude angle,  $A^\circ$ , for the zero clearance bearing indicating a periodic motion from side to side which decreases in magnitude but increases in frequency for increasing number of balls. From these results Figure 16 was prepared. It shows the variation of  $R/k_N e^{3/2}$  and  $A_{\max}^\circ$  (the maximum attitude angle) with the number of balls. The advantages to be derived from an increased number of balls are immediately apparent.

Under the influence of a constant radial load ( $R = \text{constant}$ ), these results indicate that the center of the rotor moves with a periodic motion (as defined by  $e$  and  $A^\circ$  for any ball position) with a frequency equal to the outer ball-pass frequency. The geometry is defined below in Figure 17.

The locus of the shaft center can be plotted on x-y coordinates by letting  $x = e \sin A^\circ$  and  $y = e \cos A^\circ$ .  $e$  may be expressed as

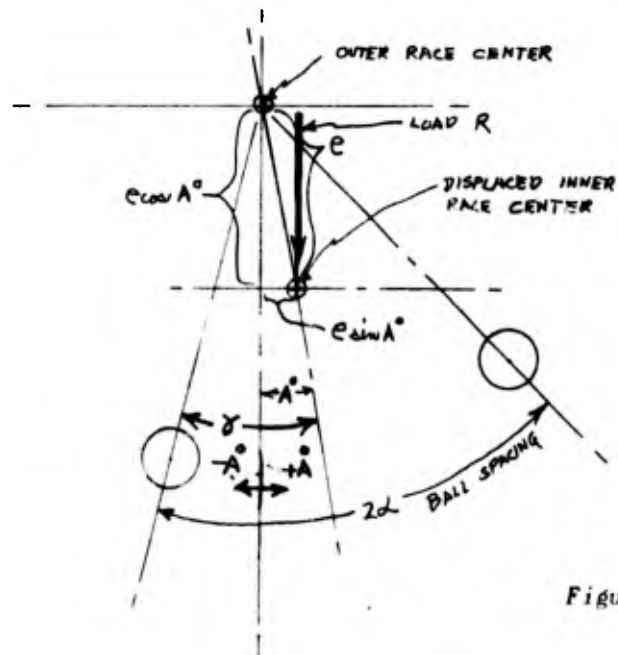


Figure 17

GEOMETRY OF DISPLACED INNER RACE

$$e = \left[ \frac{R}{k_N} \left( \frac{k_N e^{3/2}}{R} \right) \right]^{2/3} = \left( \frac{R}{k_N} \right)^{2/3} \left( \frac{k_N e^{3/2}}{R} \right)^{2/3}$$

Values of  $\left( \frac{k_N e^{3/2}}{R} \right)$  for particular ball position angle  $\gamma$  are obtained by taking the reciprocal of the data plotted in Figure 14.

$$\therefore x = \left( \frac{R}{k_N} \right)^{2/3} \left( \frac{1}{\frac{k_N e^{3/2}}{R}} \right)^{2/3} \sin A^\circ$$

Similiarly,

$$y = \left( \frac{R}{k_N} \right)^{2/3} \left( \frac{1}{\frac{R}{k_N e^{3/2}}} \right)^{2/3} \cos A^\circ$$

$$\text{Let } X = \frac{x}{\left( \frac{R}{k_N} \right)^{2/3}} \text{ and } Y = \frac{y}{\left( \frac{R}{k_N} \right)^{2/3}}$$

∴ The non-dimensional coordinates of the shaft locus are;

$$X = \left( \frac{1}{R/k_N e^{3/2}} \right)^{2/3} \sin A^\circ \leftarrow \begin{array}{l} \text{Displacement in direction} \\ \text{normal to load direction} \end{array} \quad (41)$$

$$Y = \left( \frac{1}{R/k_N e^{3/2}} \right)^{2/3} \cos A^\circ \leftarrow \begin{array}{l} \text{Displacement in direction} \\ \text{of load.} \end{array} \quad (42)$$

Equations (41) and (42) were solved (Appendix C.4) using the data plotted in Figures 14 and 15 yielding the results shown in Figure 18 for a bearing with 8 balls. The numerical results are also tabled in Table No. C-2. This periodic motion is called "ball-pass stability." Figure 18 shows the shaft center locus under the influence of a fixed direction load of constant magnitude for a zero clearance bearing containing 8 balls. The maximum x and y excursions of the locus are the amplitudes of resulting vibration and are of interest.

$$\Delta x_{\max} = \Delta X_{\max} \left( \frac{R}{k_N} \right)^{2/3} = 0.0218 \left( \frac{R}{k_N} \right)^{2/3} \text{ (in.)}$$

$$\Delta y_{\max} = \Delta Y_{\max} \left( \frac{R}{k_N} \right)^{2/3} = 0.0045 \left( \frac{R}{k_N} \right)^{2/3} \text{ (in.)}$$

I-A2321-1

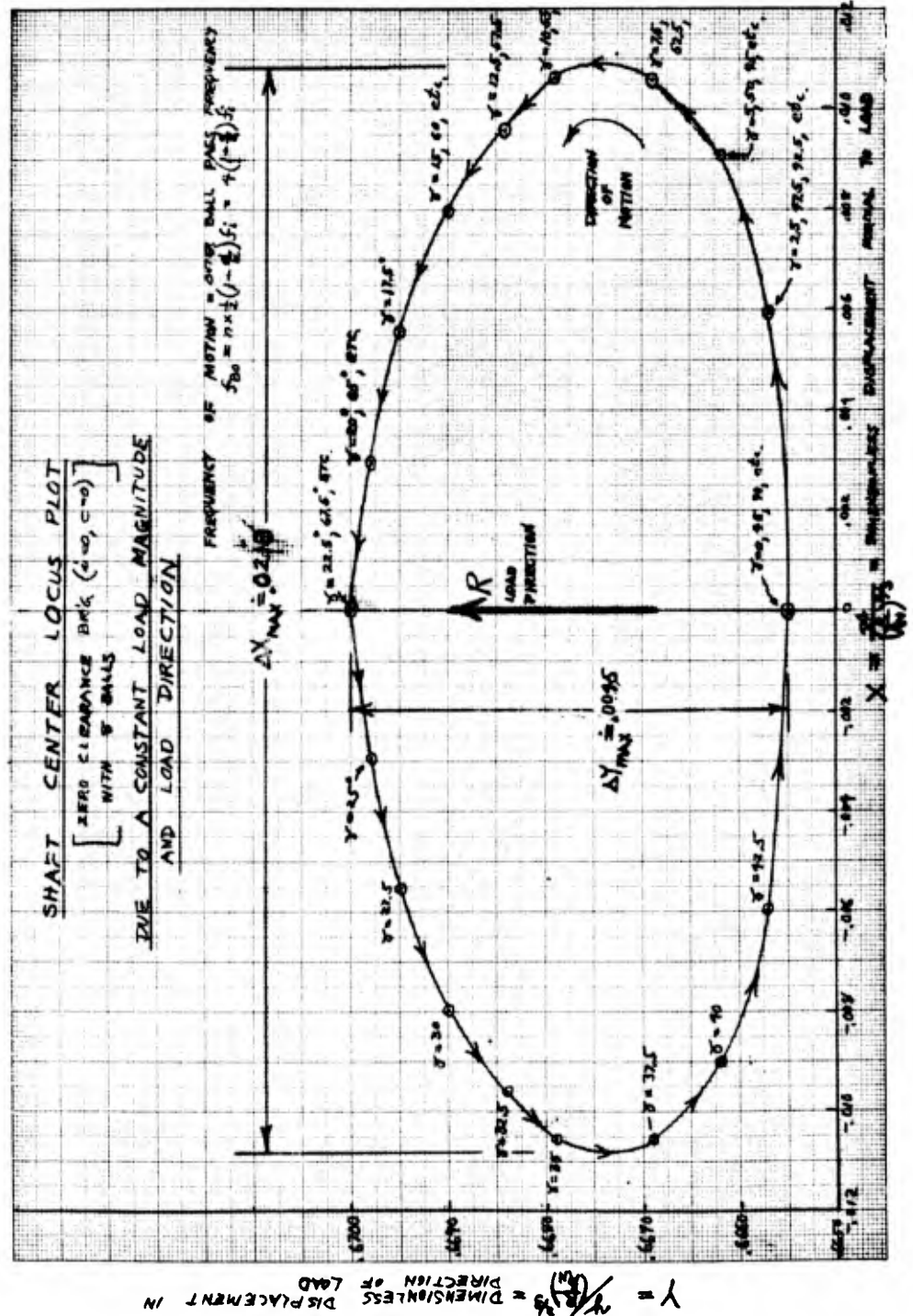


Figure 18

Equations for determining  $\Delta x_{\max}$  and  $\Delta y_{\max}$  would be

$$\Delta x_{\max} = 2 e \text{ (at } A^{\circ}_{\max}) \sin(A^{\circ}_{\max})$$

$$e \text{ (at } A^{\circ}_{\max}) \approx \frac{e_{\max} + e_{\min}}{2}$$

$$\therefore \Delta x_{\max} = (e_{\max} + e_{\min}) \sin(A^{\circ}_{\max})$$

$$\Delta x_{\max} = \left(\frac{R}{k_N}\right)^{2/3} \left\{ \left[ \frac{1}{(R/k_N e^{3/2})_{\min}} \right]^{2/3} + \left[ \frac{1}{(R/k_N e^{3/2})_{\max}} \right]^{2/3} \right\} \sin(A^{\circ}_{\max}) \text{ (in.)} \quad (43)$$

$$\Delta y_{\max} = e_{\max} - e_{\min}$$

$$\Delta y_{\max} = \left(\frac{R}{k_N}\right)^{2/3} \left\{ \left[ \frac{1}{(R/k_N e^{3/2})_{\min}} \right]^{2/3} - \left[ \frac{1}{(R/k_N e^{3/2})_{\max}} \right]^{2/3} \right\} \text{ (in.)} \quad (44)$$

The bracketed { } quantities in Equations (43) and (44) are called compliance amplitude factors. These factors are plotted in Figure 19 for various numbers of balls. To obtain the amplitude of displacement in inches, multiply the appropriate compliance amplitude factor by the quantity  $\left(\frac{R}{k_N}\right)^{2/3}$  where  $R$  = magnitude of fixed load and  $k_N$  is the constant relating normal ball load and normal approach of the raceways (See Eq. (C-11)). Values of  $k_N$  and  $k_N^{2/3}$  are tabled in appendix C.5, Table C-3.

From Figure 19 it would appear that zero clearance bearings with more balls yield less ball-pass instability vibration amplitude. However, the factor  $\left(\frac{R}{k_N}\right)^{2/3}$  must be considered. Also, the frequency must be considered since the forces generated by the vibration are proportional to the product of  $\Delta x_{\max}$  (or  $\Delta y_{\max}$ ) and the frequency squared. More will be said about this in a later section.

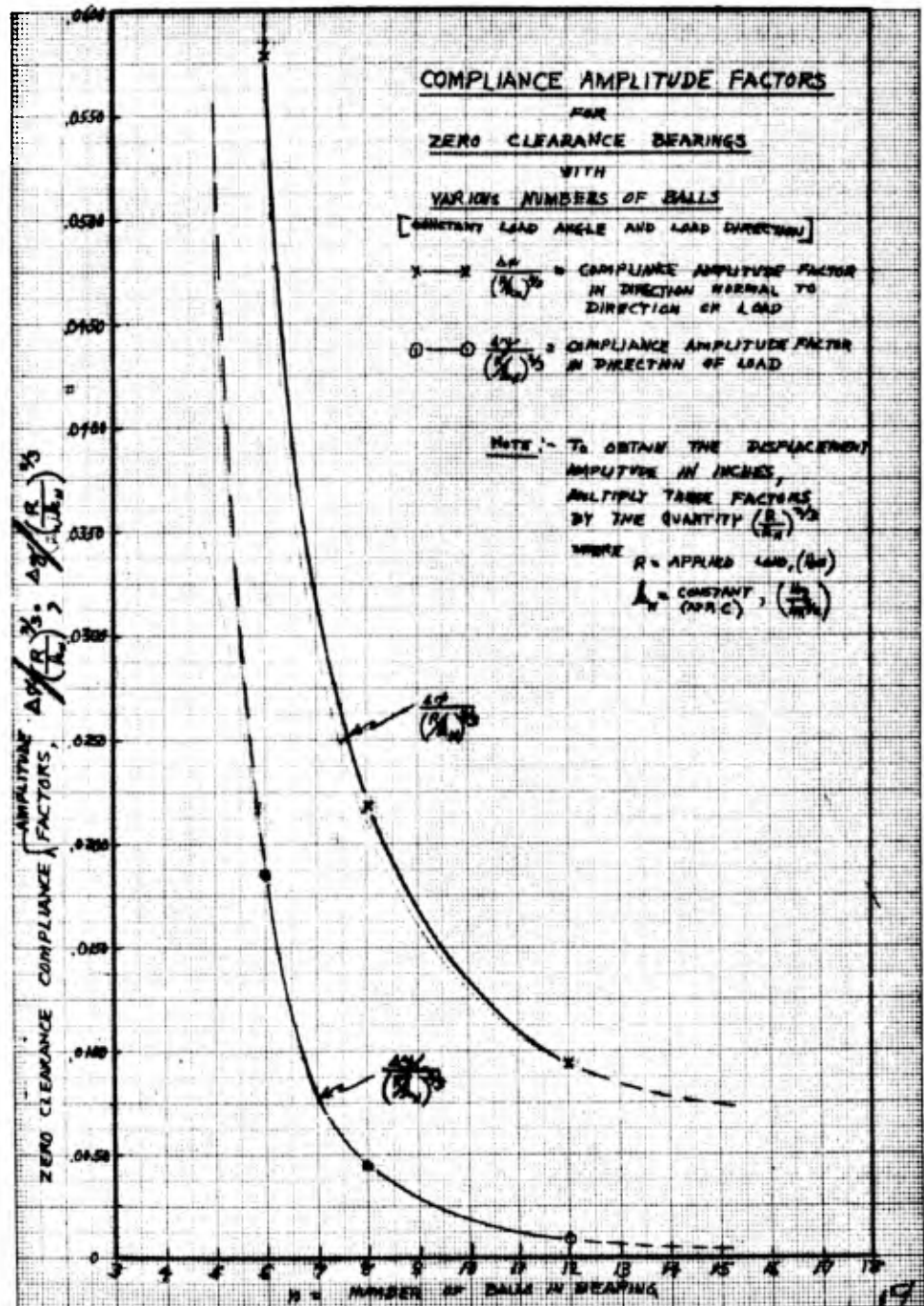


Figure 19



For a rotating load (such as due to unbalance) the instantaneous location of the shaft center exhibits a more complex periodic motion. The determination of the locus is demonstrated in Appendix C.6. The locus of a 310 zero clearance bearing with a rotating unbalance load, ( $R_u$ ), was evaluated and the results are plotted in Figure 20 in the form of a polar plot and tabled in Table C-4.  $\theta_i$  is the direction from the center of the bearing to the center of the displaced inner ring. This periodic motion is also called ball-pass instability.

The "0" of the amplitude  $\left[ e / \left( \frac{R}{k_N} \right)^{2/3} \right]$  has been suppressed to magnify the variation of amplitude. The instantaneous direction ( $\theta_L$ ) of the unbalance load is also shown on the locus curve. Notice that  $\theta_L = \theta_i$  when  $e = e_{\max}$  or  $e_{\min}$ , but  $\theta_L \neq \theta_i$  anywhere else. The starting point is ( $\theta_i = 0^\circ$ ) and  $R_u = R_{uo}$ . The locus plot was carried thru  $363.49^\circ$  rotation of  $R_u$  to  $R_{uf}$  which resulted in 5 cycles of  $\left[ e / \left( \frac{R}{k_N} \right)^{2/3} \right]$ . The frequency of this amplitude variation is  $5 \times \frac{360^\circ}{363.49^\circ} \times f_i = 4.952 f_i$ . It is seen that 4.952 is the inner ball-pass frequency factor. Hence, the frequency of the amplitude variation is equal to the inner ball-pass frequency.

I-A2321-1

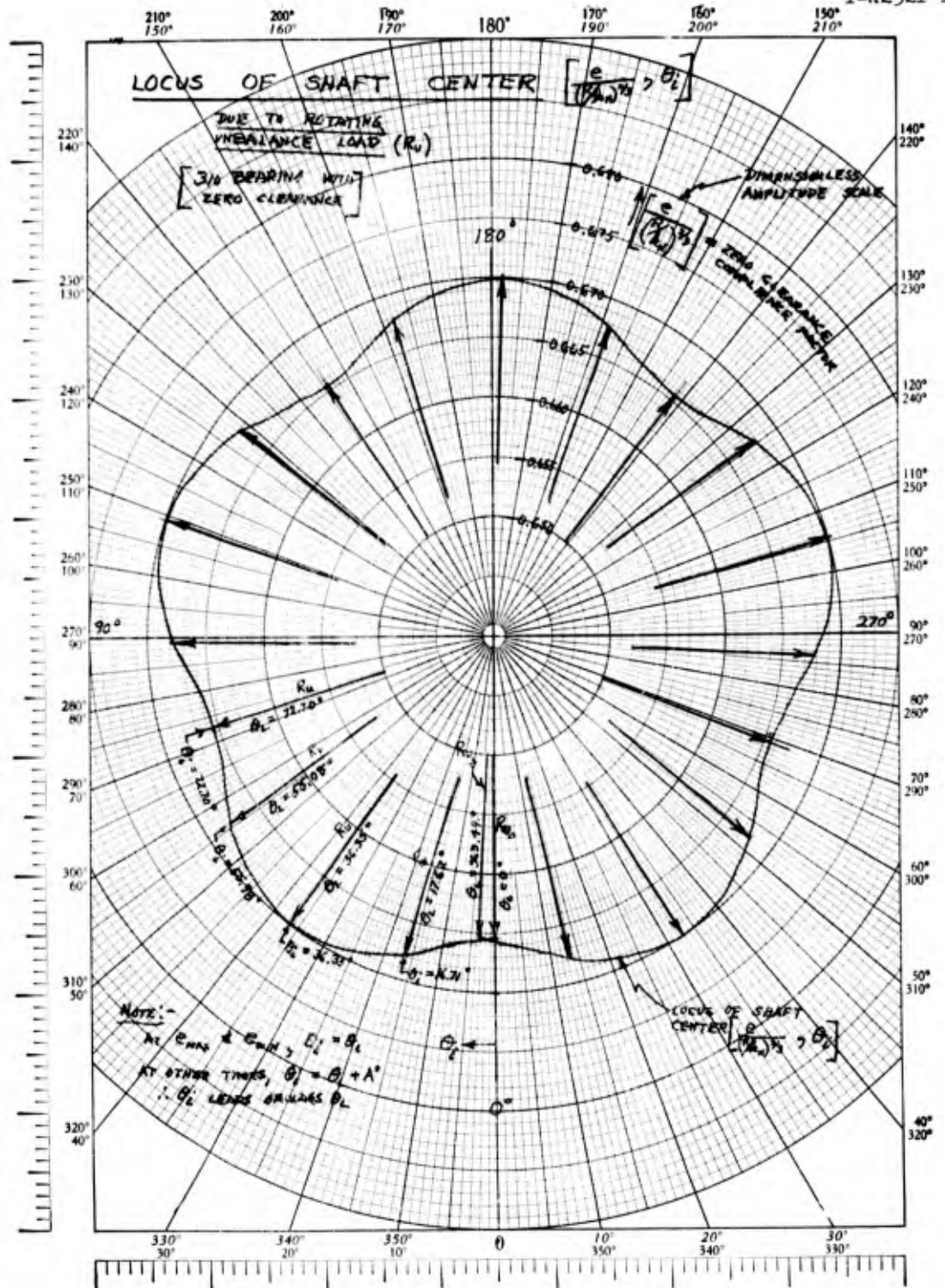


Figure 20

### 3.2.1.1.3 Bearings With Internal Clearance

The geometry of an unloaded 8-ball bearing with internal clearance is shown in Figure 21(a). Figure 21(b) shows the shaft displaced vertically down until it rests (with zero deformation) on ball 1 only ( $\gamma = 0$ ). Figure 21(c) shows the shaft position when  $\gamma = \alpha = 22.5^\circ$  and the shaft resting on balls 1 and 2. For intermediate values of  $\gamma$ , the magnitude of the displacement is

$$e = \frac{c}{\cos \alpha} = \text{constant}, \quad \therefore \epsilon = \frac{1}{\cos \alpha} \quad (45)$$

and the shaft position angle is

$$\theta_i = \alpha - \gamma \quad (\text{For } R \approx 0 \text{ and } \theta_L = 0) \quad (46)$$

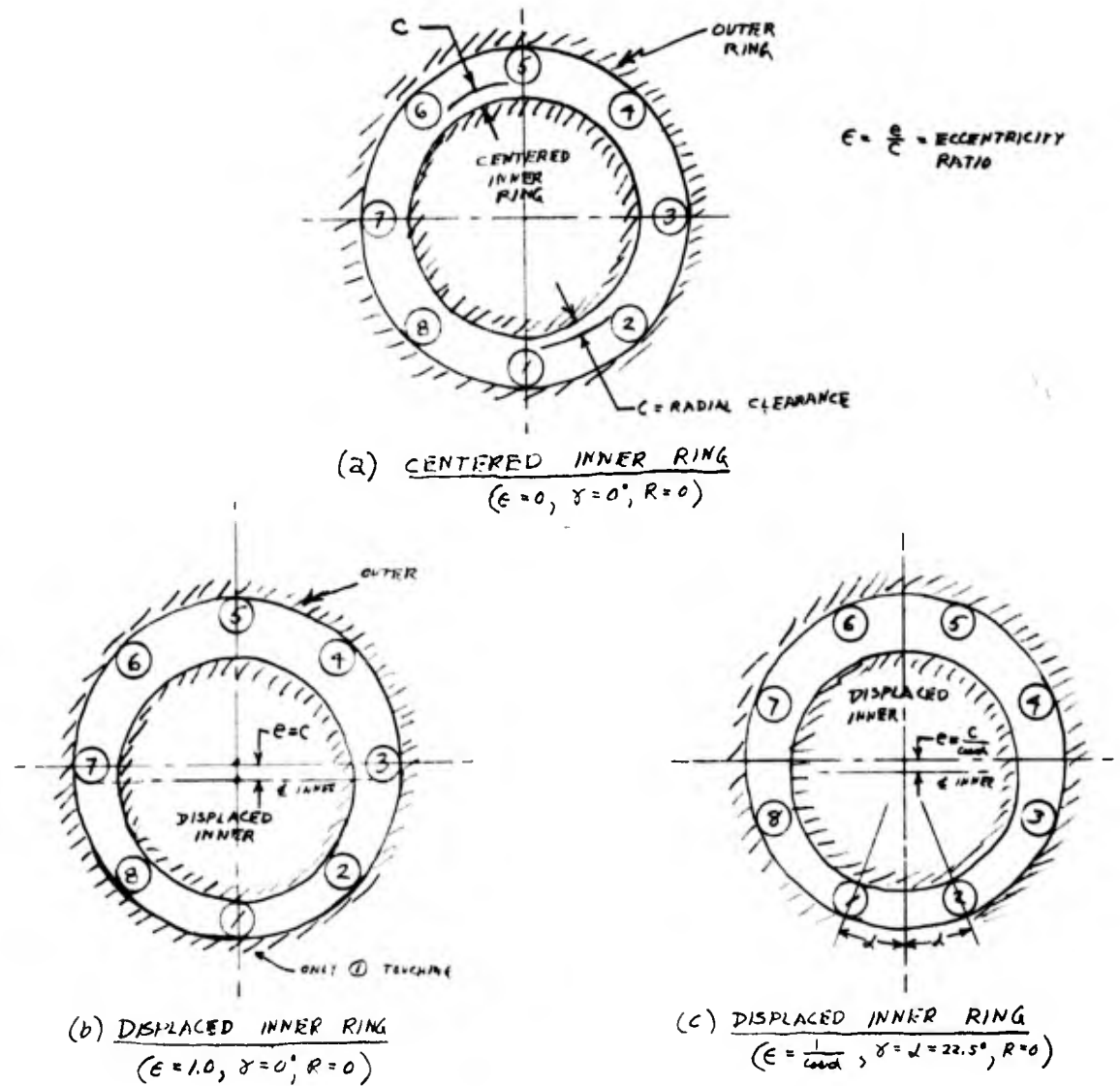
Figure 22 shows the locus plot of the center of the displaced shaft due to  $R \approx 0$  and in a fixed direction ( $\theta_L = 0$ ) for an 8-ball bearing.

$$\text{For this case, } \alpha = \frac{1}{2} \left( \frac{360^\circ}{8} \right) = 22.5^\circ$$

$$\epsilon = \frac{1}{\cos 22.5^\circ} = 1.08239$$

$$\text{and } \theta_i = 22.5^\circ - \gamma$$

The dotted portion of the locus curve occurs (instantaneously) when the shaft moves over from contacting one pair of balls to the next pair. The cycle keeps repeating as the balls move. The frequency of occurrence is equal to the outer ball-pass frequency.



GEOMETRY OF A BEARING WITH INTERNAL CLEARANCE  
(NOT LOADED)

Figure 21

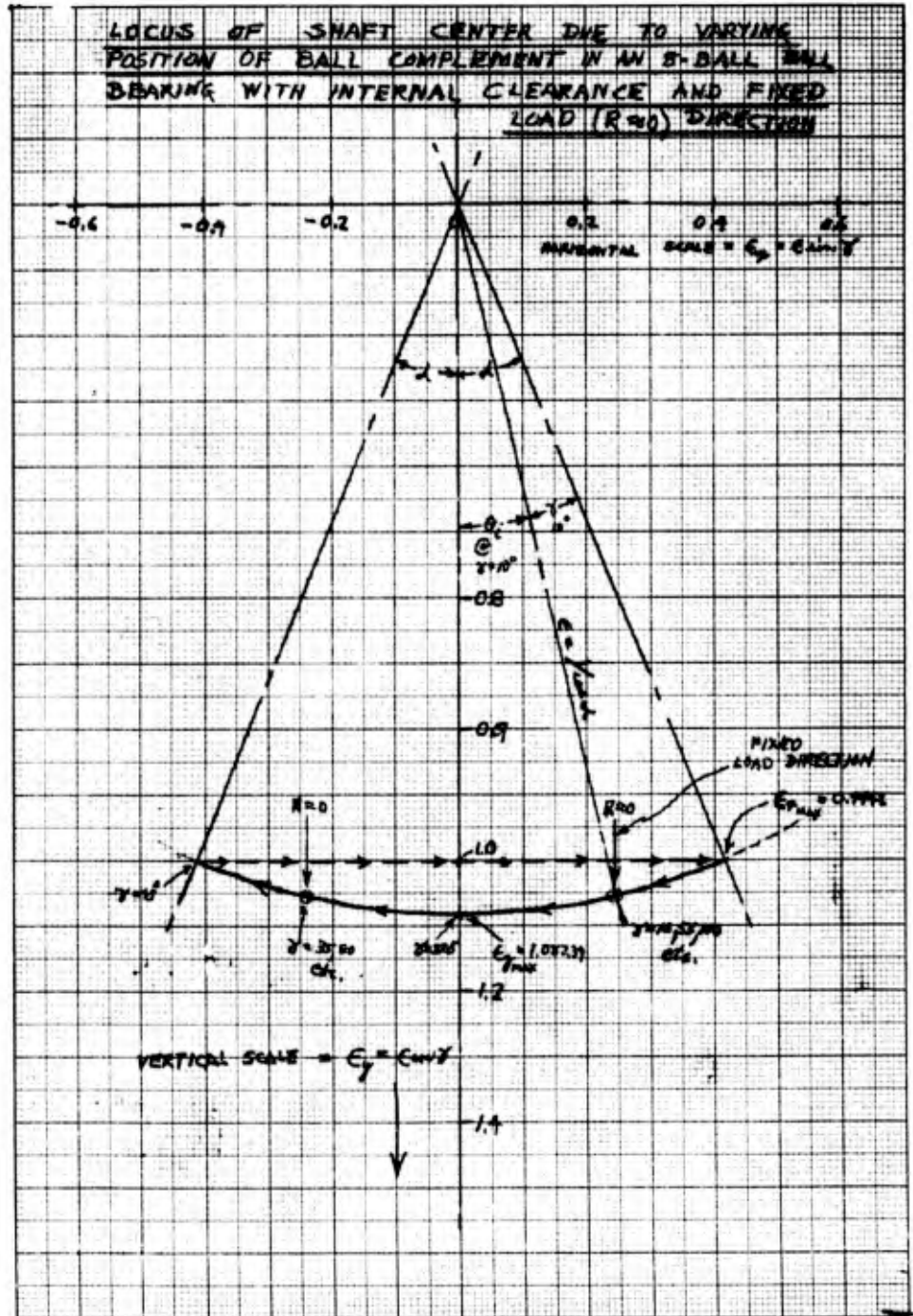


Figure 22

For the case of a very light rotating load ( $R_u \approx 0$ ) the shaft position angle may be expressed as,

$$\theta_i = j \alpha + \gamma$$

where  $j$  is an integer which changes each time the shaft rolls over a ball due to the rotating load.

Let the starting point be

$$\left. \begin{array}{l} \gamma = 0 \\ \theta_L = 0 \end{array} \right\} \theta_i = 0; \epsilon = 1.0 \text{ (ball 1 touching)}$$

As the load tends to rotate, the shaft immediately moves to (rolls over) touch two balls at

$$\theta_i = j \alpha + \gamma = (j = 1) 22.5^\circ + 0 = 22.5^\circ$$

and

$$\epsilon = \frac{1}{\cos \alpha} = 1.08239$$

For a load rotating with the shaft (unbalance load),

$$\theta_L = \frac{f_i}{f_E} \times \gamma \quad (48)$$

Also, the shaft will roll over a ball when the load angle is,

$$\theta_{Lj} = (j - 1)(2\alpha) + \gamma_j \quad (49)$$

$$\text{or } \theta_{Lj} = (j - 1)(2\alpha) + \frac{f_E}{f_i} \theta_{Lj} \quad (50)$$

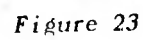
$$\therefore \theta_{Lj} = \frac{(j - 1)(2\alpha)}{0.3810} \text{ (For 310 bearing)} \quad (51)$$

This locates the angle to the locus at which  $\epsilon = 1.0$ . The extremes of the roll-over are located at  $\theta_{Lj} \pm \alpha$  with  $\epsilon = 1.08239$ . Such a locus

THE FRANKLIN INSTITUTE • *Laboratories for Research and Development*

I-A2321-1

(polar) plot is shown in Figure 23. The dotted portion represents the instantaneous roll-over condition. The frequency of the cyclic displacement is equal to the inner ball-pass frequency.





THE FRANKLIN INSTITUTE • *Laboratories for Research and Development*

I-A2321-1

For a loaded clearance bearing we must solve equations (37) and (38) to determine  $R$  and  $A^\circ$  for various combinations of  $\epsilon$  and  $\gamma$ . The equations to be solved for a bearing with 8 balls are detailed in Appendix C.7. These were programmed for our UNIVAC computer and solutions were obtained for all combinations of  $\epsilon$  and  $\gamma$  indicated below.

$1.10 \leq \epsilon \leq 2.00$  in increments of  $\Delta\epsilon = 0.05$  (19 values)

$2.25 \leq \epsilon \leq 3.75$  in increments of  $\Delta\epsilon = 0.25$  (7 values)

$4.00 \leq \epsilon \leq 20.0$  in increments of  $\Delta\epsilon = 2.0$  (5 values)

and

$0 \leq \gamma \leq 22.5^\circ$  in increments of  $\Delta\gamma = 0.5^\circ$  (46 values)

This computer work yielded data on the "clearance bearing parameter",  $\frac{R}{k_N c^{3/2}}$ , and the attitude angle,  $A^\circ$ , at  $(19 + 5 + 7) \times 46 = 1426$  points. Many of these data are shown in Appendix D, Table D-1. These data provide a wealth of information useful in determining the instantaneous position of the shaft with respect to the magnitude and direction of a pure radial load for any 8-ball, ball bearing containing any given amount of internal clearance.

The variation of bearing parameter,  $\frac{R}{k_N c^{3/2}}$ , over the eccentricity range from 1.0 to 20.0 is shown in Figure 24. Due to the compressed plotting scale used in this plot the variation of  $R/k_N c^{3/2}$  with  $\gamma$  at constant eccentricity ratio is not apparent. Figures 25 and 26 with expanded scales show this more clearly. Figure 27 shows the variation of attitude angle,  $A^\circ$ , with  $\gamma$  and  $\epsilon$ .

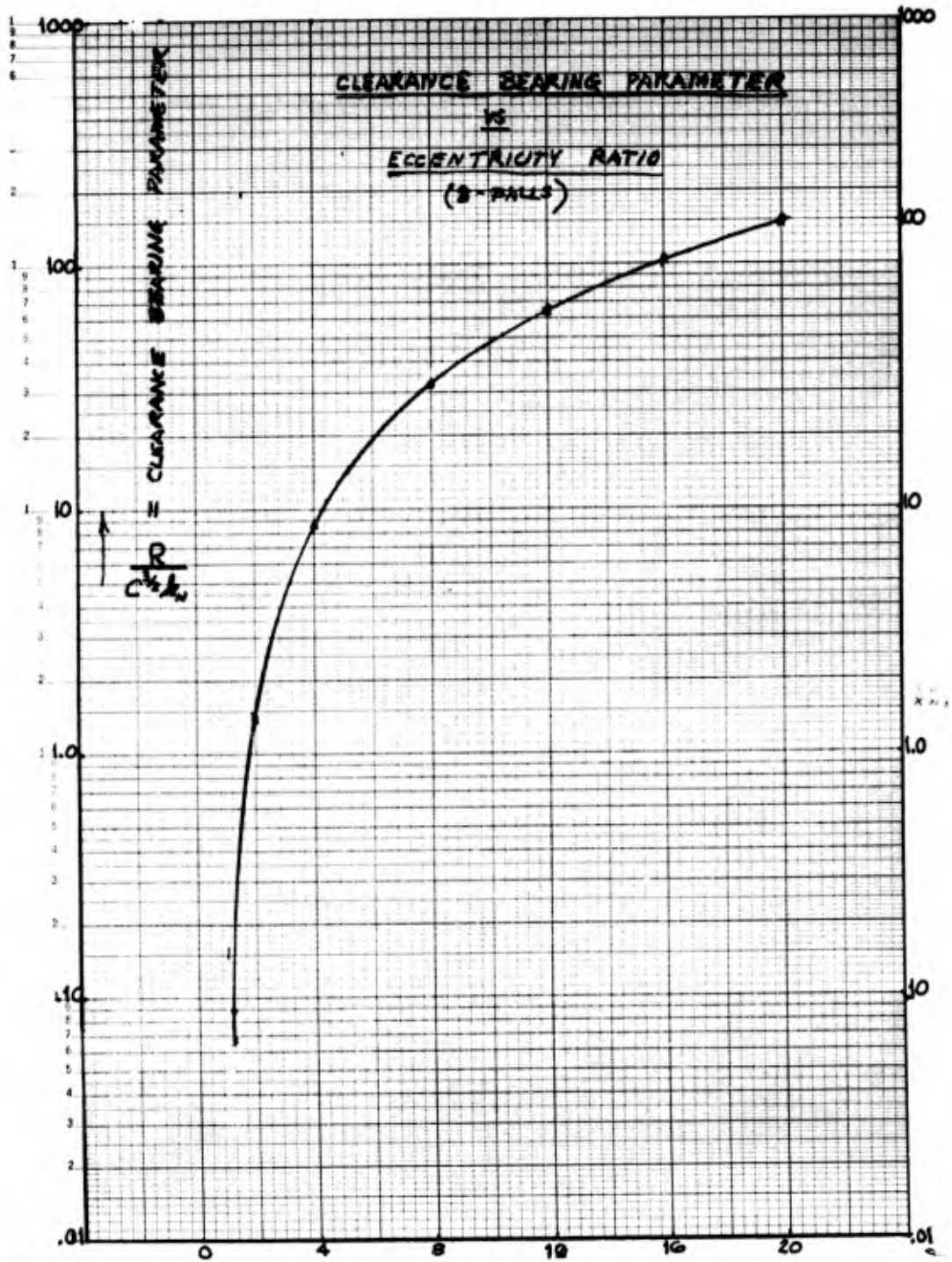


Figure 24

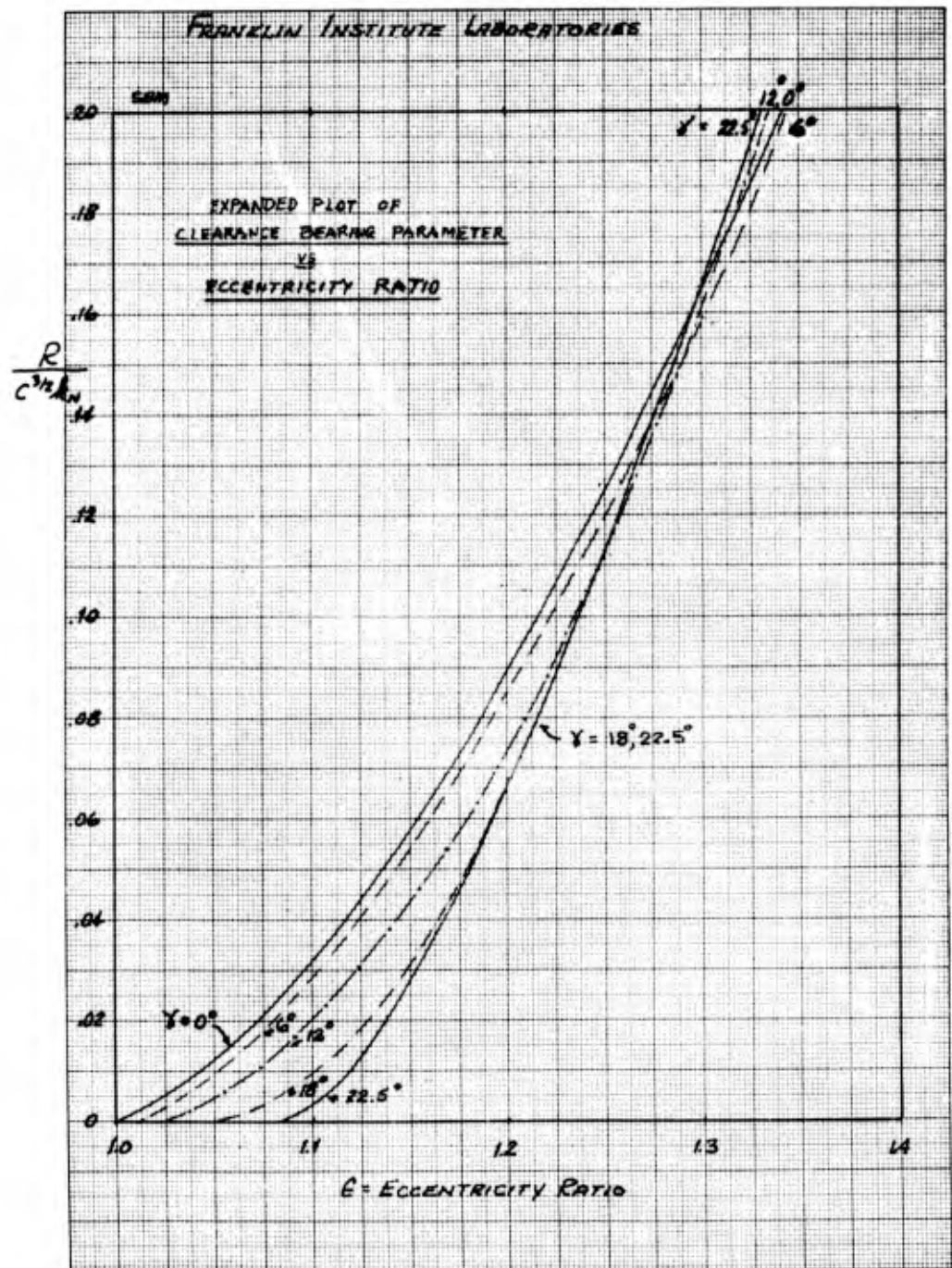


Figure 25

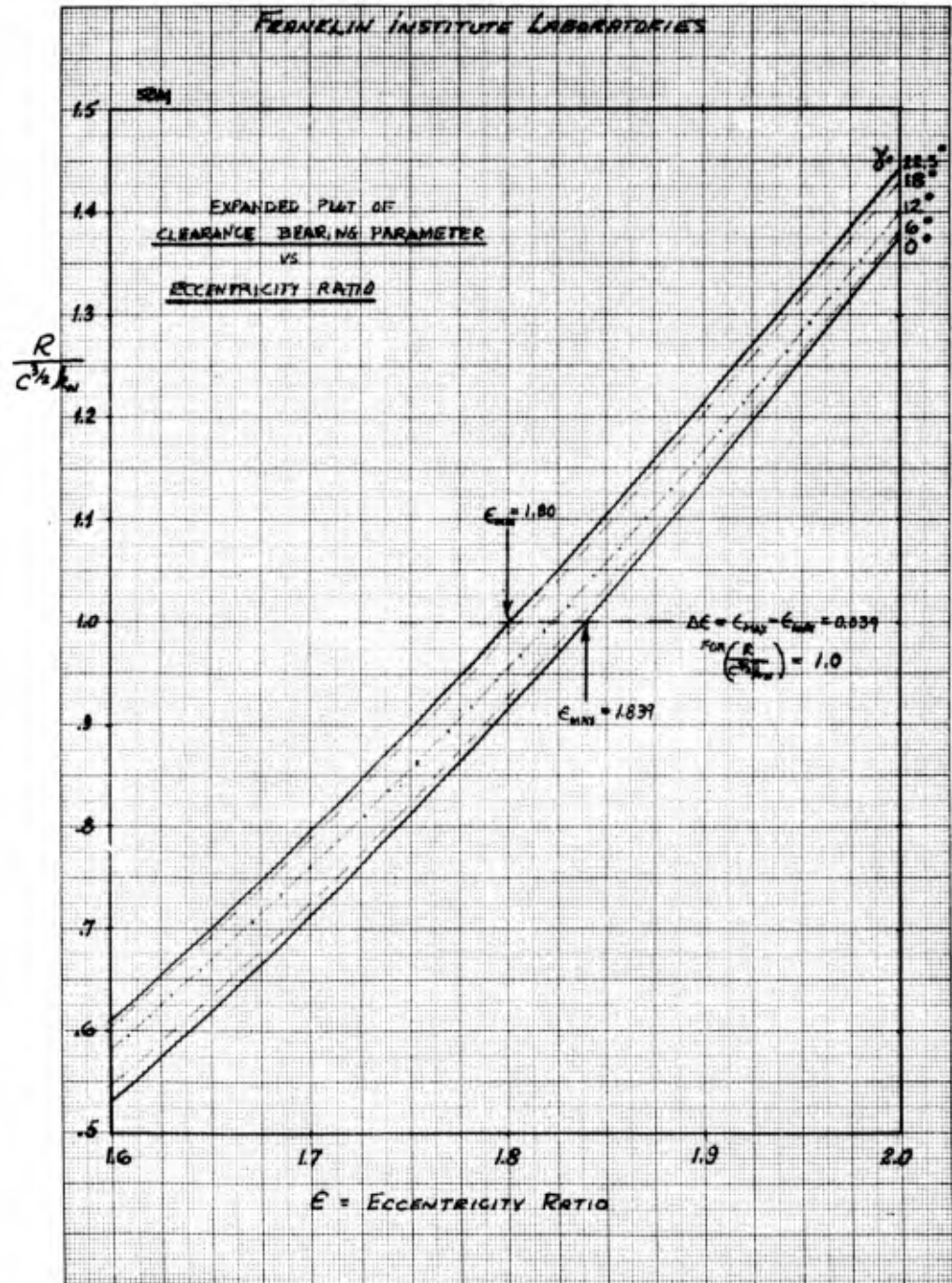


Figure 26

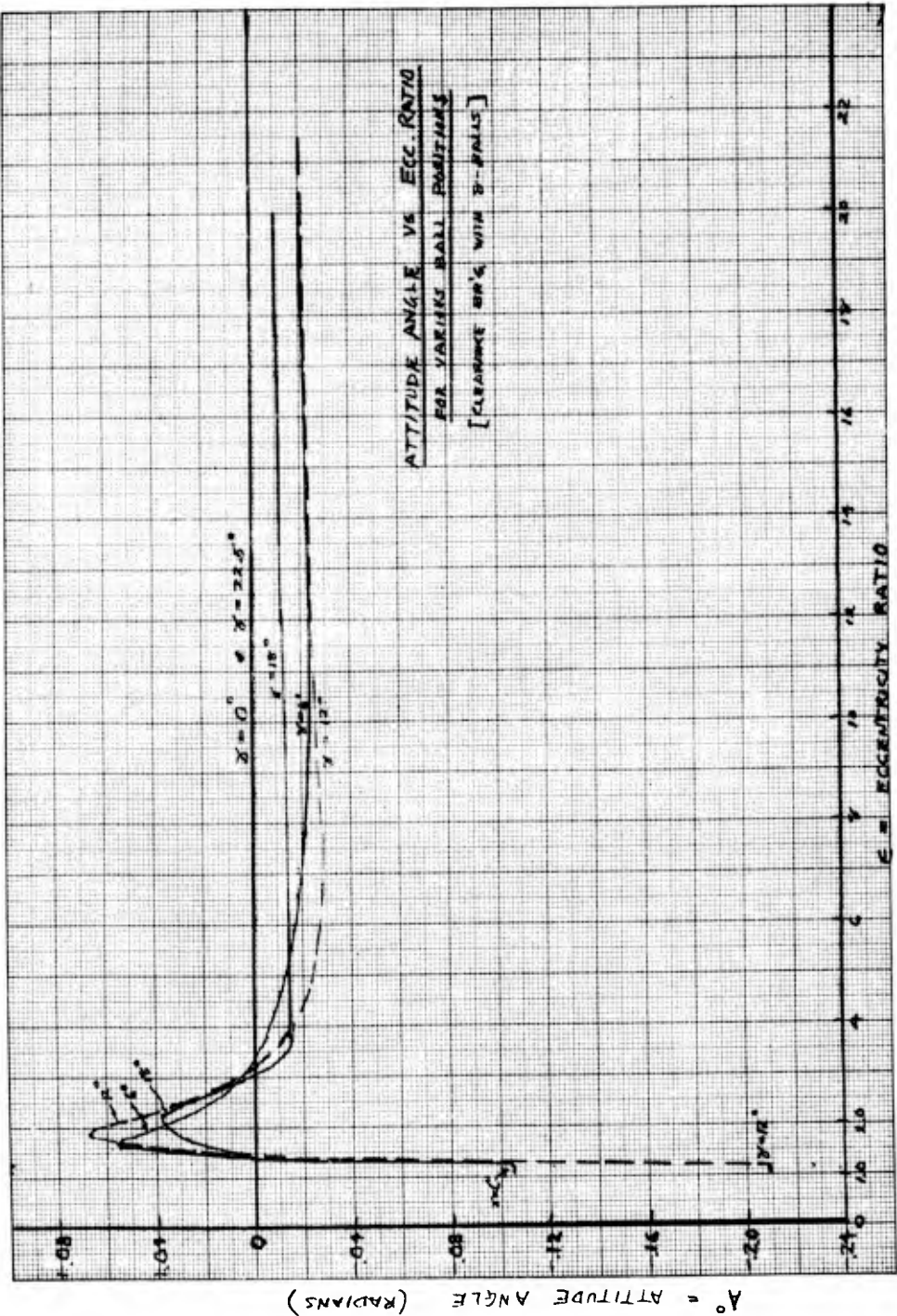


Figure 27

Under the influence of a constant radial load in a fixed direction, the center of the rotor will move with a periodic motion (as defined by  $\epsilon$  and  $A^\circ$  for any ball position) with a frequency equal to the outer ball-pass frequency and is called ball-pass instability.

In general, the locus will be an ellipse with its major and minor axis varying in magnitude with the load. To obtain the amplitude of such motion in the direction of the load, we make use of Figure 26. As an example, if  $(\frac{R}{c^{3/2} k_N}) = \text{constant} = 1.0$  we find that  $\Delta\epsilon = 0.039$ . For other values of  $(\frac{R}{c^{3/2} k_N})$ ,  $\Delta\epsilon$  will be some other value. This procedure was done for the range of  $(\frac{R}{c^{3/2} k_N})$  from 0.01 to 1000. For convenience we call this  $\Delta\epsilon = \frac{\Delta y_{\max}}{c} \cdot k_N$  radial compliance amplitude factor. (52)

where  $\Delta y_{\max}$  = maximum radial amplitude of vibration (in.)  
Figure 28 shows the results in a dimensionless fashion. This plot shows the relative radial amplitude of vibration against the clearance bearing parameter (essentially, load). There are two minimum values of  $\Delta y_{\max}$ . Notice that the amplitude never goes to zero. On this same plot the "dashed" straight line shows the equivalent amplitude for a bearing with zero clearance. At high values of load  $R$  (or for very small clearances), the value of  $\Delta y_{\max}$  approaches that of the zero clearance bearing.



I-A2321-1

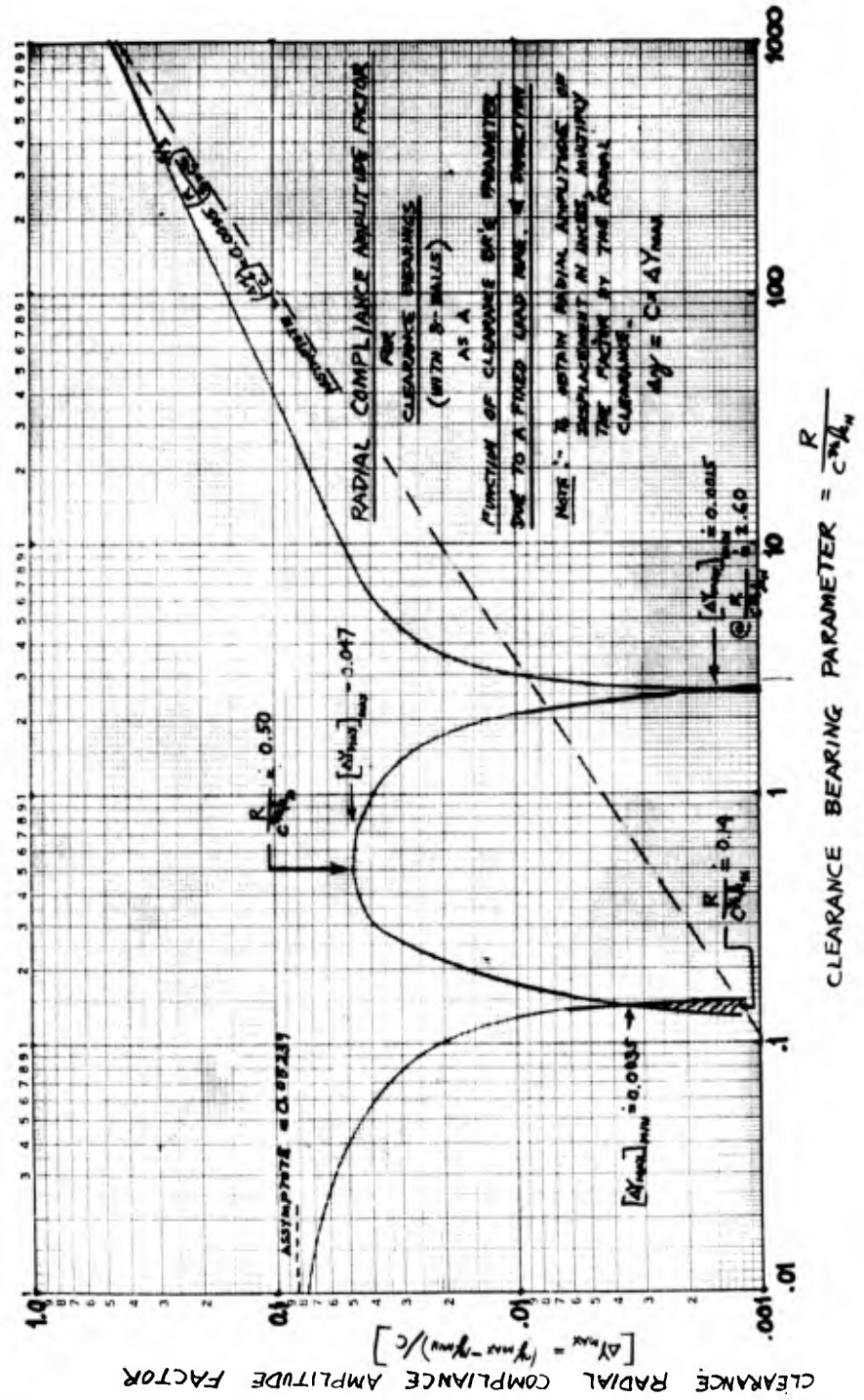


Figure 28

THE FRANKLIN INSTITUTE • *Laboratories for Research and Development*

I-A2321-1

To obtain the amplitude of vibration in the direction normal to the direction of the load we make use of the expression.

$$\Delta X_{\max} = \frac{\Delta x_{\max}}{c} = 2\epsilon \sin A^{\circ}_{\max} = \text{normal compliance amplitude factor} \quad (53)$$

From the computer data, we determine  $A^{\circ}_{\max}$  and its associated value of

$\epsilon$  a  $A^{\circ}_{\max}$ . These results are tabled in Appendix D, Table D-2 and

plotted in Figure 29. This plot shows the amplitude of vibration in the direction normal to the load direction as a function of the clearance bearing parameter. Once again, there are two regions of minimum amplitude of motion but the amplitude never goes to zero. The "dashed" straight line represents the equivalent amplitude for a bearing with zero clearance.

It is important to note from figures 28 and 29 that the minimum amplitudes of  $\Delta X_{\max}$  or  $\Delta Y_{\max}$  do not occur at the same value of  $\frac{R}{c^{3/2} k_N}$ . Thus, in a given bearing it is not possible to minimize both amplitudes. However,

since  $\Delta Y_{\max}$  is usually greater than  $\Delta X_{\max}$ , one should concentrate on reducing  $\Delta Y_{\max}$  if the overall amplitude is to be reduced. Another

interesting fact pointed out by these plots is that  $\Delta X_{\max}$  or  $\Delta Y_{\max}$  for a bearing with clearance can be made to be smaller than for a bearing with zero clearance operating under the same load by adjusting the

clearance to yield  $\frac{R}{c^{3/2} k_N}$  equal to 2.60 or 5.0. In general, for a bearing with clearance operating under a constant, pure radial load, a bearing parameter of  $\frac{R}{c^{3/2} k_N} = 5.0$  will yield a minimum amount (in inches) of amplitude of vibration.

Figure 30 shows the number of loaded balls contributing to carrying the applied load. The "dashed" curves on this plot show the

variation of  $\epsilon$  with  $\gamma$  (ball rotation) for a fixed value of  $\frac{R}{c^{3/2} k_N}$



I-A2321-1

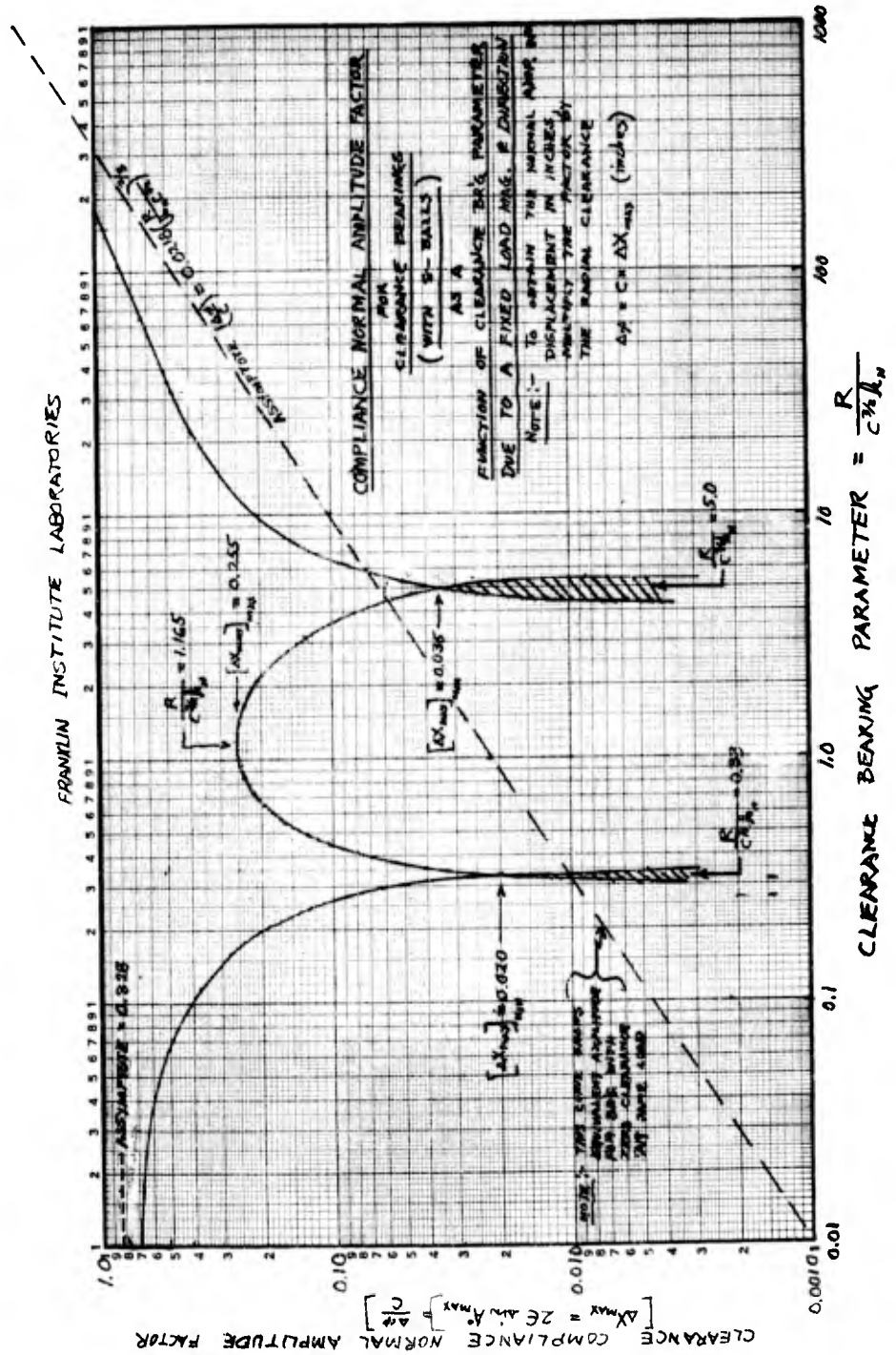
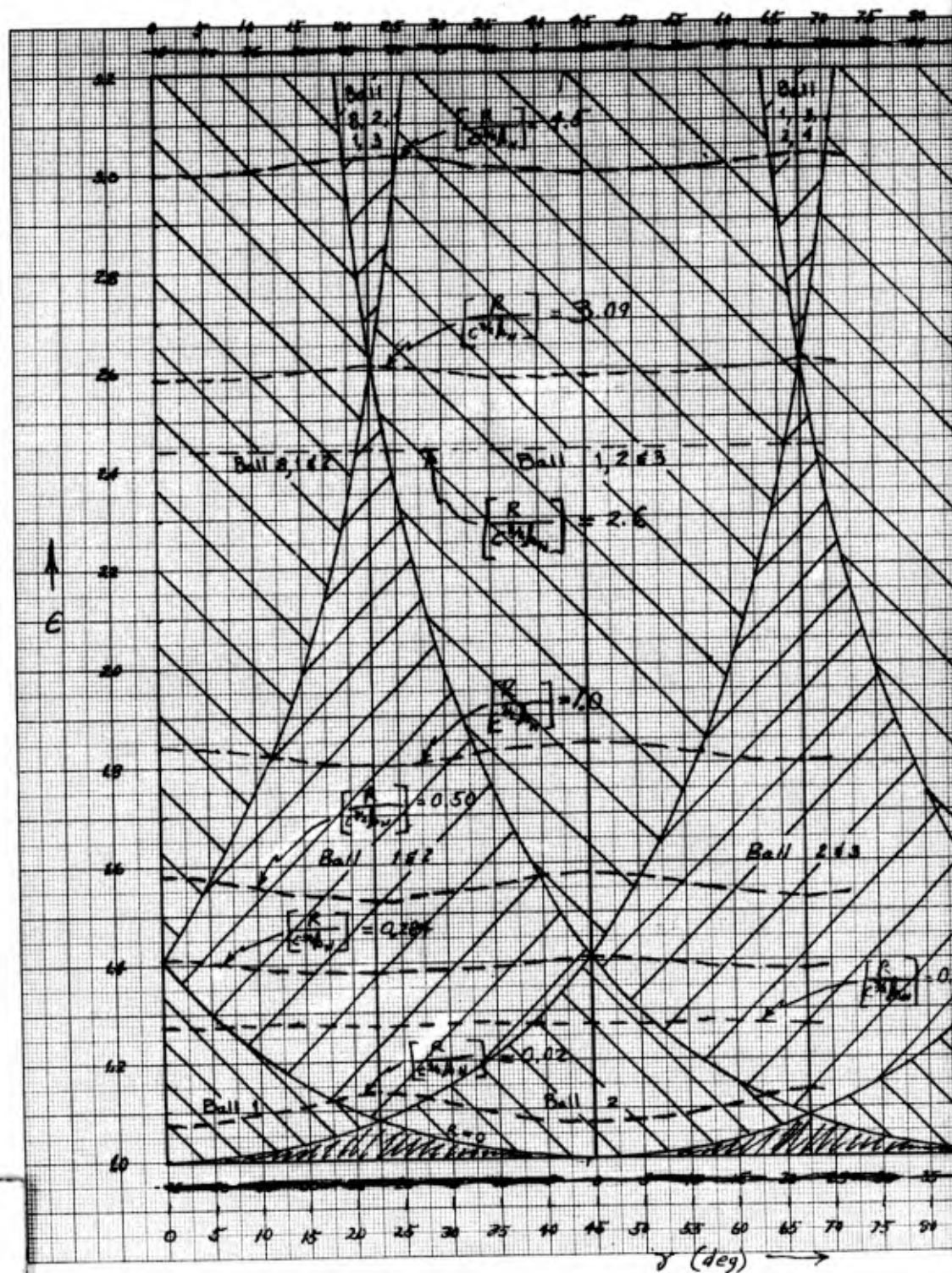


Figure 29

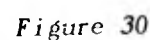
I-A2321-1

(constant load). Consider such a locus of  $\left[ \frac{R}{c^{3/2} k_N} \right] = 1.0$ . At  $\gamma = 0^\circ$ , three balls are carrying the load; namely balls 8, 1, and 2. At  $\gamma \approx 11.5^\circ$ , there is a transition from 3 balls carrying load to two balls carrying load; that is, ball 8 becomes unloaded, leaving 1 and 2 to carry the load. This continues until ball 3 becomes loaded at  $\gamma = 33.5^\circ$  and the load is then supported by balls 1, 2, and 3 until  $\gamma = 56.5^\circ$  when 1 becomes unloaded. This process continues and repeats as subsequent balls become loaded and unloaded due to ball train rotation. Several other values of  $\left[ \frac{R}{c^{3/2} k_N} \right]$  are also plotted. For  $\left[ \frac{R}{c^{3/2} k_N} \right] = 3.09$ , the load is always carried by two balls. In order for the load to be carried always by four balls,  $\left[ \frac{R}{c^{3/2} k_N} \right]$  must equal infinity which is either infinite load or zero clearance. In Figure 30, the values of  $\left[ \frac{R}{c^{3/2} k_N} \right]$  for  $[\Delta Y_{\max}]_{\min}$  (See Figure 28) are also plotted as is  $\left[ \frac{h}{c^{3/2} k_N} \right] = 0.5$  for  $[\Delta Y_{\max}]_{\max}$  (see Figure 29).

Figure 31 is a polar plot in  $c$  and  $A^\circ$  showing the loci of center of the inner ring for various values of the clearance bearing parameter  $R/c^{3/2} k_N$ . These plots were made through the use of computer data (Appendix D) and figures similar to Figures 25, 26 and 27. Figure 31 shows the growth and decay of the locus of shaft motion for various values of  $R/c^{3/2} k_N$  up to an eccentricity ratio of 2.0. If extended such a plot would again show small amplitudes of vibration at  $c = 3.0$  or  $R/c^{3/2} k_N \approx 50$ .



1





#### 3.2.1.1.4 Bearings With Radial Preload (Interference)

Using Equations (37), (C-27), (C-28) and (C-29), values of  $R/k_N i^{3/2}$  and  $A^\circ$  were obtained for various ball positions of an 8-ball bearing at various eccentricity ratios ( $\epsilon = \frac{e}{I}$ ). These equations were solved for the combinations of  $\epsilon$  and  $\gamma$  indicated below.

$$0 < \epsilon \leq 3.0 \text{ in increments of } \Delta\epsilon = 0.10 \text{ (31 values)}$$

and

$$0 < \gamma \leq 22.5^\circ \text{ in increments of } \Delta\gamma = 1.5^\circ \text{ (16 values)}$$

The computer work yielded data on the "interference bearing parameter",  $\frac{R}{k_N i^{3/2}}$ , and the attitude angle,  $[A^\circ]$ , at (31)(16) = 496 points. This data (tabled in Appendix E, Table No. E-1) provides information useful in determining the instantaneous position of the shaft with respect to the magnitude and direction of a pure radial load for any 8-ball, ball bearing containing any given amount of internal interference.

Figure 32 shows the geometry of a bearing with radial interference (or preload). The effect of increasing load is shown in Figure No. 32(a) thru (d). When the bearing is not loaded by an external force, the eccentricity ratio is zero ( $\epsilon = 0$ ), all of the ball reactions are identical, and there will be no relative motion of the center of the inner ring with respect to the center of the outer ring as the balls rotate. As load is applied, the inner ring becomes eccentric within the bearing. All of the balls remain loaded until  $\epsilon = 1.0$  at which time one of the balls just becomes unloaded, Fig. 32(c).



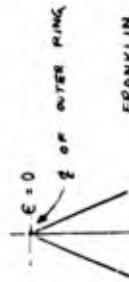
THE FRANKLIN INSTITUTE • Laboratories for Research and Development

I-A2321-1

Polar Plots

Position of Shaft -  
at an eccentricity ratio,  $e$ ,  
and an attitude angle,  $A$ ,  
with constant load  $P/c_k k_r$ .

- Points of constant, rotation angle,  $\gamma$  (deg).
- x Points of maximum angular extent of  $A$ .

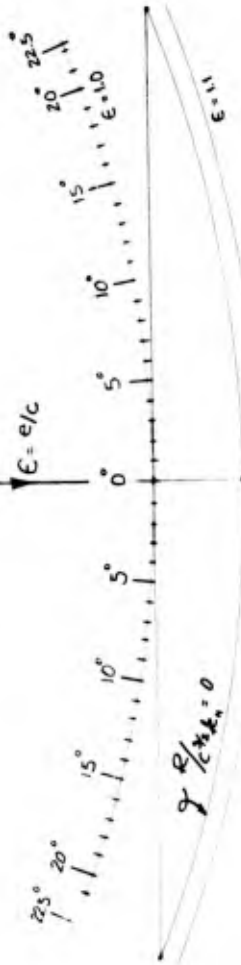


FRANKLIN INSTITUTE  
LABORATORIES

Fig. No. 33

LOCI OF INNER RING & CENTER  
FOR  
CLEARANCE BEARINGS (B-BALLS)  
OPERATING UNDER VARIOUS  
CONSTANT VALUES OF  $\left(\frac{P}{c_k k_r}\right)$

$A$



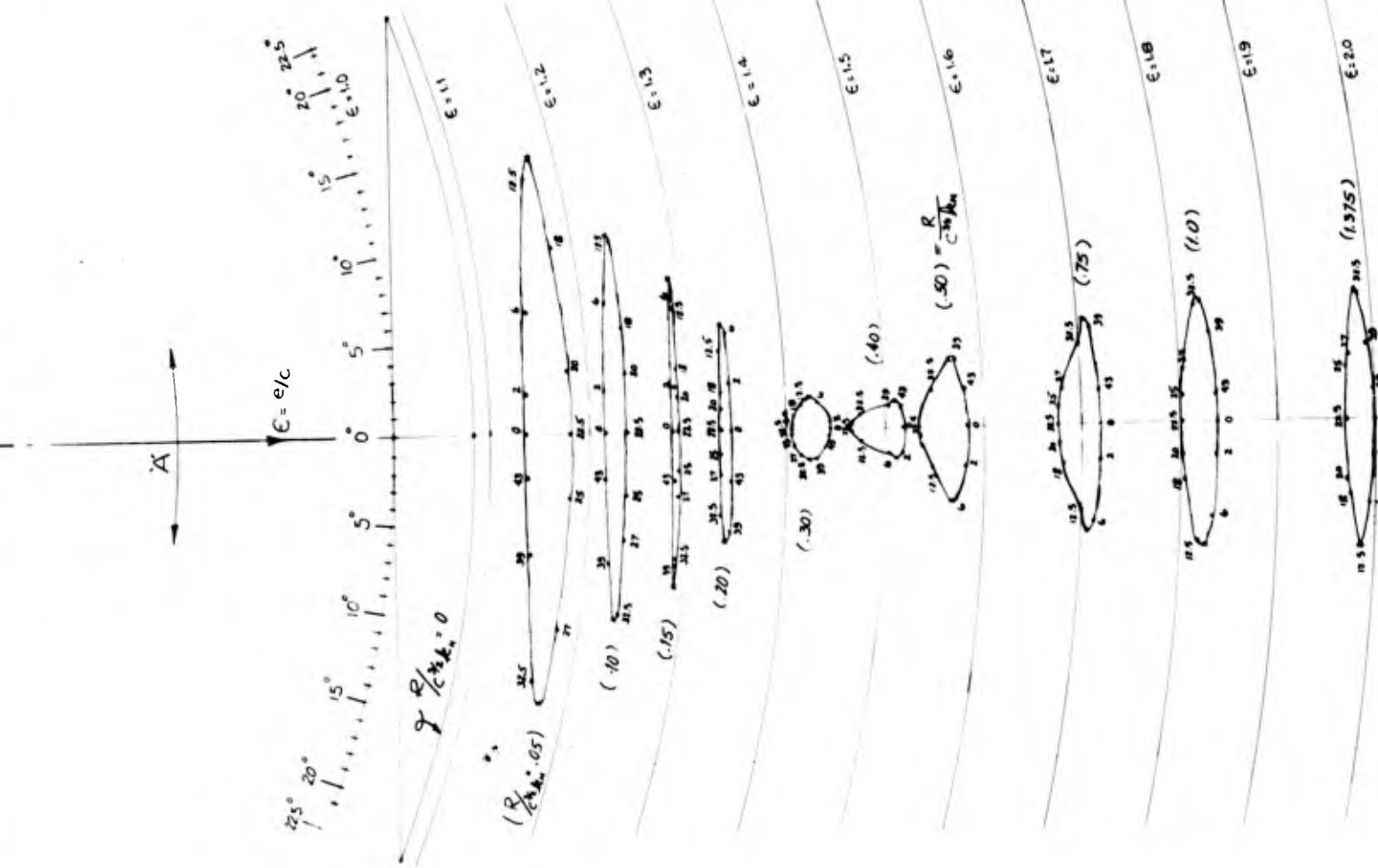


Figure 31

As more load is applied, more balls become unloaded (d). Figure 33 is a plot of interference bearing parameter  $\left[ \frac{R}{k_N i^{3/2}} \right]$  against eccentricity ratio,  $[\epsilon]$ , over the range investigated. Two interesting observations are:

1. There is a linear relationship between  $\frac{R}{i^{3/2} k_N}$  and  $\epsilon$  up to about  $\epsilon \approx 0.8$ .

Namely

$$\frac{R}{i^{3/2} k_N} = 6\epsilon \quad (54)$$

Since  $\epsilon = \frac{e}{i}$ ; this implies a linear spring rate as follows

$$R = 6k_N i^{1/2} e \quad (55)$$

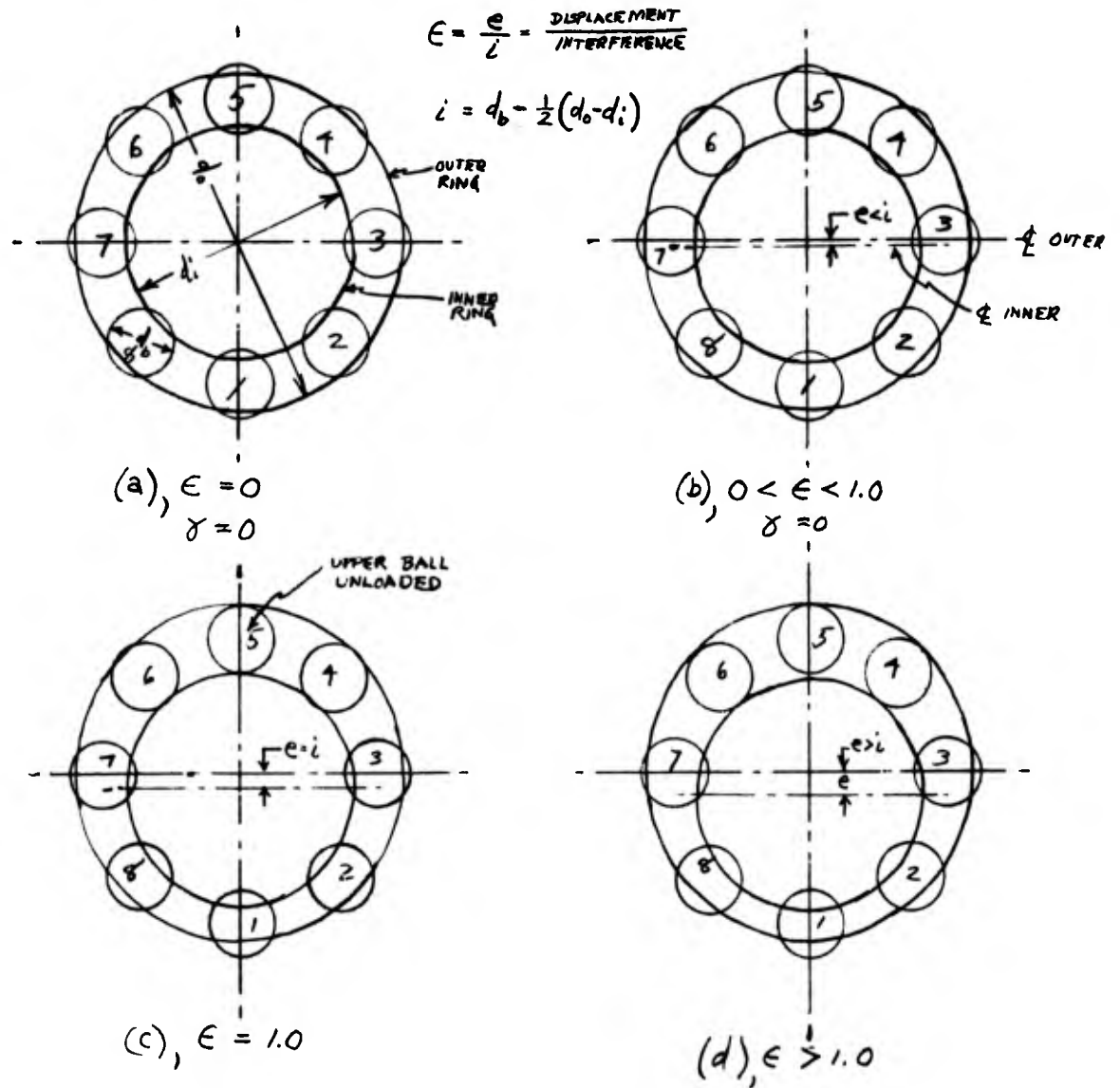
$$\text{Stiffness} = \text{spring rate} = \boxed{\frac{dR}{de} = 6k_N i^{1/2}} \quad (56)$$

2. There is a change in eccentricity ratio for constant  $\left[ \frac{R}{i^{3/2} k_N} \right]$  indicating radial periodic motion when  $\epsilon > 1$ .

Figure 34 shows the variation of attitude angle with ball rotation with  $\epsilon$  as the parameter. This indicates the presence of periodic motion in a direction normal to the load.

Using the information supplied by the computer and these two figures, (33 and 34) the maximum amplitudes of vibration in the direction of a fixed load and normal to the load were obtained. These results are plotted in Figures 35 and 36. These figures both indicate that the amplitude of periodic motion for values of the parameter  $\left[ \frac{R}{i^{3/2} k_N} \right]$





GEOMETRY OF A BEARING WITH RADIAL INTERFERENCE

Figure 32

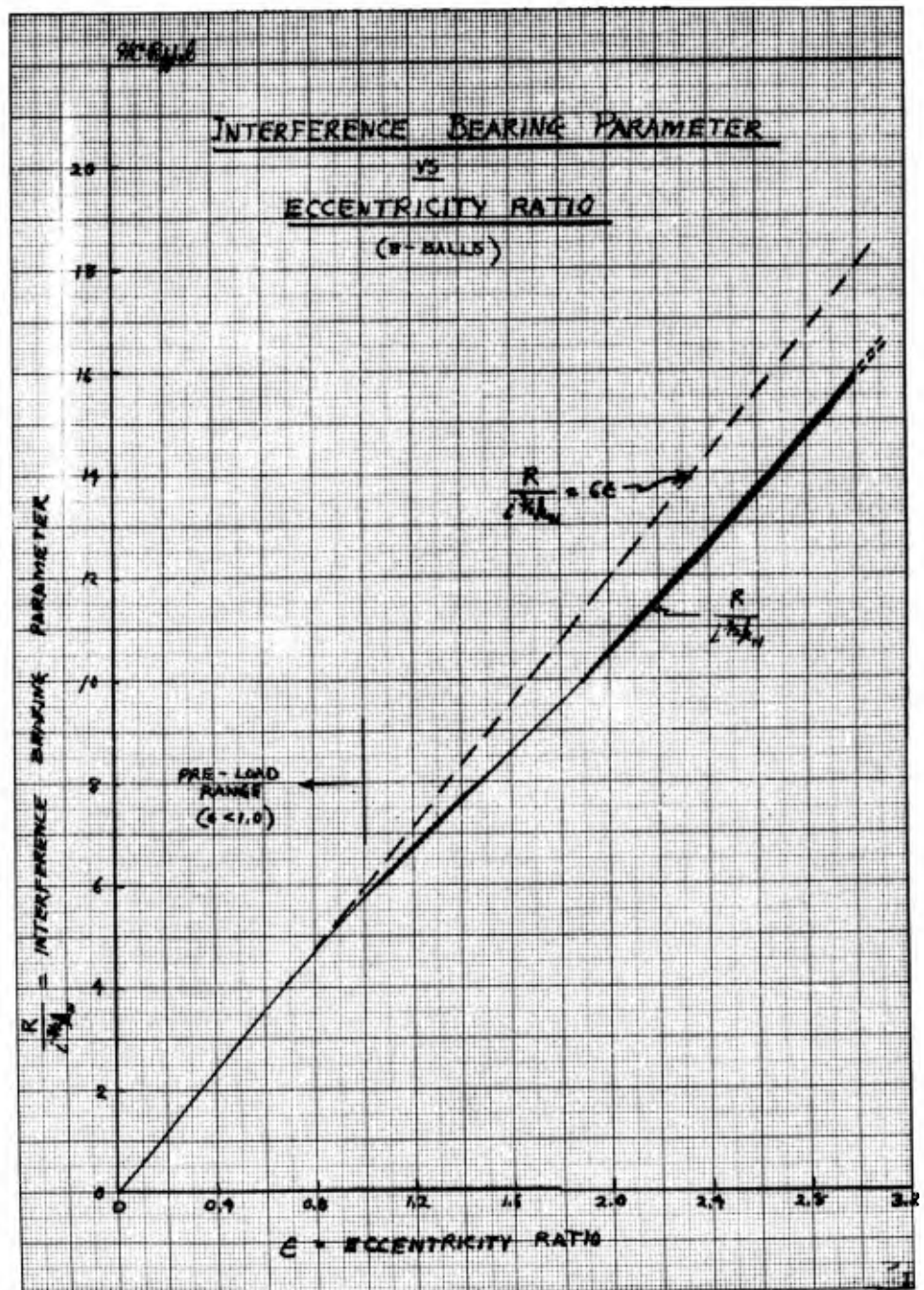
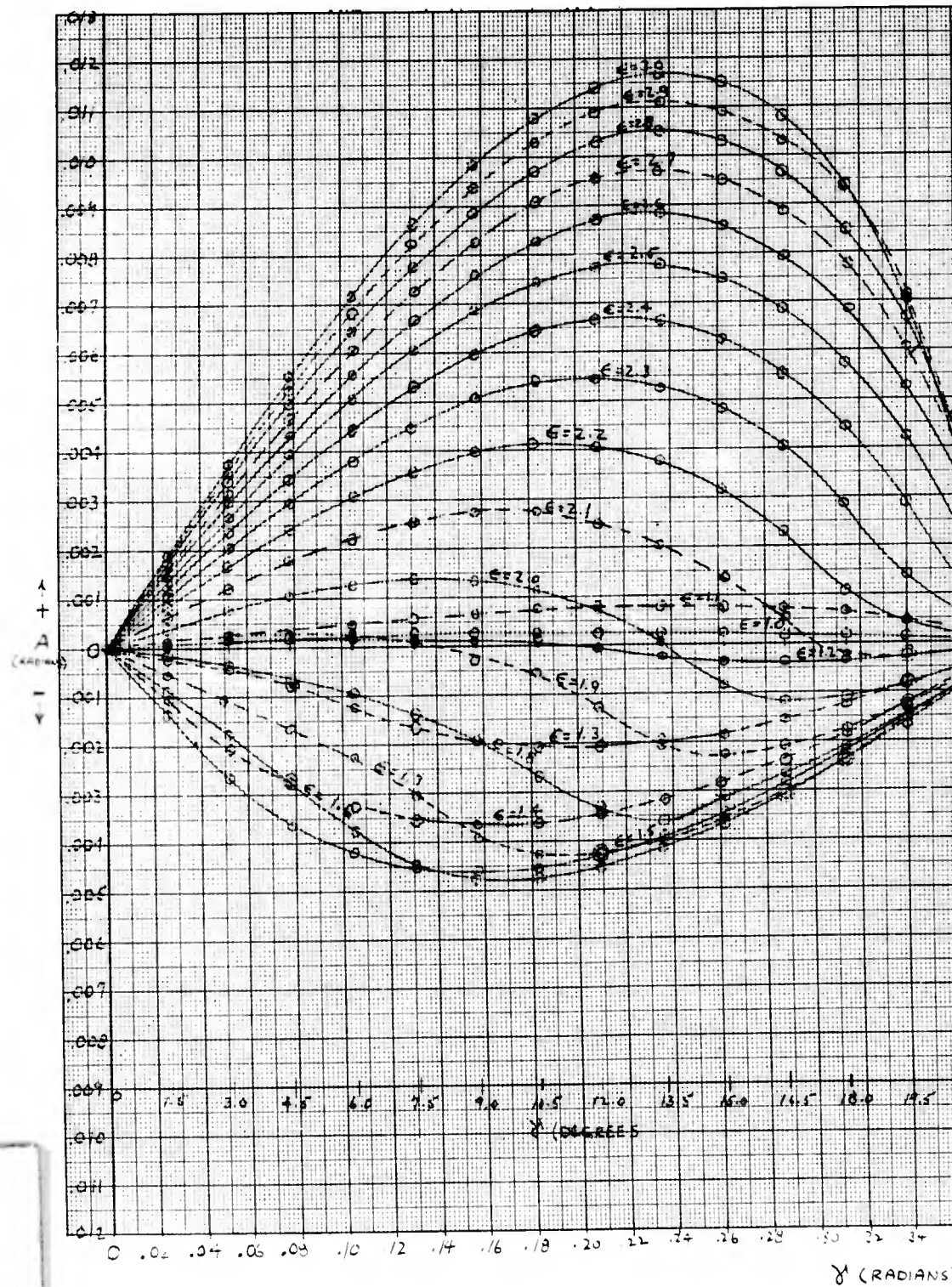


Figure 33



1

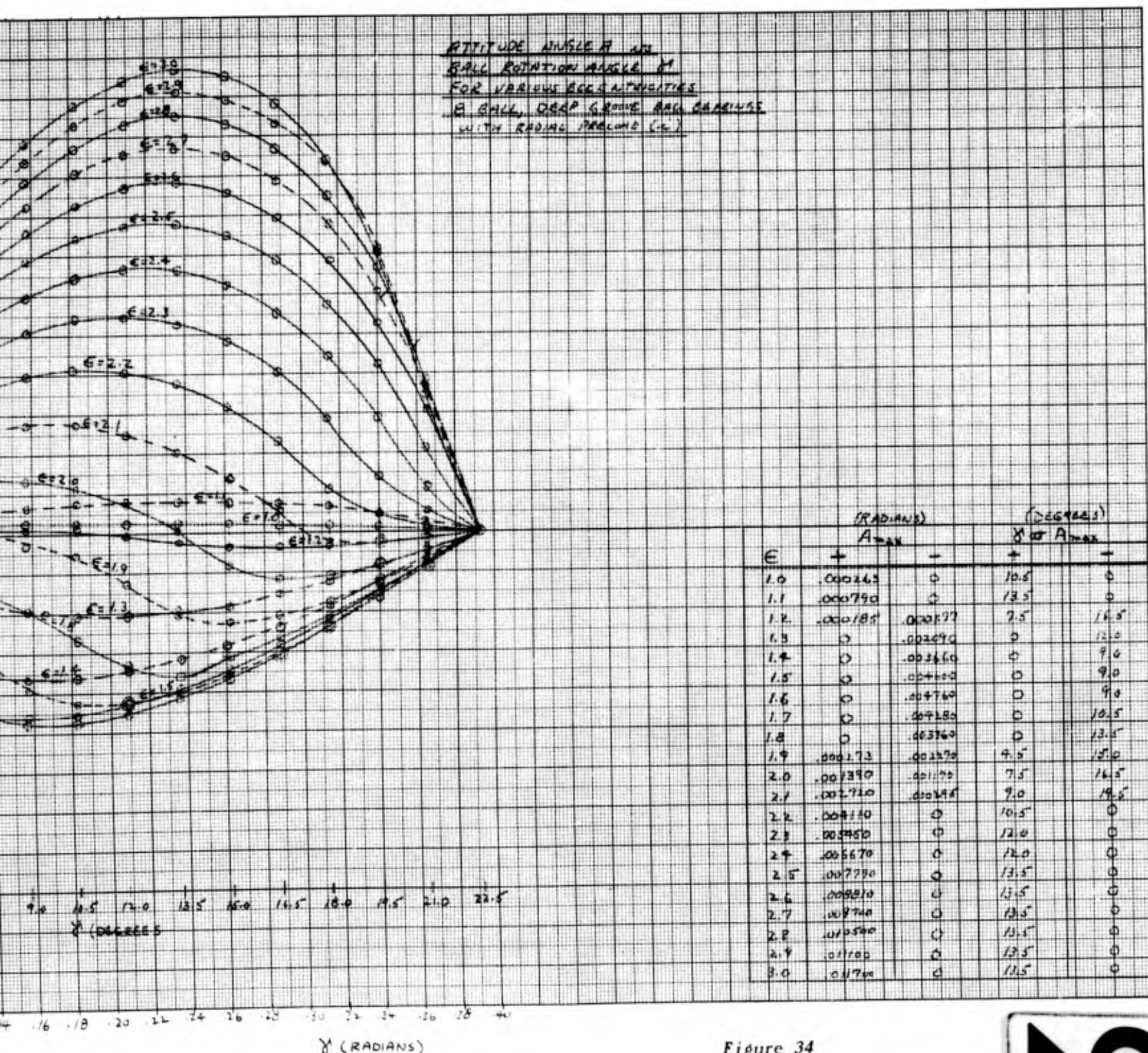


Figure 34





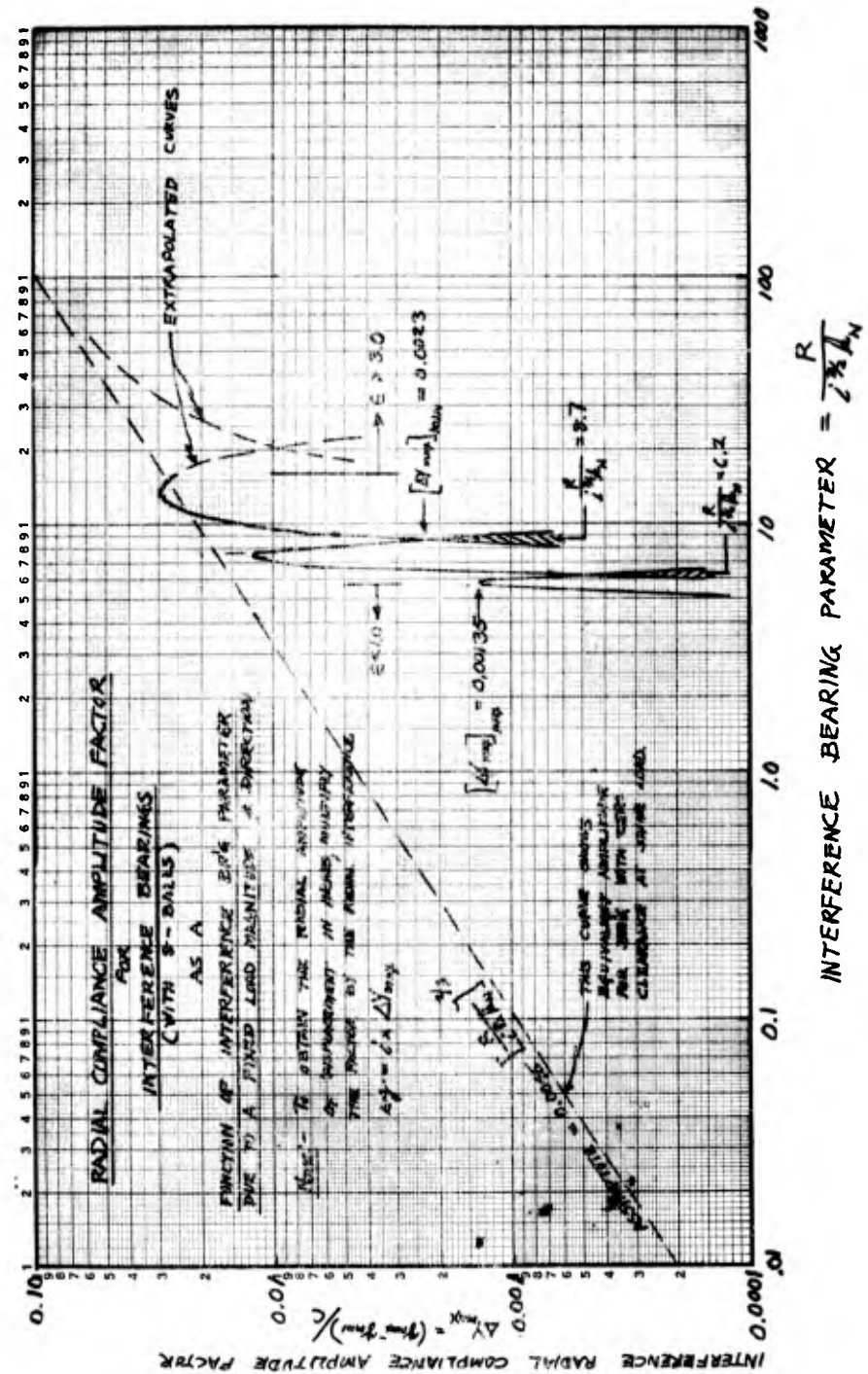


Figure 35

within the preload range  $[0 < \epsilon < 1.0]$  is virtually eliminated. For operation outside of the pre-load range, the amplitudes are less than for those present in a zero clearance bearing operating at the same load except at  $\left\{ 11.0 < \frac{R}{i^{3/2} k_N} < 15.0 \right\}$  (See Fig. 35.). Unfortunately the maximum  $\epsilon$  of 3.0 chosen for this investigation was too low to define the subsequent minimum values of  $\Delta X_{\max}$  and  $\Delta Y_{\max}$  (Fig. 36) and their asymptotic approach to the zero clearance bearing values. The reason for the existence of three minimum and maximum values of both  $\Delta X_{\max}$  and  $\Delta Y_{\max}$  for the interference bearing as opposed to only two for the clearance bearing is that the interference bearing over its range of load has 8, 7, 6, 5 or 4 balls carrying load whereas the clearance bearing has 1, 2, 3, or 4 balls carrying the load. In general, the values of  $\Delta X_{\max}$  are larger than  $\Delta Y_{\max}$  and both are less than that for a zero clearance bearing. To realize the full benefit of interference,  $\frac{R}{i^{3/2} k_N}$  should always be less than 5.0 this avoids unloading any of the balls.

Figure 37 may be used to determine the number of balls carrying load as dictated by  $\epsilon$  and  $\gamma$ . For convenience, constant values of  $\frac{R}{i^{3/2} k_N}$  are drawn as straight lines across this plot (dashed lines). Actually they should show a variation in  $\epsilon$  (just as they did for the clearance bearing, (Fig. 30), but of considerably less magnitude.

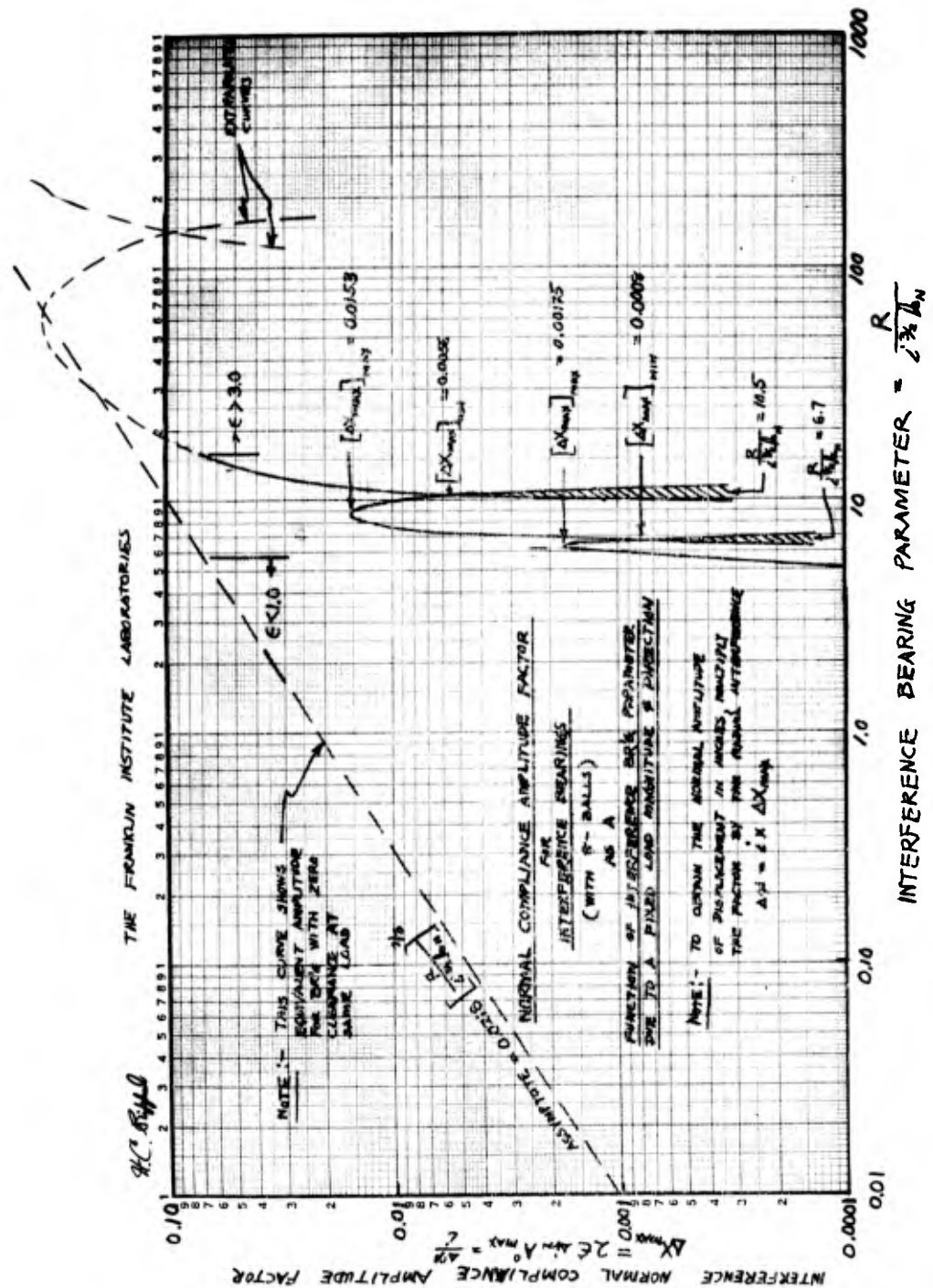


Figure 36

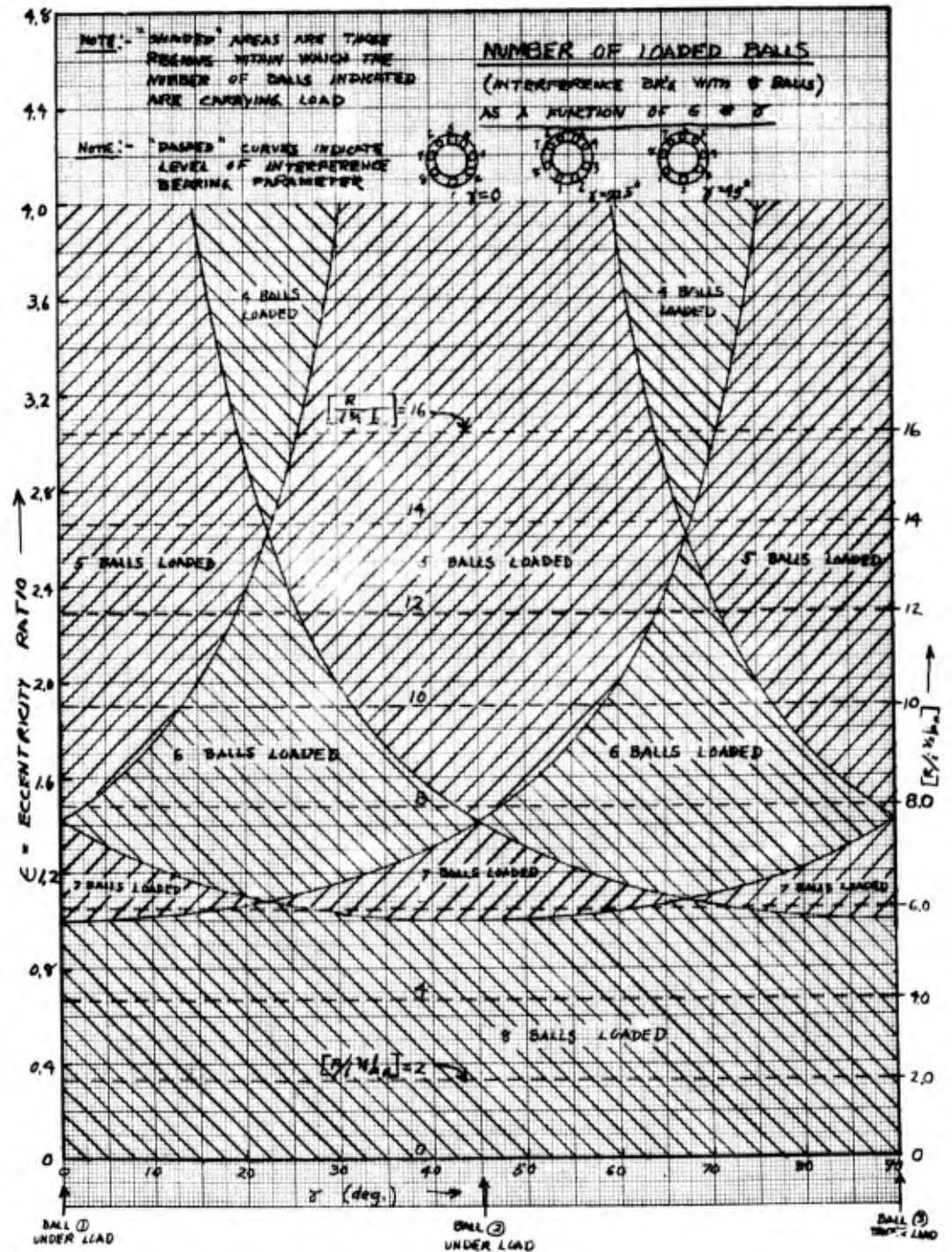


Figure 37



### 3.2.1.1.5 Bearing Spring Rates

With the information now at hand it is possible to evaluate the spring rates of deep groove, radial ball bearings containing 8 balls under the influence of a pure radial load. This is an important consideration especially with regard to their transmissibility characteristics.

#### 3.2.1.1.5.1 Bearings With Zero Clearance

From Section 3.2.1.1.2 it was found that the zero clearance bearing parameter was equal to a constant, the magnitude of which is dependent upon the number of balls in the train (See Fig. 16)

$$\therefore \frac{R}{k_N e^{3/2}} = \bar{X}_n = \text{constant}$$

$$R = k_N \bar{X}_n e^{3/2} \quad (\text{lbs.})$$

$$S_o = \text{stiffness} = \frac{dR}{de} = \frac{3}{2} k_N \bar{X}_n e^{1/2} \quad (\text{lbs/in})$$

$$\text{Since } e = \frac{R}{k_N \bar{X}_n}^{2/3}$$

$\therefore$  In terms of load,

$$S_o = \frac{3}{2} (k_N \bar{X}_n)^{2/3} R^{1/3}, \quad (\text{lbs/in}) \quad (57)$$

Since  $k_N$  and  $\bar{X}_n$  are constant quantities for a given bearing, the spring rate is non-linear with load; namely to the  $\frac{1}{3}$  power.

$$S_o \approx \text{constant} \times R^{1/3}$$

$$\text{This constant is equal to } \frac{S_o}{R^{1/3}} = \frac{3}{2} (k_N \bar{X}_n)^{2/3} \quad (58)$$

I-A2321-1

We shall call this the zero clearance load-stiffness factor.  $k_N$  is dependent upon bearing size and series and upon raceway curvature. Values of  $k_N$  are tabled in Appendix C.5, Table No. C-3.  $\Sigma_n$  is a constant depending on the number of balls (See Figure 16). Hence, (58) may be evaluated. This was done and the results are shown in Figure 38. This Figure indicates that for the same load:

1. Stiffness increases with bearing size for any given series
2. For a given size (bore code) bearing, stiffness decreases slightly with increasing series.

#### 3.2.1.1.5.2 Bearings With Internal Clearance

By the Lagrangian technique, the following analytical expression for the value of the clearance bearing parameter as a function of  $\epsilon$  was obtained.

$$\frac{R}{c^{3/2} k_N} = (16.69)10^{-6} \left[ \epsilon^6 - 58.78 \epsilon^5 + 1365 \epsilon^4 - 16099 \epsilon^3 + 119868 \epsilon^2 - 184781 \epsilon + 79705 \right] \quad (59)$$

Note: This Equation applies for  $1.0 \leq \epsilon \leq \infty$ .

At  $\epsilon = 1.0$ ,  $\frac{R}{c^{3/2} k_N} = 0$  which is correct.

This equation, if solved for  $\frac{R}{c^{3/2} k_N}$  for various values of  $\epsilon$  and the results plotted, yields the curve shown in Figure 24. Taking the derivative of (59) with respect to  $\epsilon$  yields an analytical expression for the stiffness or spring rate as follows;

$$R = (16.69)10^{-6} k_N c^{3/2} \left[ f(\epsilon) \right] = \text{bracket qty. shown in (59) above}$$

$$\frac{dR}{d\epsilon} = 1 \times 10^{-4} k_N c^{3/2} \left[ \epsilon^5 - 48.81 \epsilon^4 + 910 \epsilon^3 - 8050 \epsilon^2 + 39956 \epsilon - 30797 \right]$$

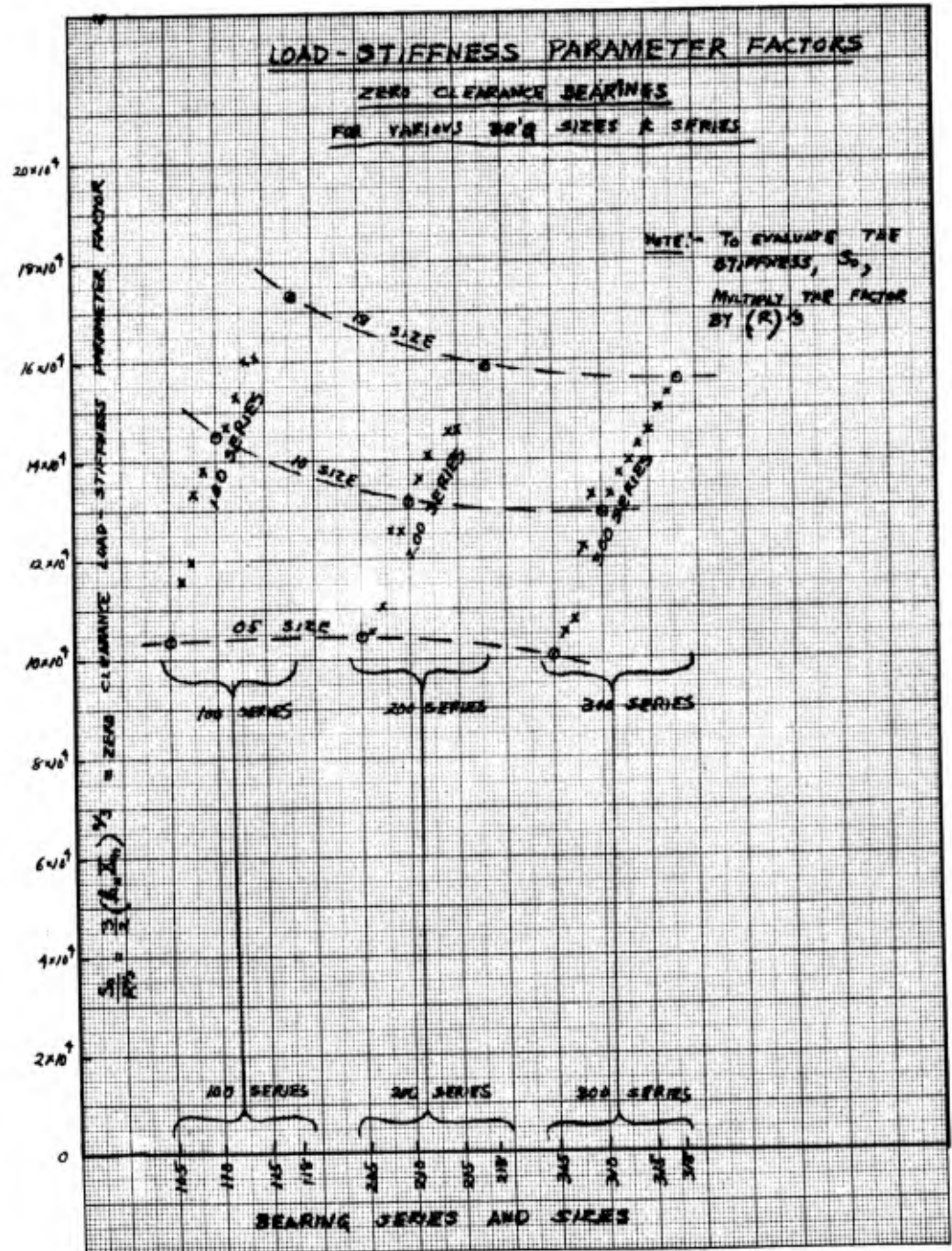


Figure 38

Since  $\epsilon = \frac{e}{c}$

$$\text{Stiffness} = S_c = \frac{dR}{de} = k_N c^{1/2} \times 10^{-4} \left[ \epsilon^5 - 48.8\epsilon^4 + 910\epsilon^3 - 8050\epsilon^2 + 39956\epsilon - 30797 \right] \quad (60)$$

If we substitute values of  $\epsilon$  in (60) and solve for  $S_c/k_N c^{1/2}$  and the same values of  $\epsilon$  in (59) and solve for  $R/k_N c^{1/2}$  we can plot  $S_c/k_N c^{3/2}$  vs  $R/k_N c^{3/2}$  and show the variation of stiffness with bearing parameter. This was done and the results are plotted in Figure 39. For low values of clearance bearing parameter (light load, large clearance), stiffness is low. As load increases or clearance decreases, stiffness increases. The "dashed" line in Figure 39 shows the equivalent stiffness for an 8-ball, ball bearing with zero clearance. Notice that spring rate for a clearance bearing approaches that for a zero clearance bearing when  $R/c^{3/2} k_N \geq 1.0$ , beyond which

$$S_c = 2.224 R k_N^{2/3} R^{1/3}, \quad \text{lbs/in} \quad (61)$$

and is independent of clearance.

Values of  $\frac{S_c}{c^{1/2} k_N}$  may also be determined by the following equation

$$\frac{S_c}{c^{1/2} k_N} = \frac{\Delta \left[ \frac{R}{c^{3/2} k_N} \right]}{\Delta \epsilon} \quad (62)$$

With  $\Delta \left[ \frac{R}{c^{3/2} k_N} \right]$  evaluated from computer data for a particular  $\Delta \epsilon$ .

I-A2321-1

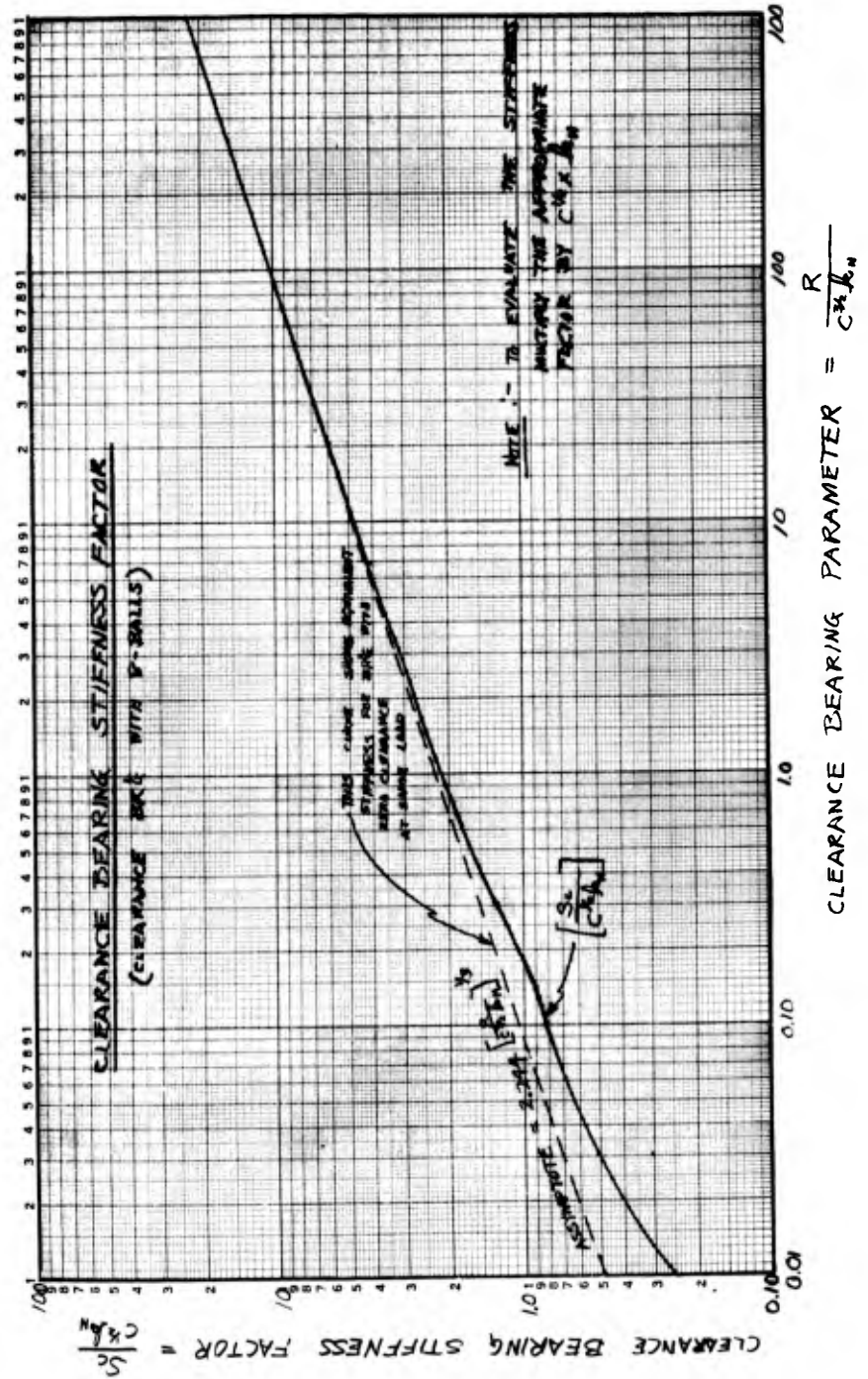


Figure 39

### 3.2.1.1.5.3 Bearings with Internal Interference

From section 3.2.1.1.4 it was found that for small values of the interference bearing parameter,  $R/i^{3/2} k_N$ , a linear spring rate was obtained; namely that

$$S_i \left| \frac{R}{i^{3/2} k_N} \right| \leq 5 \approx 6 k_N^{1/2} \quad (56)$$

At larger values of the bearing parameter there is a decreasing spring rate which becomes asymptotic to the spring rate realized in a bearing with zero clearance. The variation of  $\frac{S_i}{i^{1/2} k_N}$  (dimensionless stiffness factor) with the interference bearing parameter  $R/i^{3/2} k_N$  is shown in Figure 40. For values of  $\frac{R}{i^{3/2} k_N} \geq 10$ ,

$$S_i = 2.24 \left[ k_N^{2/3} \right] R^{1/3} \quad \text{lbs/in} \quad (63)$$

and is independent of the amount of interference.

In passing, it should be mentioned that values of  $S_i/i^{1/2} k_N$  were obtained by computing

$$\frac{S_i}{i^{1/2} k_N} = \frac{\Delta \left[ \frac{R}{i^{3/2} k_N} \right]}{\Delta \epsilon} \quad (64)$$

between all of the computer data points.

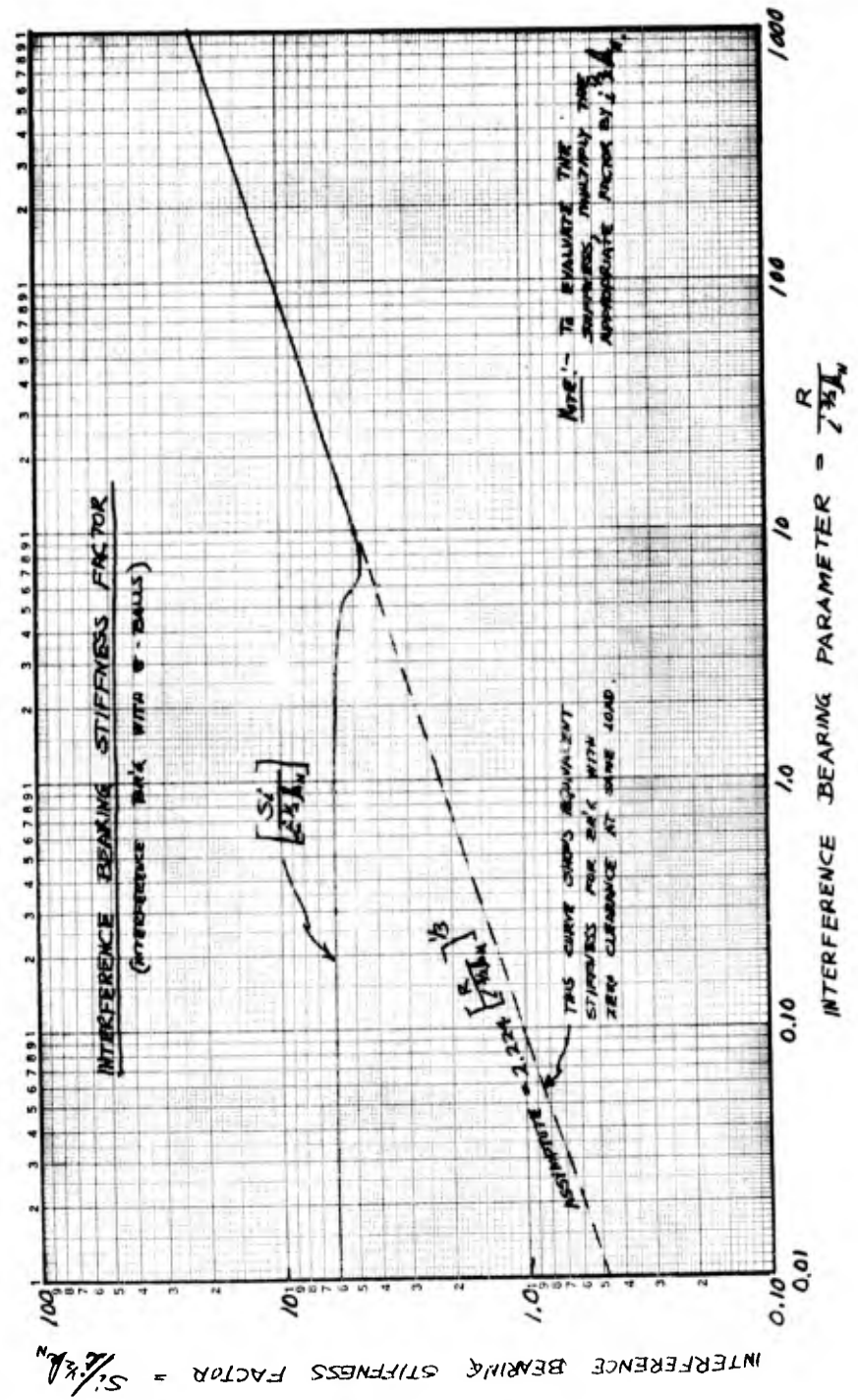


Figure 40

### 3.2.1.2 Natural Frequencies of Ball-Bearing Components

An unmounted ball bearing consists of several members each possessing their own natural frequency(s) of vibration. Since ball bearings are capable of generating frequencies of vibration of their own accord and are subjected to external varying periodic forces it would benefit us to know how such natural frequencies of bearing components compare with disturbing frequencies. Since very little damping is involved, resonance of bearing components may occur, resulting in high amplitudes of vibration and magnification of forces transmitted through the bearing.

#### 3.2.1.2.1 Natural Frequencies of Free Outer Ring

Since the outer ring is subjected to vibrations generated within the bearing and transmitted by the bearing, its natural frequency of several modes of vibration are of interest. Also, such natural frequencies may influence the contemplated technique of obtaining a measure of the bearing vibration characteristics by monitoring the vibration of the free outer ring in the subsequent experimental phase of the program (Phase III).

Pure radial, torsional, and flexural free vibrations were considered and evaluated (See Appendix F) for their natural frequencies. Of the free natural frequencies of the outer ring, summarized at the end of Appendix F, only the lower modes of flexural vibrations offer frequencies within the range of interest (10 cps to 10 kc). In general, flexural vibrations in the plane of the ring increase in frequency with decreasing bore size and increasing series, as shown in Figures 41, 42, and 43.



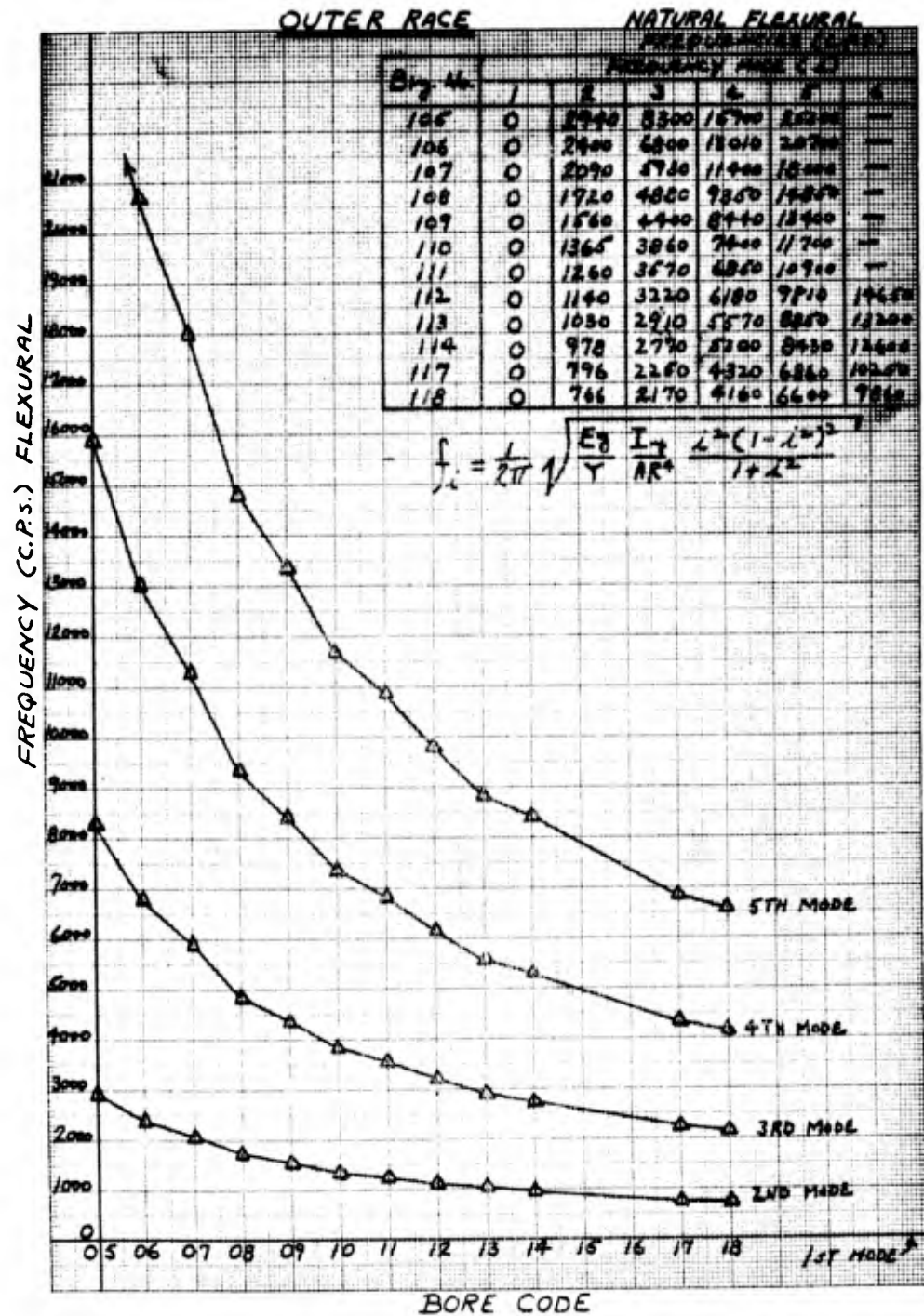


Figure 41

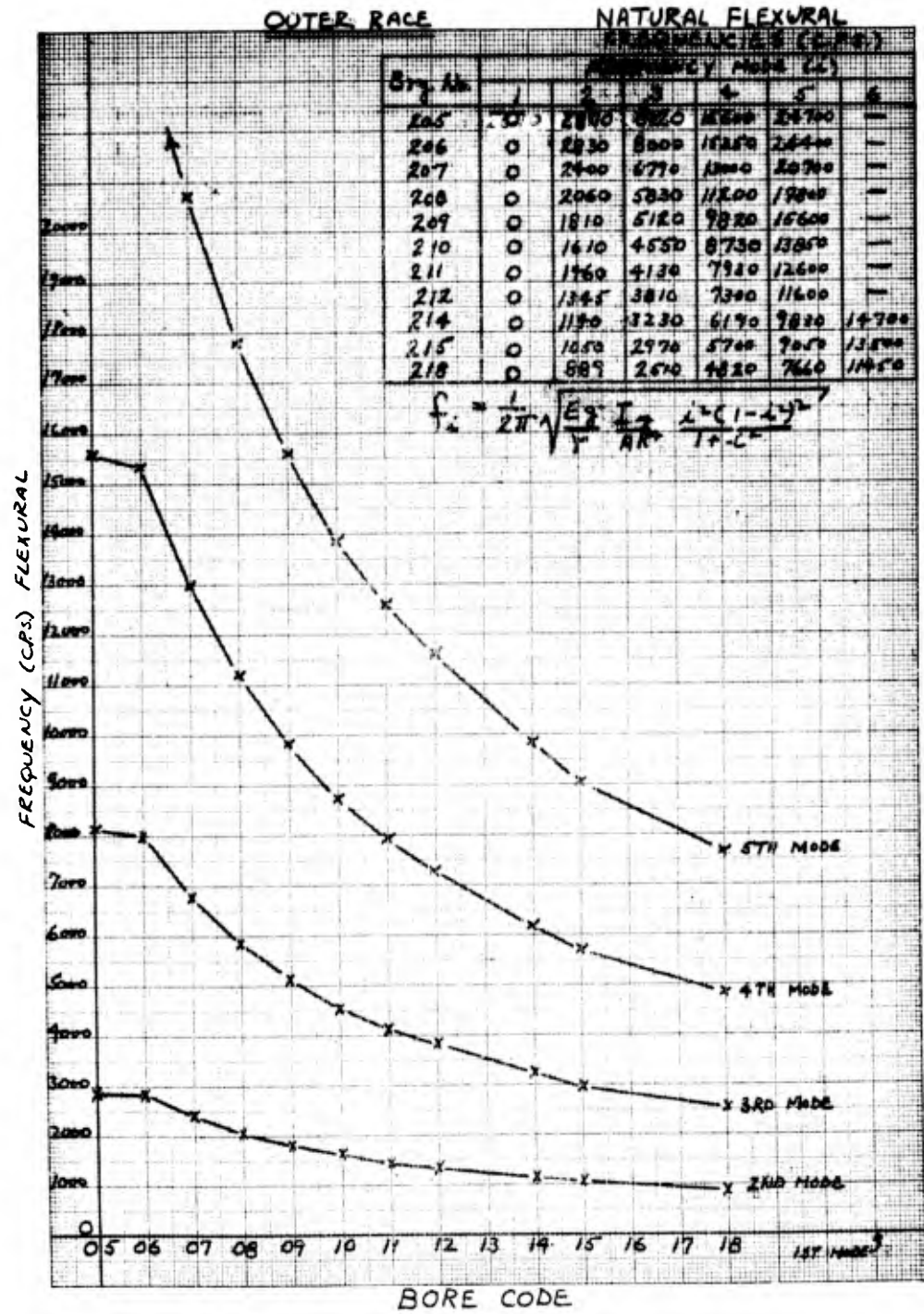


Figure 42

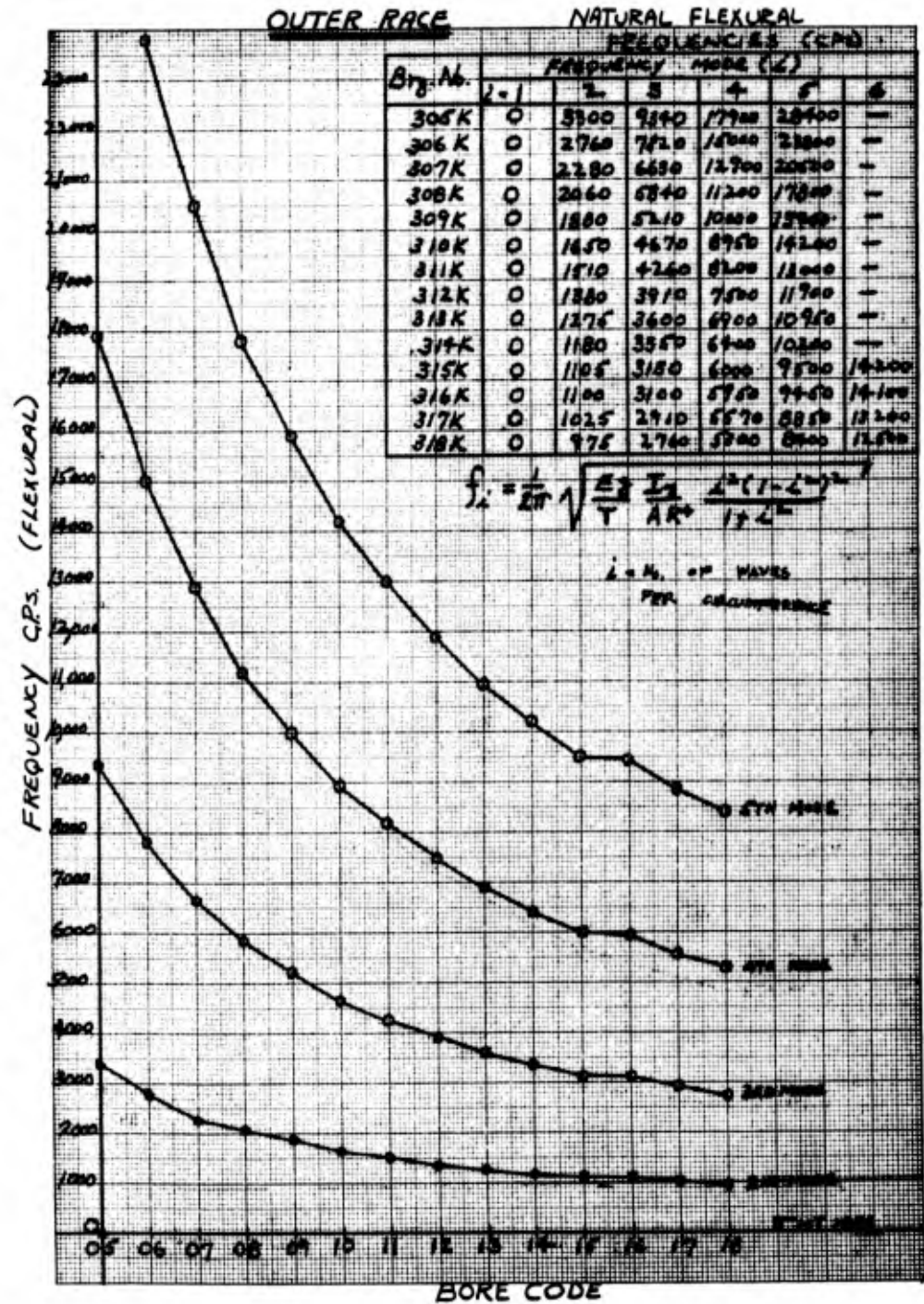


Figure 43

### 3.2.1.2.2 Natural Frequencies of Constrained Outer Ring

Normally, in an electric motor, the outer ring is mounted in its housing with a close clearance fit. For the moment, consider the case of an axially loaded bearing with its outer race touching its housing at each ball location. This condition is approximated in an electric motor when axial pre-load is high and radial load is zero. The natural frequency of vibration of the outer ring in flexure will be dictated by the number of balls since this dictates the number of nodes ("o" displacement) set up around the outer ring. For a 310 bearing with 8-balls, implying 8 nodes, the 4<sup>th</sup> mode of flexural vibration will be the fundamental frequency (since it has 8 nodes). From Figure 43 this would be 9000 cps. Higher modes of flexural vibrations having 8 nodes uniformly spaced would be the 8<sup>th</sup>, 12<sup>th</sup>, 16<sup>th</sup>, etc., all of which are out of the range of interest. For an odd number of balls the first mode of vibration would be equal to the  $n^{\text{th}}$  mode of flexural vibration where  $n$  = number of balls. Since, for the 300 series  $n_{\text{min}}$  is on the order of 7 balls, flexural frequencies with the nodes at the ball locations are beyond the range of interest in bearings having an odd number of balls. For an even number of balls, the first mode of vibration having nodes at the ball locations would be equal to the  $(\frac{n}{2})^{\text{th}}$  mode of flexural vibration, which yields frequencies in the 300 series (307→318) from approximately 5000 to 13000 cps. These frequencies are of interest to us. It is interesting to note that when measuring outer ring vibration on the Anderometer, the outer ring constraints are similar to the condition just discussed.

THE FRANKLIN INSTITUTE • *Laboratories for Research and Development*

I-A2321-1

In a perfectly circular housing, a perfectly made bearing will, theoretically, make axial line contact with the housing. Hence, it would be susceptible to being excited in its second mode of flexural vibration which produces the lowest frequency possible for flexural vibrations of the outer ring. Such frequencies are in the range of interest. This assumes that the balls offer no constraint to vibration of the outer ring. This condition is approximated by a bearing with internal clearance and essentially unloaded. The opposite situation, namely, radial interference or high axial pre-load sets up a number of internal constraints equal to the number of balls. A free outer ring subjected to uniformly spaced radial forces of equal magnitude will exhibit an increase in diameter at the ball locations and a decrease in diameter between the balls. This results in a wavy inner race and a wavy outer diameter of the outer ring. The total amplitude of this circumferential waviness may be expressed as follows.

Total variation in radial amplitude =  $\delta$

$$\delta = \frac{WR^3}{4EI_y} \times k_n$$

$W$  = radial ball load,  $R$  = outer ring radius of neutral axis,  $k_n$  is a constant which is dependent upon the number of balls. (See Roark, "Formulas for Stress and Strain", Pg. 158, 3<sup>rd</sup> Ed.). For a 310 bearing with  $R = 2.03"$ ,  $I_y = 1.9 \times 10^{-3}$  (Appendix F),  $E = 30 \times 10^6$ , and  $k_n \doteq 5.2 \times 10^{-3}$

$$\delta \doteq 0.2 \times 10^{-6} \times W, \text{ in.}$$

THE FRANKLIN INSTITUTE • *Laboratories for Research and Development*

I-A2321-1

Thus if each ball exerts a radial force of 10 lbs, the variation of radial amplitude will be 2 microinches. As the balls rotate, the radial amplitude of motion of one spot on the outer race will be of this magnitude. The natural frequency of vibration of a straight beam of length equal to one ball space is dictated by the end conditions and can be expressed as follows,

$$f = c \sqrt{\frac{gEI_y}{wL^4}}, \text{ cps} \quad w = \text{beam wt. in lbs/in.}$$

c = coefficient dependent upon end conditions  
and mode of vibration

Considering a 310 outer ring with

$$\begin{aligned} E &= 30 \times 10^6 \text{ psi} \\ I_y &= 1.4 \times 10^{-3} \text{ in}^4 \\ w &= b \cdot h \cdot (0.283) = 1.063 (.2775)(.283) = 0.0837 \text{ lbs/in.} \\ L &= R \times 2\pi/8 \text{ balls} = \pi/2 = 1.57 \text{ in.} \\ g &= 386 \text{ in/sec}^2 \\ f &= c (6580) \text{ cps} \end{aligned}$$

For radial interference, the end conditions due to the loaded balls approach a "built-in" condition for which  $c = 3.56$  for the first mode of vibration. This end condition would yield a frequency of  $3.56 (6580) = 23,500$  cps. The relationship between ball load and radial ring deflection was given as

$$\delta = 0.2 \times 10^{-6} W$$

or a spring rate of

$$\frac{\Delta W}{\Delta \delta} = 5 \times 10^6 \frac{\text{lbs}}{\text{in.}}$$

THE FRANKLIN INSTITUTE • *Laboratories for Research and Development*

I-A2321-1

If this spring rate and the beam mass for one ball span are used in the frequency equation

$$(2\pi)^2 f^2 = \frac{k}{m} = \frac{\Delta W / \Delta s}{m} = \frac{5 \times 10^6}{\frac{(0.0837 \times 1.57)}{386}}$$

$$(2\pi)^2 f^2 = 1.47 \times 10^{10}$$

$$f = 19,250 \text{ cps}$$

or an end condition coefficient of

$$c = \frac{19,250}{23,500} \times 3.56 = 2.91$$

which is, as expected, less than that for a "built-in" end condition.

In any case, frequencies of this level (20,000 cps) are at the extreme upper end of our range of interest. It would appear that the lowest natural frequency of flexural vibration of the outer race is its 2<sup>nd</sup>

mode in flexure. This could be excited in an unloaded bearing making

only line contact with its housing. Furthermore, in lightly loaded

bearings where the balls contribute only little restraint to outer race

vibration, higher modes of flexural free vibration may be excited if the

housing constraint(s) are such as to lie at nodal points. It is important

to note that increasing the number of housing constraints will suppress

the lower modes of flexural vibration. In radially preloaded bearings

I-A2321-1

the outer race may be excited at its  $\left(\frac{n}{2}\right)^{th}$  mode of flexural vibration and higher orders thereof. Since  $\frac{n}{2}$  must be an integer, it may be advantageous to use an odd number of balls.

#### 3.2.1.2.3 Natural Frequencies of Free Inner Ring

Since the radius of an inner ring is considerably less than for an outer ring, its natural frequencies of free vibration will be higher. Hence, only the lower modes of its flexural vibrations produce frequencies within the range of interest. The frequencies of the first four modes of free flexural vibration are shown plotted in Figure 44 for various bearing series and sizes. Normal mounting practice of inner rings calls for an interference fit on the shaft. This essentially precludes flexural vibrations of the inner ring. However, when measuring bearing vibration on the Anderometer, the inner ring is a close clearance fit on the test spindle. Hence, the inner ring is free to flex and conceivably can contribute to the vibrations observed.

#### 3.2.1.2.4 Cages and Retainers

The cages used to maintain the proper ball spacing in a ball bearing are of various forms and material. Electric motor bearing cages are primarily of the pressed-steel type which provide the desirable ad-



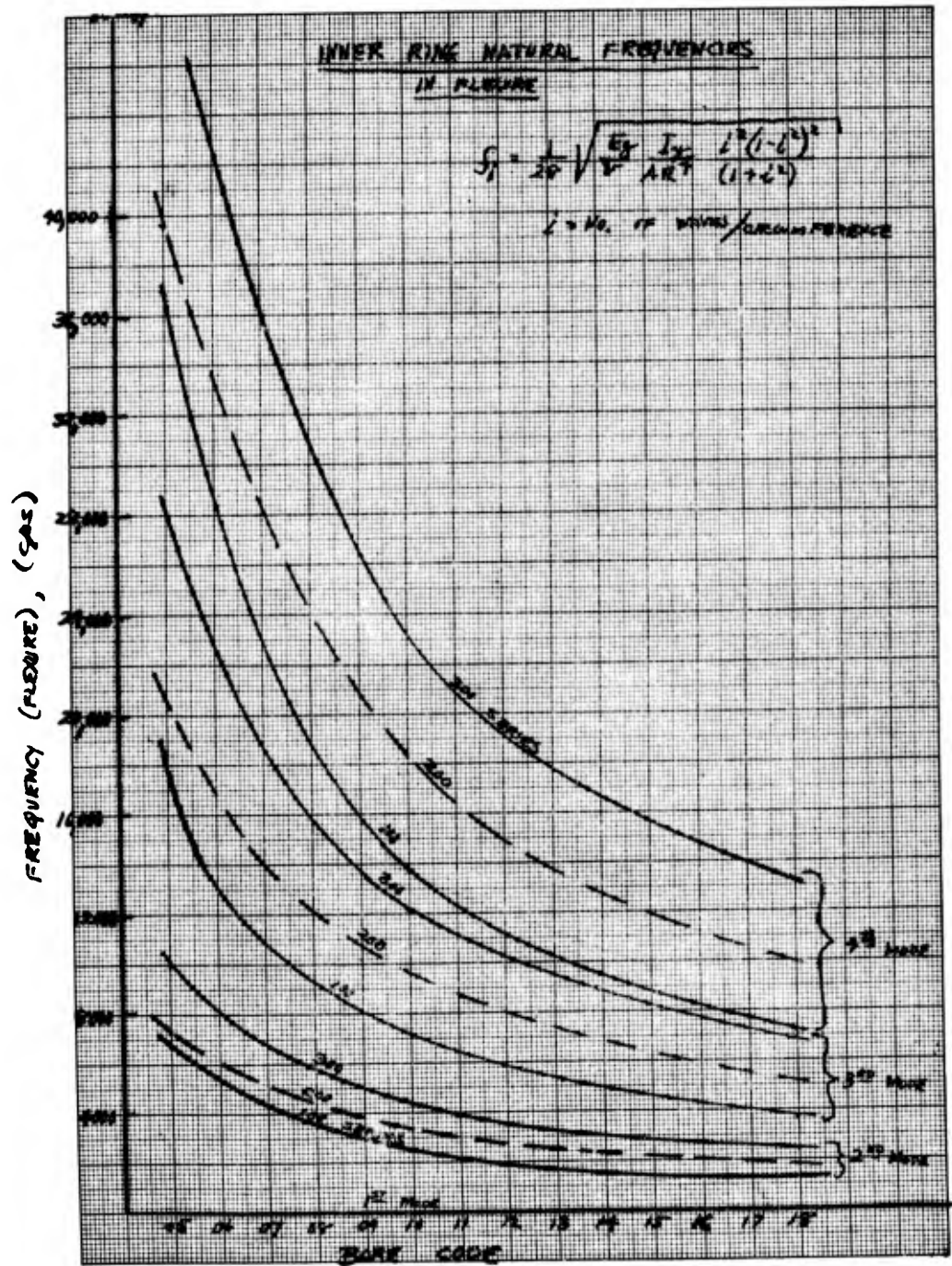


Figure 44

THE FRANKLIN INSTITUTE • *Laboratories for Research and Development*

I-A2321-1

vantages of light weight, adequate strength and minimum space. Since such a cage is supported by and given its motion by the balls, periodic sliding contact of the cage with the balls must occur. Therefore, the possibility of forcing the cage to vibrate exists. Any attempt to calculate the natural frequencies of the many possible types of vibration of such a complex configuration would be a difficult undertaking. Hence, no attempt to compute natural frequencies was made.\* Actually, the pressed-steel cage configurations, when properly assembled, offer a very rigid structure. This fact, in combination with its low mass imply relatively high natural frequencies of free vibration. It is estimated that its lowest mode of flexural vibration is on the order of 1000 cps for an average size bearing.

A ball bearing cage is subjected to a complex system of indeterminate forces that are distributed among the individual ball contacts and which may vary in a random manner as the result of residual variations within an over all tolerance control. Relatively heavy combined loads, thrust and radial, impose a cyclic variation of speed in the orbital motion of the ball and this can result in high restraining

---

\*If required, the resonant frequencies can be determined experimentally. This bit of information would be useful for airborne noise evaluation.

THE FRANKLIN INSTITUTE • *Laboratories for Research and Development*

I-A2321-1

stresses. Radial displacement of the cage under the influence of centrifugal force will induce further constraint imposed on individual ball contacts. These effects are difficult to evaluate in terms of the vibrational response of the cage structure as a whole.

Normally the cage is not an appreciable source of noise. Under relatively light loads and low speeds it may develop a tendency to "rattle" and be recognized as a source of airborne disturbance emanating from the bearing. Under these circumstances it is generally recognized that cages made from phenolic materials show little or no response of this character. Such materials provide good damping qualities and at the same time afford an inherently low frictional restraint at the areas of sliding contact with the ball.

At this time it does not seem possible to establish a rational approach to the extremely complex problem of theoretically analyzing the exciting forces and the modes of vibrational response that characterize the cage as a component of the bearing. It is believed that the contribution of the cage to the structure borne noise performance of the bearing is of minor importance, but can contribute to the airborne noise.

3.2.1.2.5. Natural Frequency of Solid Ball

The lowest natural frequency of free vibration of a solid sphere is given in Lamb's "Dynamical Theory of Sound", London, 1925, page 156 as;

$$N = 0.840 \frac{\sqrt{\mu/\rho}}{2a} \quad (\text{cps})$$

where N = Natural Freq. (cps)

$$\sqrt{\mu/\rho} \approx 0.62 \times C \quad (\text{meters/sec.})$$

C = Velocity of sound in material

$$C = \sqrt{E/\rho}$$

E = Young's Modulus

$\rho$  = Mass Density

a = Radius of Sphere

$$\therefore N = \frac{0.84 (0.62) \times \sqrt{E/\rho}}{d} \quad (\text{cps})$$

$$N = 0.5208 \frac{\sqrt{E/\rho}}{d} \quad (\text{cps})$$

where E = Young's Modulus  $\text{lbs/in}^2$

$$\rho = \text{Mass Density} = \frac{\gamma}{g} \left( \frac{\text{lbs-sec}^2}{\text{in.}^4} \right)$$

d = Ball dia. (in.)

$$\text{For steel, } \sqrt{E/\rho} = 2.02 \times 10^5 \text{ in/sec.}$$

$$\therefore N = 1.05 \times 10^5 / d \quad (\text{cps})$$

Hence, the lowest natural frequency of a ball is inversely proportional to the ball diameter. Ball diameters range from 1/4 inch to about 1-5/16 inch yielding frequencies of 420,000 to 80,000 cps respectively.

Hence, all natural frequencies of ball free vibrations are, for our purpose, much too high to consider.

### 3.2.1.3. Resonant Frequencies of a Ball on its "Springs"

In Fig. No. 12,  $k_o$  and  $k_i$  are the spring rates of the outer and inner race contacts with a ball. In an operating loaded bearing, these ball-race spring rates are continually changing. It is conceivable that the balls can vibrate on their ball-race contact "springs". Hence, we must determine the nature of these spring rates.

From previous work the relationship between ball load ( $R_N$ ) in the direction of normal approach of the races, ( $\delta_N$ ), is

$$R_N = k_N \delta_N^{3/2} \quad (C-11)$$

The combined non-linear spring rate afforded by the two ball-race contacts becomes

$$\begin{aligned} \frac{dR_N}{d\delta_N} &= \frac{3}{2} k_N \delta_N^{1/2} = k_r \\ \therefore k_r &= \frac{3}{2} k_N^{2/3} R_N^{1/3} \end{aligned} \quad (65)$$

Since the inner and outer races are separated by two "springs" in series of rates  $k_o$  and  $k_i$ ,

$$\frac{1}{k_r} = \frac{1}{k_o} + \frac{1}{k_i}$$

$$\therefore k_r = \frac{k_i k_o}{k_i + k_o}$$

If we assume that  $k_i = k_o = k_{br}$  = ball -race

spring rate

$$\therefore k_i = k_o = k_{br} = 2k_r$$

or the spring rate of a loaded ball in contact

with a single race is,

$$k_{br} = 3k_N \delta_N^{1/2} = 3k_N^{2/3} R^{1/3} \quad (66)$$

### 3.2.1.3.1 Resonant Frequency of an Un-Loaded Ball

Consider an unloaded ball in a bearing turning at a frequency

$f_i$  (shaft frequency). The load on the ball is that due to centrifugal force and it is supported on the outer race only. For this case,

$$R = C.F. = m_b \frac{E}{2} \omega_E^2, \text{ lbs.}$$

$$\omega_E = 2\pi f_E = \text{cage speed, rad./sec.}$$

$$\frac{E}{2} = \text{Radius to ball center (in.)}$$

THE FRANKLIN INSTITUTE • Laboratories for Research and Development

I-A2321-1

$$m_b = \frac{W_b}{386} = \frac{\frac{\pi(d)^3(.283)}{6}}{386} = \text{ball mass, } \frac{\text{lbs} \cdot \text{sec}^2}{\text{in}}$$

$$\therefore R = m_b \left(\frac{E}{2}\right) (2\pi f_E)^2$$

$$R = 19.75 m_b E f_E^2, \text{ lbs}$$

$$R^{1/3} = 2.7(m_b)^{1/3} (E)^{1/3} f_E^{2/3}, (\text{lbs})^{1/3}$$

(ball centrifugal force)<sup>1/3</sup>

$$\therefore k_{br} = 3k_N^{2/3} R^{1/3} = (8.1)m_b^{1/3} k_N^{2/3} E^{1/3} f_E^{2/3}, \text{ lbs/in}$$

The resonant frequency is,

$$f_n = \frac{1}{2\pi} \sqrt{\frac{k_{br}}{m_b}}$$

$$\frac{k_{br}}{m_b} = \frac{8.1 k_N^{2/3} E^{1/3} f_E^{2/3}}{m_b^{2/3}}$$

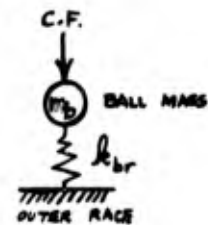
$$\sqrt{\frac{k_{br}}{m_b}} = 2.845 \frac{k_N^{1/3} (E)^{1/6} (f_E)^{2/6}}{m_b^{1/3}}$$

$$f_n = 0.454 \frac{k_N^{1/3} (E)^{1/6} (f_E)^{2/6}}{m_b^{1/3}}$$

$$m_b = \frac{W_b}{386} = \frac{\frac{\pi d^3 (.283)}{6}}{386} = 3.84 \times 10^{-4} d^3 = 0.384 \times 10^{-3} d^3$$

$$(m_b)^{1/3} = 0.726 \times 10^{-1} \times d$$

$$f_n = 6.24 \frac{k_N^{1/3} (E)^{1/6} (f_E)^{1/3}}{d}$$



(67)

THE FRANKLIN INSTITUTE • Laboratories for Research and Development

I-A2321-1

For a 310 bearing with

$$k_N = 13.85 \times 10^6 \quad \therefore k_N^{1/3} = 2.4 \times 10^2$$

$$E = 3.15 \quad " \quad E^{1/6} = 1.21$$

$$d = 3/4 \quad "$$

$$f_E = 0.381 f_i \quad f_E^{1/3} = 0.725 f_i^{1/3}$$

$$\therefore f_{n_{310}} = \frac{6.24(2.4)10^2(1.21)(.725)f_i^{1/3}}{(0.75)}$$

$$= 1750 \times f_i^{1/3}$$

@ N = 1800 RPM,  $f_i = 30$ ,  $f_i^{1/3} = 3.1$

$\therefore f_{n_{310}} = 5400 \text{ cps}$  ← Resonant frequency of an unloaded ball in a 310 br'g (operating at 1800 RPM) contacting outer race due to centrifugal force.

Thus it would appear that the natural frequency of an unloaded ball in contact with the outer race due to centrifugal force is in the range of interest. At 1800 RPM ( $f_i = 30$ ) these frequencies are from 1500 cps for large bearings to 15,000 cps for small bearings. From Equation (67), the diameter of the ball, appears to be the governing criteria since it enters as the first power. Rotational speed has some effect but not a great deal since it enters as the one-third power.

3.2.1.3.2 Resonant Frequency Of A Loaded Ball

Consider now a loaded ball that is confined between its two non-linear springs each with a spring rate of  $k_{br}$  and with the inner and outer races fixed as sketched below.





The combined spring rate is

$$k_b = 2 \times k_{br}$$

This is true even for relatively large excursions of the ball from a symmetrical arrangement. That is to say, the two opposed non-linear springs yield a more linear spring rate. This is shown in Appendix G.

$$k_b = 2 (k_{br}) = 2 (3k_N \delta_N^{1/2}) = 6 k_N \delta_N^{1/2}$$

$$\text{Since } R = k_N \delta_N^{3/2}$$

$$k_b = 6 k_N^{2/3} R_N^{1/3} \quad \text{lbs/in}$$

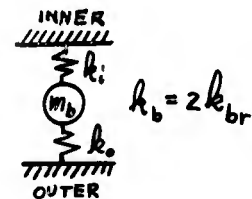
Spring rate for ball trapped and loaded between races.

$$R_N = \text{load on ball.}$$

The resonant frequency is

$$f_n = \frac{1}{2\pi} \sqrt{\frac{k_b}{m_b}}$$

$$\frac{k_b}{m_b} = \frac{6 k_N^{2/3} R_N^{1/3}}{m_b}$$



$$\sqrt{\frac{k_b}{m_b}} = 2.450 \frac{k_N^{1/3} R_N^{1/6}}{m_b^{1/2}}$$

$$f_n = 0.390 \frac{k_N^{1/3} R_N^{1/6}}{m_b^{1/2}}$$

$$m_b = \frac{\pi/6 d^3 (.283)}{386} = 3.84 \times 10^{-4} d^3$$

$$m_b^{1/2} = 1.96 \times 10^{-2} \times d^{3/2}$$

$$f_n = 20 \frac{k_N^{1/3} R_N^{1/6}}{d^{3/2}}$$

← Resonant frequency of vibration of ball trapped between two races. (69)  
d = ball dia (in)  
R<sub>N</sub> = load carried by ball

For a 310 bearing

$$k_N = 13.85 \times 10^{+6}$$

$$d = 0.75$$

$$k_N^{1/3} = 2.42 \times 10^{+2}$$

$$d^{3/2} = 0.65$$

$$f_n = \frac{20 (2.42) 10^2}{0.65} \times R_N^{1/6}$$

$$f_n = 7450 R_N^{1/6} \text{ cps}$$

(70)

In a radial bearing,  $(R_N)_{\max} \approx \frac{4.37}{n} \times R_{\max}$   
Applied load on bearing  
No. of balls

$$\text{For } n = 8, \quad (R_N)_{\max} \approx 0.5 R_{\max}$$

THE FRANKLIN INSTITUTE • *Laboratories for Research and Development*

I-A2321-1

For this size bearing,  $R_{\max}$  is on the order of 100 lbs or less in electric motor applications.

$$(R_N)_{\max} \simeq 50 \text{ lbs}$$

$$(R_N)_{\max}^{1/6} \simeq 1.92$$

As the balls move around the bearing, their minimum load (in the unloaded zone) is that due to centrifugal force, and the natural frequency will be as specified in the previous section. As the balls come into the load zone, the inner race contact comes into play and the resonant frequency increases as  $R_N$  increases until the ball is directly under the load, after which  $R_N$  decreases. Thus, for the 310 bearing

$$f_{N\max} \simeq 15,000 \text{ cps} \quad \leftarrow \quad \text{under max load}$$

$$f_{N\min} \simeq 7500 \text{ cps} \quad \leftarrow \quad \text{minimum load (2 springs)}$$

$$f_{N\min} \simeq 5400 \text{ cps (N = 1800 RPM)} \quad \leftarrow \quad \text{centrifugal force load (1 spring)}$$

For pure axial load, each ball is loaded at

$$R_N = \left(\frac{T}{n}\right) \frac{1}{\sin \beta}$$

Where  $T$  = Thrust load  
 $n$  = No. of balls  
 $\beta$  = Contact angle

Let  $\beta = 10^\circ$

$$R_N = \frac{T}{8} \times \frac{1}{0.139} \simeq 0.9T$$

From before, the resonant frequency of vibration of a loaded  $\frac{3}{4}$  inch diameter ball in a 310 bearing is  $\{Eq. (70)\}$  ;

$$f_n = 7450 R_N^{1/6}$$

$$\therefore f_n = 7450 T^{1/6} (.9)^{1/6}$$

$$f_n = 7310 T^{1/6}$$

← Resonant frequency of vibration of loaded ball due to axial load T.

<u>T</u>	<u>T<sup>1/6</sup></u>	<u>f<sub>n</sub></u>	
5	1.31	9,560	
10	1.47	10,750	
15	1.57	11,500	← Anderometer test load
20	1.65	12,050	
30	1.76	12,900	
50	1.92	14,000	
100	2.16	15,800	← Electric motor preload
150	2.30	16,800	

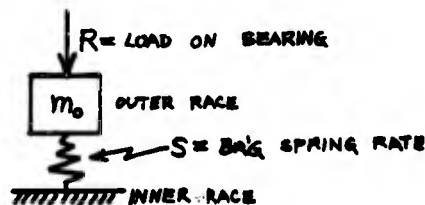
#### 3.2.1.4 Resonant Frequencies of Vibration of Inner and Outer Rings

In this section, we shall neglect the mass of the balls and consider a rigid outer race and a rigid inner race coupled together by the bearing's resultant spring rate (Section 3.2.1.1.5). In the work which follows, three modes of vibration are considered:

1. Free outer race and fixed inner race.
2. Free inner race and fixed outer race.
3. Free inner race and free outer race.

### 3.2.1.4.1 Free Outer Race And Fixed Inner Race

In most bearing vibration studies, the outer race is free and the inner race is supported on a rotating spindle. If the spindle runs true and if the bore of the bearing has an interference fit, the assumed conditions of free outer and fixed inner would be approximated. Neglecting the ball masses, we would have the simple spring-mass system shown below.



Assuming small vibrations ( $S \approx \text{constant}$ )

$$\omega_n^2 = \frac{S}{m_o}$$

$S$  is dictated by these following considerations

1. Bearing clearance or interference
2. Magnitude of applied load
3. Size and series of bearing
4. No. of balls in bearing

$m_o$  is dependent upon bearing size and series.

To evaluate frequencies, we shall investigate a 310 bearing.

Consider first a 310 bearing with zero clearance,

From Figure 38

$$S_o = 12.93 \times 10^4 \times R^{1/3} \quad \text{lbs/in}$$

$$m_o = \frac{15.5/16 \text{ lbs}}{386} = 25 \times 10^{-4} \frac{\text{lbs} \cdot \text{sec}^2}{\text{in.}}$$

$$\therefore \omega_n^2 = \frac{12.93 \times 10^4}{25 \times 10^{-4}} \times R^{1/3}$$

$$\omega_n^2 = 0.517 \times 10^8 R^{1/3}$$

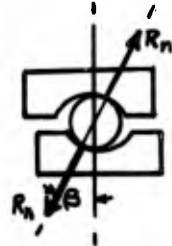
$$\omega_n = 0.72 \times 10^4 R^{1/6}$$

$$f_n = 11.5 \times 10^2 R^{1/6} \text{ cps}$$

<u>R</u> <u>lbs</u>	<u>R</u> <sup>1/6</sup>	<u>f<sub>n</sub></u> <u>cps</u>	
1	1	1150	← outer ring wt = 1 lb.
10	1.47	1690	
20	1.65	1900	
30	1.76	2020	← typical } for 310 br'g ≈ 30 lbs
40	1.85	2130	rotor wt. }
50	1.92	2210	
100	2.16	2480	
500	2.82	3240	
1000	3.16	3630	
5000	4.15	4770	

Virtually the same frequencies would be obtained for a bearing with clearance (See Figure 39) since spring rates are of almost the same magnitude for all but the very smallest loads ( $R < 1 \text{ lb}$ ).

For a bearing with interference, a linear spring rate of high magnitude is available over an appreciable load range beyond which spring rates similar to a zero clearance bearing are obtained. (See Fig. 40). In practice, radial interference is achieved by axial pre-load (T).



$$T_n = \frac{T}{n} = \frac{\text{AXIAL PRELOAD}}{\text{No. OF BALLS}} ; \beta = \text{CONTACT ANGLE}$$

$$R_n = \left(\frac{T}{n}\right) \frac{1}{\sin \beta} = k_n \delta_n^{3/2}$$

A vector diagram showing a right-angled triangle. The horizontal base is labeled \$(T/n)\$. The hypotenuse is labeled \$R\_n\$. The angle between the vertical side and the hypotenuse is labeled \$\beta\$.

$$\therefore \text{The radial interference } \delta_n \times \cos \beta = \left[ \left(\frac{T}{n}\right) \frac{1}{k_n} \cdot \frac{1}{\sin \beta} \right]^{2/3} \times \cos \beta$$

For 310 br'g (\$\beta \approx 10^\circ\$)

$$\therefore \delta_n \cos \beta = 0.98481 \left[ \frac{T}{8(13.85)10^6 \times (.17865)} \right]^{2/3}$$

$$\delta_n = 0.139 \times 10^{-4} [T]^{2/3} \quad (71)$$

T = axial preload

When preloaded and with no radial load

$$S_i = 6 k_N \delta_n^{1/2}$$

$$\therefore S_i = 6(13.85)10^6 \left\{ 0.139 \times 10^{-4} T^{2/3} \right\}^{1/2}$$

$$S_i = 83.10 \times 10^6 \left\{ 0.372 \times 10^{-2} T^{1/3} \right\}$$

$$S_i = 31 \times 10^4 T^{1/3}$$

The resonant frequency of vibration is

$$\omega_n^2 = \frac{S_i}{m_o} = \frac{31 \times 10^4 T^{1/3}}{25 \times 10^{-4}} = 1.24 \times 10^8 T^{1/3}$$

$$\omega_n = 1.11 \times 10^4 T^{1/6}$$

$$f_n = 17.7 \times 10^2 T^{1/6} \quad \text{cps}$$

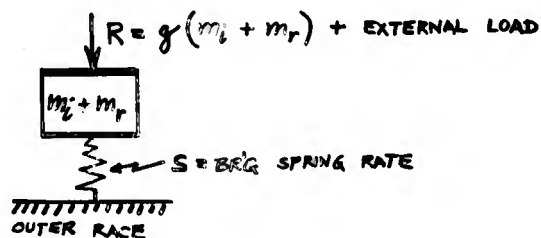
T = total axial preload

( $\beta = 10^\circ$ )

<u>T</u> (lbs)	<u>T</u> <sup>1/6</sup>	<u>f<sub>n</sub></u> (cps)	
5	1.31	2320	
10	1.47	2600	
15	1.57	2780	← Anderometer test load
20	1.65	2920	
30	1.76	3120	
50	1.92	3400	
100	2.16	3820	← Electric motor preload
150	2.30	4070	

### 3.2.1.4.2 Free Inner Race And Fixed Outer Race

This condition is approximated in an electric motor. In this case, the outer race is confined and the inner race mounted on the rotor is free.





The moving mass is the inner race and the rotor

As before,

$$\omega_n^2 = \frac{S}{m_i + m_r}$$

For a 310 bearing with or without clearance,

$$S_c \approx S_o = 12.93 \times 10^4 \times R^{1/3}$$

For zero external load (rotor load only)

$$R = 386(m_i + m_r)$$

$$S_c \approx S_o = 12.93 \times 10^4 (7.3)(m_i + m_r)^{1/3} = 94.5 \times 10^4 (m_i + m_r)^{1/3}$$

$$\therefore \omega_n^2 = \frac{S_o}{m_i + m_r} = \frac{94.5 \times 10^4}{(m_i + m_r)^{2/3}}$$

$$\omega_n = \frac{9.8 \times 10^2}{(m_i + m_r)^{1/3}}$$

$$f_n = \frac{1.56 \times 10^2}{(m_i + m_r)^{1/3}}$$

$$m_i \approx \frac{10.5/16}{386} = 1.71 \times 10^{-3}$$

$$m_r \approx \frac{60/2}{386} \quad 0.077 = 77 \times 10^{-3}$$

$$m_i + m_r \approx 79 \times 10^{-3}$$

$$(m_i + m_r)^{1/3} = (79)^{1/3} \times 10^{-1} = 0.43$$

$$f_n = \frac{156}{0.43}$$

$$f_n = 362 \text{ cps}$$

↙ Resonant frequency of 60 lb rotor supported on two-310

bearings as dictated by zero clearance spring rates and rotor mass  
(outer race fixed) No. axial preload.

For a substantial axial preload ( $T \approx 2 \times \text{rotor wt.}$ )

$$S_i = 31 \times 10^4 T^{1/3} \text{ (See previous section)}$$

$$\text{Let } T = 2 \times (\text{rotor wt.}) = 120 \text{ lbs.}$$

$$\therefore S_i = 152 \times 10^4$$

$$\omega_n^2 = \frac{152 \times 10^4}{(m_i + m_r)} = \frac{150 \times 10^4}{7.9 \times 10^{-4}} = 19 \times 10^6$$

$$f_n = \frac{\omega_n}{2\pi} = \frac{4.35 \times 10^3}{6.28} =$$

$$f_n = 692 \text{ cps}$$

↙ Natural frequency of 60 lb rotor supported on two-310

br'gs with 120 lb axial preload ( $\beta \approx 10^\circ$ ).

With the outer race fixed and the inner race free and axially  
preloaded with no rotor mass,

$$\omega_n^2 = \frac{S_i}{m_i} = \frac{31 \times 10^4 T^{1/3}}{0.171 \times 10^{-2}}$$

$$f_n = \frac{\omega_n}{2\pi} = \frac{13.5 \times 10^3 T^{1/6}}{2\pi}$$

$$f_n = 2140 \times T^{1/6} \text{ cps}$$

$T$  = total axial preload

$$\beta \approx 10^\circ$$

For a 15-lb axial load only (Anderometer test load) this yields a frequency of 3360 cps.



### 3.2.1.4.3 Free Inner And Outer Rings

With both the inner and outer rings free to vibrate

$$\omega_n^2 = S \left( \frac{m_i + m_o}{m_i m_o} \right)$$

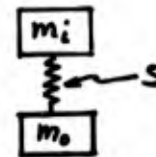
For axially preloaded 310 br'gs

$$S = S_i = 31 \times 10^4 T^{1/3}$$

$$\omega_n^2 = 31 \times 10^4 T^{1/3} \left( \frac{25 + 17.1}{25 \times 17.1} \right) \frac{10^{-4}}{10^{-8}}$$

$$\omega_n^2 = 31 \times 10^4 T^{1/3} (.0984) 10^4 = 3.05 \times 10^8 T^{1/3}$$

$$f_n = 2720 \times T^{1/6} \text{ cps} \quad T = \text{total axial preload}$$



For a 15-lb axial load only (Anderometer test load) this yields a frequency of 4300 cps.

### 3.2.1.5 Resonant Frequencies of Vibration of Inner Ring-Balls-Outer Ring System

In this section we shall consider a rigid outer ring, rigid inner ring and rigid balls coupled together by the individual ball-race contact springs. In the work which follows, three modes of vibration are considered.

1. Free outer race and fixed inner ring
2. Free inner ring and fixed outer ring
3. Free inner ring and free outer ring

The vibrational characteristics of these several multi-degree of freedom systems will be dependent upon the ball-race contact spring rates existing within the bearing as dictated by the loading conditions

I-A2321-1

to which the bearing is subjected. In a 310 bearing, 10 masses (2 rings and 8 balls) may vibrate when coupled together by as many as 16 non-linear springs. An analog computer solution would be the only practical way of evaluating the frequency response of such a complex system. As a very simple approach to the problem, we shall combine the ball masses to obtain a total of three masses and reduce the number of springs to two which couple the balls to the inner and outer rings. The problem will be even further simplified to consider only axially preloaded bearings. If this were the case, the system could be represented as shown below.



$$\text{where } k_i = k_o = 3k_N i^{1/2} = 3k_N \left\{ 0.139 \times 10^{-4} (T)^{2/3} \right\}^{1/2}$$

$$k_i = k_o = 1.13 k_N \times 10^{-2} (T^{1/3})$$

$$\text{For a 310 br'g, } k_N = 13.85 \times 10^6$$

$$k_i = k_o = 15.7 \times 10^4 (T^{1/3})$$

Assume that the lumped ball mass is equal to that of 4 balls,

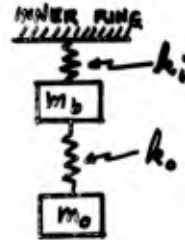
$$\therefore m_b = 4 \times (3.84 \times 10^{-4} d^3) = 15.36 \times 10^{-4} (d)^3$$

$$m_b = 6.47 \times 10^{-4}$$

$$m_o = 25 \times 10^{-4}$$

### 3.2.1.5.1 Free Outer Ring and Fixed Inner Ring

For this case we have



The two natural frequencies are

$$\omega_n^2 = \frac{1}{2} \left[ \frac{k_i + k_o}{m_b} + \frac{k_o}{m_o} \right] \pm \frac{1}{2} \sqrt{\left[ \frac{k_i + k_o}{m_b} + \frac{k_o}{m_o} \right]^2 - 4 \frac{k_i k_o}{m_b m_o}}$$

$$k_i = k_o = 2 \left[ 15.7 \times 10^4 T^{1/3} \right]$$

$$\frac{k_i + k_o}{m_b} = \frac{31.4 \times 10^4 T^{1/3}}{6.47 \times 10^{-4}} = 4.85 \times 10^8 T^{1/3}$$

$$\frac{k_o}{m_o} = \frac{15.7 \times 10^4 T^{1/3}}{25 \times 10^{-4}} = 0.628 \times 10^8 T^{1/3}$$

$$\therefore \frac{1}{2} \left[ \frac{k_i + k_o}{m_b} + \frac{k_o}{m_o} \right] = 2.74 \times 10^8 T^{1/3}$$

$$\left[ \frac{k_i + k_o}{m_b} + \frac{k_o}{m_o} \right]^2 = 30 \times 10^{16} T^{2/3}$$

$$\frac{4 k_i k_o}{m_b m_o} = \frac{4 \left[ 15.7 \times 10^4 T^{1/3} \right]^2}{6.47 \times 10^{-4} (25 \times 10^{-4})} = 6.08 \times 10^{16} T^{2/3}$$

$$\therefore \frac{1}{2} \sqrt{\left[ \frac{k_i + k_o}{m_b} + \frac{k_o}{m_o} \right]^2 - 4 \frac{k_i k_o}{m_b m_o}} = 2.45 \times 10^8 T^{1/3}$$

$$\therefore \omega_n^2 = [2.74 \pm 2.45] 10^8 T^{1/3}$$

$$\omega_n^2 = [5.19 \text{ or } 0.3] 10^8 T^{1/3}$$

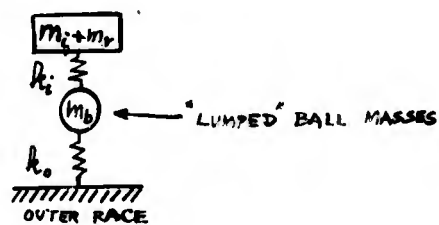
$$\omega_n = [2.28 \text{ or } 0.55] 10^4 \times T^{1/6}$$

$$f_n = (3630 \text{ and } 870) \times T^{1/6} \text{ cps} \quad T = \text{axial preload}$$

<u>T</u> <u>lbs</u>	<u>T<sup>1/6</sup></u>	<u>f<sub>n1</sub></u> <u>(cps)</u>	<u>f<sub>n2</sub></u> <u>(cps)</u>	
5	1.31	1140	4750	
10	1.47	1280	5350	
15	1.57	1370	5700	← Anderometer test load
20	1.65	1430	6000	
30	1.76	1530	6400	
50	1.92	1670	7000	
100	2.16	1880	7850	
150	2.30	2000	8350	

### 3.2.1.5.2 Fixed Outer Ring And Free Inner Ring

In this case we have



The natural frequency is,

$$\omega_n^2 = \frac{k}{2(m_i + m_r)} \left( \frac{2(m_i + m_r)}{m_b} \right) \left[ 1 \pm \sqrt{1 - \frac{m_b}{m_i + m_r}} \right]$$

Since  $(m_i + m_r) \gg m_b$

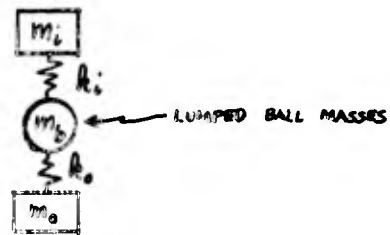
$$\omega_{n1}^2 \approx \frac{k}{2(m_i + m_r)} = \text{natural frequency of rotor neglecting ball mass}$$

$$\omega_{n2}^2 \approx \frac{2k}{m_b} = \text{natural frequency of trapped balls between two springs}$$

These frequencies have been evaluated previously.

### 3.2.1.5.3 Free Outer Ring and Free Inner Ring

For this case



For this situation, the natural frequency is

$$\omega^4 - \frac{k_i k_o}{m_i m_b m_o} \left[ \frac{m_i m_b + m_i m_o}{k_i} + \frac{m_b m_o + m_i m_o}{k_o} \right] \omega^2 + \frac{k_i k_o (m_i + m_b + m_o)}{m_i m_b m_o} = 0$$

Since  $k_i = k_o = k$

I-A2321-1

This can be reduced to the following

$$\omega^2 = \frac{k}{2m_1m_bm_o} [m_1m_b + 2m_1m_o + m_bm_o] \left\{ 1 \pm \sqrt{1 - \frac{4(m_1 + m_b + m_o)(m_1m_bm_o)}{[m_1m_b + 2m_1m_o + m_bm_o]^2}} \right\}$$

For a 310 BR'G with  $m_1 = 17 \times 10^{-4}$ ,  $m_b = 6.5 \times 10^{-4}$  and  $m_o = 25 \times 10^{-4}$

$$\omega^2 = \frac{k(11.23 \times 10^{-6})}{2(27.6)10^{-10}} \left\{ 1 \pm \sqrt{1 - \frac{4(48.5 \times 10^{-4})(27.6 \times 10^{-10})}{126.5 \times 10^{-12}}} \right\}$$

$$\omega^2 = 0.204 \times 10^4 k \left\{ 1 \pm \sqrt{1 - .424} \right\} = 0.204 \times 10^4 k \left\{ 1 \pm 0.76 \right\}$$

$$\omega^2 = (0.36 \text{ and } 0.049)10^4 \times k$$

Since  $k = k_1 = k_o = 15.7 \times 10^4 T^{1/3}$

$$\omega^2 = (5.65 \text{ and } 0.77)10^8 T^{1/3}$$

$$\omega = (2.38 \text{ and } 0.85) 10^4 T^{1/6}$$

$$\therefore f_n = (3.8 \text{ and } 1.35)10^3 T^{1/6} \text{ cps}$$

T = axial load

<u>T</u> (lbs)	<u>T<sup>1/6</sup></u>	<u>f<sub>n1</sub></u> (cps)	<u>f<sub>n2</sub></u> (cps)
5	1.31	1770	5000
10	1.47	1980	5600
15	1.57	2120	5960
20	1.65	2230	6270
30	1.76	2380	6700
50	1.92	2600	7500
100	2.16	2920	8200
150	2.30	3100	8750

← Anderometer test load



3.2.1.6 Summary of Ball Bearing Vibrational Response Characteristics

The lower modes of natural vibration of the inner and outer rings and the cage lie within the range of frequencies generated within a ball bearing. Hence, if these components are excited at frequencies close to their natural frequencies, vibration will be amplified. Figures 45 and 46 show this for amplification of vibration in flexure of the outer race as a function of the waviness of inner and outer races of a 310 bearing. As can be seen, considerable amplification is possible for certain, discrete values of waviness.

The multiple ball-race contact spring rates and ball, race and rotor masses combine to yield a multitude of resonant frequencies in the range of 300 cps to 15,000 cps.

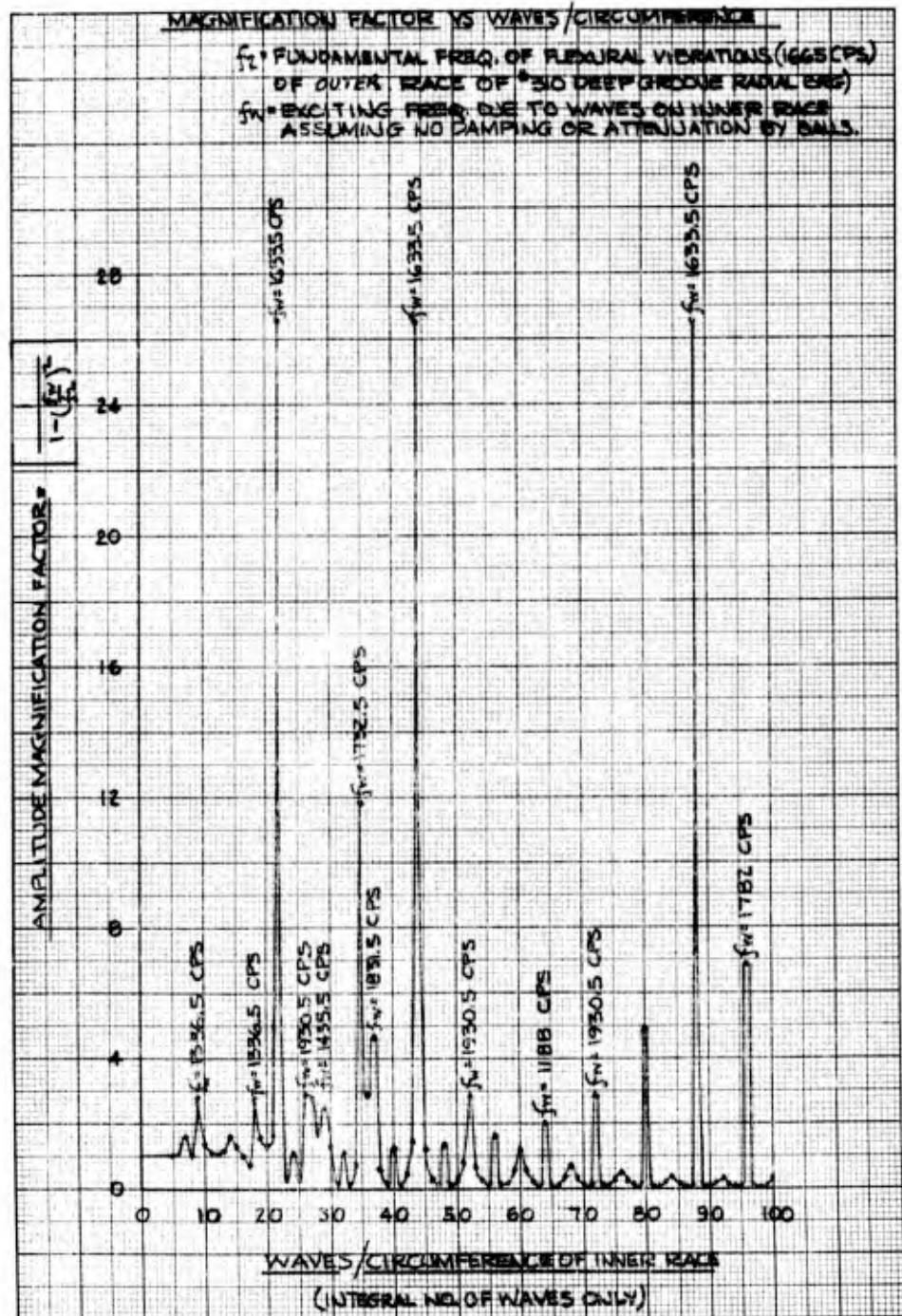


Figure 45

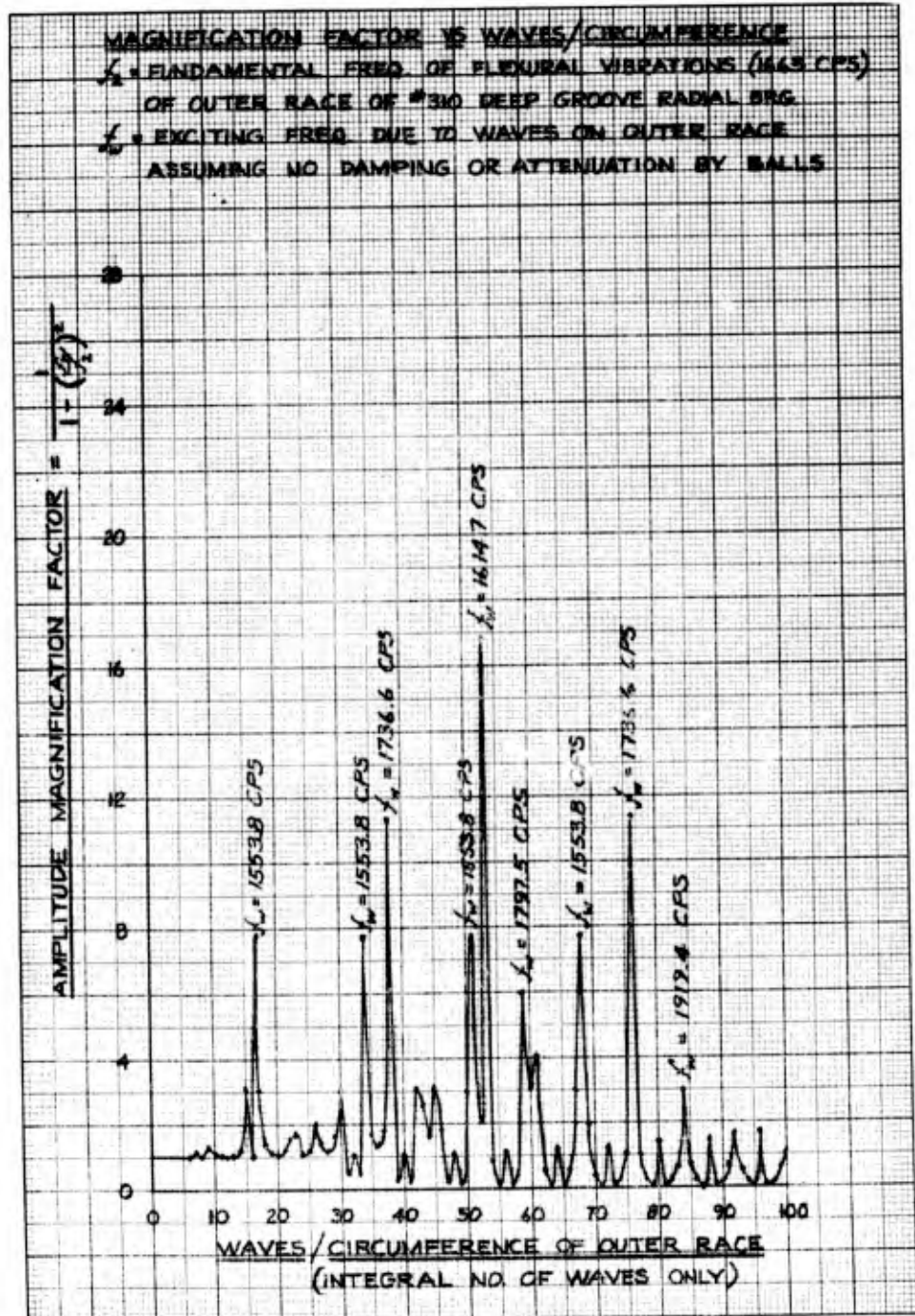
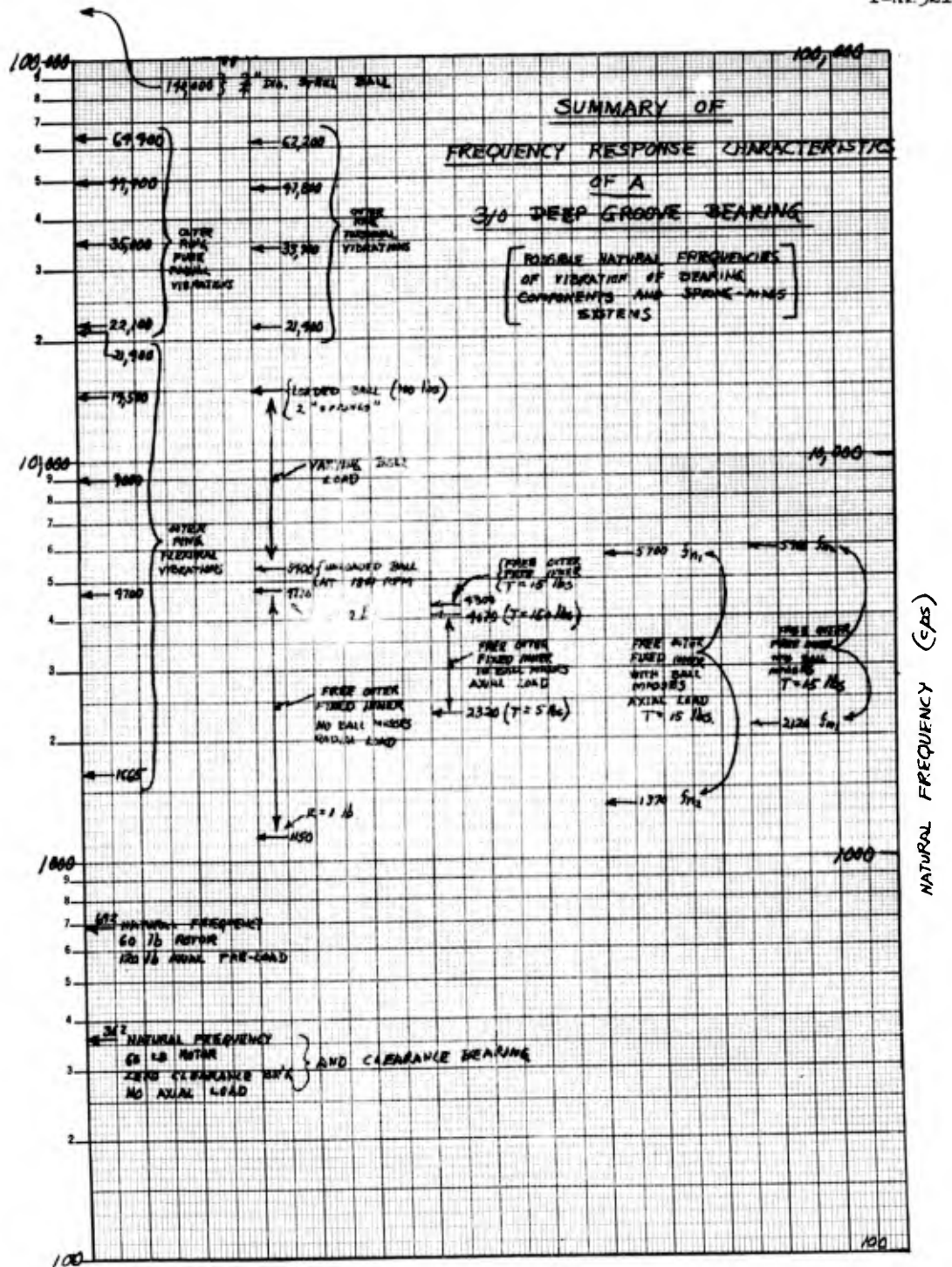


Figure 46

THE FRANKLIN INSTITUTE • *Laboratories for Research and Development*

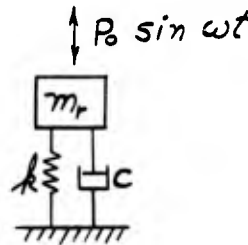
I-A2321-1

Figure 47 presents a graphic summary of the vibrational response characteristics of a 310 bearing as determined within section 3.2.1. These results indicate that disturbing frequencies of relatively high frequency (greater than approximately 300 cps) and comparatively low amplitude can be amplified by the bearing due to the excitation of resonant frequencies of vibration. This is discussed in more detail in the study on noise and vibration transmission. In a ball bearing there are many sources of vibration (See Fig. 10) covering the frequency range (at 1800 RPM) from 10 cps to 30,000 cps which, conceivably, could excite the bearing components and various spring-mass systems to vibrate at high amplitudes at particular frequencies to which they will respond.



### 3.2.2 Sliding Surface Bearings

The vibrational response of a journal bearing supported system to periodic disturbing forces is dictated by the fluid film spring rate, damping and the mass being vibrated. Since the journal is an integral part of the rotor and the bearing is an integral part of the housing, none of the bearing components can exhibit natural frequencies of free vibration nor are other vibrating spring mass systems established by the bearing. Hence, assuming only a single degree system, the vibrating system may be represented schematically, as shown below.\*



The response of such a damped-single degree of freedom system may be written in terms of the amplification factor,  $x_o/x_{st}$ , as

$$\frac{x_o}{x_{st}} = \left[ \frac{1}{(1 - \frac{\omega^2}{\omega_n^2})^2 + 4(\frac{c}{c_c})^2(\frac{\omega}{\omega_n})^2} \right]^{1/2} \quad (72)$$

The undamped natural frequency of the system,  $\omega_n$ , requires knowledge of the fluid film spring rate. The critical damping constant,  $c_c$  in turn is dependent upon spring rate and mass. Thus, in what follows, the load-displacement characteristics of journal bearings are investigated and means developed for computing spring rates. This is followed by the

\* A somewhat more rigorous approach to the problem is outlined in Section 3.3.2.1.

determination of the damping ratio,  $(\frac{c}{c_c})$  afforded by journal bearings, which then allows the determination of vibrational response as dictated by Equation (72).

### 3.2.2.1 Load-Displacement Characteristics and Spring Rates

The relationship between load and displacement for finite length, 360° journal bearings operating on a full film of lubricant with unidirectional load is well known. Figure 48 shows the eccentricity ratio (displacement of journal from center of bearing) and attitude angle (line of journal and bearing centers) as a function of bearing characteristic number for an L/D ratio = 1.0. These plots are based on material in the reference 1. Nomenclature is indicated on the figure. By means of this chart, one may find the magnitude and direction of displacement of the center of the journal as a function of applied load (W), speed (N), viscosity of lubricant (Z), and bearing dimensions (L, D and C). Figure 49 shows the journal center locus. At very light loads the journal is virtually centered within the bearing. As load is applied, the journal moves off the center of the bearing and becomes eccentric.

Notice that, in this case, the journal moves almost at right angles to the direction of the load. As load increases the journal follows the path shown. At  $\epsilon \approx 0.72$ , additional load causes further displacement only in the direction of load. For still further loading, the journal will move back in toward the vertical centerline of the bearing.



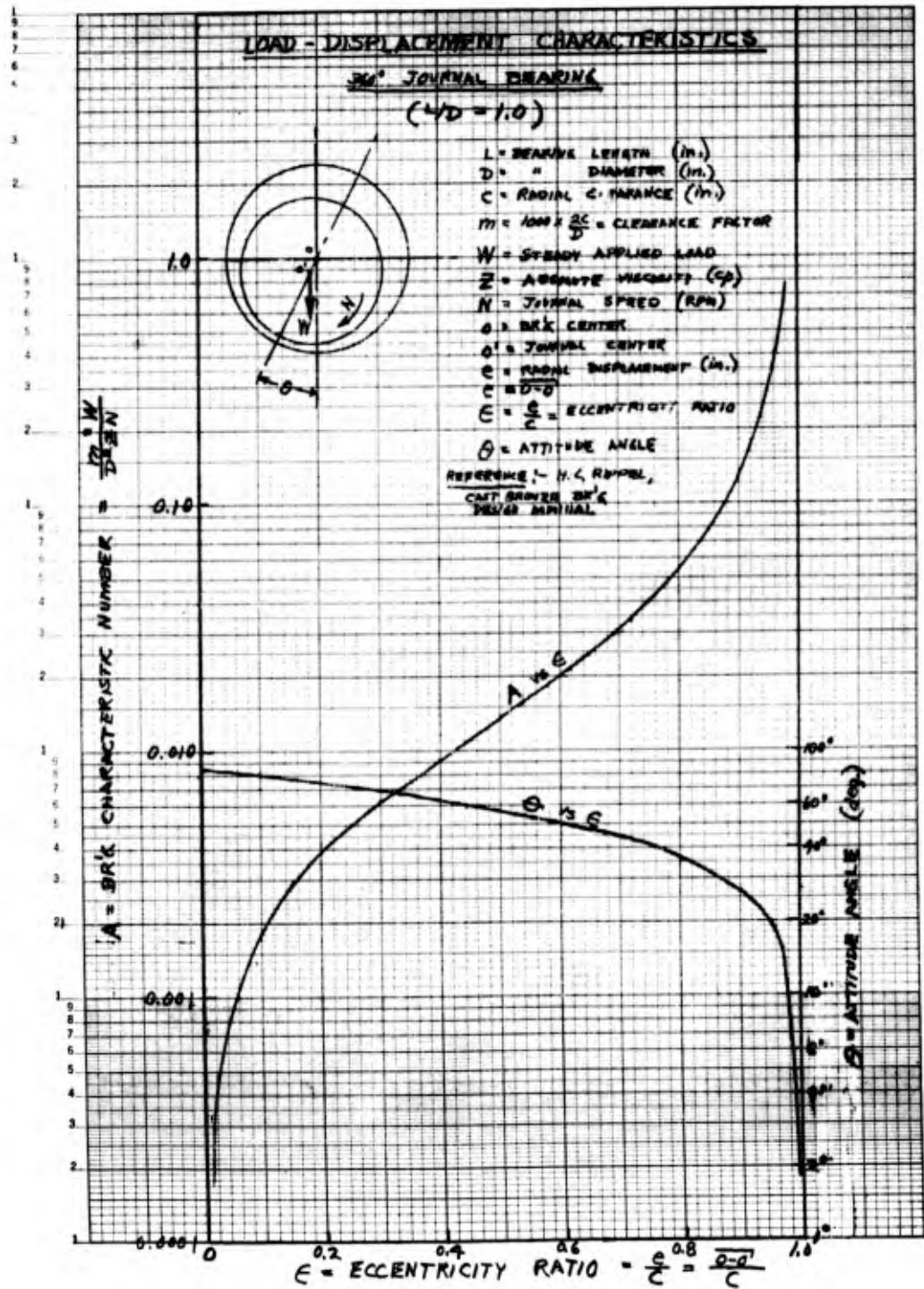


Figure 48



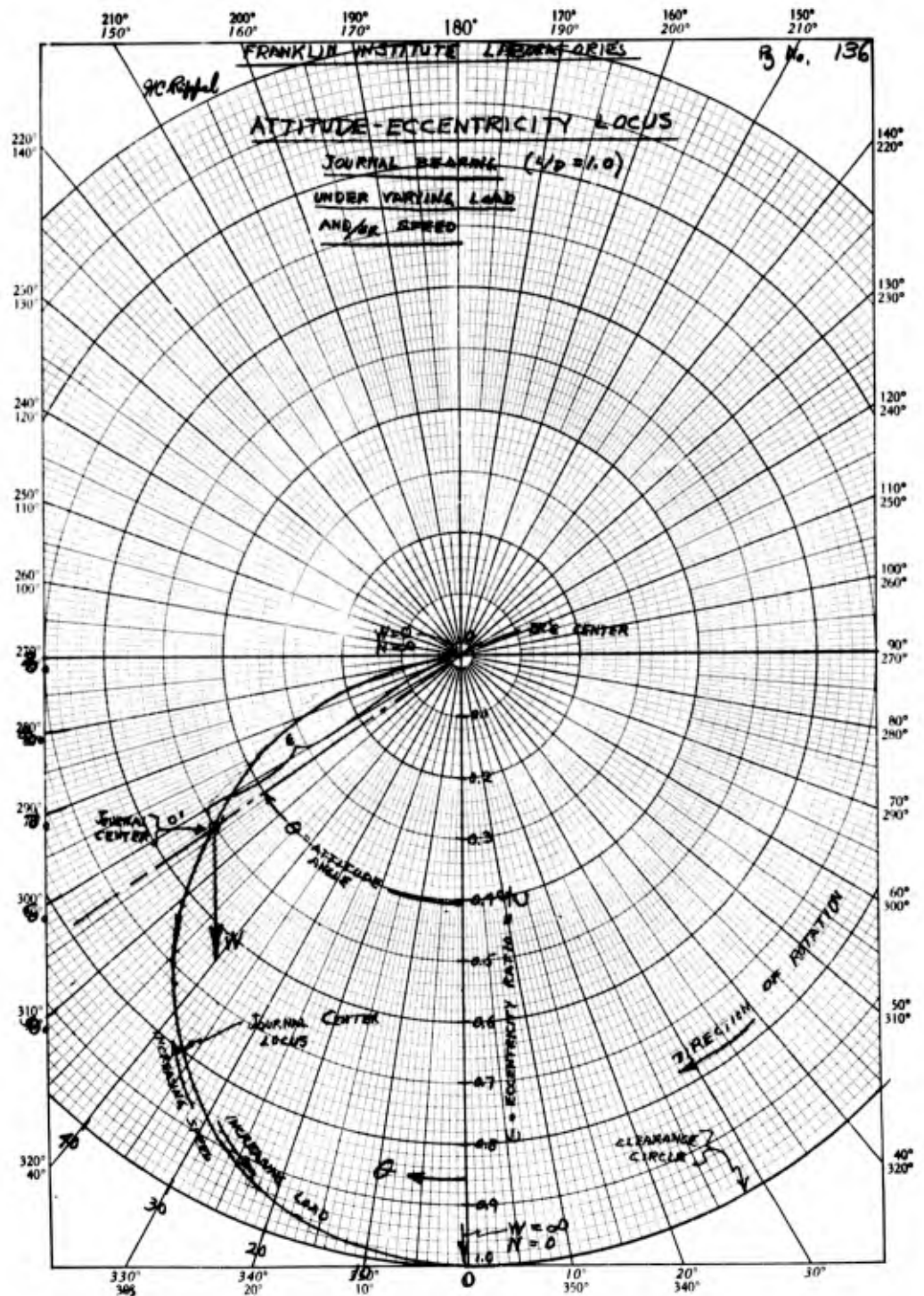


Figure 49

The load-displacement characteristics of a full-film lubricated bearing are quite non-linear particularly at appreciable levels of load. Hence, spring rates, as such, are a function of the bearing characteristic number. Also, for a given set of operating conditions ( $A = \text{constant}$ ), the spring rate will vary with direction. For example, the spring rate in the direction of the applied (steady) load will be different from the spring rate in any other direction. Such "local spring rates" are defined as follows. (See Figure 50).

$$k_a = \frac{d(W \cos \alpha)}{c \cdot d \left( \frac{\epsilon \cos \theta}{\cos \alpha} \right)}, \text{ lbs/in.} \quad (73)$$

where  $k_a$  = local spring rate in " $\alpha$ " direction (lbs/in.)

$\alpha$  = angle between direction of spring rate  $k_a$  and direction of applied load (deg.)

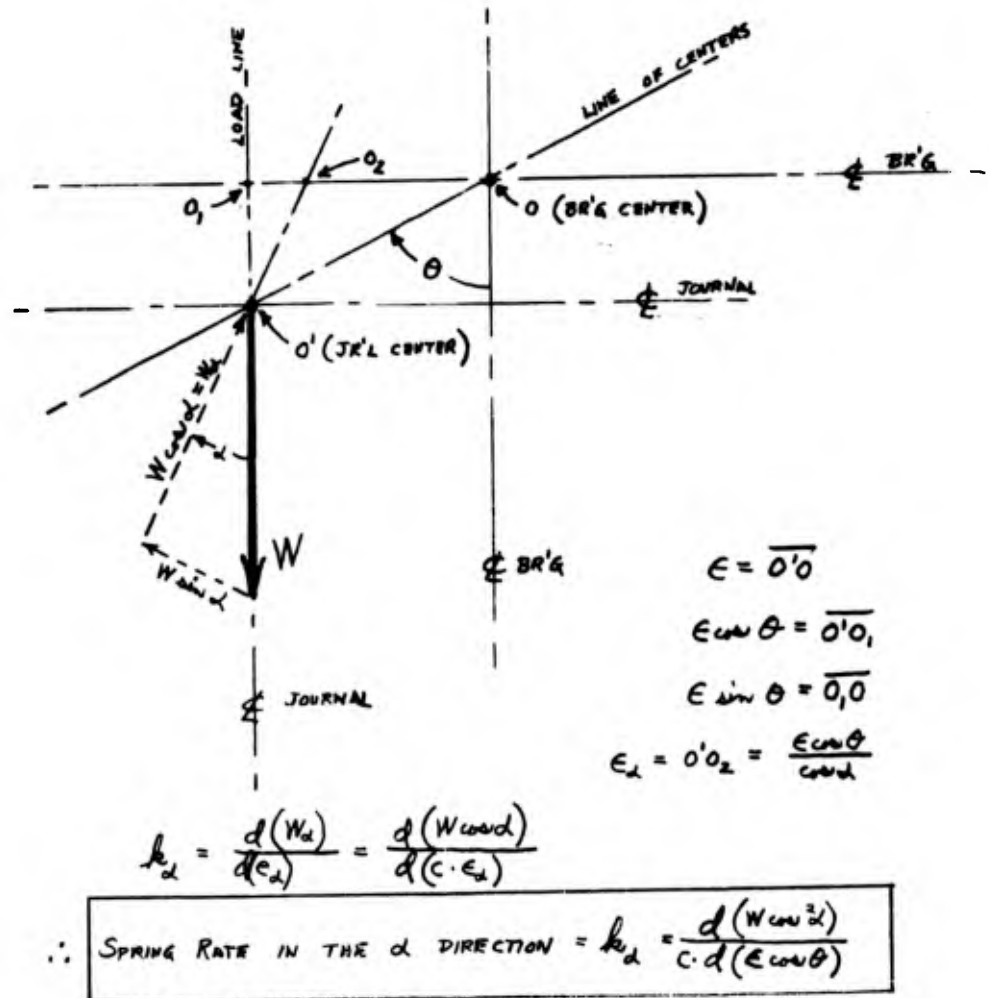
$\theta$  = attitude angle (line of centers) (deg.)

$W$  = applied load (lbs.)

$C$  = radial clearance (in.)

Substituting for  $W$  in terms of the bearing characteristic number, ( $A$ ), gives

$$k_a = \frac{d(A \cdot \cos \alpha)}{d \left( \frac{\epsilon \cos \theta}{\cos \alpha} \right)} \times \frac{2 D Z N \times 10^3}{m^3}, \text{ lbs/in.}$$



SLEEVE BEARING LOAD-DISPLACEMENT (SPRING RATE) GEOMETRY

Figure 50

THE FRANKLIN INSTITUTE • Laboratories for Research and Development

I-A2321-1

$$\text{Let } \frac{d(A \cdot \cos \alpha)}{d\left(\frac{e \cos \theta}{\cos \alpha}\right)} = S_{\alpha} = \text{local spring rate factor}$$

$$\therefore k_{\alpha} = \frac{2 D Z N \times 10^3}{m^3} (S_{\alpha}), \text{ lbs/in.} \quad (74)$$

For the radial spring rate (along the line of centers)

$$\alpha = \theta$$

$$S_{\theta} = \frac{d(A \cos \theta)}{d(e)} \quad (75)$$

This spring rate factor was evaluated by taking the slope of the  $A \cdot \cos \theta$  vs.  $e$  curve at various values of  $A$ . The results are shown in Figure 51 as  $S_{\theta}$  vs.  $A$ . Spring rate factors in the  $\alpha$  direction may then be evaluated as

$$S_{\alpha}|_A = S_{\theta}|_A \cdot \frac{\cos^2 \alpha}{\cos^2 \theta}|_A \quad (76)$$

These results are also plotted in Figure 51 as  $S_{\alpha}$  vs  $A$  for various values of  $\alpha$ .

Since, in Equation (74),  $D$ ,  $Z$ ,  $N$ ,  $m$ , and  $c$  are constant quantities for a given bearing,  $S_{\alpha}$  is proportional to the local spring rate. Hence, the variation in spring rate with "A" is shown in Figure 51. Since  $W$  is the only variable in "A" free to change, these plots of  $S_{\alpha}$  show the variation of spring rate with load.

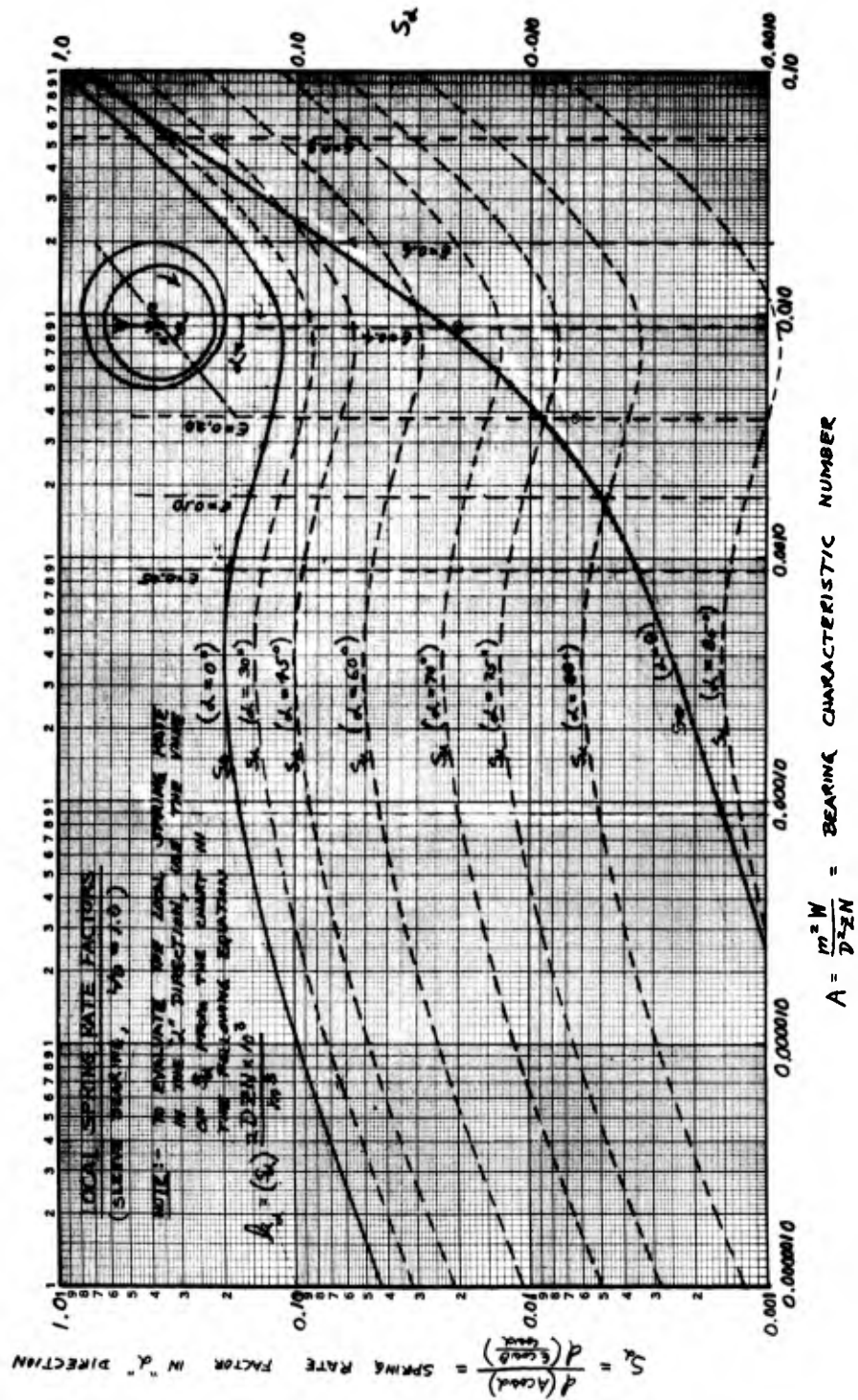


Figure 51

THE FRANKLIN INSTITUTE • *Laboratories for Research and Development*

I-A2321-1

Most sleeve bearings operate in the bearing characteristic number range from 0.00010 (light load, high speed) to 0.10 (high load, low speed). As may be seen in Figure 51, the radial spring rate factor, ( $S_0$ ), is quite low compared with the spring rate factor in the direction of load ( $S_\alpha$ ). The operating speed for the onset of one-half frequency whirl instability is dictated by the radial spring rate. The spring rate in a given direction ( $\alpha$ ) varies considerably as load changes. For a given set of operating conditions,  $S_\alpha$  decreases quite dramatically with increasing  $\alpha$ . Theoretically, the sleeve bearing has zero "stiffness" in the direction normal to the applied load.

Sleeve bearings can exhibit quite high stiffness as will be illustrated for a typical case. Consider a 60-lb. rotor supported by two, 2-inch diameter x 2-inch long sleeve bearings lubricated by an SAE 20 motor oil @ 130°F operating at 1800 RPM with a radial clearance of  $1.25 \times 10^{-3}$  inch.

From Equation (74)

$$k_\alpha = \frac{2 D Z N \times 10^3}{m^3} (S_\alpha) = \frac{2 \times 2(30)(1800)10^3}{(1.25)^3} S_\alpha$$

$$k_\alpha = 110 \times 10^6 S_\alpha \quad (77)$$

The bearing characteristic number for just the dead weight load is

$$A = \frac{m^2 W}{D^2 Z N} = \frac{(1.25)^2 \left( \frac{60}{2} \right)}{4 (30)(1800)} = 2.07 \times 10^{-4}$$

THE FRANKLIN INSTITUTE • *Laboratories for Research and Development*

I-A2321-1

From Figure 48

$$c \approx 0.010$$

$$\theta \approx 85^\circ$$

From Figure 51

$$S_o = 0.185$$

$$S_\theta = 0.00195$$

$$\therefore k_o = 110 \times 10^6 (0.185) = 20.5 \times 10^6 \text{ lbs/in.}$$

$$k_\theta = 110 \times 10^6 (.00195) = 0.216 \times 10^6 \text{ lbs/in.}$$

From section 3.2.1.1.5.2, the spring rate for a 310 bearing with clearance is;

$$R = 30 \text{ lbs.}$$

$$c \approx 2 \times 10^{-4} \text{ in.}$$

$$k_N = 13 \times 10^6$$

$$\frac{R}{c^{3/2} k_N} = \frac{30}{(2 \times 10^{-4})^{3/2} 13 \times 10^6} = \frac{30}{2.83(13)} = 0.786$$

From Figure 39

$$S_{c/1}^{1/2} k_N = 1.9$$

$$S_c = 1.9 (2 \times 10^{-4})^{1/2} 13 \times 10^6 = 34.9 \times 10^4$$

$$S_c = 0.349 \times 10^6 \text{ lbs/in.}$$

This value should be compared to  $k_o$  for the journal bearing since it is the spring rate in the direction of load.

THE FRANKLIN INSTITUTE • *Laboratories for Research and Development*

I-A2321-1

From section 3.2.1.1.5.1, the spring rate for a 310 bearing with zero clearance is

$$\frac{S_o}{R^{1/3}} = 12.9 \times 10^4 \text{ (Fig. No. 38)}$$

$$\therefore S_o = 12.9(30)^{1/3} \times 10^4$$

$$S_o = 0.401 \times 10^6 \text{ lbs/in.}$$

From section 3.2.1.1.5.3, the spring rate for a 310 interference bearing is,

$$S_i = 6 \times i^{1/2} k_N \text{ (Fig. 40; with all balls loaded)}$$

$$\text{For } i = 2 \times 10^{-4} \text{ in.}$$

$$S_i = 6(2 \times 10^{-4})^{1/2} 13 \times 10^6$$

$$S_i = 1.1 \times 10^6 \text{ lbs/in.}$$

$$\frac{R}{i^{3/2} k_N} = \frac{30}{(2 \times 10^{-4})^{3/2} (13)10^6}$$

$$\frac{R}{i^{3/2} k_N} = 0.786$$

Thus, at this level of load (30 lbs), sleeve bearing spring rates compare favorably with ball bearings.



THE FRANKLIN INSTITUTE • *Laboratories for Research and Development*

I-A2321-1

Maximum loads for bearings of 310 size (2" bore) are approximately 1500 pounds.

Therefore, for the sleeve bearing

$$A_{1500} = 2.07 \times 10^{-4} \times \frac{1500}{30} = 0.0104$$

From Figure 48, @  $A = .0104$

$$\epsilon \approx 0.44$$

$$\theta \approx 60^\circ$$

From Figure 51, @  $A = .0104$

$$S_o = 0.120$$

$$S_\theta = .028$$

From Equation (77)

$$k_a = 110 \times 10^6 S_a$$

$$\therefore k_o = 110 \times 10^6 (.120) = 13.2 \times 10^6 \text{ lbs/in.}$$

$$k_\theta = 110 \times 10^6 (.028) = 3.08 \times 10^6 \text{ lbs/in.}$$

For a 310 bearing with clearance ( $c = 2.0 \times 10^{-4}$  in.)

$$\frac{R}{c^{3/2} k_N} = \frac{1500}{(2 \times 10^{-4})^{3/2} 13 \times 10^6} = 39.3$$

From Figure 39, @  $R/c^{3/2} k_N = 39.3$ ,  $\frac{S_c}{c^{1/2} k_N} = 7.5$

$$S_c = 7.5 (2 \times 10^{-4})^{1/2} 13 \times 10^6$$

$$S_c = 1.38 \times 10^6 \text{ lbs/in.}$$

From Figure 39, we also see that the spring rate for a zero clearance 310 bearing is the same at this level.

Also with an interference 310 bearing

$$(i = 2.0 \times 10^{-4})$$

$$\frac{R}{i^{3/2} k_N} = 39.3$$

From Figure 40, the spring rate for this value of interference bearing parameter  $(\frac{R}{i^{3/2} k_N})$  gives the same spring rate as a zero clearance bearing. Thus, whether the 310 bearing has clearance, zero clearance, or interference, the spring rate at this level of load will be

$$S \approx 1.38 \times 10^6 \text{ lbs/in.},$$

which is considerably less than for the sleeve bearing.

Thus, it would appear that sleeve bearing spring rates are of the same order of magnitude (or greater) as for ball bearings. The sleeve bearing exhibits various spring rates in various directions as do ball bearings except for the lightly loaded interference bearing.

### 3.2.2.2 Damping Characteristics

The critical damping constant associated with the rotor mass-fluid film spring system is defined as,

$$c_c = 2 \left[ m_r k_a \right]^{1/2} \quad (78)$$

Considering a typical electric motor rotor weighing 60 pounds,

$$m_r = \frac{60/2}{g} = 0.0776 \frac{\text{lbs} \cdot \text{sec}^2}{\text{in.}}$$

For the same motor the journal bearing would have the following dimensions.

$$D = 2", L = 2", C = 1.25 \times 10^{-3} \text{ in.}$$

THE FRANKLIN INSTITUTE • *Laboratories for Research and Development*

I-A2321-1

For  $N = 1800$  RPM and a lubricant having a viscosity of 30 centripoises, we can use equation (74) to calculate  $k_a$  as,

$$k_a = \frac{2 D Z N \times 10^3}{m^3} \cdot S_a = \frac{2(2)(30)(1800)10^3}{(1.25)^3}$$

$$k_a = 110 \times 10^6 S_a \quad (79)$$

Substituting for  $m_r$  and  $k_a$  in (78) gives

$$\therefore c_c = 2 [ .0776 ]^{1/2} [ 110 \times 10^6 S_a ]^{1/2} = 5850 [ S_a ]^{1/2} \quad (80)$$

Virtually all journal bearings operate with a bearing characteristic number within the range,

$$0.000010 < A < 0.10.$$

From Figure 51 then

$$0.0010 < S_a < 1.0$$

Substituting in Equation (80) gives a range of  $c_c$  as,

$$185 < c_c < 5850 \frac{\text{lbs} - \text{sec}}{\text{in.}}$$

Sternlight\* gives some insight into damping as follows

$$c = L\mu \left(\frac{D}{C}\right)^3 \cdot \beta$$

$$L = 2", Z = 30 \text{ cp}, C = \text{diametral clearance} = 2.5 \times 10^{-3} \text{ in.}$$

$$\mu = \frac{Z}{6.875 \times 10^6} = 4.4 \times 10^{-6}$$

---

\* B. Sternlight, "Elastic And Damping Properties Of Cylindrical Journal Bearings, Jr'l of Basic Eng. Trans. ASME, June, 1959 pp. 101-110.

THE FRANKLIN INSTITUTE • *Laboratories for Research and Development*

I-A2321-1

$$\begin{aligned} \left(\frac{D}{C}\right) &= 0.8 \times 10^3 \\ c &= (2)(4.4)10^{-6}(.512)10^9 \cdot \beta \\ c &= 4.5 \times 10^3 \cdot \beta \end{aligned} \quad (81)$$

$\beta$  is the dissipation factor. From the same reference

$$10 < \beta < 100 \quad (L/D = 1.0)$$

$$\therefore c_{\min} = 4500 \frac{\text{lb} - \text{sec}}{\text{in.}}$$

$$c_{\max} = 450 \times 10^3 \frac{\text{lb} - \text{sec}}{\text{in.}}$$

Normally,  $c_c$  is high when  $c$  is high and  $c_c$  is low when  $c$  is low.

Hence, gross extremes of  $\left(\frac{c}{c_c}\right)$  are

$$\left(\frac{c}{c_c}\right)_{\min} = \frac{c_{\min}}{(c_c)_{\max}} = \frac{4500}{5850}$$

$$\left(\frac{c}{c_c}\right)_{\min} \approx 0.8$$

$$\left(\frac{c}{c_c}\right)_{\max} = \frac{c_{\max}}{(c_c)_{\min}} = \frac{4500 \times 10^2}{185}$$

$$\left(\frac{c}{c_c}\right)_{\max} \approx 2500$$

Thus, it would appear that sleeve bearings (as used in electric motor applications) are quite highly overdamped or, at the least, critically damped. This implies no amplification of vibration amplitudes. Thinking ahead, it also implies essentially unity transmission of disturbing forces regardless of frequency.

### 3.2.2.3 Vibrational Response

The vibrational amplitude amplification factor as given in (72) can also be written as,

$$\frac{x_o}{x_{st}} = \left[ \frac{1}{\left(1 - \frac{f^2}{f_n^2}\right)^2 + 4\left(\frac{c}{c_c}\right)^2 \left(\frac{f}{f_n}\right)^2} \right]^{1/2} \quad (82)$$

The undamped natural frequency is

$$f_n = \frac{1}{2\pi} \left[ \frac{k_a}{m_r} \right]^{1/2} \quad (83)$$

For the same typical rotor and journal bearings as cited in the previous section,

$$\begin{aligned} f_n &= \frac{1}{2\pi} \left[ \frac{110 \times 10^6 S_a}{0.0776} \right]^{1/2} \\ f_n &= 6000 S_a^{1/2} \end{aligned} \quad (84)$$

It is interesting to note that for

$$0.0010 < S_a < 1.0,$$

the undamped natural frequency range is,

$$190 < f_n < 6000 \text{ cps}$$

For common motor speeds,

$$5 < \frac{f_n}{f_i} < 200$$

THE FRANKLIN INSTITUTE • *Laboratories for Research and Development*

I-A2321-1

Since the journal bearing does not generate disturbing forces in this frequency range, the excitation must come from some other source.

Consider the typical motor to be horizontal with its two journal bearings each supporting 30 pounds. The bearing characteristic number, A, becomes,

$$A = \frac{m_W^2}{D^2 Z N} = \frac{(1.25)^2 (30)}{(4)(30)(1800)} \approx 0.0002$$

For this condition, from Figure 48

$$\epsilon = 0.010, \theta = 85^\circ$$

From Figure 51 @ A = .0002

$$S_\theta = 0.00195$$

$$S_{0^\circ} = 0.185$$

$$S_{90^\circ} \rightarrow 0$$

From Equation (81),

$$c = 4.5 \times 10^3 \beta \frac{\text{lb} - \text{sec}}{\text{in.}}$$

In reference 2, values of  $\beta$  vary with direction. However in this case since  $\epsilon \neq 0$ ,  $\beta \approx \beta @ \epsilon = 0$  for all directions. From the same reference  $\beta = 5 @ \epsilon = 0$  for an L/D ratio of 1.0.

Substituting in Equation (81)

$$c = 22.5 \times 10^3 \frac{\text{lb} - \text{sec}}{\text{in.}}$$

In the radial direction, ( $\alpha = \theta$ ) using Equation (84)

$$f_n = 6000 (19 \times 10^{-4})^{1/2}$$

$$f_{n\theta} = 265 \text{ cps}$$

$c_c$  at this condition (From (80))

$$c_c = 5850 (S_a)^{1/2} = 5850 (19.5 \times 10^{-4})^{1/2}$$

$$c_c = 260 \frac{\text{lb} - \text{sec}}{\text{in.}}$$

$$\therefore \frac{c}{c_c} = \frac{225 \times 10^2}{260}$$

$$\left( \frac{c}{c_c} \right) = 87 \text{ @ } A = 0.0002, \alpha = \theta$$

From Equation (82)

$$\frac{x_o}{x_{st}} = \left[ \frac{1}{\left( 1 - \frac{f^2}{(265)^2} \right)^2 + 4(87)^2 \left( \frac{f}{265} \right)^2} \right]^{1/2}$$

This can be reduced to

$$\frac{x_o}{x_{st}} = \left[ \frac{1}{1 + \left( \frac{f}{265} \right)^2 \cdot \left[ \left( \frac{f}{265} \right)^2 + 30,276 \right]} \right]^{1/2}$$

$$\text{Since } 30,276 \gg \left( \frac{f}{265} \right)^2$$

$$\frac{x}{x_{st}} = \left[ \frac{1}{1 + \left(\frac{f}{265}\right)^2 (30,276)} \right]^{1/2}$$

$$@ f = f_1 = 30 \text{ cps}, x_o/x_{st} = \left(\frac{1}{400}\right)^{1/2} \approx 0.05$$

$$x_o = 4.7 \times 10^{-6} P_o \times 0.05$$

$$x_o = 0.235 \times 10^{-6} P_o$$

$$x_{st} = \frac{P_o}{k_s} = \frac{P}{110(S_s)10^6}$$

$$x_{st} = \frac{P \times 10^{-6}}{.214}$$

In the load direction ( $\alpha = 0^\circ$ )

$$S_o = 0.185$$

$$f_{n_o} = 6000 (S_o)^{1/2} = 6000(.185)^{1/2}$$

$$f_{n_o} = 2680 \text{ cps}$$

$c_c$  for this direction is,

$$c_c = 5850(.185)^{1/2}$$

$$c_c = 2520 \frac{\text{lb} - \text{sec}}{\text{in.}}$$

$$c \text{ (as before)} = 22.5 \times 10^3$$

$$\therefore \left(\frac{c}{c_c}\right) = 8.9$$

$$\therefore \frac{x_o}{x_{st}} = \left[ \frac{1}{\left[1 - \left(\frac{f}{2520}\right)^2\right]^2 + 4(8.9)^2 \left(\frac{f}{2520}\right)^2} \right]^{1/2}$$

$$@ f = f_1 = 30 \text{ cps}$$



$$\frac{x_o}{x_{st}} = \left[ \frac{1}{1 + .45} \right]^{1/2}$$

$$\frac{x_o}{x_{st}} = 0.83$$

$$x_o = x_{st} \times 0.83 P_o = 0.041 \times 10^{-6} P_o$$

$$x_{st} = \frac{P_o \times 10^{-6}}{20.4} = 0.049 P_o \times 10^{-6}$$

At right angles to the load, ( $\alpha = 90^\circ$ )

$$s_{90^\circ} = 0$$

$$\therefore f_n = 0$$

$$c_c = 0$$

Several equations may be written for this  $k = 0$  condition

$$x_o = P \sin \phi / c\omega \quad (85)$$

$$x_o = - \frac{P \cos \phi}{m\omega^2} \quad (86)$$

$$\tan \phi = - \frac{c}{m_r \omega} \quad (87)$$

$P$  = magnitude of disturbing force (lbs)

For A ( $\frac{60}{2}$ ) lb rotor,  $m_r = 7.76 \times 10^{-2}$

Also (from before)  $c = 22.5 \times 10^3$

$$\tan \phi = - \frac{22.5 \times 10^3}{7.76(10^{-2}) 2\pi \cdot f} = \frac{4.6 \times 10^4}{f}$$

$$@ f_1 = 30 \text{ cps}$$

$$\tan \phi = 1540$$

$$\therefore \phi \approx 90^\circ$$

$$\therefore x_0 = \frac{P \sin \phi}{c\omega} = \frac{P (1)}{22.5(10^3)(2\pi)(30)}$$

$$x_0 = 0.234 \times P \times 10^{-6}$$

For a disturbing force equal to the applied load

$$P = 30$$

$$x_0 = 7 \times 10^{-6} \text{ in.}$$

For heavier loads, the spring rates increase (or decrease) and the damping will increase or decrease depending upon the direction of displacement.

At a load of 1500 lbs,

$$A \approx 0.0104$$

$$S_\theta = .028$$

$$\epsilon = 0.44$$

$$S_0 = 0.120$$

$$\theta = 60^\circ$$

$$S_{90^\circ} = 0$$

In the radial direction ( $\alpha = \theta$ )

$$f_n = 6000(.028)^{1/2} = 1000 \text{ cps}$$

$$\beta \approx 13 (\text{in direction of minimum film})$$

From Equation (81)

$$\therefore c = 4.5 \times 10^3 \cdot \beta$$

$$c = 58.5 \times 10^3$$

From Equation (80)

$$c_c = 5850 (2.8 \times 10^{-2})^{1/2}$$

$$c_c = 995$$

$$\therefore \frac{c}{c_c} = \frac{58.5 \times 10^3}{.995 \times 10^3} = 58.9$$

$$@ f = f_1 = 30 \text{ From equation (82)}$$

$$\frac{x_o}{x_{st}} = \left[ \frac{1}{1 + 4(59)^2 \left(\frac{30}{1000}\right)^2} \right]^{1/2}$$

$$\frac{x_o}{x_{st}} = 0.272$$

$$x_{st} = \frac{P_o \times 10^{-6}}{3.08} = 0.324 P_o \times 10^{-6}$$

$$x_o = P_o \times 10^{-6} (.324)(.272) -$$

$$x_o = .088 \times 10^{-6} P_o$$

In the load direction ( $\alpha = 0$ )

$$f_n = 6000 (S_a)^{1/2} = 6000(.12)^{1/2}$$

$$f_n = 2080 \text{ cps}$$

The value of " $\beta$ " must be less than that used for radial displacement.

Figure 10 of Reference 2 may be applied as an approximation since it is for an  $\epsilon \approx 0.5$ .

THE FRANKLIN INSTITUTE • Laboratories for Research and Development

I-A2321-1

$$\therefore \beta_{\alpha=0} = \beta_{\alpha=0} \times \frac{19.7}{24.8} = 13 \cdot \frac{19.7}{24.8}$$

$$\theta = 60^\circ$$

$$\beta_{\alpha=0} \approx 10$$

$$\therefore c = 4.5 \times 10^3 \times 10$$

$$c = 45,000 \text{ lb - sec/in.}$$

$$c_c = 5850 (.12)^{1/2} = 2020 \text{ lb - sec/in.}$$

$$\frac{c}{c_c} = 22.5$$

$$@ f = f_1 = 30 \text{ cps}$$

From (82)

$$\frac{x_o}{x_{st}} = 0.45$$

$$x_{st} = \frac{P_o \times 10^{-6}}{13.2} = .076 \times 10^{-6} P_o$$

$$x_o = 0.45 (.076 \times 10^{-6}) P_o$$

$$x_o = 0.034 \times 10^{-6} P_o$$

At right angles to the load ( $\alpha = 90^\circ$ )

$$S_{90^\circ} = 0$$

$$f_n = 0$$

$$c_c = 0$$

$$\beta (@ \alpha = 0) \approx \frac{20.4}{24.8} \times 13 \approx 10.7$$

$$c = 4.5 \times 10^3 (10.7)$$

$$c = 48.2 \times 10^3$$

From Equation (87) with  $m_r = 7.76 \times 10^{-2}$  and  $f = 30$  cps

$$\phi \approx 90^\circ$$

From equation (85)

$$x_o = \frac{P_o \sin \phi}{c\omega} = \frac{P_o (1)}{48.2(10^3)(2\pi)(30)}$$

$$x_o = 0.108 P_o \times 10^{-6}$$

For a disturbing force equal to the applied load

$$P_o = 30$$

$$x_o = 3.24 \times 10^{-6} \text{ in.}$$

Summarizing briefly, the following conclusions regarding the response of a sleeve bearing of typical size for an electric motor application may be made

1.  $\frac{x_o}{x_{st}} < 1.0$  (No amplification of vibration)
2.  $x_o$ , at the worst, falls in the range  
 $0 < x_o < 1.0 \times 10^{-6} \times P_o$
3. At typical electric motor speeds, no inherent instabilities should occur.

$$\omega_{c_{min}} = 2 \sqrt{\frac{k_{\theta_{min}}}{m}} \approx 2 \left[ \frac{0.11 \times 10^6}{0.0776} \right]^{1/2} = 2(1.2 \times 10^3)$$

$$f_{c_{min}} = 382 \text{ cps}$$

$$f_{whirl_{min}} = f_{c_{min}} \approx 10 f_i$$

4. Demagnification of  $x_0$  will be present at all disturbing frequencies since  $(\frac{c}{c} - ) > 1.0$ .

5. There is one exception to No. 1, No. 2, and No. 4 (above).

If the disturbing frequency is equal to one-half the rotor frequency, the bearing theoretically, cannot carry any load (due to film instability). Hence, a resonant condition will exist.

### 3.3 Transmission of Vibration Forces

The noise and vibration generated within the bearing and other disturbing forces (attributed to the rotor being supported) must be transmitted through the bearing to its housing. It is of interest to determine how such forces are transmitted; that is, are they amplified or suppressed by the bearing? Transmissibility, or the ratio of "force-out" to "force-in", is dictated by the springs, damping and masses involved. Also, the frequency and nature of the disturbing forces are of importance. Both ball bearings and sleeve bearings exhibit non-linear spring rates that vary with the direction and magnitude of the disturbing force. Also, some degree of damping is present, (particularly with sleeve bearings), that varies with operating conditions and direction and nature of the applied load. Thus, a strict analysis of noise and vibration transmission presents a formidable problem that requires numerous assumptions thereby detracting from its worth. In the work which follows hereafter, several such gross assumptions are made in an attempt to determine whether vibration is amplified, suppressed, or not affected in being transmitted through the bearing.

Transmissibility is defined as

$$\tau = \frac{\text{Transmitted Force}}{\text{Imposed Force}} = \frac{|F|}{|P|}$$

for a damped, single degree of freedom spring-mass system,

$$\tau = \left[ \frac{1 + 4 \left( \frac{c}{c_c} \right)^2 \left( \frac{f}{f_n} \right)^2}{\left( 1 - \frac{f^2}{f_n^2} \right)^2 + 4 \left( \frac{c}{c_c} \right)^2 \left( \frac{f}{f_n} \right)^2} \right]^{1/2} \quad (88)$$

Equation (88) is plotted in Figure 52. Damping is advantageous over the frequency range of  $0 < \frac{f}{f_n} < \sqrt{2}$  in that the build-up of peak forces due to resonance is suppressed. At frequencies of  $\frac{f}{f_n} > \sqrt{2}$ , low damping is advantageous. Relatively high damping, while minimizing vibration peak response, promotes unity transmission of imposed forces.

### 3.3.1 Rolling Contact Bearings

An axially preloaded ball bearing rotor can exhibit five modes of vibration - translation along each of the three axes and rotation about 2 axes. Radial and axial bearing spring rates in combination with rotor mass and moment of inertia will dictate the several natural frequencies.

Consider the radial spring rate of a deep groove ball bearing that is pre-loaded. Within its pre-load range, the spring rate is

$$s_i \doteq 6k_N i^{1/2} \quad (56)$$

The natural frequency in the radial direction is

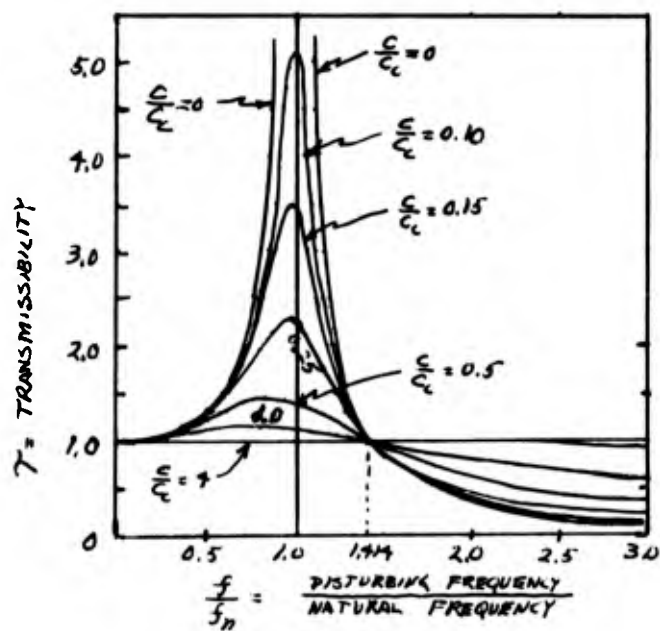
$$f_n = \frac{1}{2\pi} \left[ \frac{s_i}{m_r} \right]^{1/2} = \frac{0.39}{(m_r)^{1/2}} (k_N)^{1/2} (i)^{1/4} \quad (89)$$

The radial interference in an axially pre-loaded bearing is;

$$i \approx \delta_N \times \cos \beta \approx \left[ \frac{T}{n} \cdot \frac{1}{k_N} \cdot \frac{1}{\sin \beta} \right]^{2/3} \cos \beta \quad (90)$$

Note: Equation (56) is based on  $n = 8$  balls. Substituting in (89) gives





TRANSMISSIBILITY - FREQUENCY CURVES

Figure 52

I-A2321-1

$$f_n = 0.276 \left( \frac{1}{m_r} \right)^{\frac{1}{2}} (k_N)^{\frac{1}{3}} (T)^{\frac{1}{6}} (\cos \beta)^{\frac{1}{4}} \left( \frac{1}{\sin \beta} \right)^{\frac{1}{6}} \quad (91)$$

For  $0 \leq \beta \leq 30^\circ$

$$\cos^{\frac{1}{4}} \beta \approx 1.0$$

$$f_n \approx 0.276 \left( \frac{1}{m_r} \right)^{\frac{1}{2}} (k_N)^{\frac{1}{3}} (T)^{\frac{1}{6}} \left( \frac{1}{\sin \beta} \right)^{\frac{1}{6}} \quad (92)$$

For 308 to 318 BR'GS ( $n = 8$  balls)

$$10^2 \times 2.33 \underset{(308)}{\leq} (k_N)^{\frac{1}{3}} \underset{(318)}{\leq} 2.63 \times 10^2 \quad (\text{see Appendix C.5})$$

$$\therefore (k_N)^{\frac{1}{3}} \approx 2.5 \times 10^2$$

$$f_n = 0.69 \left( \frac{1}{m_r} \right)^{\frac{1}{2}} (T)^{\frac{1}{6}} \left( \frac{1}{\sin \beta} \right)^{\frac{1}{6}} \times 10^2 \quad (93)$$

The recommended axial preload is (see Appendix K),

$$T \approx 2 \times W_R$$

$$\text{The rotor mass is } = \frac{W_r/2}{386} = m_r$$

$$\therefore \frac{(T)^{\frac{1}{6}}}{(m_r)^{\frac{1}{2}}} = \frac{1.123 W_R^{\frac{1}{6}}}{\frac{W_R^{\frac{1}{2}}}{27.8}} = \frac{31.2}{W_R^{\frac{1}{3}}}$$

$$f_n = \frac{21.6 \times 10^2}{W_R^{\frac{1}{3}}} \left( \frac{1}{\sin \beta} \right)^{\frac{1}{6}} \quad (94)$$

For  $5^\circ \leq \beta \leq 30^\circ$

$$1.5 \geq \left( \frac{1}{\sin \beta} \right)^{\frac{1}{6}} \geq 1.1$$

$$\therefore \left( \frac{1}{\sin \beta} \right)^{\frac{1}{6}} \approx 1.30$$

$$\therefore \boxed{f_n \approx \frac{2800}{(W_R)^{\frac{1}{3}}}} \text{ cps} \quad (95)$$

THE FRANKLIN INSTITUTE • Laboratories for Research and Development

I-A2321-1

Equation (95) is an approximate expression for the natural frequency of an axially pre-loaded rotor of weight  $W_R$  supported on 2 - 8-ball, ball bearings. From Appendix H we obtain the following rotor weights and computed resonant frequencies

BR'G Size	Rotor Weight $W_R$ (lbs)	$(W_R)^{\frac{1}{3}}$	$f_n$ (cps)
308	34	3.24	863
309	42	3.47	807
310	57	3.84	730
311	68	4.08	685
312	80	4.31	650
313	97	4.58	611
314	114	4.84	578
315	132	5.09	550
316	150	5.31	527
317	170	5.55	505
318	190	5.75	487

Natural frequencies  
of radial vibration  
due to preloaded  
bearings ( $T \approx 2W_R$ )

From these results and consideration of zero damping in Figure 52, it is evident that disturbing forces generated within the bearing (or rotor) lying in the frequency range from 250 cps to 1250 cps will be magnified in being transmitted through the bearing. The troublesome frequency range will of course be more narrow for a particular motor (i.e., 400 to 1000 cps for a 310 bearing motor).

The foregoing was based on a rigidly mounted outer race. In practice, the outer race is normally a free fit within the bearing. This allows intimate contact of outer race with housing in the loaded region and a "free" outer race on the opposite side. It is conceivable,

THE FRANKLIN INSTITUTE • *Laboratories for Research and Development*

I-A2321-1

therefore, that a portion of the outer race will "ring" at one of its natural frequencies if excited. Depending upon the amplitude of "ringing", the outer race will make periodic contact with the race where it normally might not touch the housing and vice-versa where it normally touches. High damping is undoubtedly provided at the outer race by the housing which serves to minimize vibrational amplitudes of the outer race and, thereby, allow unity transmission of disturbing forces at the race-housing interface. However, it is important to remember that these disturbing forces at the race-housing interface are the result of the transmissibility characteristics of the outer race and are magnified in magnitude (in the neighborhood of resonant frequencies) when compared to the magnitude of disturbing forces exciting the outer race.

Summarizing briefly, it would appear that disturbing forces of relatively low frequency ( $f < 250$  cps) (such as due to unbalance, eccentricity, inner and outer ball pass, low order ball and raceway waviness) have a transmissibility ratio of approximately one. Medium frequency disturbances ( $250 < f < 1250$ ) may become amplified due to excitation of mass (rotor) - spring (bearing) system. Disturbing frequencies within this range may be generated by higher order waviness. Relatively high frequency disturbing forces ( $f > \sqrt{2} f_n > 1250$  cps, approx.), such as generated by high frequency waviness, may be amplified due to ringing of the outer race at its several natural modes of vibration.

### 3.3.2 Sliding Surface Bearing Vibration Force Transmission

#### 3.3.2.1 An Approach to the Problem

In this section it is desired to evaluate the ability of oil-lubricated journal bearings to transmit forces of periodic nature. Such periodic forces may be generated in the bearing or originate in the rotor being supported. Both of these cases can be studied as the response of the bearing to a periodic load. A steady load on the bearing may also be considered to be present.

Since the forces within the fluid film can be computed for every position and velocity of the shaft center, a solution can be obtained for the path of the journal center during steady state oscillation. The equations of motion can be solved on a computer and the locus of the center can be found for any combination of the steady load and of the magnitude and frequency of the disturbing load. The computer could start from any state and work through the transient condition. Once the steady state is reached, the fluid film forces would represent the transmitted forces and the "transmissibility" would be the ratio of transmitted force to disturbing force.

A simplified but significant solution can be obtained considering the shaft free to move only along the direction of the line of centers. In this direction, the dissipation is the highest for any given velocity of the shaft center. However, even in this case, the solution is rather complicated due to the fact that the spring rate and damping factors of the fluid film are highly non-linear functions of the position of the shaft center. Also, the damping factor assumes different values for velocities of different sign.

THE FRANKLIN INSTITUTE • *Laboratories for Research and Development*

I-A2321-1

A possible numerical solution could be obtained in the following manner. Assume any set of initial conditions ( $t=0$ ). Then assign a value to the first time interval  $t=t_1$ . Then  $F(t)$  has a definite numerical value. We can then proceed to draw a set of curves (one for each  $\dot{x}$ ) on the  $\ddot{x}$ - $x$  plane, (see Figure 53).

$$\ddot{x} = \frac{F}{M}(t) - \frac{B(x)}{M} \dot{x} - \frac{K(x)}{M} \cdot x \quad (119)$$

Now we notice if  $B$  does not depend on  $\dot{x}$ , two curves will be sufficient for interpolation because  $\ddot{x}$  depends linearly on  $\dot{x}$ . If we now pass to the  $\dot{x}$ - $x$  plane we can find the slope of the curves at any point  $(\dot{x}, x)$  by recognizing that

$$\frac{d\dot{x}}{dx} = \text{slope} = \frac{\ddot{x}}{\dot{x}}$$

which can be read off the  $\ddot{x}$ - $x$  plane plots at every value of  $x$  on any curve (and  $\dot{x}$  really because we can interpolate linearly). At the same time, the average velocity obtained in the interval  $\Delta x$  chosen will have to match the ratio of  $\Delta x / \Delta t$  used. By a few approximations, this can lead to the correct choice of the point  $(\dot{x}, x)$ . The knowledge of the slope will allow us to draw the curve (in the  $\dot{x}$ - $x$  plane). Successive steps for time  $t = t_2, t_3$ , etc., will allow us to draw the complete time cycle on the  $\dot{x}$ - $x$  plane and will lead to the determination of the limiting cycle.

As an example, if we pick a value  $t = t_1$  and use it in the equation for  $\ddot{x}$ , we might generate the two curves  $\dot{x} = a$ , and  $\dot{x} = b$  in Figure 53. Then, if the position  $x_1$  and the velocity  $\dot{x}_1$  are known at  $t = t_1$  (initial conditions), we know the slope of the solution curve for our problem at  $(x_1, \dot{x}_1)$ .

I-A2321-1

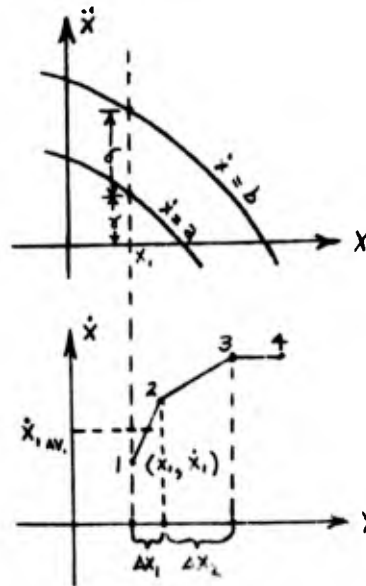


Figure 53

ACCELERATION AND  
VELOCITY - DISPLACEMENT  
PLANE CURVES

$$\text{slope} = \frac{\ddot{x}_1}{\dot{x}_1} = \left[ \gamma + \frac{(\dot{x}_1 - a)}{(b - a)} \delta \right] / \dot{x}_1$$

The size of the interval  $\Delta x$  is such that

$$\frac{\Delta x_1}{\Delta t_1} = \dot{x}_{1 \text{ avg}}$$

Now, by using  $t = t_2 = t_1 + \Delta t_1$ , we obtain

$$F(t_2) = F(t_1) + T_1$$

where  $T_1$  is the amount by which we have to shift the  $x$  axis in the  $\ddot{x}$ - $x$  plane plot toward the negative  $\ddot{x}$  direction. A new step can now be taken. The size of the steps should be small enough to describe  $F(t)$  accurately.

I-A2321-1

If the above procedure is repeated a sufficient number of times, it can be expected that the  $\dot{x}$ - $x$  curve will stabilize on a limit cycle which will be the steady state solution. The function  $F(t)$  might include the term representing the steady load as a constant. It is to be expected that the steady state solution will be the same for all initial conditions chosen.

This type of solution is perfectly general and can be applied to any unsymmetrical, non-linear, forced vibration problem in one dimension. If  $B = B(x, \dot{x})$ , then more than two curves will be necessary in the  $\dot{x}$ - $x$  plot.

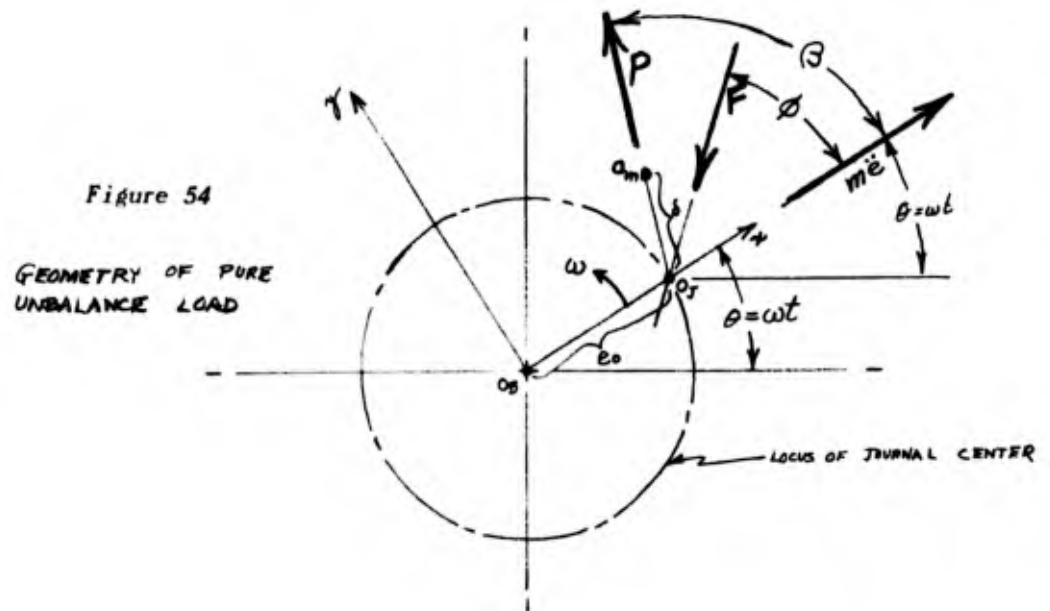
#### 3.3.2.2 Transmissibility of Special Cases of Disturbing Forces

Ways and means of using the above described procedure for evaluating transmissibility were explored. Computer facilities were available but we could not justify such work due to limited funds and time on the existing program. However, the special case, which is fairly common, of a pure unbalance load on a journal was considered. As will be shown in the work which follows hereafter, the transmissibility is equal to unity for a typical motor journal bearing. Consideration is also given to treating the bearing as a single degree of freedom, damped spring-mass system.

##### 3.3.2.2.1 Pure Unbalance Load

In this case, the geometric center of the journal, " $O_j$ ", will rotate in a circular path about the geometric center of the bearing, " $O_B$ ", the radius of which is  $e_o$  (see Figure 54).





Let the center of mass be at " $O_m$ " a distance  $\delta$  from " $O_J$ " for equilibrium, the force vectors must satisfy the following equation

$$m\ddot{e} + F = P \quad (96)$$

where  $m\ddot{e}$  = inertia force, (lbs)  
 $F$  = fluid film force, (lbs)  
 $P$  = unbalance disturbing force, (lbs)  
 $m$  = rotor mass, (lbs-sec<sup>2</sup>/in.)  
 $\omega$  = rotor rotational speed, (rad/sec)  
 $e_o$  = radial distance to journal center, (in.)  
 $\delta$  = distance from journal geometric center to mass center, (in.)  
 $\beta$  = phase angle between  $P$  and x-axis  
 $\phi$  = phase angle between  $F$  and x-axis

Letting

$$\begin{aligned} \ddot{e} &= e_o \omega^2 \\ P &= m \delta \omega^2 \\ F &= \frac{1}{2} \pi \mu \omega L D \left( \frac{R}{c} \right)^2 \cdot f \\ e_o &= \epsilon_o \cdot c \\ \delta &= \Delta \cdot c \end{aligned}$$

Substituting in (96), simplifying and rearranging we obtain,

$$\bar{X} = \frac{f}{\epsilon_o \cos \phi \pm \sqrt{\Delta^2 - \epsilon_o \sin^2 \phi}} \quad (97)$$

where

$$\bar{X} = \left\{ \frac{\omega}{\left[ \frac{\mu LD (R/c)^2}{2\pi mc} \right]} \right\} = \text{dimensionless frequency}$$

$\mu$  = lubricant absolute viscosity,  $\left( \frac{\text{lbs-sec}}{\text{in}^2} \right)$

$L$  = bearing length (in.)

$D$  = bearing diam. (in.)

$c$  = radial clearance (in.)

$$f = \frac{2\pi F}{\mu \omega LD \left( \frac{R}{c} \right)^2} = \text{dimensionless film force}$$

Defining transmissibility as

$$\tau = \frac{|F|}{|P|}$$

Substituting for  $F$  and  $P$  from above gives the transmissibility as

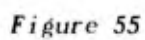
$$\tau = \frac{f}{\Delta} \cdot \frac{1}{\bar{X}} \quad (98)$$

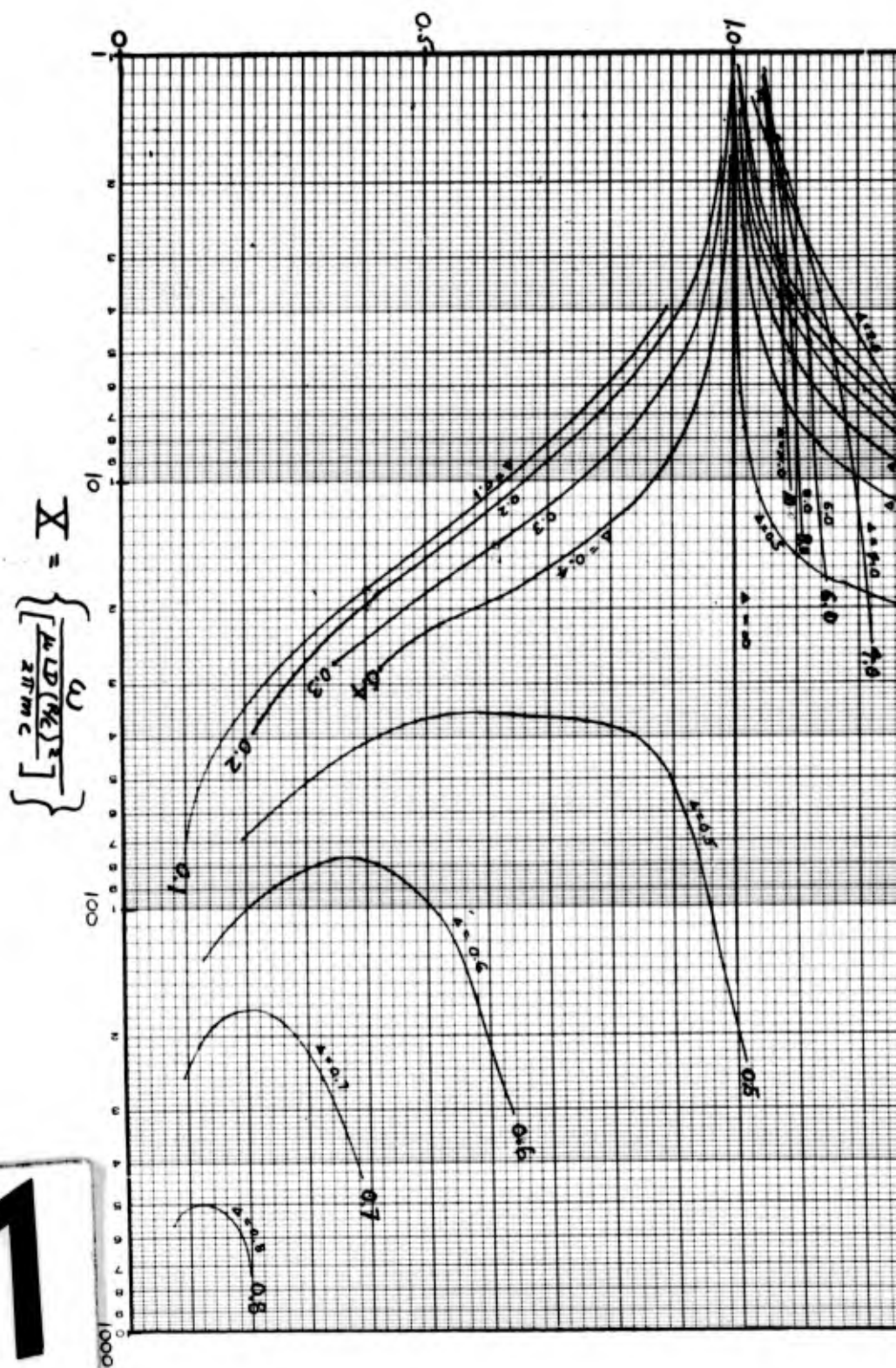
or

$$\tau = \frac{\epsilon_o \cos \phi \pm \sqrt{\Delta^2 - \epsilon_o \sin^2 \phi}}{\Delta} \quad (99)$$

Reference 3 gives the necessary relationships among  $f$ ,  $\phi$ , and  $\epsilon_o$ , for a pure unbalance force which allows the determination of the frequency response curves (Equation (97)) and the transmissibility curves (Equation (99)) for various values of  $\Delta$ , the dimensionless unbalance arm. Figure 55 shows the frequency response curves and Figure 56 shows the transmissibility characteristics. The complete derivation and development of the equations and method of solution to obtain the resulting curves is given in Appendix J.







1



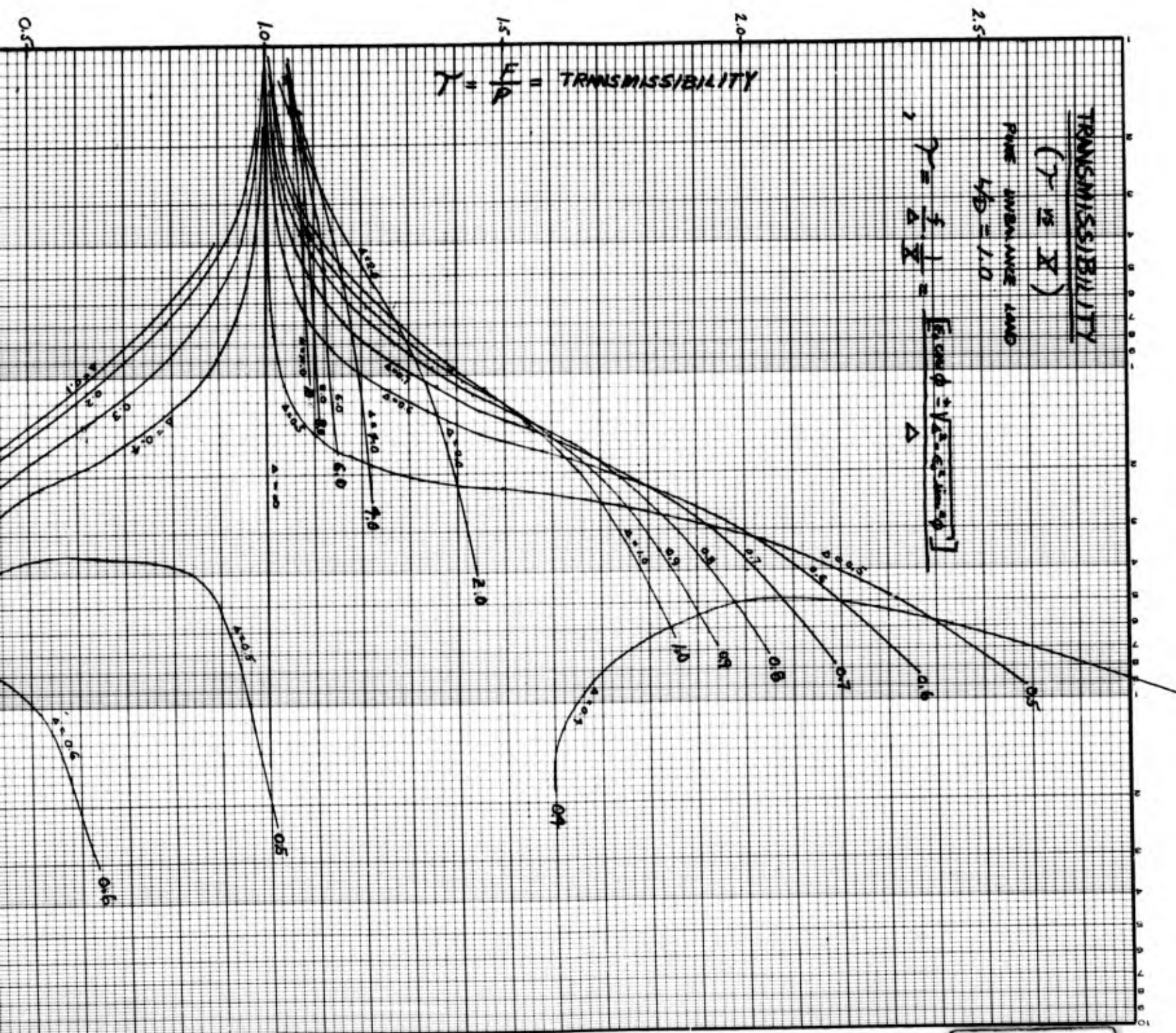


Figure 56

Consider the frequency response curves (Fig. 55) for relatively large unbalance, ( $\Delta > 0.5$ ), eccentricity increases with increasing  $\bar{X}$ . For a given bearing, given lubricant, and given mass, increasing  $\bar{X}$  implies increasing speed,  $\omega$ . Thus, for a given unbalance, the effect of changing speed is immediately apparent. Notice that for small unbalance eccentricity increases initially with speed, attains a maximum and then decreases with further increase in speed. This "resonant" condition occurs when  $\Delta = \epsilon \sin \phi$  for which Eq [97] reduces to

$$\bar{X}_{\text{res}} = \frac{f}{\epsilon \cos \phi} \quad (100)$$

$(\Delta = \epsilon \sin \phi)$

Eq. 100 is plotted as the dashed line in Fig. 55. The intersection of this line with those of small  $\Delta$  curves is the "resonance" condition.

The significance of the secondary branches of the curves in the upper right hand corner of Fig. 55 is not known and may be physically impossible to achieve. In any case, the primary curves point out the advantages of good balancing.

Fig. 56 shows the transmissibility of a pure unbalance load in a sleeve bearing ( $L/D = 1.0$ ). If we consider only the primary branches (Low  $\bar{X}$ ), the following observations may be made.

1. For low values of  $\bar{X}$ , ( $\bar{X} < 1.0$ ),

$$\tau = \frac{F}{P} \approx 1$$

This implies that

$$F(\text{Force on Bearing}) \approx P(\text{Unbalance Force})$$

2. For  $\bar{X} > 1.0$ ,

a. Well balanced rotors ( $\Delta < 0.5$ )

$$\tau = \frac{F}{P} < 1.0$$

and  $F < P$ , therefore, absorption is achieved.

b. Poorly balanced rotors ( $\Delta \geq 0.5$ )

$$\tau = \frac{F}{P} > 1.0$$

and  $F > P$ , therefore, magnification is present.

3. For large unbalance ( $\Delta > 10$ )

$$\tau = \frac{F}{P} \approx 1$$

∴ No absorption or magnification is present

Thus, in order to evaluate the transmissibility of sleeve bearings (for pure unbalance load) we need to know the value of  $\bar{X}$  and  $\Delta$ .

Let us first consider  $\bar{X}$ . From before

$$\bar{X} = \left\{ \frac{\omega^2}{\frac{\mu L D \left(\frac{R}{c}\right)^2}{2\pi m R^c}} \right\}$$

Let us select a 2 inch diameter bearing 310 BR'G Size  
Frame No. 365  
60 P at 1800 RPM

$$\therefore D = 2 \text{ in.} \quad \therefore R = 1$$

$$\text{If } L/D = 1$$

$$\therefore L = 2 \text{ in.}$$

$$\text{Let } \frac{R}{c} = 0.8 \times 10^{-3} \quad \therefore c = 1.25 \times 10^{-3} \text{ in.}$$



The rotor mass for this size motor is  $\approx \frac{80 \text{ lbs}}{386 \text{ in/sec}^2} = 0.21$

Considering that each bearing carries half the mass,

$$m_r = 0.10$$

The rotational speed,  $\omega$ , is

$$\omega = \frac{2\pi N}{60} = \frac{2\pi(1800)}{60}$$

$$\omega = 60\pi \text{ rad/sec.}$$

Assume an S.A.E. 20 oil at 140°F, then

$$\mu = 3 \times 10^{-6} \text{ Reyns, } \frac{\text{lb-sec}}{\text{in}^2}$$

$$\bar{X} = \left\{ \frac{60 \pi}{\left[ \frac{(3 \times 10^{-6})(2)(2)(.8)^2 (10^6)}{2\pi (.13)(1.25)10^{-3}} \right]} \right\}$$

$$\bar{X} = 0.020$$

This low value of  $\bar{X}$  implies (see Fig. No. 56) that the transmissibility ratio is essentially unity regardless of the degree of unbalance,  $\Delta$ . Other bearing sizes for electric motor rotors were investigated, but  $\bar{X}$  was always less than 1.0. This leads to the conclusion that No absorption (or magnification) is afforded by sleeve bearings when subjected to a pure unbalance load, at least for the  $\bar{X}$ 's dictated by the mass, size and speed associated with electric motors. To achieve good absorption requires, first of all, good balance ( $\Delta < 0.5$ ), and

THE FRANKLIN INSTITUTE • *Laboratories for Research and Development*

I-A2321-1

high  $\bar{X}$ , which means, large mass, high speed, low viscosity, small bearings, and large clearance.

Typical values of  $\Delta$  for sleeve bearing motors may be determined from Appendix H.

$$\delta_{avg} \approx 3 \times 10^{-3} \times \text{Bore Dia.}$$

$\left\{ \begin{array}{l} \text{Slope of curve} \\ \text{on Fig. H-6} \end{array} \right\}$

$$\delta \approx 3 \times D \times 10^{-3}$$

$$\Delta = \frac{\delta}{c} = 3 \times \frac{D \times 10^{-3}}{c} = 6 \times 10^{-3} \frac{R}{c}$$

$$\frac{R}{c} = \text{clearance ratio}$$

For this type of equipment

$$10^{-3} \times 0.65 < \frac{R}{c} < 0.85 \times 10^{-3}$$

$$4.0 < \Delta < 5.0$$

It should be pointed out that this is maximum allowable unbalance as per mil. spec. Mil-M-17060 B (Ships), 2/25/59 for "precision balanced" motors (see Appendix H). Super-precision balancing would yield  $1.5 < \Delta < 2.0$  as maximum unbalance. In any case, minimum unbalance is probably on the order of  $\Delta = 1.0$

Therefore, since

$$\bar{X} < 1.0$$

$$\Delta > 1.0$$

Sleeve bearing transmissibility for a pure unbalance load is,

$$\tau = \frac{F}{P} \approx 1.0$$

THE FRANKLIN INSTITUTE • *Laboratories for Research and Development*

I-A2321-1

This leads to the interesting fact that if the fluid film force,  $F$ , is equal in magnitude to the unbalance force,  $P$ , then one could expect agreement between the steady-state operating eccentricity for a steady state load and the rotating eccentricity for a rotating unbalance load,  $P$ .

To illustrate this point, we shall use the work of Raimondi and Boyd<sup>4</sup>. The bearing characteristic number (Summerfeld No.),  $S$ , given in this work is

$$S = \left(\frac{R}{c}\right)^2 \frac{\mu N}{P} \quad , \quad (101)$$

where:-  $R$  = Br'g Radius, (in.)

$c$  = Br'g Rad. Clearance, (in.)

$\mu$  = Abs. Viscosity,  $\left(\frac{\text{lbs-sec}}{\text{in}^2}\right)$

$N$  = Rotational Speed, (Rev. per second)

$P$  = Unit Load =  $\frac{W}{L \cdot D}$  ,  $\left(\frac{\text{lbs}}{\text{in}^2}\right)$

$L$  = Br'g Length , (in.)

$W$  = Total Br'g Load, (lbs)

$D$  = Br'g Dia. (in.)

Let us determine the relationship among  $S$ ,  $\bar{X}$  and  $\Delta$

$$S = \left(\frac{R}{c}\right)^2 \cdot \frac{\mu N}{P} = \left(\frac{R}{c}\right)^2 \cdot \frac{\mu N L D}{W} \quad (102)$$

$$\bar{X} = \frac{\omega (2\pi R c)}{\mu L D \left(\frac{R}{c}\right)^2} \quad (103)$$

$$\Delta = \frac{\delta}{c} \quad (104)$$

From (102)

$$\frac{1}{S} = \frac{W}{\mu_{NLD} \left(\frac{R}{c}\right)^2} = \frac{1}{\mu_{LD} \left(\frac{R}{c}\right)^2} \cdot \frac{W}{N}$$

$$N = \frac{\omega}{2\pi}$$

$$\frac{1}{S} = \frac{2\pi}{\mu_{LD} \left(\frac{R}{c}\right)^2} \cdot \frac{W}{\omega} \cdot \frac{\omega}{\omega} \cdot \frac{mc}{mc}$$

$$\frac{1}{S} = \left[ \frac{\omega(2\pi mc)}{\mu_{LD} \left(\frac{R}{c}\right)^2} \right] \frac{W}{\omega^2 mc}$$

$$\frac{1}{S} = \bar{X} \cdot \frac{W}{\omega^2 mc}$$

For a pure unbalance load,

$$W = m\delta\omega^2$$

$$\therefore \frac{1}{S} = \bar{X} \cdot \frac{m\delta\omega^2}{\omega^2 mc} = \bar{X} \cdot \frac{\delta}{c}$$

From (104)

$$\therefore \frac{1}{S} = \bar{X} \cdot \Delta$$

Solving for  $\bar{X}$

$$\bar{X} = \frac{1}{S \cdot \Delta}$$

THE FRANKLIN INSTITUTE • Laboratories for Research and Development

I-A2321-1

From Ref. 4, Table I,  $L/D = 1.0$

$\epsilon$	S	$\frac{1}{S}$	$\bar{X} = \frac{1}{S} \frac{1}{\Delta}$			
			$\Delta=0.1$	$\Delta=1.0$	$\Delta=10$	$\Delta=100$
.1	.240	4.16	41.6	4.16	.416	.0416
.2	.123	8.12	81.2	8.12	.812	.0812
.4	.0626	16.0	160	16.0	1.60	.160
.6	.0389	25.7	257	25.7	2.57	.257
.8	.0210	47.6	476	47.6	4.76	.476
.9	.0115	87.0	870	87.0	8.70	.870

These results for  $\bar{X}$  are shown plotted on Fig. 55 as circled points connected by dashes. Notice that for  $\Delta > 10$  the steady state solution (from Ref. 3) shows good agreement with the frequency response curves. For  $\Delta = 1$ , the steady state solution gives optimistic values of eccentricity for  $\bar{X} > 3$ , indicating that the transmissibility is greater than unity. This is substantiated in Fig. 56. For  $\Delta = 0.1$ , the steady state solution gives pessimistic values of eccentricity for  $\bar{X} > 5$  indicating that transmissibility is less than unity. This likewise is indicated by Fig. 56.

Summary of Sleeve Bearing Transmissibility

For a Pure Unbalance Load

(or Load Rotating with Shaft)

(Based on  $L/D = 1$ )

1. The transmissibility is essentially unity (no absorption or magnification of unbalance) for the mass, size and speed associated with electric motors.

2. For very high speed (Large  $\bar{X} > 5.0$ )

$$\left. \begin{array}{l} \tau < 1.0 \text{ when } \Delta < 0.5 \\ \tau > 1.0 \text{ when } \Delta > 0.5 \end{array} \right\} L/D = 1$$

3. For very poor balance ( $\Delta > 10$ )

$$\tau = 1.0 \quad \left. \begin{array}{l} \text{steady state} \\ \text{solution valid} \end{array} \right\}$$

4. For good balance ( $0.5 < \Delta < 10$ )

$$\tau > 1.0 \text{ when } \bar{X} > 5.0 \quad \left. \begin{array}{l} \text{steady state} \\ \text{solution optimistic} \end{array} \right\}$$

5. Extremely good balance ( $0.5 > \Delta$ )

$$\tau < 1.0 \text{ when } \bar{X} > 5.0 \quad \left. \begin{array}{l} \text{steady state} \\ \text{solution pessimistic} \end{array} \right\}$$

#### 3.3.2.2.2 Transmissibility of Damped, Forced Vibrations

Transmissibility of a damped single degree of freedom system was defined in Eq. (88) as,

$$\tau = \left[ \frac{1 + 4 \left( \frac{c}{c_c} \right)^2 \left( \frac{f}{f_n} \right)^2}{\left( 1 - \frac{f^2}{f_n^2} \right)^2 + 4 \left( \frac{c}{c_c} \right)^2 \left( \frac{f}{f_n} \right)^2} \right]^{1/2} \quad (88)$$

In section 3.2.2.3,  $c$ ,  $c_c$ , and  $f_n$  were determined for

- a. Dead weight load (30 lbs)
- b. Max load (1500 lbs)
- c. Three directions of motion

$$\begin{array}{l} \alpha = \theta \\ \alpha = 0^\circ \\ \alpha = 90^\circ \end{array}$$

THE FRANKLIN INSTITUTE • Laboratories for Research and Development

1-A2321-1

These results were substituted in Eq [88] and the results are shown below.

W	$\epsilon$	$\alpha$	c	$c_c$	$\left(\frac{c}{c_c}\right)$	$f_n$	$\left(\frac{c}{c_c}\right)^2$	$\tau_{Eq [88]}$
30	0.01	$\theta = 85^\circ$	$22.5 \times 10^3$	260	87	265	$76 \times 10^2$	$\sim 1.0$
30	0.01	0	$22.5 \times 10^3$	2520	8.9	2680	$0.79 \times 10^2$	$\sim 1.0$
30	0.01	$90^\circ$	$22.5 \times 10^3$	0	$\infty$	0	$\infty$	$\sim 1.0$
1500	0.44	$\theta = 60^\circ$	$58.5 \times 10^3$	995	58.9	1000	$34.7 \times 10^2$	$\sim 1.0$
1500	0.44	0	$45.0 \times 10^3$	2020	22.5	2080	$5.07 \times 10^2$	$\sim 1.0$
1500	0.44	$90^\circ$	$48.2 \times 10^3$	0	$\infty$	0	$\infty$	$\sim 1.0$

Transmissibility  
at  $f = f_1 = 30$  cps

For a once-per-revolution disturbing force ( $f = f_1 = 30$  cps) using the tabled values of  $c$ ,  $c_c$  and  $f_n$  in Eq [88] yielded  $\tau \approx 1.0$ . These results are in line with the results obtained in section 3.3.2.2.1 for a pure unbalance load.

Due to the high damping ratios,  $\left(\frac{c}{c_c}\right) > 1$ , present in sleeve bearings, transmissibility at all frequencies is essentially unity. This is obvious by inspection of Figure 52.

### 3.3.3. Summary of Vibration Force Transmissibility

As used in electric motors;

- A. Journal Bearings, because of their high damping qualities, exhibit unity transmission of disturbing forces regardless of frequency.
- B. Rolling Contact Bearings exhibit varying transmissibility of disturbing forces depending upon the frequency of such forces.

In general, for axially preloaded bearings.

- |    |                                 |                            |
|----|---------------------------------|----------------------------|
| 1. | $0 < f < 300 \text{ cps}$       |                            |
|    | $\tau \approx 1$                |                            |
| 2. | $300 < f < 1000 \text{ cps}$    | } Bearing<br>Spring rate   |
|    | $\tau > 1$                      |                            |
| 3. | $1000 < f < 2000 \text{ cps}$   |                            |
|    | $\tau \leq 1$                   |                            |
| 4. | $2000 < f < 20,000 \text{ cps}$ | } Outer<br>Race<br>Ringing |
|    | $\tau > 1$                      |                            |



#### 4. CONCLUSIONS

All of the preceding work has dealt with the determination of how bearings of the rolling contact and sliding surface types as used in electric motors:

- a. Contribute to Vibration Generation (Section 3.1)
- b. Respond to Periodic Disturbing Forces (Section 3.2)
- c. Transmit Periodic Disturbing Forces (Section 3.3)

The more important findings and the conclusions to be drawn from this study are indicated below.

##### 4.1 ROLLING ELEMENT BEARINGS

###### 4.1.1. VIBRATION GENERATION

- A. Rolling contact bearings generate vibration producing forces of a periodic nature.
- B. The frequency range of such generated forces ranges from a fraction of the shaft frequency to approximately 1000 x shaft frequency depending upon kinematic considerations and geometry imperfections.
- C. In general, the frequencies generated will be dependent upon;

<u>Frequency</u>	<u>Cause</u>
$0 < \frac{f}{f_s} < 1.0$	Cage
$1 < \frac{f}{f_s} < 10$	Inner and outer ball-pass, ball rotation, low order ball and ring waviness.
$10 < \frac{f}{f_s} < 1000$	Higher order ball and ring waviness.

I-A2321-1

- D. A ball bearing, having perfect geometry of all of its components, when subjected to a constant radial load will, of necessity, exhibit an inherent instability at a frequency equal to ball-pass frequency. The amplitudes of vibratory motion are primarily dependent upon

1. Clearance (or interference)
2. Load
3. Ball deformation-load constant
4. Number of balls in the bearing

Preloading to effectively eliminate the clearance and promote uniform ball loading serves to minimize the amplitude of vibration. It is recommended that  $T_0 \approx 2 \times$  rotor weight (see Appendix K).

- E. Higher order ball and ring wavinesses and ball size variations of the order of  $10 \times 10^{-6}$  inch can produce vibratory forces of the same order of magnitude as the once per revolution force generated by the allowable inner race runout.
- F. If one considers the possibility of higher harmonics, gross changes in contact angle, varying ball path, variation of ball rotational axis, surface finish, and ball skidding, it becomes apparent that rolling contact bearings generate a multitude of frequencies.

#### 4.1.2. VIBRATIONAL RESPONSE

- A. Consideration was given to the order of the natural frequencies of vibration of bearing components. It was found that;

Balls:-  $f_n \geq 80,000$  cps

Cages:-  $f_n \approx 1,000$  cps

Outer Rings:- Flexure  $1,500 < f_n < 50,000$  cps

Radial  $15,000 < f_n < 90,000$  cps

Torsion  $15,000 < f_n < 90,000$  cps

Inner Ring Flexure  $2,000 < f_n$

Of these, flexure of the outer ring is believed to be most critical in light of bearing mounting practice and bearing vibration measuring techniques.

THE FRANKLIN INSTITUTE • *Laboratories for Research and Development*

I-A2321-1

- B. Ball loading and bearing housing fit and preloading practice introduce constraints and damping to the "ringing" of the outer race. In this regard, it would be advantageous to use an odd number of balls to avoid establishing nodal points of vibration at the ball-race contacts. For example, the 300 series have, for the most part, 8 balls which would favor the 4<sup>th</sup> mode of flexural vibration having 8 nodes. In normal practice and usage, an appreciable portion of the outer ring may be free within its housing, hence, "ringing" of the outer ring is a distinct possibility. Amplitudes of flexure are, because of the high frequency, probably an order of magnitude less than outer race-housing clearances. However, such amplitudes may affect ball loads.
- C. Consideration of the ball-race contact "springs" and ring and ball masses for various boundary conditions simulating electric motor application and bearing vibration measuring methods, indicates possible resonant frequencies all falling in the range from 1,000 to 20,000 cps for 310 size bearings. The combination of rotor mass and bearing spring rate for this size bearing would yield natural frequencies of vibration in the range 350 to 1,000 cps depending upon preload.
- D. In this work, no attempt was made to evaluate the small damping inherent in ball bearings. Based on the assumption, of zero damping, a free outer ring of an assembled bearing should be particularly responsive to disturbing frequencies in the neighborhood of its natural flexural frequencies. Bearing vibration measurements are normally made with the outer race free. Hence, it is believed that "ringing" of the outer race in the frequency range 2,000 to 10,000 cps would produce consistently high vibration levels in this frequency range. Support for this conclusion may be drawn from the current Anderometer vibration limits (Mil. Spec. Mil-B-17931 A). Excitation frequencies in this frequency range may originate from waviness of high order, or by "spring-back" as the ball loads sweep by the outer race at the location of vibration measurement. This latter consideration is always present thereby implying an irreducible minimum vibration level short of changing outer ring dimensions or introducing damping by one means or another.
- E. In an electric motor, resonance of the rotor on its "springs" (bearings) can occur. Disturbing forces in the frequency range 350 to 1000 cps will lead to serious vibration. Higher harmonics of ball-pass frequency and low order waviness can generate frequencies in the range.

THE FRANKLIN INSTITUTE • *Laboratories for Research and Development*

I-A2321-1

- F. A free outer ring, although not particularly responsive to ball pass frequency, will flex as the loaded balls pass a particular location on the outer ring. Hence, when monitoring outer ring vibrations, outer ball-pass frequency should always be present.

G. Expected Frequencies in Bearing Vibration Measurement

Most bearing vibration measurement work is accomplished by monitoring the vibration of the free outer ring while the inner ring is supported and driven by a smooth-running spindle operating at constant speed. In particular, the current Navy specification dealing with rolling element bearing noise and vibration, revolves around the use of the Anderometer which, using a velocity type pick-up, provides a measure of bearing "noise" quality within each of these frequency bands covering a total frequency range from 50 cps to approximately 10,000 cps when the inner ring is driven at 1800 rpm. A nominal thrust load is applied during test to stabilize the ball path and allow reasonably consistent measurement of the radial velocity of vibration of the outer ring. The following is a discussion of what considerations do not, do, and might contribute to the measurement of bearing noise quality as obtained from the Anderometer. These comments are based on the results of our study and, of course, assume that the bearing vibration is truthfully evaluated and not influenced by the test spindle on pick-up characteristics.

1. Frequencies not Included in Frequency Range

Vibrations at frequencies less than 50 cps and higher than 10,000 cps are not measured by the Anderometer. Hence, once per revolution cage-to-inner and cage-to-outer disturbing force frequencies are unaccounted for. The higher modes of outer ring "ringing" are on the order of 10,000 cps. Hence, depending upon bearing size, such

THE FRANKLIN INSTITUTE • *Laboratories for Research and Development*

I-A2321-1

ringing may be out of the measuring range. For 310 bearings, disturbing frequencies at 10,000 cps are generated by approximately 85 waves on a ball circumference, 109 waves on the outer raceway circumference or 67 waves on the inner raceway circumference. Hence, 10,000 cps appears adequate for ball waviness and outer raceway waviness, but may be exceeded by high order inner raceway waviness.

2. Low Band (50 to 300 cps)

Outer ball-pass frequency and its higher harmonics are the major contributors in this frequency band due to flexing of the outer ring as the loaded balls pass the point of vibration measurement. The vibration wave form will have appreciable higher harmonic content due to the instantaneous nature of the ball load. Along these lines, axially loaded bearings having very little radial clearance will exhibit higher amplitudes of ball-pass flexing than those with appreciable clearance due to the necessarily higher ball loads required to produce the required axial load carrying capacity. Low order ball and raceway waviness will also contribute to the generation of disturbing forces in this frequency range. If the radial runout is excessive, the higher harmonics of the once per revolution occurrence will contribute. Also, under such condition a disturbance at inner ball-pass frequency will be generated.

3. Medium Band (300 to 1800 cps)

Waviness of ball bearing components (on the order of 5 to 50 waves per circumference) if present, can generate frequencies in this

THE FRANKLIN INSTITUTE • *Laboratories for Research and Development*

I-A2321-1

range. Also, sub-frequencies of higher order waviness can also contribute. Since the magnitude of these disturbing forces is relatively low the forced vibrational amplitude will, in this frequency range, also probably be low compared to ball-pass flexing in the low-band and outer ring "ringing" in the high band.

4. High Band (1800 to 10,000 cps)

With the outer ring free and constrained only by the ball loads, "ringing" of the outer ring at one or more of its natural modes of vibration must occur. Such ringing frequencies are on the order of 100 times the ball-pass frequency, hence, are not suppressed to any large degree. Another peak frequency would be the resonant frequency of the outer ring mass vibrating on the springs provided by the ball-race contacts. Depending upon bearing size, clearance and axial load, this particular frequency will be on the order of 2500 to 4000 cps. Other resonant systems within the high band may also be excited. High order waviness of bearing components will generate disturbing frequencies in this frequency range.

4.1.3 Transmission of Vibration Forces Through the Bearing

A. Low Frequency Disturbing Forces ( $f < 300$  cps)

Disturbing forces of relatively low frequency (such as due to unbalance, eccentricity, inner and outer ball pass, and low order ball and race wavinesses) have a transmissibility ratio of:  $r = 1$

I-A2321-1

B. Medium Frequency Disturbances ( $300 < f < 1000$ )

Disturbing forces in this frequency range may be magnified due to resonance of the rotor on its bearings (higher harmonics of ball-pass and higher order waviness can produce frequencies in this range). Thus, in this range,

$$r > 1$$

C. High Frequency Disturbances ( $1000 < f < \infty$ )

Disturbing forces in this frequency range may be magnified due to excitation of the several natural modes of vibration of the outer ring. Hence,

$$r > 1$$

Hence, the rolling element bearing is an active transmitter and potential amplifier of disturbing forces originating in the rotor or generated in the bearing.

4.2 Sliding Surface Bearings

4.2.1 Vibration Generation

A. Sleeve bearings, as used in electric motor applications, should not suffer from the inherent instabilities of half-frequency whirl and oil whip (see "F" below also).

B. Low frequency waviness of the journal will generate vibration ( $f_{\max} = 10 f_i$ )



C. High frequency journal waviness ( $w_j > 10$ ) will not contribute to vibration generation unless waviness amplitudes are on the order of  $100 \times 10^{-6}$  inches.

D. The large angular and axial extent of the fluid film pressure distribution tend to average out geometry imperfections of bearing members.

E. Inadequate design or mis-application of sleeve bearings can promote vibration generation. It is important to note that the frequencies of vibration generated will, in general, be less than  $10 \times f_i$ .

F. In some cases, (extremely light load, high speed, high mass) inherent instability may be encountered. Methods of predicting instability are available and can be prevented by correct design.

#### 4.2.2 Vibrational Response

A. Sleeve bearings are relatively highly damped. Hence, resonant frequencies as such should not exist.

B. Disturbing forces at any frequency except at one-half shaft speed will not produce excessive vibrations of the spindle.

C. Since the journal is an integral part of the rotor and the bearing is normally a press fit in the housing, "resonance" of bearing members is not a problem.

D. Vibrational amplitudes within the bearing due to disturbing forces will be less than static displacement under influence of static forces of the same magnitudes.

#### 4.2.3 Transmission of Disturbing Forces

A. Transmissibility of disturbing forces in sleeve bearings is essentially unity for all frequencies. This may be attributed to its relatively high damping qualities.

#### 4.3 Comparison of Rolling Contact and Sliding Surface Bearings

From the standpoints of vibration generation and transmission it would appear that sliding surface bearings have the advantage over rolling contact bearings for noise critical applications for reasons such as;

1. Sleeve bearings generate only low frequency noise

$$\left(0.5 < \frac{f}{f_i} < 10\right)$$

2. Ball bearings generate vibrations over a broader range

$$\left(0.4 < \frac{f}{f_i} < 1000\right)$$

3. Sleeve bearings offer high damping to eliminate bearing "resonances" as such and allow only unity transmission of all disturbing forces.

4. Ball bearing components, particularly the outer ring, are subject to excitation of one or more of their natural modes of vibration.

5. In ball bearings, the components are subjected to continually varying and highly concentrated forces of varying magnitude and direction because load carrying capacity is achieved through high stress contact of the rotating balls and races. In the sleeve bearing, however, the

THE FRANKLIN INSTITUTE • *Laboratories for Research and Development*

I-A2321-1

"infinite" number of oil molecules allow a single, stationary pressure distribution to support the load over a large area rather than at several distinct points which are continually changing.

The chief disadvantages of journal bearings are;

a. Require a continuous, adequate supply of clean lubricant at the proper temperature. This usually means increased space requirements and increased maintenance. The use of a fluid lubricant (non-grease) is often undesirable.

b. Separate thrust bearings usually required.

c. Lubrication system may limit rotor orientation.

d. Grooving may restrict direction of load application.

e. Effective oil seals are required.

f. Emergency replacement involving shaft damage.

g. Noise of lubricant supply system (pumps, etc.).

The apparent advantages of journal bearings with regard to bearing noise and vibration must be weighed in the light of the practical problems associated with their use (cited above). Such problems, of course, can be overcome, and, with diligence, the apparent penalties minimized.

4.4 Means for Improving the Vibrational Quality of Ball Bearings

Conventional ball bearings are designed for maximum load carrying capacity within the dimensional limits of standard bearing sizes. However, when load capacity is not of primary importance (as in electric motors) the internal construction of the bearing may be

I-A2321-1

modified to meet other functional requirements in special types of application. This study serves to relate design features of the bearing to vibrational performance in service, and suggests the following means by which the noise generating and transmitting tendencies can be moderated in some degree.

1. Internal Design of the Bearing

A decrease in ball size with a corresponding increase in number, reduces the individual ball load and tends to minimize the effect of residual errors. Increase in ball number also contributes to the reduction of amplitudes of inherent vibration due to ball-pass instability. Also, an increased number of balls promotes a greater number of constraints upon the outer ring thereby not favoring the lower modes of outer race flexural vibrations.

An increase in the relative thickness of the outer race will tend to minimize the free "ringing" of this part in its natural modes of vibration. The ringing frequencies will then be higher and thus more difficult to excite. The additional stiffness of the section will be less responsive to bending under the individual ball loads, where the ring is not directly supported by the housing fit.

2. Manufacturing Controls

Residual errors in the surface geometry of balls and raceways give rise to periodic forces identified with the relative rotation of the component parts. This study has shown the manner in which raceway waviness can interact to generate high frequency vibration.

I-A2321-1

It seems appropriate that suitable manufacturing controls be devised to limit this geometrical error on component parts that are intended for special quiet service. It may prove desirable to expand the specification of ball quality to include some control of waviness of its surface geometry and ball complement size variation.

### 3. Installation and Mounting of the Bearing

The simple expedient of correctly applying a given amount of axial pre-load considerably enhances the bearing's vibration performance by stabilizing the ball path and ball loads. Axial thrust preloads on the order of 4 times the radial load will minimize ball load variation around the bearing. Axial preload in electric motors should be approximately twice the rotor weight.

### 4. Damping

It should be possible to introduce damping into ball bearing design or application by such things as;

- a. laminated construction
- b. vibration tapes
- c. use of high specific damping capacity materials  
such as  
Mn-Cu alloys  
NIVCO 10  
403 alloy  
Tungsten and other carbides for rings and/or  
balls, and visco-elastic adhesives for rings.

5. ACKNOWLEDGEMENTS

The authors are indebted to many different parties who contributed directly and indirectly to the work contained herein. These, not previously acknowledged include the following;

Mr. William W. Shugarts, Jr., Manager, Friction and Lubrication Branch, Franklin Institute, for his administrative assistance during the course of the program.

Mr. Robert Gustafson and his associates at the Naval Engineering Experiment Station for giving us the benefit of their past and continuing experience in the field of bearing noise and vibration.

We are particularly grateful to technical representatives of the following rolling element bearing companies for the courtesies extended to us during technical discussions devoted to rolling element bearing noise and vibration.

The Fafnir Bearing Company  
New Departure Division, General Motors Corporation  
Marlin-Rockwell Corporation

Mr. R. Hershey and his associates in the Vibrations and Noise Section of the Designs Division, Philadelphia Navy Yard for telling us of their experience in the overhauling and rebuilding of electric motors for submarines.

THE FRANKLIN INSTITUTE • *Laboratories for Research and Development*

I-A2321-1

Mr. A. J. Ruffini, Bearings Branch, Code 644B, Bureau of  
Ships under whose supervision the program was conducted.

*Harry C. Rippel*

Harry C. Rippel  
Project Engineer

Approved by:

*W. W. Shugarts, Jr.*

W. W. Shugarts, Jr., Manager  
Friction and Lubrication Laboratory

*N. R. Droulard*

N. R. Droulard  
Technical Director

*F. L. Jackson*

F. L. Jackson, Assistant  
Director of Laboratories

THE FRANKLIN INSTITUTE • *Laboratories for Research and Development*

I-A2321-1

APPENDIX A

DEEP GROOVE BALL BEARING DIMENSIONS



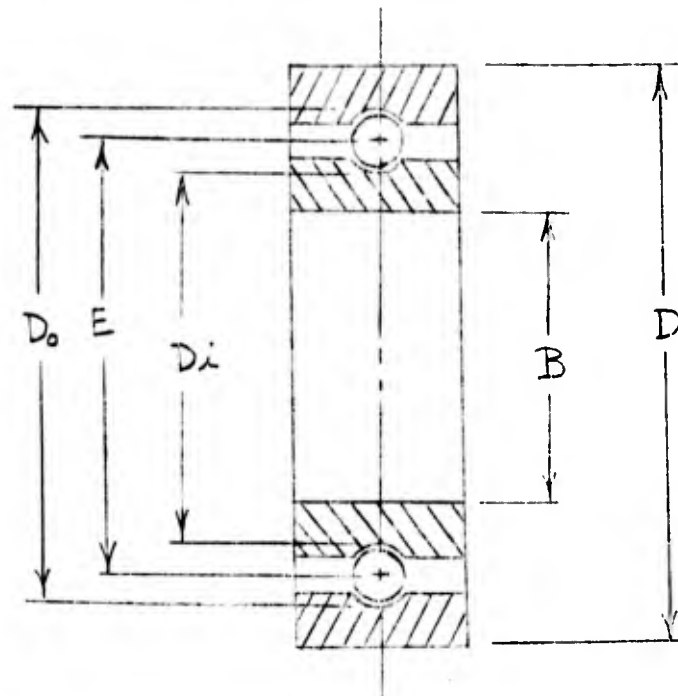
APPENDIX A

A.1. Deep Groove Ball Bearing Dimensions

$$\left. \begin{array}{l} B \\ d \\ D \end{array} \right\} \text{ Given}$$

$$\left. \begin{array}{l} D_o = E + d \\ D_i = E - d \end{array} \right\} \text{ Neglecting Clearance}$$

$$E = \frac{B + D}{2}$$



Series  
100  
200  
300

Follow:

THE FRANKLIN INSTITUTE • Laboratories for Research and Development

I-A2321-1

Bearing No.	B inches	D inches	Balls		D <sub>o</sub> inches	D <sub>i</sub> inches	E inches
			(n) No.	(d) Size inches			
100	.3937	1.0236	7	.1875	.8962	.5212	.7087
101	.4724	1.1024	7	.1875	.9749	.5999	.7874
102	.5906	1.2598	9	.1875	1.1127	.7377	.9252
103	.6693	1.3780	10	.1875	1.2112	.8362	1.0237
104	.7874	1.6535	8	.2500	1.4705	.9705	1.2205
105	.9843	1.8504	10	.2500	1.6674	1.1674	1.4174
106	1.1811	2.1654	11	.2812	1.9545	1.3921	1.6733
107	1.3780	2.4409	11	.3125	2.2220	1.5970	1.9095
108	1.5748	2.6772	13	.3125	2.4385	1.8135	2.1260
109	1.7717	2.9528	13	.3437	2.7060	2.0186	2.3623
110	1.9685	3.1496	14	.3437	2.9028	2.2154	2.5591
111	2.1654	3.5433	13	.4062	3.2606	2.4482	2.8544
112	2.3622	3.7402	14	.4062	3.4574	2.6450	3.0512
113	2.5591	3.9370	15	.4062	3.6543	2.8419	3.2481
114	2.7559	4.3307	14	.4687	4.0120	3.0746	3.5433
117	3.3465	5.1181	15	.5312	4.7635	3.7011	4.2323
118	3.5433	5.5118	14	.5937	5.1213	3.9339	4.5276
200	.3937	1.1811	7	.2187	1.0061	.5687	.7874
201	.4724	1.2598	7	.2344	1.1005	.6317	.8661
202	.5906	1.3780	7	.2500	1.2343	.7343	.9843
203	.6693	1.5748	8	.2812	1.4033	.8409	1.1221
204	.7874	1.8504	8	.3125	1.6314	1.0064	1.3189
205	.9843	2.0472	9	.3125	1.8283	1.2033	1.5158
206	1.1811	2.4409	8	.4062	2.2172	1.4048	1.8110
207	1.3780	2.8346	8	.4687	2.5750	1.6376	2.1063
208	1.5748	3.1496	9	.5000	2.8622	1.8622	2.3622
209	1.7717	3.3465	9	.5000	3.0591	2.0591	2.5591
210	1.9685	3.5433	10	.5000	3.2559	2.2559	2.7559
211	2.1654	3.9370	10	.5625	3.6137	2.4887	3.0512
212	2.3622	4.3307	10	.6250	3.9715	2.7215	3.3465
214	2.7559	4.9213	10	.6875	4.5261	3.1511	3.8386
215	2.9528	5.1181	10	.6875	4.7230	3.3480	4.0355
218	3.5433	6.2992	10	.875	5.7963	4.0463	4.9213

THE FRANKLIN INSTITUTE • Laboratories for Research and Development

I-A2321-1

Bearing No.	B inches	D inches	Balls		D <sub>o</sub> inches	D <sub>i</sub> inches	E inches
			n	(d) Size inches			
No.	inches	inches	No.	inches	inches	inches	inches
300	.3937	1.3780	6	.2812	1.1671	.6047	.8859
301	.4724	1.4567	6	.2812	1.2458	.6834	.9646
302	.5906	1.6535	6	.3437	1.4658	.7784	1.1221
303	.6693	1.8504	7	.3437	1.6036	.9162	1.2599
304	.7874	2.0472	7	.3750	1.7923	1.0423	1.4173
305	.9843	2.4409	7	.4687	2.1813	1.2439	1.7126
306	1.1811	2.8346	7	.5312	2.5391	1.4767	2.0079
307	1.3780	3.1496	7	.5625	2.8263	1.7013	2.2638
308	1.5748	3.5433	8	.6250	3.1841	1.9341	2.5591
309	1.7717	3.9370	8	.6875	3.5419	2.1669	2.8544
310	1.9685	4.3307	8	.7500	3.8996	2.3996	3.1496
311	2.1654	4.7244	8	.8125	4.2574	2.6324	3.4449
312	2.3622	5.1181	8	.8750	4.6151	2.8651	3.7401
313	2.5591	5.5118	8	.9375	4.9729	3.0979	4.0354
314	2.7559	5.9055	8	1.0000	5.3307	3.3307	4.3307
315	2.9528	6.2992	8	1.0625	5.6885	3.5635	4.6260
316	3.1496	6.6929	8	1.1875	6.1088	3.7338	4.9213
317	3.3465	7.0866	8	1.2500	6.4666	3.9666	5.2166
318	3.5433	7.4803	8	1.3125	6.8243	4.1993	5.5118

A.2. Fundamental Frequency Factors

Bearing No.	$\frac{d}{E}$	$1 + \frac{d}{E}$	$1 - \frac{d}{E}$	$\frac{1}{2} (1 + \frac{d}{E})$	$\frac{1}{2} (1 - \frac{d}{E})$	$\frac{1}{2} \frac{E}{d} (1 - \frac{d}{E})(1 + \frac{d}{E})$
100	.2649	1.2649	.7351	.5325	.3676	Not Req'd
101	.2381	1.2381	.7619	.6191	.3810	Not Req'd
102	.2027	1.2027	.7973	.6014	.3987	Not Req'd
103	.1832	1.1832	.8168	.5916	.4084	Not Req'd
104	.2048	1.2048	.7952	.6025	.3976	Not Req'd
105	.1764	1.1764	.8236	.5882	.4118	2.747
106	.1681	1.1681	.8319	.5841	.4160	2.891
107	.1637	1.1637	.8363	.5819	.4182	2.973
108	.1470	1.1470	.8530	.5735	.4265	3.328
109	.1455	1.1455	.8545	.5728	.4273	3.364
110	.1343	1.1343	.8657	.5672	.4329	3.656
111	.1423	1.1423	.8577	.5712	.4289	3.443
112	.1331	1.1331	.8669	.5666	.4335	3.690
113	.1251	1.1251	.8749	.5626	.4375	3.934
114	.1323	1.1323	.8677	.5662	.4339	3.714
117	.1255	1.1255	.8745	.5628	.4373	3.921
118	.1311	1.1311	.8689	.5656	.4345	3.749

THE FRANKLIN INSTITUTE • Laboratories for Research and Development

I-A2321-1

Bearing No.	$\frac{d}{E}$	$1 + \frac{d}{E}$	$1 - \frac{d}{E}$	$\frac{1}{2} (1 + \frac{d}{E})$	$\frac{1}{2} (1 - \frac{d}{E})$	$\frac{1}{2} \frac{E}{d} (1 - \frac{d}{E})(1 + \frac{d}{E})$
200	.2777	1.2777	.7223	.6389	.3612	Not Req'd
201	.2706	1.2706	.7294	.6353	.3647	Not Req'd
202	.2540	1.2540	.7460	.6270	.3730	Not Req'd
203	.2506	1.2506	.7494	.6253	.3747	Not Req'd
204	.2369	1.2369	.7631	.6185	.3816	Not Req'd
205	.2062	1.2062	.7938	.6031	.3969	2.322
206	.2243	1.2243	.7757	.6122	.3879	2.117
207	.2225	1.2225	.7775	.6113	.3888	2.136
208	.2117	1.2117	.7883	.6059	.3892	2.228
209	.1954	1.1954	.8046	.5977	.4023	2.461
210	.1814	1.1814	.8186	.5907	.4093	2.666
211	.1844	1.1844	.8156	.5922	.4078	2.620
212	.1868	1.1868	.8132	.5934	.4066	2.583
214	.1791	1.1791	.8209	.5896	.4105	2.702
215	.1704	1.1704	.8296	.5852	.4148	2.849
218	.1778	1.1778	.8222	.5889	.4111	2.723
300	.3174	1.3174	.6826	.6587	.3413	Not Req'd
301	.2915	1.2915	.7085	.6458	.3542	Not Req'd
302	.3063	1.3063	.6937	.6532	.3468	Not Req'd
303	.2728	1.2728	.7272	.6364	.3636	Not Req'd
304	.2646	1.2646	.7354	.6323	.3677	Not Req'd
305	.2737	1.2737	.7263	.6368	.3632	1.690
306	.2646	1.2646	.7354	.6323	.3677	1.758
307	.2485	1.2485	.7515	.6242	.3758	1.888
308	.2442	1.2442	.7558	.6221	.3779	1.926
309	.2408	1.2408	.7592	.6204	.3796	1.956
310	.2381	1.2381	.7619	.6190	.3810	1.981
311	.2358	1.2358	.7642	.6179	.3821	2.003
312	.2340	1.2340	.7660	.6170	.3830	2.020
313	.2323	1.2323	.7677	.6162	.3838	2.036
314	.2309	1.2309	.7691	.6154	.3846	2.050
315	.2297	1.2297	.7703	.6148	.3852	2.062
316	.2413	1.2413	.7587	.6206	.3794	1.952
317	.2396	1.2396	.7604	.6198	.3802	1.967
318	.2381	1.2381	.7619	.6190	.3810	1.981

I-A2321-1

A.3. Ball-Pass Frequency Factors

Bearing No.	$\frac{n}{2} (1 - \frac{d}{E})$	$\frac{n}{d} (1 + \frac{d}{E})$
105	4.118	5.882
106	4.576	6.425
107	4.600	6.401
108	5.545	7.456
109	5.555	7.446
110	6.061	7.941
111	5.576	7.426
112	6.069	7.932
113	6.563	8.439
114	6.075	7.927
117	6.560	8.442
118	6.083	7.918
205	3.572	5.428
206	3.103	4.898
207	3.110	4.890
208	3.503	5.497
209	3.621	5.379
210	4.093	5.907
211	4.078	5.922
212	4.066	5.934
214	4.105	5.896
215	4.148	5.852
218	4.111	5.889
305	2.542	4.457
306	2.574	4.426
307	2.631	4.369
308	3.023	4.977
309	3.037	4.963
310	3.048	4.952
311	3.057	4.943
312	3.064	4.936
313	3.070	4.930
314	3.077	4.923
315	3.082	4.918
316	3.035	4.965
317	3.042	4.958
318	3.048	4.952

THE FRANKLIN INSTITUTE • *Laboratories for Research and Development*

I-A2321-1

APPENDIX B

DETERMINATION OF Q FOR USE IN EQUATIONS (17) & (18)

THE FRANKLIN INSTITUTE • *Laboratories for Research and Development*

I-A2321-1

APPENDIX B

B.1. Determination of Q for use in Equations (17) & (18)

$$\text{Outer Waviness Frequency factor} = \frac{f_{w_0}}{f_1} = \frac{n}{Q} \times w_0 \times \frac{1}{2} \left(1 - \frac{d}{E}\right) \quad (17)$$

Similarly,

$$\text{Inner Waviness Frequency factor} = \frac{f_{w_1}}{f_1} = \frac{n}{Q} \times w_1 \times \frac{1}{2} \left(1 + \frac{d}{E}\right) \quad (18)$$

$n$ ,  $w_1$ ,  $w_0$ ,  $d$  and  $E$  are known values, but  $Q$  must be determined.

$Q$  is always an integer in the range  $1 \leq Q \leq n$ . Its numerical value for a particular combination of  $w$  and  $n$  is equal to the largest integer which can be divided into both  $w$  and  $n$  yielding  $\bar{w}$  and  $\bar{n}$  (also in tegers) respectively.

$$Q = \frac{n}{\bar{n}} = \frac{w}{\bar{w}}$$

Consider the following examples:

$$1. \quad n = 8 \quad w = 20$$

$$\frac{n}{w} = \frac{8}{20} = \frac{2}{2} \times \frac{4}{10} = \frac{2}{2} \times \frac{2}{2} \times \frac{2}{5} = \frac{4}{4} \times \frac{2}{5}$$

$$\therefore \frac{n}{w} = \frac{4}{4} \times \frac{2}{5}$$

$$\frac{n}{w} = \frac{4}{4} \times \frac{\bar{n}}{\bar{w}}$$

THE FRANKLIN INSTITUTE • *Laboratories for Research and Development*

I-A2321-1

$$\therefore \left. \begin{array}{l} Q = 4 \\ \frac{n}{w} = 2 \\ w = 5 \end{array} \right\} \begin{array}{l} Q \times \bar{n} = n = 8 \\ Q \times \bar{w} = w = 12 \end{array}$$

2.  $n = 8, w = 21$

$$\frac{n}{w} = \frac{8}{21} = \frac{1}{1} \times \frac{8}{21}$$

$$\therefore \frac{n}{w} = \frac{1}{1} \times \frac{8}{21}$$

$$\therefore \left. \begin{array}{l} Q = 1 \\ \frac{n}{w} = 8 \\ w = 21 \end{array} \right\} \begin{array}{l} Q \times \bar{n} = 8 \\ Q \times \bar{w} = w = 21 \end{array}$$

3.  $n = 8, w = 8$

$$\frac{n}{w} = \frac{8}{8} = \frac{8}{8} \times \frac{1}{1} = \frac{Q}{Q} \cdot \frac{\bar{n}}{\bar{w}}$$

$$\therefore \left. \begin{array}{l} Q = 8 \\ \frac{n}{w} = 1 \\ w = 1 \end{array} \right\} \begin{array}{l} Q \times \bar{n} = n = 8 \\ Q \times \bar{w} = w = 8 \end{array}$$

Values of Q for many combinations of w and n are given in Table No. B-1.

Notice that the pattern of Q repeats every  $n^{\text{th}}$  Ball.



Table B-1

NO. OF BALLS TOUCHING RACEWAY WAVE PEAKS  
AT ANY INSTANT (Q)

No. OF WAVES W	Q																	
	n=6	n=7	n=8	n=9	n=10	n=11	n=12	n=13	n=14	n=15	n=16							
0	6	7	8	9	10	11	12	13	14	15	16							
1	1	1	1	1	1	1	1	1	1	1	1							
2	2	1	2	1	2	1	2	1	2	1	2							
3	3	1	1	3	1	1	3	1	1	3	1							
4	2	1	4	1	2	1	4	1	2	1	4							
5	1	1	1	1	5	1	1	1	1	5	1							
6	6	1	2	3	2	1	6	1	2	3	2							
7	1	7	1	1	1	1	1	1	7	1	1							
8	2	1	8	1	2	1	4	1	2	1	8							
9	3	1	1	9	1	1	3	1	1	3	1							
10	2	1	2	1	10	1	2	1	2	5	2							
11	1	1	1	1	1	11	1	1	1	1	1							
12	6	1	4	3	2	1	12	1	2	3	4							
13	REPEATS ↓	1	1	1	1	1	1	13	1	1	1							
14		7	2	1	2	1	2	1	14	1	2							
15		REPEATS ↓	1	1	3	5	1	3	1	15	1							
16	REPEATS ↓		8	1	2	1	4	1	2	1	16							
17			REPEATS ↓	1	1	1	1	1	1	1	1							
18	REPEATS ↓	REPEATS ↓		9	2	1	6	1	2	3	2							
19				REPEATS ↓	1	1	1	1	1	1	1	1						
20					10	1	4	1	2	5	4							
21	REPEATS ↓	REPEATS ↓	REPEATS ↓		REPEATS ↓	1	3	1	7	3	1							
22						11	2	1	2	1	2							
23						REPEATS ↓	1	1	1	1	1							
24	REPEATS ↓	REPEATS ↓	REPEATS ↓				12	1	2	3	8							
25							REPEATS ↓	1	1	5	1							
26								13	2	1	2							
27	REPEATS ↓	REPEATS ↓	REPEATS ↓					REPEATS ↓	1	3	1							
28									14	1	4							
29									REPEATS ↓	5	1							
30	REPEATS ↓	REPEATS ↓	REPEATS ↓							REPEATS ↓	2							
31											1							
32											16							
33	REPEATS ↓	REPEATS ↓	REPEATS ↓								REPEATS ↓							
34																		

THE FRANKLIN INSTITUTE • *Laboratories for Research and Development*

I-A2321-1

B.2 Development of an Expression for Outer Waviness Sub-Frequency Factor

1<sup>st</sup> - Locate where (angle from 0°) in the bearing the first contact takes place, call this  $\theta_{1st}$ .  
 $\theta_{1st}$  is positive if less than 180°. If it turns out to be more than 180°, subtract 360° from it.

2<sup>nd</sup> - Divide  $\theta_{1st}$  by 360°

$$\therefore f_{wo_{sub}} = \frac{\theta_{1st}}{360} \times f_{wo} \quad \text{Outer Waviness Sub-Frequency}$$

From (17)

$$f_{wo_{sub}} = \frac{\theta_{1st}}{360} \times \frac{w_o}{Q} \times n f_E$$

$\theta_{1st}$  may be expressed as:

$$\theta_{1st} = \frac{360}{n} (k_B \pm \frac{Q}{w_o})$$

where  $k_B$  = smallest No. of ball spaces between successive ball contacting peaks

+ sign used if 2<sup>nd</sup> ball is closer in direction of cage movement

- sign used if 2<sup>nd</sup> ball is closer in opposite direction

$$\therefore f_{wo_{sub}} = (k_B \pm \frac{Q}{w_o}) \frac{w_o}{Q} \times f_E$$

$$\frac{f_{wo_{sub}}}{f_1} = \left( \frac{w_o}{Q} k_B \pm 1 \right) \times \frac{1}{2} \left( 1 - \frac{d}{E} \right) \quad (19)$$

Table B-2

OUTER-WAVINESS SUB-FREQUENCIES (n=8 Balls)

$$f_{w_{0SUB}} = \left[ \frac{w_0}{Q} b_D \pm 1 \right] f_E$$

$$f_{w_{0SUB}} = \left[ \frac{w_0}{Q} b_D \pm 1 \right] \frac{1}{2} \left( 1 - \frac{d}{L} \right) f_i$$

n = 8 BALLS

310 BRG

$w_0$	Q	1 <sup>ST</sup> BALL TO CONTACT AFTER TIME "0"	$b_D$	$\frac{w_0}{Q} b_D$	$\left[ \frac{w_0}{Q} b_D \pm 1 \right]$	PATTERN	$(0.381) \left[ \frac{w_0}{Q} b_D \pm 1 \right]$
1	1	7	1 ⊖	1	0	+8 =	0
2	2	7, 3	1 ⊖	1	0	+4 =	0
3	1	5	3 ⊖	9	8	+24 =	3.048
4	1	7, 1, 3, 5	1 ⊖	1	0	+2 =	0
5	1	3	3 ⊖	15	16	+24 =	6.096
6	2	5, 1	3 ⊖	9	8	+12 =	3.048
7	1	1	1 ⊕	7	8	+8 =	3.048
8	8	7, 1, 3, 5, 6	1 ⊖	1	0	+1 =	0
9	1	7	1 ⊖	9	8	← +16 =	3.048
10	2	7	1 ⊖	5	4	← +4 =	1.524
11	1	5	3 ⊖	33	32	← +24 =	12.192
12	4	7	1 ⊖	3	2	← +2 =	0.762
13	1	3	3 ⊖	39	40	← +24 =	15.240
14	2	5	3 ⊖	21	20	← +12 =	7.620
15	1	1	1 ⊕	15	16	← +8 =	6.096
16	8	7	1 ⊖	2	1	← +1 =	0.381
17	1	7	1 ⊖	17	16	←	6.096
18	2	7	1 ⊖	9	8	←	3.048
19	1	5	3 ⊖	57	56	←	21.336
20	4	7	1 ⊖	5	4	←	1.524
21	1	3	3 ⊕	63	64	←	24.384
22	2	5	3 ⊖	33	32	←	12.192
23	1	1	1 ⊕	23	24	←	9.144
24	8	7	1 ⊖	3	2	←	0.762

CONTINUED ON NEXT PAGE

THE FRANKLIN INSTITUTE • Laboratories for Research and Development

I-A2321-1

Table B-2 (Cont'd)

OUTER-WAVINESS SUB-FREQUENCIES (n = 8 Balls)

$$f_{w_{o\text{sub}}} = \left[ \frac{w_o}{Q} k_B \pm 1 \right] f_E = \left[ \frac{w_o}{Q} k_B \pm 1 \right] \frac{1}{2} \left( 1 - \frac{d}{E} \right) f_1$$

$$\frac{1}{2} \left( 1 - \frac{d}{E} \right) = 0.381 \text{ for 310 BR'G}$$

		310 BRG				310 BRG				310 BRG	
$w_o$	$\left[ \frac{w_o}{Q} k_B \pm 1 \right]$	$0.381 \left[ \frac{w_o}{Q} k_B \pm 1 \right]$	$\left[ \frac{w_o}{Q} k_B \pm 1 \right]$	$w_o$	$\left[ \frac{w_o}{Q} k_B \pm 1 \right]$	$0.381 \left[ \frac{w_o}{Q} k_B \pm 1 \right]$	$\left[ \frac{w_o}{Q} k_B \pm 1 \right]$	$w_o$	$\left[ \frac{w_o}{Q} k_B \pm 1 \right]$	$0.381 \left[ \frac{w_o}{Q} k_B \pm 1 \right]$	$\left[ \frac{w_o}{Q} k_B \pm 1 \right]$
25	24	9.144		57	56	21.336		89	88	33.528	
26	12	4.572		58	28	10.668		90	44	16.764	
27	80	30.480		59	176	67.056		91	272	103.632	
28	6	2.286		60	14	5.334		92	22	8.382	
29	88	33.528		61	184	70.104		93	280	106.680	
30	44	16.764		62	92	35.052		94	140	53.340	
31	32	12.192		63	64	24.384		95	96	36.576	
32	3	1.143		64	7	2.667		96	11	4.191	
33	32	12.192		65	64	24.384		97	96	36.576	
34	16	6.096		66	32	12.192		98	48	18.288	
35	104	39.624		67	200	76.200		99	296	112.776	
36	8	3.048		68	16	6.096		100	24	9.144	
37	112	42.672		69	208	79.248		101	304	115.824	
38	56	21.336		70	104	39.624		102	152	57.912	
39	40	15.240		71	72	27.432		103	104	39.624	
40	4	1.524		72	8	3.048		104	12	4.572	
41	40	15.240		73	72	27.432		105	104	39.624	
42	20	7.620		74	36	13.716		106	52	19.812	
43	128	48.768		75	224	85.344		107	320	121.920	
44	10	3.810		76	18	6.858		108	26	9.906	
45	136	51.816		77	232	88.392		109	328	124.968	
46	68	25.908		78	116	44.196		110	164	62.484	
47	48	18.288		79	80	30.480		111	112	42.672	
48	5	1.905		80	9	3.429		112	13	4.953	
49	48	18.288		81	80	30.480		113	112	42.672	
50	24	9.144		82	40	15.240		114	56	21.336	
51	152	57.912		83	248	94.488		115	344	131.064	
52	12	4.572		84	20	7.620		116	28	10.668	
53	160	60.960		85	256	97.536		117	352	134.112	
54	80	30.480		86	128	48.768		118	176	67.056	
55	56	21.336		87	88	33.528		119	120	45.720	
56	6	2.286		88	10	3.810		120	14	5.334	

THE FRANKLIN INSTITUTE • Laboratories for Research and Development

I-A2321-1

Using the examples cited in Section 3.1.1.1.6;

$$\begin{array}{l}
 n = 8 \\
 w_o = 15 \\
 Q = 1 \\
 k_B = 1 \text{ (ball ①)} \\
 \therefore \text{use } \oplus \text{ sign}
 \end{array}
 \left\{
 \begin{array}{l}
 f_{wo_{sub}} = \left[ \frac{w_o}{Q} k_B \pm 1 \right] f_E \\
 = \left[ \frac{15}{1} (1) + 1 \right] f_E \\
 f_{wo_{sub}} = 16 f_E
 \end{array}
 \right\}
 \begin{array}{l}
 f_{wo} = \frac{w_o}{Q} n f_E \\
 = \frac{15}{1} \times 8 f_E \\
 f_{wo} = 120 f_E
 \end{array}$$

$$\begin{array}{l}
 n = 8 \\
 w_o = 17 \\
 Q = 1 \\
 k_B = 1 \text{ (ball ⑦)} \\
 \therefore \text{use } \ominus \text{ sign}
 \end{array}
 \left\{
 \begin{array}{l}
 f_{wo_{sub}} = \left[ \frac{17}{1} (1) - 1 \right] f_E \\
 f_{wo_{sub}} = 16 f_E
 \end{array}
 \right\}
 \begin{array}{l}
 f_{wo} = \frac{17}{1} \times 8 f_E \\
 f_{wo} = 136 f_E
 \end{array}$$

$$\begin{array}{l}
 n = 8 \\
 w_o = 19 \\
 Q = 1 \\
 k_B = 3 \text{ (ball ⑤)} \\
 \therefore \text{use } \ominus \text{ sign}
 \end{array}
 \left\{
 \begin{array}{l}
 f_{wo_{sub}} = \left[ \frac{19}{1} (3) - 1 \right] f_E \\
 f_{wo_{sub}} = 56 f_E
 \end{array}
 \right\}
 \begin{array}{l}
 f_{wo} = \frac{19}{1} \times 8 f_E \\
 f_{wc} = 152 f_E
 \end{array}$$

Other examples

$$\begin{array}{l}
 n = 8 \\
 w_o = 20 \\
 Q = 4 \\
 k_B = 1 \text{ (ball ⑦)} \\
 \therefore \text{use } \oplus \text{ sign}
 \end{array}
 \left\{
 \begin{array}{l}
 f_{wo_{sub}} = \left[ \frac{20}{4} (1) - 1 \right] f_E \\
 f_{wo_{sub}} = 4 f_E
 \end{array}
 \right\}
 \begin{array}{l}
 f_{wo} = \frac{20}{4} \times 8 f_E \\
 f_{wo} = 40 f_E
 \end{array}$$

$$\begin{array}{l}
 n = 8 \\
 w_o = 99 \\
 Q = 1 \\
 k_B = 3 \text{ (ball ⑤)} \\
 \therefore \text{use } \ominus \text{ sign}
 \end{array}
 \left\{
 \begin{array}{l}
 f_{wo_{sub}} = \left[ \frac{99}{1} (3) - 1 \right] f_E \\
 f_{wo_{sub}} = 298 f_E
 \end{array}
 \right\}
 \begin{array}{l}
 f_{wo} = \frac{99}{1} \times 8 f_E \\
 f_{wo} = 792 f_E
 \end{array}$$

### B.3 Development of an Expression for Inner Waviness Sub-Frequency Factor

As in the case of outer ring waviness, somewhere in the bearing a ball will be  $\frac{360}{n} \frac{Q}{W_1}$  degrees removed from a wave peak at the time one ball is in contact with some other wave peak. Consider a bearing with 15 waves on the inner race and 8 balls (see Figure B-1). The inner race rotates at  $\omega_i = 2\pi f_i$  in a clockwise direction while the ball complement rotates in the same direction at  $\omega_E = 2\pi f_E$ . For this case, balls (7) and (1) are closer to wave peaks than any other ball. They are removed from peaks 13 and 2 respectively by  $\frac{360^\circ}{n} \cdot \frac{Q}{W_1}$  degrees or  $\frac{360}{n} \cdot \frac{1}{15} = 3^\circ$ . Since  $\omega_i > \omega_E$ , ball (7) will contact wave peak 13 at time  $= \frac{1}{f_{wi}}$  at some angle  $\theta_{1st}$  removed from the vertical or

$$\theta_{1st} = \frac{360^\circ}{n} \times k_B \pm \Delta\theta_E$$

where  $k_B$  = smallest number of ball spaces from ball in contact to next ball to touch,  $\Delta\theta_E$  = angle cage moves through from  $t = 0$  to  $t = \frac{1}{f_{wi}}$ , + sign used if 2<sup>nd</sup> ball is closer in direction of cage rotation, - sign used if 2<sup>nd</sup> ball is closer in opposite direction,  $\theta_{1st}$  and  $\Delta\theta_E$  are shown in Figure B-1. From Figure B-1,

$$\theta_{1st} = \frac{360^\circ}{n} k_B \pm \Delta\theta_E$$

also

$$\begin{aligned} \Delta\theta_i &= \frac{360}{n} \frac{Q}{W_1} + \Delta\theta_E \\ \Delta\theta_i = \omega_i t &\quad \left\{ \quad \Delta\theta_E = \omega_E t \right. \\ \Delta\theta_i = \frac{\omega_i}{\omega_E} \Delta\theta_E &= \frac{f_i}{f_E} \Delta\theta_E \end{aligned}$$

Inner Wave Peak-Ball Contact Geometry

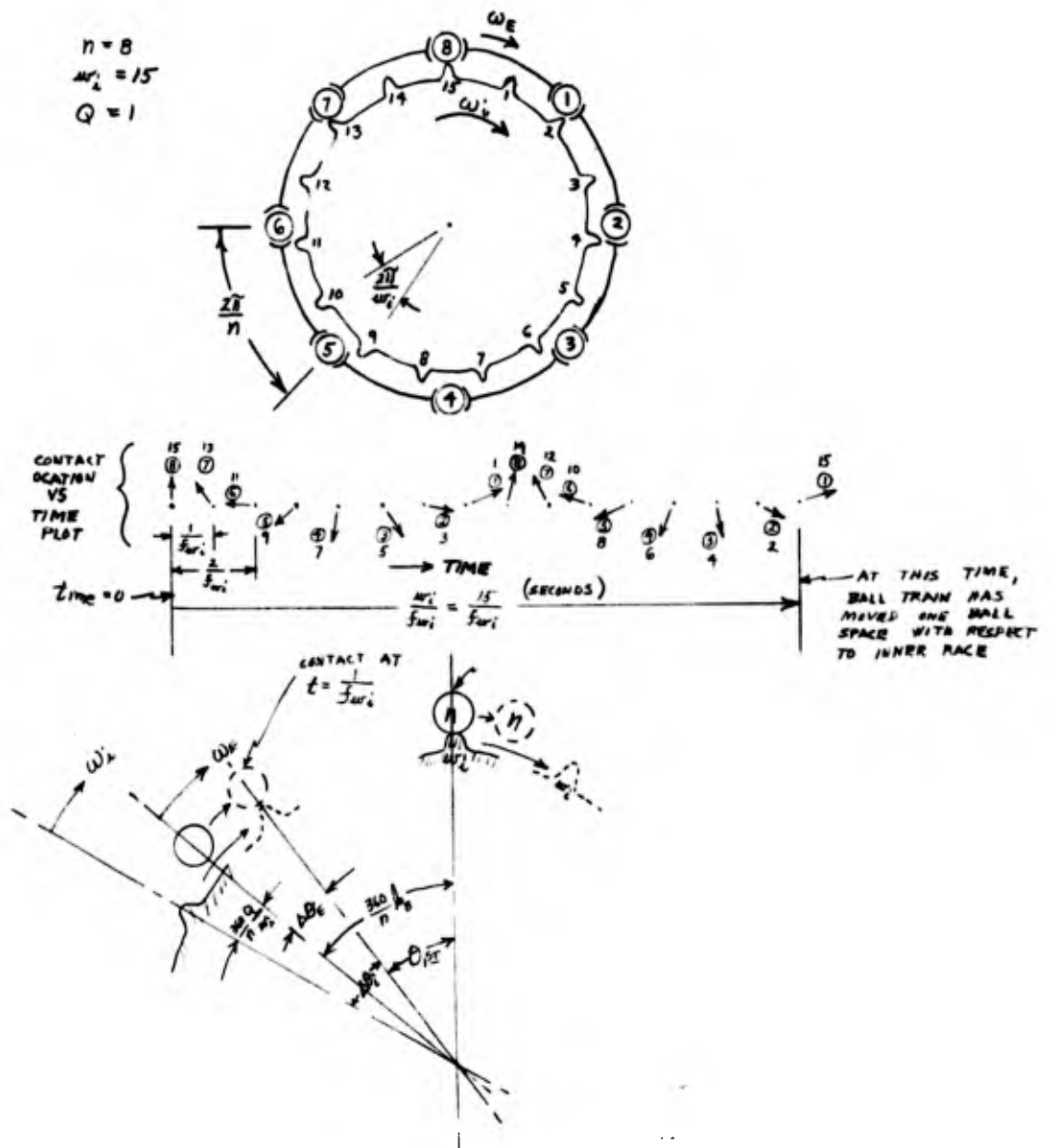


Figure B1

$$\begin{aligned}\frac{f_i}{f_E} \Delta\theta_E &= \frac{360}{n} \frac{Q}{w_i} + \Delta\theta_E \\ \left[ \frac{f_i}{f_E} - 1 \right] \Delta\theta_E &= \frac{360}{n} \frac{Q}{w_i} \\ \Delta\theta_E &= \frac{360}{n} \frac{Q}{w_i} \times \frac{f_E}{f_i - f_E} \\ \theta_{1st} &= \frac{360^\circ}{n} k_B \pm \frac{Q}{w_i} \frac{360^\circ}{n} \frac{f_E}{f_i - f_E} \\ \theta_{1st} &= \frac{360}{n} \left[ k_B \pm \frac{Q}{w_i} \frac{f_E}{f_i - f_E} \right]\end{aligned}$$

From (4)

$$\begin{aligned}f_E &= \frac{1}{2} \left( 1 - \frac{d}{E} \right) \\ \theta_{1st} &= \frac{360^\circ}{n} \left[ k_B \pm \frac{Q}{w_i} \frac{\left( 1 - \frac{d}{E} \right)}{\left( 1 + \frac{d}{E} \right)} \right], \text{degrees}\end{aligned} \quad (B-1)$$

Thus, the lower frequency, (as before for outer waviness) may be expressed as

$$f_{wi\_sub} = \frac{\theta_{1st}}{360^\circ} \times f_{wi}$$

Substituting for  $\theta_{1st}$  from (B-1) and  $f_{wi}$  from (18) yields

$$f_{wi\_sub} = \frac{\frac{360^\circ}{n} \left[ k_B \pm \frac{Q}{w_i} \frac{\left( 1 - \frac{d}{E} \right)}{\left( 1 + \frac{d}{E} \right)} \right]}{360^\circ} \times \frac{n}{Q} w_i \frac{1}{2} \left( 1 + \frac{d}{E} \right) f_i$$

or

$$\frac{f_{wi\_sub}}{f_i} = \left[ \frac{w_i}{Q} k_B \pm \frac{\left( 1 - \frac{d}{E} \right)}{\left( 1 + \frac{d}{E} \right)} \right] \frac{1}{2} \left( 1 + \frac{d}{E} \right) \text{ cps} \quad (20)$$

$\left[ \frac{w_i}{Q} k_B \pm \frac{\left( 1 - \frac{d}{E} \right)}{\left( 1 + \frac{d}{E} \right)} \right] \frac{1}{2} \left( 1 + \frac{d}{E} \right)$  for a 310 bearing are tabulated in Table B-3 for various values of  $w_i$ . Sub-frequency factors are plotted in Figure 8.



INNER WAVINESS SUB-FREQUENCIES (n=8 Balls)

$$f_{w_{i,j10}} = \left[ \frac{w_i}{Q} h_u \pm \frac{(1-\frac{d}{Q})}{(1+\frac{d}{Q})} \right] f_E$$

$$f_{w_{i,j20}} = \left[ \frac{w_i}{Q} h_u \pm \frac{(1-\frac{d}{Q})}{(1+\frac{d}{Q})} \right] \frac{1}{2} (1+\frac{d}{Q}) f_i$$

FOR 3/16 BR'G  
 $(1-\frac{d}{Q}) = 0.7619$   
 $(1+\frac{d}{Q}) = 1.2381$   
 $\frac{1}{2}(1+\frac{d}{Q}) = 0.619$

$w_i$	Q	1 <sup>ST</sup> BAIL TO CONTACT AFTER TIME = "0"	$h_u$	$\frac{w_i}{Q} h_u$	$\frac{w_i}{Q} h_u \pm \frac{(1-\frac{d}{Q})}{(1+\frac{d}{Q})}$	PATTERN	$(0.6M) \left[ \frac{w_i}{Q} h_u \pm 0.615 \right]$
1	1	1	1 ⊕	1	1.615	+8 =	1.000
2	2	1, 5	1 ⊕	1	1.615	+9 =	1.000
3	1	3	3 ⊕	9	9.615	+29 =	5.952
4	4	1, 3, 5, 7	1 ⊕	1	1.615	+2 =	1.000
5	1	5	3 ⊕	15	14.385	+24 =	8.904
6	2	3, 7	3 ⊕	9	9.615	+12 =	5.952
7	1	7	1 ⊕	7	6.385	+8 =	3.952
8	8	1, 2, 3, 4, 5, 6, 7, 8	1 ⊕	1	1.615	+1 =	1.000
9	1	1	1 ⊕	9	9.615	+8 =	5.952
10	2	1	1 ⊕	5	5.615	+4 =	3.476
11	1	3	3 ⊕	33	33.615	+29 =	20.808
12	4	1	1 ⊕	3	3.615	+2 =	2.238
13	1	5	3 ⊕	39	38.385	+24 =	23.760
14	2	3	3 ⊕	21	21.615	+12 =	13.380
15	1	7	1 ⊕	15	14.385	+8 =	8.904
16	8	1	1 ⊕	2	2.615	+1 =	1.619
17	1	1	1 ⊕	17	17.615		10.904
18	2	1	1 ⊕	9	9.615		5.952
19	1	3	3 ⊕	57	57.615		35.664
20	4	1	1 ⊕	5	5.615		3.476
21	1	5	3 ⊕	63	62.385		38.616
22	2	3	3 ⊕	33	33.615		20.808
23	1	7	1 ⊕	23	22.385		13.856
24	8	1	1 ⊕	3	3.615		2.238

CONT'D ON NEXT PAGE

THE FRANKLIN INSTITUTE • Laboratories for Research and Development

I-A2321-1

INNER WAVINESS SUB-FREQUENCIES (n=8 Balls)

CONT'D

$$f_{w_{i,sub}} = \left[ \frac{w_i}{Q} h_0 \pm \frac{(1-\frac{1}{Q})}{(1+\frac{1}{Q})} \right] f_E = \left[ \frac{w_i}{Q} h_0 \pm \frac{(1-\frac{1}{Q})}{(1+\frac{1}{Q})} \right] \frac{1}{2} \left( 1 + \frac{1}{Q} \right) f_i$$

3rd Ball  
 $(1-\frac{1}{Q}) = 0.762$   
 $\frac{1}{2}(1+\frac{1}{Q}) = 0.619$

$w_i$	$\left[ \frac{w_i}{Q} h_0 \pm 0.15 \right]$	$0.619 \left[ \frac{w_i}{Q} h_0 \pm 0.15 \right]$	$w_i$	$\left[ \frac{w_i}{Q} h_0 \pm 0.15 \right]$	$0.619 \left[ \frac{w_i}{Q} h_0 \pm 0.15 \right]$	$w_i$	$\left[ \frac{w_i}{Q} h_0 \pm 0.15 \right]$	$0.619 \left[ \frac{w_i}{Q} h_0 \pm 0.15 \right]$
25	25.615	15.856	57	57.615	35.664	89	89.615	55.972
26	13.615	8.428	58	29.615	18.332	90	45.615	28.236
27	81.615	50.520	59	177.615	109.974	91	273.615	169.368
28	7.615	4.714	60	15.615	9.666	92	23.615	14.618
29	86.385	53.972	61	182.385	112.896	93	278.385	172.320
30	45.615	28.236	62	93.615	57.998	94	141.615	87.660
31	30.385	18.808	63	62.385	38.616	95	94.385	58.424
32	4.615	2.857	64	8.615	5.333	96	12.615	7.809
33	33.615	20.808	65	65.615	40.616	97	97.615	60.424
34	17.615	10.904	66	33.615	20.808	98	49.615	30.172
35	105.615	65.376	67	201.615	124.800	99	297.615	189.224
36	9.615	5.952	68	17.615	10.904	100	25.615	15.856
37	110.385	68.328	69	206.385	127.752	101	302.385	187.176
38	57.615	35.664	70	105.615	65.376	102	153.615	95.088
39	38.385	23.760	71	70.385	43.568	103	102.385	63.376
40	5.615	3.476	72	9.615	5.952	104	13.615	8.428
41	41.615	25.760	73	73.615	45.568	105	105.615	65.376
42	21.615	13.380	74	37.615	23.284	106	53.615	33.188
43	129.615	80.232	75	225.615	139.656	107	321.615	199.080
44	11.615	7.190	76	19.615	12.142	108	27.615	17.094
45	134.385	83.184	77	230.385	142.608	109	326.385	202.032
46	69.615	43.092	78	117.615	72.804	110	165.615	102.516
47	46.385	28.712	79	78.385	48.520	111	110.385	68.328
48	6.615	4.095	80	10.615	6.571	112	14.615	9.047
49	49.615	30.712	81	81.615	50.520	113	113.615	70.328
50	25.615	15.856	82	41.615	25.760	114	57.615	35.664
51	153.615	95.088	83	249.615	154.512	115	345.615	213.936
52	13.615	8.428	84	21.615	13.380	116	29.615	18.332
53	158.385	98.040	85	254.385	157.964	117	359.385	216.888
54	81.615	50.520	86	129.615	80.232	118	177.615	109.944
55	54.385	33.664	87	86.385	53.472	119	118.385	73.280
56	7.615	4.714	88	11.615	7.190	120	15.615	9.666

THE FRANKLIN INSTITUTE • *Laboratories for Research and Development*

I-A2321-1

APPENDIX C

GENERALIZED EQUATIONS FOR THE GEOMETRY OF BALL BEARING COMPONENTS

## APPENDIX C

C.1 Generalized Equations for the Geometry  
of Ball Bearing Components

The geometry of a ball and the inner and outer raceways (in 2 dimensions) may be defined by the equations of a circle. The general equation, in polar coordinates, of a circle of radius "r" centered at position angle " $\phi$ " a distance "R" from some reference point ( $x=0, y=0$ ) as shown in Figure C-1 is derived below.

In rectangular coordinates we may

write

$$(x-x_o)^2 + (y-y_o)^2 = r^2$$

or

$$(x^2+y^2) + (x_o^2+y_o^2) - 2x_o x$$

$$- 2y_o y = r^2$$

but

$$x_o^2+y_o^2 = R^2 \text{ and } x^2+y^2 = \rho^2.$$

Also,

$$x = \rho \cos \theta \quad \text{and} \quad y = \rho \sin \theta$$

$$x_o = R \cos \phi \quad y_o = R \sin \phi$$

Substituting these in the above yields

$$\rho^2 + R^2 - 2R \cos \phi \cdot \rho \cos \theta - 2R \sin \phi \cdot \rho \sin \theta - r^2 = 0$$

$$\rho^2 - 2R (\cos \phi \cos \theta + \sin \phi \sin \theta) \rho + (R^2 - r^2) = 0$$

$$\rho^2 - 2R [\cos (\phi - \theta)] \rho + (R^2 - r^2) = 0$$

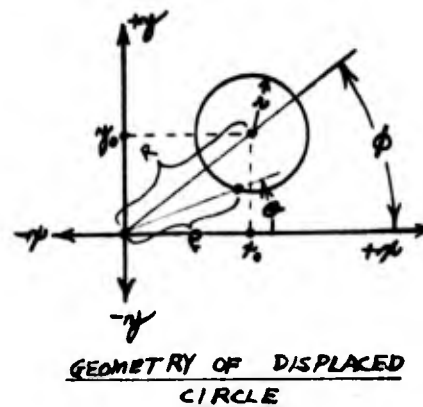


Figure C1

THE FRANKLIN INSTITUTE • Laboratories for Research and Development

I-A2321-1

Applying the quadratic equation gives the equation for a displaced circle in polar coordinates

$$\rho = R [\cos (\phi - \theta)] \pm \sqrt{r^2 - R^2 [\sin^2 (\phi - \theta)]}, \text{ (in.)} \quad (C-1)$$

Consider a displaced inner ring. Physically, it is displaced only very slightly with respect to the center of the stationary ring. If, in Eq.(C-1), we let

$R$  = shaft displacement magnitude =  $e$ , (in.)

$\phi$  = shaft displacement angle =  $\phi_1$ , (deg)

$r$  = inner race radius =  $R_i$ , (in.)

$\rho$  = distance from ( $x=0$ ,  $y=0$ ) to displaced inner race =  $\rho_1$ , (in.)

Then (C-1) may be written as

$$\rho_1 = e [\cos (\phi_1 - \theta)] \pm \sqrt{R_i^2 - e^2 [\sin^2 (\phi_1 - \theta)]}$$

since

$$\begin{aligned} R_i &\gg e \\ \therefore e^2 &\approx 0 \end{aligned}$$

$$\therefore \boxed{\rho_1 = e [\cos (\phi_1 - \theta)] + R_i} \quad (C-2)$$

Equation for displaced inner race

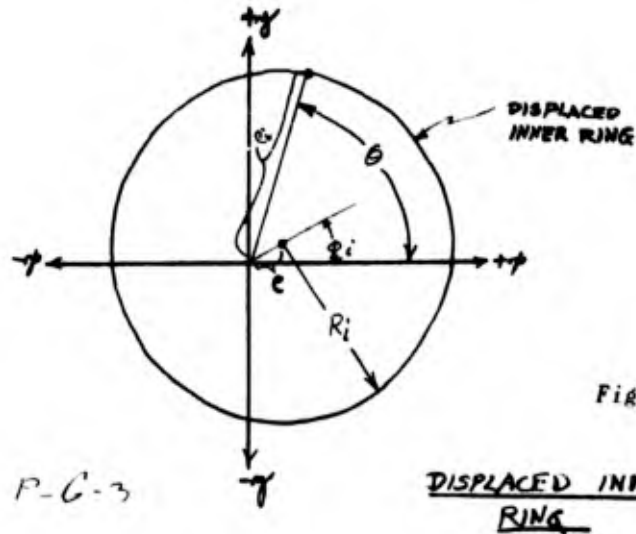


Figure C2

The center of the  $n^{\text{th}}$  ball in the train is assumed to be located at an angle  $\phi_n$  and at a radial distance from the center of the outer race equal to  $\frac{1}{2} (\rho_o + \rho_i)_{\theta = \phi_n}$  (this assumes equal deformation of inner and outer races).

Let

$$R_{Bn} = \frac{1}{2} (\rho_o + \rho_i)_{\theta = \phi_n}$$

$\rho_o$  is simply equal to  $R_o$

$\rho_i$  from (C-1) is  $e[\cos(\phi_i - \theta_n)] + R_i$

$$\therefore R_{Bn} = \frac{1}{2} [R_o + \{e \cos(\phi_i - \phi_n) + R_i\}]$$

$R_o$  can be written as

$$R_o = R_i + 2r_B + c - i \quad (C-3)$$

THE FRANKLIN INSTITUTE • Laboratories for Research and Development

I-A2321-1

where

$r_B$  = ball radius, (in.)

$c$  = radial clearance =  $\frac{1}{2}$  total radial play, (in.)

$i$  = radial interference =  $\frac{1}{2}$  total interference, (in.)

} For a BR'G with  
radial play,  $i=0$   
For a BR'G with  
interference,  $c=0$   
For a BR'G with  
no play and no  
interference,  
 $c=0$  and  $i=0$

Substituting for  $R_o$  from (C-3) gives,

$$R_{Bn} = (R_i + r_B) + \frac{1}{2} [c - i + e \cos (\phi_i - \phi_n)] \quad (C-4)$$

The equation for any ball in the train would be (from C-1),

$$\rho_{Bn} = R_{Bn} [\cos (\phi_n - \theta)] \pm \sqrt{r_B^2 - R_{Bn}^2 [\sin^2 (\phi_n - \theta)]} \quad (C-5)$$

where

$R_{Bn}$  is distance to center of ball

$\phi_n$  = angle to center of ball

$r_B$  = ball radius

$R_{Bn}$  is defined by Eq. (C-4). Substituting for  $R_{Bn}$  in (C-5)

$$\rho_{Bn} = \{R_i + r_B + \frac{1}{2} [c - i + e \cos (\phi_i - \phi_n)]\}$$

$$\pm \sqrt{r_B^2 - \{R_i + r_B + \frac{1}{2} [c - i + e \cos (\phi_i - \phi_n)]\}^2 \sin^2 (\phi_n - \theta)} \quad (C-6)$$

## C.2 Normal Approach of Inner and Outer Races (Ball Deformation)

In order to evaluate the load on each ball we must determine the magnitude of the normal approach of the inner and outer races (amount of squeeze on the ball).

$$\therefore \text{Normal Approach} = \delta_{N_n} = \delta_{o_n} + \delta_{i_n} \quad (C-7)$$

where

$\delta_{o_n}$  = deformation at outer race at  $\theta = \phi_n$

$\delta_{i_n}$  = deformation at inner race at  $\theta = \phi_n$

Now  $\delta_{o_n}$  is the difference between  $\rho_{Bn}$  and  $\rho_o$

$$\therefore \delta_{o_n} = -\rho_o + \rho_{Bn}$$

Since  $\rho_o = R_o$  and substituting  $\theta = \phi_n$  in (C-6)

$$\delta_{on} = -R_o + \left\{ R_i + r_B + \frac{1}{2} [c-i + e \cos (\phi_i - \phi_n)] \right\} \\ \pm \sqrt{r_B^2 - \left\{ R_i + r_B + \frac{1}{2} [c-i + e \cos (\phi_i - \phi_n)] \right\}^2 \sin^2 (\phi_n - \phi_n)}$$

Since  $\sin (0) = 0$

$$\therefore \delta_{o_n} = -R_o + \left\{ R_i + r_B + \frac{1}{2} [c-i + e \cos (\phi_i - \phi_n)] \right\} + (\pm r_B)$$



THE FRANKLIN INSTITUTE • Laboratories for Research and Development

I-A2321-1

Since we are concerned with ball-outer squeeze use  $\oplus$  sign.

$$\therefore \delta_{on} = R_i - R_o + 2r_B + \frac{1}{2} [c - i + e \cos (\phi_i - \phi_n)] \quad (C-8)$$

$\delta_{in}$  is the difference between  $\rho_i$  and  $\rho_{Bn}$  at  $\theta = \phi_n$

$$\therefore \delta_{in} = \rho_{in} - \rho_{Bn}$$

Substituting from (C-2) and (C-6) gives

$$\therefore \delta_{in} = e [\cos (\phi_i - \phi_n)] + R_i - \left\{ R_i + r_B + \frac{1}{2} [c - i + e \cos (\phi_i - \phi_n)] \pm r_B \right\}$$

Since we are concerned with ball-inner contact use  $\ominus$  sign

$$\therefore \delta_{in} = e [\cos (\phi_i - \phi_n)] - \frac{c-i}{2} - \frac{e}{2} \cos (\phi_i - \phi_n)$$

$$\delta_{in} = \frac{1}{2} [e \cos (\phi_i - \phi_n) - c + i] \quad (C-9)$$

Substituting (C-8) and (C-9) in (C-7) gives

$$\begin{aligned} \delta_{Nn} &= \delta_{on} + \delta_{in} = R_i - R_o + 2r_B + \frac{1}{2} [c - i + e \cos (\phi_i - \phi_n)] \\ &\quad + \frac{1}{2} [e \cos (\phi_i - \phi_n) - c + i] \end{aligned}$$

$$\delta_{Nn} = (R_i - R_o + 2r_B) + e \cos (\phi_i - \phi_n)$$

THE FRANKLIN INSTITUTE • *Laboratories for Research and Development*

I-A2321-1

From (C-3)  $(R_i - R_o + 2r_B) = i - c$

$$\therefore \delta_{N_n} = e \cos (\phi_i - \phi_n) - c + i \quad (C-10)$$

normal approach of raceways  
(total squeeze of ball)

THE FRANKLIN INSTITUTE • Laboratories for Research and Development

I-A2321-1

C.3 Ball Deformation - Load Relationships

The relationship between ball load ( $R_n$ ) and normal approach

$\delta_{N_n}$  is

$$R_n = k_N (\delta_{N_n})^{3/2}, \text{ (lbs)} \quad (C-11)$$

where

per A.B. Jones\*

$$k_N = \text{constant} = \frac{d^{\frac{1}{2}} \times 10^9}{[7.8107 (c_{\phi_0} + c_{\phi_1})]^{3/2}} \quad (C-12)$$

$d$  = ball dia.

$c_{\phi_0}$  &  $c_{\phi_1}$  from Jones Chart 56.

Combining equations (C-10) and (C-11) gives

$$R_n = k_N [e \cos (\phi_i - \phi_n) - c + i]^{3/2} \quad (C-13)$$

Let

$$\epsilon_c = e/c \text{ and } \epsilon_i = i/c$$

$$R_n = k_N \left[ c[\epsilon_c \cos (\phi_i - \phi_n) - 1] + i[\epsilon_i \cos (\phi_i - \phi_n) + 1] \right]^{3/2} \quad (C-14)$$

---

\*A. B. Jones, "Analysis of Stresses and Deflections", New Departure Div., General Motors Corp., 1946.

For a bearing with clearance ( $i=0$ )

$$\frac{R_n}{k_N c^{3/2}} = \left[ \epsilon_c \cos (\phi_i - \phi_n) - 1 \right]^{3/2}, \text{ (dimensionless)} \quad (C-15)$$

For a bearing with interference ( $c=0$ )

$$\frac{R_n}{k_N i^{3/2}} = \left[ \epsilon_i \cos (\phi_i - \phi_n) + 1 \right]^{3/2}, \text{ (dimensionless)} \quad (C-16)$$

For a bearing with  $c=0$  and  $i=0$

$$\frac{R_n}{k_N e^{3/2}} = \left[ \cos (\phi_i - \phi_n) \right]^{3/2}, \text{ (dimensionless)} \quad (C-17)$$

The vector addition of all of the ball loads due to  $n$  equally spaced balls gives the resultant load magnitude and direction.

For a bearing with clearance;

$$\therefore \frac{R}{k_N c^{3/2}} = \sum_{n=1}^{n=n} \frac{R_n}{k_N c^{3/2}} = \sum_{n=1}^{n=n} \left[ \epsilon_c \cos (\phi_i - \phi_n) - 1 \right]^{3/2} \quad (C-18)$$

Since the balls rotate we may restrict the shaft displacement angle,  $\phi_i$ , to a single angle; say zero for convenience.

$$\therefore \frac{R}{k_N c^{3/2}} = \sum_{n=1}^{n=n} \left[ \epsilon_c \cos (-\phi_n) - 1 \right]^{3/2} = \sum_{n=1}^{n=n} \left[ \epsilon_c \cos (\phi_n) - 1 \right]^{3/2} \quad (C-19)$$

Let

$$\left( \frac{R}{k_N c^{3/2}} \right)^2 = \left( \frac{R_c}{k_N c^{3/2}} \right)^2 + \left( \frac{R_t}{k_N c^{3/2}} \right)^2 \quad (C-20)$$

where

$R_c$  = component of  $R$  in direction of displacement  $c$ .

$R_t$  = component of  $R$  in direction of normal to displacement  $c$ .

$$\therefore A = \tan^{-1} \frac{R_t}{R_c} \quad (C-21)$$

where  $A$  = angle of resultant load.

$$R_{cn} = R_n \times \cos \phi_n$$

$$\therefore \frac{R_c}{k_N c^{3/2}} = \sum_{n=1}^{n=n} [c_c \cos \phi_n - 1]^{3/2} \times \cos \phi_n \quad (C-22)$$

likewise

$$\frac{R_t}{k_N c^{3/2}} = \sum_{n=1}^{n=n} [c_c \cos \phi_n - 1]^{3/2} \times \sin \phi_n \quad (C-23)$$

Similar equations may be derived for a bearing with interference and one with no clearance or interference. All pertinent equations for each case are tabled below.

Table C-1

LOAD-DISPLACEMENT RELATIONSHIPS FOR A  
DEEP GROOVE BALL BEARING UNDER PURE RADIAL LOAD

$\frac{1}{2}(D_o - D_i - 2d)$	Load-Displacement	Load Angle and Eccentricity Ratio
$c$ (Clearance)	$\frac{R_e}{k_N c^{3/2}} = \sum_{n=1}^{n=n} [\epsilon \cos \phi_n - 1]^{3/2} \times \cos \phi_n \quad (C-22)$ $\frac{R_t}{k_N c^{3/2}} = \sum_{n=1}^{n=n} [\epsilon \cos \phi_n - 1]^{3/2} \times \sin \phi_n \quad (C-23)$ $\left( \frac{R}{k_N c^{3/2}} \right)^2 = \left( \frac{R_e}{k_N c^{3/2}} \right)^2 + \left( \frac{R_t}{k_N c^{3/2}} \right)^2 \quad (C-20)$	$\epsilon = \frac{e}{c}$ $A = \tan^{-1} \frac{R_t}{R_e} \quad (C-21)$
$0$ ( $c=0, i=0$ )	$\frac{R_e}{k_N e^{3/2}} = \sum_{n=1}^{n=n} [\cos \phi_n]^{3/2} \times \cos \phi_n \quad (C-24)$ $\frac{R_t}{k_N e^{3/2}} = \sum_{n=1}^{n=n} [\cos \phi_n]^{3/2} \times \sin \phi_n \quad (C-25)$ $\left( \frac{R}{k_N e^{3/2}} \right)^2 = \left( \frac{R_e}{k_N e^{3/2}} \right)^2 + \left( \frac{R_t}{k_N e^{3/2}} \right)^2 \quad (C-26)$	$A = \tan^{-1} \frac{R_t}{R_e} \quad (C-21)$
$i$ (interference)	$\frac{R_e}{k_N i^{3/2}} = \sum_{n=1}^{n=n} [\epsilon \cos \phi_n + 1]^{3/2} \times \cos \phi_n \quad (C-27)$ $\frac{R_t}{k_N i^{3/2}} = \sum_{n=1}^{n=n} [\epsilon \cos \phi_n + 1]^{3/2} \times \sin \phi_n \quad (C-28)$ $\left( \frac{R}{k_N i^{3/2}} \right)^2 = \left( \frac{R_e}{k_N i^{3/2}} \right)^2 + \left( \frac{R_t}{k_N i^{3/2}} \right)^2 \quad (C-29)$	$\epsilon = \frac{e}{i}$ $A = \tan^{-1} \frac{R_t}{R_e} \quad (C-21)$

## C.4 Zero Clearance Bearing

This is the easiest case to consider. Using equations (C-24), (C-25), (C-26) and (C-27), values of  $\frac{R}{k_N e^{3/2}}$  and  $A^\circ$  were obtained for various ball positions of bearings with 6, 8 and 12 balls.

$$\underline{6 \text{ Balls}} \quad (2\alpha = \frac{360^\circ}{6} = 60^\circ)$$

From (C-24)

$$\frac{R}{k_N e^{3/2}} = \sum_{n=1}^{n=6} [\cos \phi_n]^{3/2} \times \cos \phi_n \quad (60)$$

$$\phi_1 = -\gamma = -\gamma$$

$$\phi_2 = 2\alpha - \gamma = 60 - \gamma$$

$$\phi_3 = 4\alpha - \gamma = 120 - \gamma$$

$$\phi_4 = 6\alpha - \gamma = 180 - \gamma$$

$$\phi_5 = 8\alpha - \gamma = 240 - \gamma$$

$$\phi_6 = 10\alpha - \gamma = 300 - \gamma$$

$$\begin{aligned} \therefore \frac{R}{k_N e^{3/2}} &= [\cos (-\gamma)]^{3/2} \times \cos (-\gamma) + [\cos (60-\gamma)]^{3/2} \times \cos (60-\gamma) \\ &+ [\cos (120-\gamma)]^{3/2} \times \cos (120-\gamma) + [\cos (180-\gamma)]^{3/2} \times \cos (180-\gamma) \\ &+ [\cos (240-\gamma)]^{3/2} \times \cos (240-\gamma) + [\cos (300-\gamma)]^{3/2} \times \cos (300-\gamma). \end{aligned}$$

$\gamma$  was varied from 0 to  $\alpha$ , ( $30^\circ$ ) in steps of  $5^\circ$  with the following results

THE FRANKLIN INSTITUTE • Laboratories for Research and Development

I-A2321-1

$\gamma^\circ$	$R_c/k_N e^{3/2}$		$\gamma^\circ$	$R_c/k_N e^{3/2}$
0	1.354	Due to symmetry →	60	1.354
5	1.355		55	1.355
10	1.362		50	1.362
15	1.371		45	1.371
20	1.382		40	1.382
25	1.392		35	1.392
30	1.396		30	1.396

Equation (C-25) gave the following results for  $\frac{R_t}{k_N e^{3/2}}$

$\gamma$	$R/k_N e^{3/2}$		$\gamma$	$R_t/k_N e^{3/2}$
0	0	Symmetry →	60	0
5	.0195		55	.0195
10	.0334		50	.0334
15	.0476		45	.0476
20	.0490		40	.0490
25	.0343		35	.0343
30	0		30	0

From (C-26) 
$$\frac{R}{k_N e^{3/2}} = \sqrt{\left(\frac{R_c}{k_N e^{3/2}}\right)^2 + \left(\frac{R_t}{k_N e^{3/2}}\right)^2}$$

and (57)

$A^\circ = \tan^{-1} \frac{R_t}{R_c}$  we obtain

$\gamma$	$R/k_N e^{3/2}$	$A^\circ$ (deg.)		$\gamma$	$R/k_N e^{3/2}$	$A^\circ$ (deg.)
0	1.3540	0	1 ball space	60	1.3540	0
5	1.3551	-0.8217		55	1.3551	+0.8217
10	1.3624	-1.4050		50	1.3624	+1.4050
15	1.3718	-1.9883		45	1.3718	+1.9883
20	1.3828	-2.0333		40	1.3828	+2.0333
25	1.3924	-1.4100		35	1.3924	+1.4100
30	1.3960	0		30	1.3960	0

If applied load is constant, then  $e$  is some max value (at  $\gamma = 0^\circ$ ) decreasing to a minimum (at  $\gamma = 30^\circ = \alpha$ ) then increasing to a max again (at  $\gamma = 60^\circ = 2\alpha$ ).

Load angle increases negatively from 0 to a max value, back to 0 and then goes through a positive cycle to a max value and back to 0.



I-A2321-1

$$12 \text{ Balls } \left( 2\alpha = \frac{360^\circ}{12} = 30^\circ \right)$$

The results of  $R/k_N e^{3/2}$  and  $A^\circ$  for 12 balls are tabled below

$\gamma$	$R/k_N e^{3/2}$	$A^\circ$ (deg)	$\gamma$	$R/k_N e^{3/2}$	$A^\circ$ (deg)
0	2.74948	0	30	2.74948	0
1	2.74935	0.118	29	2.74935	-0.118
2	2.74901	0.193	28	2.74901	-0.193
3	2.74852	0.292	27	2.74852	-0.292
6	2.74669	0.312	24	2.74669	-0.312
9	2.74485	0.265	21	2.74485	-0.265
12	2.74353	0.147	18	2.74353	-0.147
15	2.74296	0	15	2.74296	0

The pattern of variation of  $R$  and  $A^\circ$  with  $\gamma$  is opposite to that for 6 balls and of considerably less magnitude. The reversal of variation is due to the fact that more balls carry the load at  $\gamma=15$  than at  $\gamma=0$ , whereas the opposite is true for 6-balls.

$$8 \text{ Balls } \left( 2\alpha = \frac{360^\circ}{12} = 45^\circ \right)$$

The results of  $R/k_N e^{3/2}$  and  $A^\circ$  for 8 balls are tabled below.

$\gamma$	$R/k_N e^{3/2}$	$A^\circ$ (deg)	$\gamma$	$R/k_N e^{3/2}$	$A^\circ$ (deg)
0	1.8408	0	45	1.8408	0
2.5	1.8395	0.5080	42.5	1.8395	-0.5080
5	1.8377	0.7778	40	1.8377	-0.7778
7.5	1.8352	0.9083	37.5	1.8352	-0.9083
10	1.8317	0.9083	35	1.8317	-0.9083
12.5	1.8290	0.8208	32.5	1.8290	-0.8208
15	1.8259	0.6805	30	1.8259	-0.6805
17.5	1.8235	0.4957	27.5	1.8235	-0.4757
20	1.8225	0.2500	25	1.8225	-0.2500
22.5	1.8220	0	22.5	1.8220	0

The variation of  $e$  and  $A^\circ$  for 8 balls is similar to that for 12 balls but of greater amplitude.

THE FRANKLIN INSTITUTE • Laboratories for Research and Development

I-A2321-1

For a zero clearance bearing with 8 balls we may compile the following table.

Table C-2

ZERO CLEARANCE BR'G SHAFT LOCUS

$\gamma$	$R/k_N e^{\frac{3}{2}}$	$\left(\frac{k_N e^{3/2}}{R}\right)^{2/3}$	$A^\circ$	$\sin A^\circ$	$\cos A^\circ$	$X = \left(\frac{k_N e^{3/2}}{R}\right)^{2/3} \sin A^\circ$	$Y = \left(\frac{k_N e^{3/2}}{R}\right)^{2/3} \cos A^\circ$
0	1.8408	.6655	0	0	1.00000	0	.6655
2.5	1.8391	.6657	.508	.00890	.99996	.00592	.6657
5	1.8377	.6662	.778	.01357	.99991	.00904	.6661
7.5	1.8352	.6670	.908	.01585	.99988	.01057	.6669
10	1.8317	.6680	.908	.01585	.99988	.01059	.6679
12.5	1.8290	.6685	.821	.01431	.99990	.00957	.6684
15	1.8259	.6690	.681	.01188	.99993	.00795	.6690
17.5	1.8235	.6695	.476	.00830	.99996	.00556	.6695
20	1.8225	.6698	.250	.00436	.99999	.00292	.6698
22.5	1.8220	.6700	0	0	1.00000	0	.6700
25	1.8225	.6698	-.250	-.00436	.99999	-.00292	.6698
27.5	1.8233	.6695	-.476	-.00830	.99996	-.00556	.6695
30	1.8259	.6690	-.681	-.01188	.99993	-.00795	.6690
32.5	1.8290	.6685	-.821	-.01431	.99990	-.00957	.6684
35	1.8317	.6680	-.908	-.01585	.99988	-.01059	.6679
37.5	1.8352	.6670	-.908	-.01585	.99988	-.01057	.6669
40	1.8377	.6660	-.778	-.01357	.99991	-.00904	.6661
42.5	1.8391	.6657	-.508	-.00890	.99996	-.00592	.6657
45	1.8408	.6655	0	0	1.00000	0	.6655

One ball space, start another cycle.

THE FRANKLIN INSTITUTE • Laboratories for Research and Development

I-A2321-1

C.5 Values of  $k_N$  and  $k_N^{3/2}$ ;  $\left(\frac{\text{lbs}}{\text{in.}^{3/2}}\right)$ ,  $\left(\frac{\text{lbs}^{2/3}}{\text{in.}}\right)$

(Constant Relating Normal Ball Load and Normal Approach of Races)

Table C-3

BALL LOAD-NORMAL APPROACH CONSTANT

Extra Light BR'G Size	$k_N \times 10^{-6}$ $\left(\frac{\text{lbs}}{\text{in.}^{3/2}}\right)$	$k_N^{2/3} \times 10^{-4}$ $\left(\frac{\text{lb}^{2/3}}{\text{in.}}\right)$	Light BR'G Size	$k_N \times 10^{-6}$	$k_N^{2/3} \times 10^{-4}$	Medium BR'G Size	$k_N \times 10^{-6}$	$k_N^{2/3} \times 10^{-4}$
105	8.00	4.00	205	8.95	4.31	305	10.93	4.91
106	8.50	4.17	206	10.20	4.70	306	11.67	5.14
107	8.95	4.31	207	10.93	4.91	307	12.00	5.25
108	8.95	4.31	208	11.30	5.05	308	12.65	5.44
109	9.38	4.45	209	11.30	5.05	309	13.65	5.71
110	9.38	4.45	210	11.30	5.05	310	13.85	5.77
111	10.20	4.70	211	12.00	5.25	311	14.42	5.94
112	10.20	4.70	212	12.65	5.44	312	15.00	6.08
113	10.20	4.70	-	-	-	313	15.50	6.21
114	10.93	4.91	214	13.25	5.60	314	16.00	6.33
-	-	-	215	13.25	5.60	315	16.50	6.48
-	-	-	-	-	-	316	17.45	6.73
117	11.67	5.14	-	-	-	317	17.88	6.82
118	12.31	5.33	218	15.0	6.08	318	18.32	6.92

Note:  $k_N$  computed from the following

As defined by A. B. Jones, "Analysis of Stresses and Deflections", New Departure Division, G. M. Corp., 1946.

$$k_N = \frac{d^{1/2} \times 10^9}{\left[7.8107 (c_{d0} + c_{d1})\right]^{3/2}}$$

Using a 51% curvature for the inner race and 52% for outer race and

$$\frac{d}{E} \cos \beta \approx + 0.25 \text{ (for } \beta = 0 \text{ \& } \frac{d}{E} \approx 0.25 \text{)}$$

From A. B. Jones' Chart No. 56,

$$c_{\delta o} \approx 1.07$$

$$c_{\delta i} \approx 0.95$$

$$\therefore k_N = \frac{d^{1/2} \times 10^9}{62.5}$$

### C.6 Locus of Shaft Due to Rotating Load

For a rotating load (such as an unbalance force) the instantaneous location of the shaft center can be determined as shown below.

From Figure C-3 we may write that

$$\theta_i = \theta_L - A(-\gamma) \quad \text{Note:-} \quad (C-30)$$

$$\theta_i = \theta_E + (-\gamma) \quad A(-\gamma) \text{ signifies} \quad (C-31)$$

the value of A°  
at  $\gamma = -\gamma$

Subtracting yields

$$\theta_L - \theta_E = A(-\gamma) + (-\gamma) \quad (C-32)$$

$$\theta_L \left( 1 - \frac{\theta_E}{\theta_L} \right) = A(-\gamma) + (-\gamma)$$

From Figure C-3 it is seen that  $A(-\gamma) = -A\gamma$

$$\therefore \theta_L = \frac{-A\gamma - \gamma}{\left( 1 - \frac{\theta_E}{\theta_L} \right)}$$

$$\frac{\theta_E}{\theta_L} = \frac{\omega_E}{\omega_L}$$

$$\therefore \theta_L = - \frac{A\gamma + \gamma}{\left( 1 - \frac{\omega_E}{\omega_L} \right)}$$

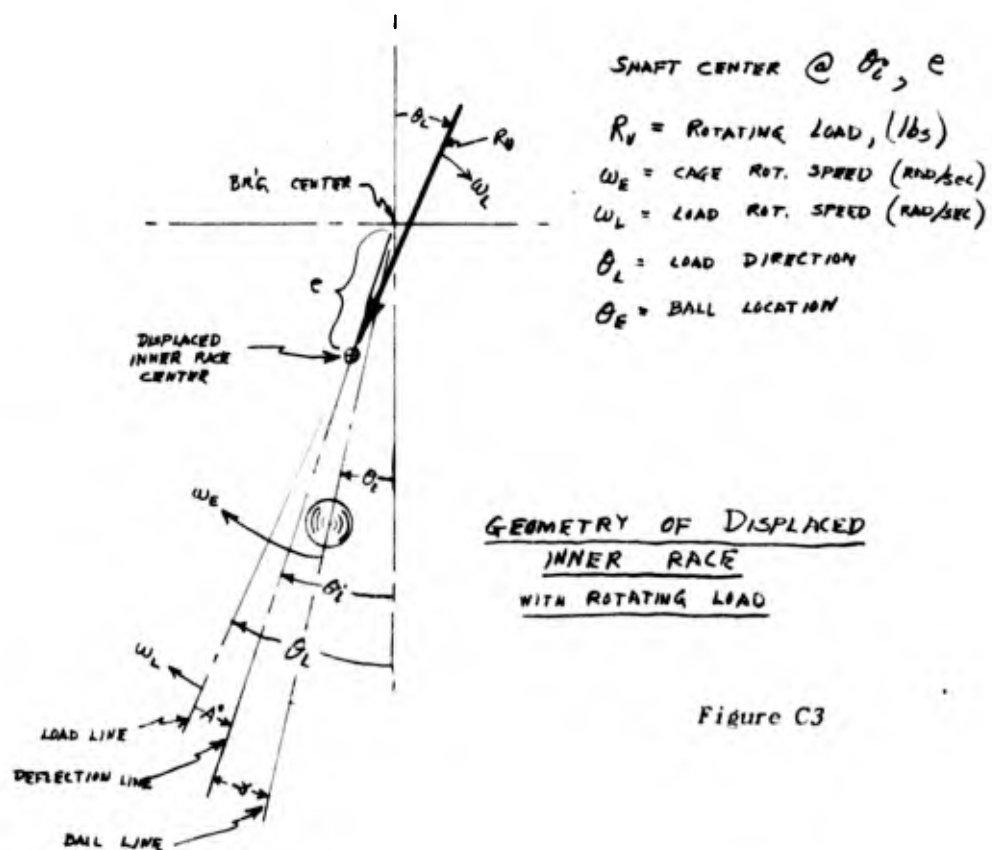


Figure C3

Substituting in (C-30) gives

$$\theta_1 = - \left[ \frac{A_Y + Y}{1 - \frac{\omega_E}{\omega_L}} \right] + A_Y \quad (C-33)$$

The amplitude of displacement ( $e$ ) associated with the angle of displacement may be evaluated as,

$$e = \left( \frac{R}{k_N} \right)^{2/3} \left[ \frac{k_N e^{3/2}}{R} \right]^{2/3} Y$$

A dimensionless amplitude may be written as,

$$\frac{e}{(R/k_N)^{2/3}} = \left[ \frac{k_N e^{3/2}}{R} \right]^\gamma \quad (\text{dimensionless}) \quad (C-34)$$

We shall call  $\frac{e}{(R/k_N)^{2/3}}$  the "zero clearance compliance factor". Notice that it is equal to the reciprocal of the zero clearance bearing parameter to the two-thirds power.

To illustrate the use of Eqs. (C-33) and (C-34) consider an unbalance load rotating with the shaft.

$$\therefore \omega_L = \omega_1 = 2\pi f_1$$

$$\omega_E = 2\pi f_E$$

$$\therefore \frac{\omega_E}{\omega_L} = \frac{2\pi f_E}{2\pi f_1} = \frac{f_E}{f_1}$$

$$\therefore \left( 1 - \frac{\omega_E}{\omega_L} \right) = 1 - \frac{f_E}{f_1} = \frac{f_1 - f_E}{f_1}$$

$$\therefore \left( 1 - \frac{\omega_E}{\omega_L} \right) = \frac{f_{E1}}{f_1}$$

$$\text{From (6), } f_{E1} = \frac{1}{2} \left( 1 + \frac{d}{E} \right) f_1$$

$$\therefore \left( 1 - \frac{\omega_E}{\omega_L} \right) = \frac{1}{2} \left( 1 + \frac{d}{E} \right) = \text{cage factor}$$

Thus for an unbalance load, Eq. (C-33) becomes

$$\theta_{i_u} = - \frac{A_\gamma + \gamma}{\text{cage factor}} + A_\gamma$$

For a 310 bearing, (n = 8 balls), this becomes

$$\theta_{i_u} = - \frac{A_\gamma + \gamma}{0.6190} + A_\gamma$$

Values of  $\theta_{i_u}$  were evaluated for the 310 bearing for various values of  $\gamma$  and appear in the following table along with values for  $e/(R/k_N)^{2/3}$ .

I-A2321-1

Table C-4

## SHAFT LOCUS ANGLE AND DISPLACEMENT FOR AN UNBALANCE LOAD

$\gamma$ (deg)	$\frac{R}{k_N e^{3/2}}$	$A_\gamma$ (deg)	$A_\gamma + \gamma$ (deg)	$\theta_L = \frac{A_\gamma + \gamma}{0.619}$ (deg)	$\theta_1 = \theta_L + A_\gamma$ (deg)	$\frac{e}{(R/k_N)^{3/2}}$
0	1.8408	0	0	0	0	.6655
2.5	1.8395	.5080	3.0080	-4.8594	-4.3414	.6657
5	1.8377	.7778	5.7778	-9.3340	-8.5562	.6662
7.5	1.8352	.9083	8.4083	-13.5836	-12.6753	.6670
10	1.8317	.9083	10.9083	-17.6224	-16.7141	.6680
12.5	1.8290	.8208	13.3208	-21.5197	-20.6989	.6685
15	1.8259	.6805	15.6805	-25.3318	-24.6513	.6690
17.5	1.8235	.4757	17.9757	-29.0397	-28.5640	.6695
20	1.8225	.2500	20.2500	-32.7139	-32.4639	.6698
22.5	1.8220	0	22.5	-36.3488	-36.3488	.6700
25	1.8225	-.2500	24.7500	-39.9836	-40.2336	.6698
27.5	1.8235	-.4757	27.0243	-43.6578	-44.1335	.6695
30	1.8259	-.6805	29.3195	-47.3657	-48.0462	.6690
32.5	1.8290	-.8208	31.6792	-51.1777	-51.9985	.6685
35	1.8317	-.9083	34.0917	-55.0751	-55.9834	.6680
37.5	1.8352	-.9083	36.5917	-59.1139	-60.0222	.6670
40	1.8377	-.7778	39.2222	-63.3635	-64.1413	.6662
42.5	1.8395	-.5080	41.9920	-67.8381	-68.3461	.6657
45	1.8408	0	45	-72.6925	-72.6975	.6655
47.5	↓	↓	48.0080			↓
50			50.7778			
52.5	R	R	53.9083	& so	& so	R
	E	E		forth	forth	E
& so	P	P	& so			P
forth	E	E	forth			E
	A	A				A
	T	T				T
	S	S				S

I-A2321-1

### C.7 Bearings With Internal Clearance

Using Eqs. (C-20), (C-21), (C-22), and (C-23), values of  $\frac{R}{k_N c^{3/2}}$  and  $A^\circ$  were obtained for various ball positions of an 8-ball ball bearing at various ecc. ratios ( $\epsilon$ ) when deformation is present [ $\epsilon \approx 1.10$ ]

$$\frac{R \epsilon}{k_N c^{3/2}} = \sum_{n=1}^{n=n_t=8} [\epsilon \cos \phi_n - 1]^{3/2} \times \cos \phi_n \quad (C-22)$$

where  $\epsilon$  = eccentricity ratio =  $\frac{e}{c}$   
 $e$  = radial displacement from centerline outer race, (in.)  
 $c$  = radial clearance =  $\frac{1}{2}$  total radial play, (in.)  
 $\phi_1 = -\gamma$   
 $\phi_2 = 2\alpha - \gamma = 45 - \gamma$   
 $\phi_3 = 4\alpha - \gamma = 40 - \gamma$   
 $\phi_4 = 6\alpha - \gamma = 135 - \gamma$   
 $\phi_5 = 8\alpha - \gamma = 180 - \gamma$   
 $\phi_6 = 10\alpha - \gamma = 225 - \gamma$   
 $\phi_7 = 12\alpha - \gamma = 270 - \gamma$   
 $\phi_8 = 14\alpha - \gamma = 315 - \gamma$

$$\begin{aligned} \therefore \frac{R \epsilon}{k_N c^{3/2}} &= [\epsilon \cos (-\gamma) - 1]^{3/2} \cos (-\gamma) + [\epsilon \cos (45-\gamma) - 1]^{3/2} \cos (45-\gamma) \\ &+ [\epsilon \cos (90-\gamma) - 1]^{3/2} \cos (90-\gamma) + [\epsilon \cos (135-\gamma) - 1]^{3/2} \cos (135-\gamma) \\ &+ [\epsilon \cos (180-\gamma) - 1]^{3/2} \cos (180-\gamma) + [\epsilon \cos (225-\gamma) - 1]^{3/2} \cos (225-\gamma) \\ &+ [\epsilon \cos (270-\gamma) - 1]^{3/2} \cos (270-\gamma) + [\epsilon \cos (315-\gamma) - 1]^{3/2} \cos (315-\gamma) \end{aligned}$$

This equation along with the one for  $\frac{R_t}{k_N c^{3/2}}$ ,  $\frac{R}{k_N c^{3/2}}$  and  $A^\circ$  were solved for all combinations of  $\epsilon$  and  $\gamma$  indicated in Section 3.2.1.1.3 (on the F.I.L. UNIVAC Computer).



THE FRANKLIN INSTITUTE • *Laboratories for Research and Development*

I-A2321-1

**APPENDIX D**

COMPUTER DATA FOR CLEARANCE BEARING

## APPENDIX D

## COMPUTER DATA FOR CLEARANCE BEARING

$\epsilon$	$\gamma$ (deg.)	$\frac{R}{C^{1/2} L_N}$	$A^\circ$ (rad.)		$\epsilon$	$\gamma$ (deg.)	$\frac{R}{C^{1/2} L_N}$	$A^\circ$ (rad.)
1.10	0	$.3162 \times 10^{-1}$	.0000		1.30	0	$.1643 \times 10^0$	.0000
	3	.3091	-.0523			3	.1628	-.0523
	6	.2880	-.1047			6	.1592	-.1000
	9	.2542	-.1570			9	.1598	-.1050
	12	.2093	-.2094			12	.1618	-.0906
	15	$.1563 \times 10^{-1}$	-.2681			15	.1639	-.0680
	18	$.9918 \times 10^{-2}$	-.3141			18	.1655	-.0417
	21	.4670	-.3145			21	.1664	-.0140
	22.5	$.3833 \times 10^{-2}$	.0000			22.5	$.1665 \times 10^0$	.0000
1.15	0	$.5809 \times 10^{-1}$	.0000		1.35	0	$.2070 \times 10^0$	.0000
	3	.5718	-.0523			3	.2055	-.0517
	6	.5447	-.1047			6	.2083	-.0677
	9	.5006	-.1570			9	.2131	-.0641
	12	.4412	-.2094			12	.2180	-.0529
	15	.3688	-.2618			15	.2223	-.0387
	18	.3154	-.2272			18	.2253	-.0233
	21	.2914	-.0869			21	.2269	-.0078
	22.5	$.2884 \times 10^{-1}$	.0000			22.5	$.2271 \times 10^0$	.0000
1.20	0	$.8944 \times 10^{-1}$	.0000		1.40	0	$.2529 \times 10^0$	.0000
	3	.8834	-.0523			3	.2569	-.0300
	6	.8506	-.1047			6	.2648	-.0349
	9	.7971	-.1570			9	.2731	-.0316
	12	.7280	-.2044			12	.2806	-.0253
	15	.6918	-.1822			15	.2868	-.0180
	18	.6721	-.1214			18	.2911	-.0106
	21	.6629	-.0423			21	.2934	-.0035
	22.5	$.6617 \times 10^{-1}$	.0000			22.5	$.2937 \times 10^0$	.0000
1.25	0	$.1250 \times 10^0$	.0000		1.45	0	$.3075 \times 10^0$	.0000
	3	.1237	-.0523			3	.3155	-.0039
	6	.1198	-.1047			6	.3274	-.0069
	9	.1144	-.1496			9	.3388	-.0062
	12	.1128	-.1427			12	.3488	-.0044
	15	.1124	-.1121			15	.3569	-.0026
	18	.1125	-.0705			18	.3624	-.0013
	21	.1125	-.0240			21	.3653	-.0004
	22.5	$.1125 \times 10^0$	.0000			22.5	$.3657 \times 10^0$	.0000

$\epsilon$	$\gamma$ (deg.)	$\frac{R}{C^{\frac{3}{2}}L_N}$	$A^\circ$ (rad.)		$\epsilon$	$\gamma$ (deg.)	$\frac{R}{C^{\frac{3}{2}}L_N}$	$A^\circ$ (rad.)
1.50	0	$.3746 \times 10^\circ$	.0000		1.70	0	$.7141 \times 10^\circ$	.0000
	3	.3799	.0195			3	.7168	.0307
	6	.3954	.0161			6	.7250	.0554
	9	.4098	.0139			9	.7402	.0643
	12	.4223	.0117			12	.7618	.0513
	15	.4321	.0090			15	.7785	.0373
	18	.4389	.0057			18	.7899	.0227
	21	.4423	.0019			21	.7956	.0076
	22.5	$.4428 \times 10^\circ$	.0000			22.5	$.7964 \times 10^\circ$	.0000
1.55	0	$.4499 \times 10^\circ$	.0000		1.75	0	$.8131 \times 10^\circ$	.0000
	3	.4539	.0287			3	.8155	.0292
	6	.4685	.0353			6	.8229	.0538
	9	.4858	.0302			9	.8357	.0675
	12	.5006	.0247			12	.8570	.0576
	15	.5121	.0183			15	.8754	.0418
	18	.5201	.0113			18	.8879	.0253
	21	.5241	.0038			21	.8942	.0085
	22.5	$.5246 \times 10^\circ$	.0000			22.5	$.8950 \times 10^\circ$	.0000
1.60	0	$.5320 \times 10^\circ$	.0000		1.80	0	$.9170 \times 10^\circ$	.0000
	3	.5354	.0314			3	.9192	.0275
	6	.5465	.0505			6	.9259	.0513
	9	.5664	.0437			9	.9371	.0667
	12	.5834	.0352			12	.9559	.0630
	15	.5967	.0259			15	.9760	.0456
	18	.6058	.0158			18	.9896	.0276
	21	.6104	.0053			21	.9966	.0092
	22.5	$.6110 \times 10^\circ$	.0000			22.5	$.9974 \times 10^\circ$	.0000
1.65	0	$.6203 \times 10^\circ$	.0000		1.85	0	$.1025 \times 10^1$	.0000
	3	.6233	.0316			3	.1027	.0257
	6	.6325	.0552			6	.1033	.0484
	9	.6512	.0549			9	.1043	.0643
	12	.6706	.0439			12	.1058	.0671
	15	.6856	.0321			15	.1080	.0490
	18	.6958	.0196			18	.1095	.0296
	21	.7010	.0065			21	.1102	.0099
	22.5	$.7016 \times 10^\circ$	.0000			22.5	$.1103 \times 10^1$	.0000

$\epsilon$	$\gamma$ (deg.)	$\frac{R}{C^{\frac{1}{2}}k_N}$	$A^\circ$ (rad)		$\epsilon$	$\gamma$ (deg.)	$\frac{R}{C^{\frac{1}{2}}k_N}$	$A^\circ$ (rad)
1.90	0	$.1138 \times 10^1$	.0000		8.00	0	$.3273 \times 10^2$	.0000
	3	.1140	.0240			3	.3270	-.0109
	6	.1145	.0454			6	.3261	-.0219
	9	.1154	.0612			9	.3248	-.0292
	12	.1167	.0670			12	.3235	-.0280
	15	.1188	.0519			15	.3224	-.0226
	18	.1203	.0314			18	.3216	-.0145
	21	.1212	.0105			21	.3213	-.0082
	22.5	$.1213 \times 10^1$	.0000			22.5	$.3211 \times 10^2$	.0000
1.95	0	$.1255 \times 10^1$	.0000		12.0	0	$.6544 \times 10^3$	.0000
	3	.1257	.0223			3	.6538	-.0129
	6	.1262	.0424			6	.6521	-.0240
	9	.1270	.0578			9	.6500	-.0265
	12	.1281	.0649			12	.6479	-.0245
	15	.1299	.0545			15	.6461	-.0194
	18	.1316	.0329			18	.6448	-.0124
	21	.1324	.0110			21	.6441	-.0042
	22.5	$.1326 \times 10^1$	.0000			22.5	$.6440 \times 10^2$	.0000
2.00	0	$.1377 \times 10^1$	.0000		16.0	0	$.1049 \times 10^3$	.0000
	3	.1378	.0207			3	.1048	-.0139
	6	.1382	.0395			6	.1045	-.0225
	9	.1389	.0542			9	.1042	-.0243
	12	.1399	.0620			12	.1039	-.0223
	15	.1413	.0568			15	.1037	-.0177
	18	.1431	.0343			18	.1035	-.0113
	21	.1441	.0114			21	.1034	-.0038
	22.5	$.1442 \times 10^1$	.0000			22.5	$.1034 \times 10^3$	.0000
4.00	0	$.8692 \times 10^1$	.0000		20.0	0	$.1501 \times 10^3$	.0000
	3	.8686	-.0035			3	.1500	-.0143
	6	.8667	-.0072			6	.1497	-.0213
	9	.8635	-.0113			9	.1493	-.0228
	12	.8590	-.0161			12	.1489	-.0209
	15	.8534	-.0210			15	.1485	-.0165
	18	.8495	-.0158			18	.1483	-.0106
	21	.8475	-.0057			21	.1481	-.0036
	22.5	$.8473 \times 10^1$	.0000			22.5	$.1481 \times 10^3$	.0000

$\epsilon$	$\gamma$ (deg.)	$\frac{R}{C^{3/2}k_N}$	$A^\circ$ (rad.)		$\epsilon$	$\gamma$ (deg.)	$\frac{R}{C^{3/2}k_N}$	$A^\circ$ (rad.)
2.25	0	.2040 $\times 10^1$	.0000		3.25	0	.5466 $\times 10^1$	.0000
	3	.2040	.0140			3	.5463	.0007
	6	.2042	.0270			6	.5453	.0012
	9	.2044	.0377			9	.5437	.0010
	12	.2048	.0447			12	.5415	.0001
	15	.2052	.0461			15	.5386	.0028
	18	.2057	.0380			18	.5350	.0076
	21	.2068	.0131			21	.5330	.0038
	22.5	.2070 $\times 10^1$	.0000			22.5	.5328 $\times 10^1$	.0000
2.50	0	.2788 $\times 10^1$	.0000		3.50	0	.6485 $\times 10^1$	.0000
	3	.2788	.0092			3	.6481	.0009
	6	.2787	.0177			6	.6469	.0021
	9	.2785	.0247			9	.6448	.0038
	12	.2782	.0294			12	.6418	.0064
	15	.2778	.0305			15	.6380	.0103
	18	.2773	.0265			18	.6340	.0124
	21	.2768	.0135			21	.6321	.0048
	22.5	.2769 $\times 10^1$	.0000			22.5	.6319 $\times 10^1$	.0000
2.75	0	.3613 $\times 10^1$	.0000		3.75	0	.7562 $\times 10^1$	.0000
	3	.3612	.0056			3	.7556	.0023
	6	.3608	.0107			6	.7541	.0049
	9	.3601	.0148			9	.7514	.0079
	12	.3592	.0172			12	.7477	.0117
	15	.3580	.0171			15	.7429	.0165
	18	.3565	.0134			18	.7389	.0146
	21	.3547	.0044			21	.7371	.0054
	22.5	.3542 $\times 10^1$	.0000			22.5	.7368 $\times 10^1$	.0000
3.00	0	.4507 $\times 10^1$	.0000					
	3	.4505	.0029					
	6	.4498	.0054					
	9	.4487	.0071					
	12	.4472	.0075					
	15	.4451	.0061					
	18	.4426	.0019					
	21	.4403	.0016					
	22.5	.4400 $\times 10^1$	.0000					

Table D-2

DATA FOR MAXIMUM DISPLACEMENT  
 NORMAL TO APPLIED LOAD ( $\Delta X_{\max} = 2c \sin A_{\max}^{\circ}$ )

(Clearance Bearing  
 with 8 Balls)

$c$	$A_{\max}^{\circ}$ (rad)	$\frac{R}{c^{3/2} k_N}$ at $A_{\max}^{\circ}$	$\gamma$ at $A_{\max}^{\circ}$ (deg)	$\sin A_{\max}^{\circ}$	$\Delta X_{\max} = 2c \sin A_{\max}^{\circ}$	$X_{\max} = c \sin A_{\max}^{\circ}$
1.10	-.3538	.005306	19.5	-.3465	-.7623	-.3812
1.15	-.2702	.03456	16.0	-.2669	-.6139	-.3070
1.20	-.2051	.07200	12.5	-.2036	-.4886	-.2443
1.25	-.1515	.1137	10.0	-.1509	-.3773	-.1887
1.30	-.1065	.1594	8.0	-.1063	-.2764	-.1382
1.35	-.0680	.2091	6.5	-.0679	-.1833	-.0917
1.40	-.0350	.2648	6.0	-.0350	-.0980	-.0490
1.45	{ -.0070	.3313	1.0	-.0070	-.0203	-.0102
	{ +.0016	.3085	7.0	+.0016	+.0046	+.0023
1.50	+.0196	.3800	3.0	+.0196	+.0588	+.0294
1.55	+.0371	.4623	5.0	+.0371	+.1150	+.0750
1.60	+.0506	.5465	6.0	+.0506	+.1619	+.0810
1.65	+.0596	.6403	7.5	+.0596	+.1967	+.0984
1.70	+.0651	.7369	8.5	+.0650	+.2210	+.1105
1.75	+.0680	.8386	9.5	+.0679	+.2377	+.1189
1.80	+.0688	.9450	10.5	+.0687	+.2473	+.1237
1.85	+.0685	1.0529	11.0	+.0684	+.2531	+.1266
1.90	+.0671	1.1651	11.5	+.0670	+.2546	+.1273
1.95	+.0650	1.2814	12.0	+.0649	+.2531	+.1266
2.0	+.0624	1.3995	12.5	+.0623	+.2492	+.1246
2.25	+.0465	2.0506	14.0	+.0465	+.2093	+.1047
2.50	+.0307	2.7792	14.5	+.0307	+.1535	+.0768
2.75	+.0176	3.5871	13.5	+.0176	+.0968	+.0484
3.00	{ +.0076	4.4751	11.5	+.0076	+.0456	+.0228
	{ +.0019	4.4080	20.0	-.0019	-.0114	-.0057
3.25	{ +.0013	5.4493	7.0	+.0013	+.0085	+.0043
	{ -.0078	5.3453	18.5	-.0078	-.0507	-.0254
3.50	-.0133	6.3508	17.0	-.0133	-.0931	-.0466
3.75	-.0177	7.4133	16.0	-.0177	-.1328	-.0664
4.0	-.0211	8.5344	15.0	-.0211	-.1688	-.0844
8.0	-.0295	32.441	10.0	-.0295	-.4720	-.2360
12.0	-.0265	65.006	9.0	-.0265	-.6360	-.3180
16.0	-.0243	104.34	8.5	-.0243	-.7776	-.3888
20.0	-.0229	149.39	8.5	-.0229	-.9160	-.4580

THE FRANKLIN INSTITUTE • *Laboratories for Research and Development*

I-A2321-1

**APPENDIX E**

COMPUTER DATA FOR INTERFERENCE BEARING

## APPENDIX E

Table E-1

COMPUTER DATA FOR INTERFERENCE BEARING

$\epsilon$	$\gamma$ (deg.)	$\frac{R}{i^{3/2} k_N}$	$A^\circ$ (rad.)	$\epsilon$	$\gamma$ (deg.)	$\frac{R}{i^{3/2} k_N}$	$A^\circ$ (rad.)
.10	0	$.5998 \times 10^0$	0	.50	0	$.2975 \times 10^1$	0
	3	.5998	↑		3	.2975	↑
	6	.5998	↑		6	.2975	↑
	9	.5998	↑		9	.2975	↑
	12	.5998	↑		12	.2975	↑
	15	.5998	↑		15	.2975	↑
	18	.5998	↑		18	.2975	↑
	21	.5998	↓		21	.2975	↓
	22.5	$.5998 \times 10^0$	0		22.5	$.2975 \times 10^1$	0
.20	0	$.1198 \times 10^1$	0	.60	0	$.3556 \times 10^1$	0
	3	.1198	↑		3	.3556	↑
	6	.1198	↑		6	.3556	↑
	9	.1198	↑		9	.3556	↑
	12	.1198	↑		12	.3556	↑
	15	.1198	↑		15	.3556	↑
	18	.1198	↑		18	.3556	↑
	21	.1198	↓		21	.3556	↓
	22.5	$.1198 \times 10^1$	0		22.5	$.3556 \times 10^1$	0
.30	0	$.1794 \times 10^1$	0	.70	0	$.4129 \times 10^1$	0
	3	.1794	↑		3	.4129	↑
	6	.1794	↑		6	.4129	↑
	9	.1794	↑		9	.4129	↑
	12	.1794	↑		12	.4129	↑
	15	.1794	↑		15	.4129	↑
	18	.1794	↑		18	.4129	↑
	21	.1794	↓		21	.4129	↓
	22.5	$.1794 \times 10^1$	0		22.5	$.4129 \times 10^1$	0
.40	0	$.2387 \times 10^1$	0	.80	0	$.4691 \times 10^1$	0
	3	.2387	↑		3	.4691	↑
	6	.2387	↑		6	.4691	↑
	9	.2387	↑		9	.4691	↑
	12	.2387	↑		12	.4691	↑
	15	.2387	↑		15	.4691	↑
	18	.2387	↑		18	.4691	↑
	21	.2387	↓		21	.4691	↓
	22.5	$.2387 \times 10^1$	0		22.5	$.4691 \times 10^1$	0



$\epsilon$	$\gamma$ (deg.)	$\frac{R}{i^{3/2} k_N}$	$A^\circ$ (rad.)	$\epsilon$	$\gamma$ (deg.)	$\frac{R}{i^{3/2} k_N}$	$A^\circ$ (rad.)
.90	0	.5237 $\times 10^1$	.0000	1.3	0	.7215 $\times 10^1$	.0000
	3	.5237	.3232 $\times 10^{-4}$		3	.7213	-.4644 $\times 10^{-3}$
	6	.5237	.5896		6	.7204	-.1242 $\times 10^{-2}$
	9	.5238	.7531		9	.7192	-.1941
	12	.5238	.7860		12	.7181	-.2091
	15	.5238	.6832		15	.7172	-.1808
	18	.5238	.4632		18	.7167	-.1211 $\times 10^{-2}$
	21	.5238	.1639 $\times 10^{-4}$		21	.7164	-.4250 $\times 10^{-3}$
	22.5	.5238 $\times 10^1$	.0000		22.5	.7163 $\times 10^1$	.0000
1.0	0	.5758 $\times 10^1$	.0000	1.4	0	.7686 $\times 10^1$	.0000
	3	.5758	.1141 $\times 10^{-3}$		3	.7678	-.2073 $\times 10^{-2}$
	6	.5759	.2040		6	.7668	-.3242
	9	.5761	.2546		9	.7657	-.3657
	12	.5762	.2601		12	.7648	-.3469
	15	.5763	.2222		15	.7640	-.2814
	18	.5764	.1488 $\times 10^{-3}$		18	.7635	-.1823 $\times 10^{-2}$
	21	.5765	.5230 $\times 10^{-4}$		21	.7632	-.6302 $\times 10^{-3}$
	22.5	.5765 $\times 10^1$	.0000		22.5	.7632 $\times 10^1$	.0000
1.1	0	.6247 $\times 10^1$	.0000	1.5	0	.8136 $\times 10^1$	.0000
	3	.6247	.2508 $\times 10^{-3}$		3	.8138	-.2644 $\times 10^{-2}$
	6	.6247	.4792		6	.8135	-.4201
	9	.6248	.6615		9	.8128	-.4601
	12	.6248	.7716		12	.8121	-.4277
	15	.6249	.7786		15	.8115	-.3424
	18	.6250	.6416		18	.8110	-.2201 $\times 10^{-2}$
	21	.6249	.2623 $\times 10^{-3}$		21	.8108	-.7583 $\times 10^{-3}$
	22.5	.6249 $\times 10^1$	.0000		22.5	.8107 $\times 10^1$	.0000
1.2	0	.6734 $\times 10^1$	.0000	1.6	0	.8592 $\times 10^1$	.0000
	3	.6733	.1024 $\times 10^{-3}$		3	.8595	-.1792 $\times 10^{-2}$
	6	.6731	.1740		6	.8601	-.3772
	9	.6727	.1687 $\times 10^{-3}$		9	.8603	-.4760
	12	.6720	-.8269 $\times 10^{-4}$		12	.8599	-.4544
	15	.6711	-.3583 $\times 10^{-3}$		15	.8595	-.3672
	18	.6706	-.3357		18	.8592	-.2369 $\times 10^{-2}$
	21	.6703	-.1321 $\times 10^{-3}$		21	.8590	-.8170 $\times 10^{-3}$
	22.5	.6702 $\times 10^1$	.0000		22.5	.8590 $\times 10^1$	.0000

$\epsilon$	$\gamma$ (deg.)	$\frac{R}{i^{3/2} k_N}$	$A^\circ$ (rad)	$\epsilon$	$\gamma$ (deg.)	$\frac{R}{i^{3/2} k_N}$	$A^\circ$ (rad)
1.7	0	.9057 $\times 10^1$	.0000	2.1	0	.1099 $\times 10^2$	.0000
	3	.9060	-.1038 $\times 10^{-2}$		3	.1100	.1233 $\times 10^{-2}$
	6	.9067	-.2274		6	.1101	.2220
	9	.9078	-.3903		9	.1102	.2717
	12	.9082	-.4260		12	.1104	.2489
	15	.9082	-.3572		15	.1107	.1313 $\times 10^{-2}$
	18	.9081	-.2340 $\times 10^{-2}$		18	.1109	.2221 $\times 10^{-3}$
	21	.9080	-.8121 $\times 10^{-3}$		21	.1110	.1859 $\times 10^{-3}$
	22.5	.9080 $\times 10^1$	.0000		22.5	.1110 $\times 10^2$	.0000
1.8	0	.9530 $\times 10^1$	.0000	2.2	0	.1150 $\times 10^2$	.0000
	3	.9533	-.3677 $\times 10^{-3}$		3	.1150	.1656 $\times 10^{-2}$
	6	.9541	-.8464 $\times 10^{-3}$		6	.1151	.3053
	9	.9554	-.1942 $\times 10^{-2}$		9	.1153	.3937
	12	.9569	-.5313		12	.1155	.4059
	15	.9574	-.3118		15	.1158	.3181
	18	.9576	-.2122 $\times 10^{-2}$		18	.1160	.1068 $\times 10^{-2}$
	21	.9576	-.7467 $\times 10^{-3}$		21	.1162	.1416 $\times 10^{-3}$
	22.5	.9576 $\times 10^1$	.0000		22.5	.1162 $\times 10^2$	.0000
1.9	0	.1001 $\times 10^2$	.0000	2.3	0	.1201 $\times 10^2$	.0000
	3	.1001	.2285 $\times 10^{-3}$		3	.1201	.2033 $\times 10^{-2}$
	6	.1002	.2341		6	.1202	.3796
	9	.1003	-.2017 $\times 10^{-3}$		9	.1204	.5021
	12	.1005	-.1289 $\times 10^{-2}$		12	.1207	.5447
	15	.1007	-.2267		15	.1209	.4818
	18	.1007	-.1712 $\times 10^{-2}$		18	.1212	.2877 $\times 10^{-2}$
	21	.1007	-.6221 $\times 10^{-3}$		21	.1214	.5683 $\times 10^{-3}$
	22.5	.1007 $\times 10^2$	.0000		22.5	.1214 $\times 10^2$	.0000
2.0	0	.1050 $\times 10^2$	.0000	2.4	0	.1253 $\times 10^2$	.0000
	3	.1050	.7597 $\times 10^{-3}$		3	.1253	.2371 $\times 10^{-2}$
	6	.1051	.1284 $\times 10^{-2}$		6	.1254	.4459
	9	.1052	.1343 $\times 10^{-2}$		9	.1256	.5984
	12	.1054	.7157 $\times 10^{-3}$		12	.1259	.6672
	15	.1057	-.8119 $\times 10^{-3}$		15	.1262	.6249
	18	.1058	-.1094 $\times 10^{-2}$		18	.1265	.4432
	21	.1058	-.4368 $\times 10^{-3}$		21	.1267	.1149 $\times 10^{-2}$
	22.5	.1058 $\times 10^2$	.0000		22.5	.1267 $\times 10^2$	.0000

$\epsilon$	$\gamma$ (deg.)	$\frac{R}{i^{3/2} k_N}$	$A^\circ$ (rad)		$\epsilon$	$\gamma$ (deg.)	$\frac{R}{i^{3/2} k_N}$	$A^\circ$ (rad.)
2.5	0	$.1305 \times 10^2$	.0000		2.9	0	$.1523 \times 10^2$	.0000
	3	.1306	$.2672 \times 10^{-2}$			3	.1524	$.3587 \times 10^{-2}$
	6	.1307	.5049			6	.1525	.6828
	9	.1309	.6839			9	.1528	$.9377 \times 10^{-2}$
	12	.1312	.7751			12	.1531	$.1087 \times 10^{-1}$
	15	.1315	.7494			15	.1534	$.1093 \times 10^{-1}$
	18	.1318	.5754			18	.1537	$.9026 \times 10^{-2}$
	21	.1320	$.2123 \times 10^{-2}$			21	.1538	$.3671 \times 10^{-3}$
	22.5	$.1321 \times 10^2$	.0000			22.5	$.1538 \times 10^2$	.0000
2.6	0	$.1359 \times 10^2$	.0000		3.0	0	$.1579 \times 10^2$	.0000
	3	.1359	$.2941 \times 10^{-2}$			3	.1580	$.3756 \times 10^{-2}$
	6	.1361	.5575			6	.1581	.7155
	9	.1363	.7596			9	.1584	$.9833 \times 10^{-2}$
	12	.1365	.8699			12	.1587	$.1141 \times 10^{-1}$
	15	.1368	.8571			15	.1590	$.1147 \times 10^{-1}$
	18	.1372	.6861			18	.1593	$.9387 \times 10^{-2}$
	21	.1374	$.3060 \times 10^{-2}$			21	.1594	$.3493 \times 10^{-3}$
	22.5	$.1375 \times 10^2$	.0000			22.5	$.1594 \times 10^2$	.0000
2.7	0	$.1413 \times 10^2$	.0000					
	3	.1413	$.3181 \times 10^{-2}$					
	6	.1415	.6043					
	9	.1417	.8266					
	12	.1420	.9528					
	15	.1423	.9495					
	18	.1426	.7768					
	21	.1428	$.3677 \times 10^{-2}$					
	22.5	$.1428 \times 10^2$	.0000					
2.8	0	$.1468 \times 10^2$	.0000					
	3	.1468	$.3396 \times 10^{-2}$					
	6	.1470	.6459					
	9	.1472	$.8857 \times 10^{-2}$					
	12	.1475	$.1025 \times 10^{-1}$					
	15	.1478	$.1027 \times 10^{-1}$					
	18	.1481	$.8488 \times 10^{-2}$					
	21	.1483	$.3859 \times 10^{-3}$					
	22.5	$.1483 \times 10^2$	.0000					

TABLE E-2

DATA FOR MAXIMUM DISPLACEMENT NORMAL TO APPLIED LOAD

$$\Delta X_{\max} = 2c \sin A^{\circ}_{\max}$$

$F$	$A^{\circ}_{\max}$ (rad)	$\frac{R}{i^{3/2}k_N}$ at $A^{\circ}_{\max}$	$\gamma$ at $A^{\circ}_{\max}$ (deg)	$\sin A^{\circ}_{\max}$	$\Delta X_{\max} =$ $2c \sin A^{\circ}_{\max}$	$X_{\max} =$ $c \sin A^{\circ}_{\max}$
0	0	0	-	0	0	0
0.1	0	.5998	-	0	0	0
.2	0	1.19849	-	0	0	0
.3	0	1.79486	-	0	0	0
.4	$+.2640 \times 10^{-6}$	2.38768	12.0	$+.264 \times 10^{-6}$	$.21120 \times 10^{-6}$	$.0806 \times 10^{-6}$
0.5	$+.976 \times 10^{-6}$	2.97556	11.0	$+.976 \times 10^{-6}$	$.976 \times 10^{-6}$	$.488 \times 10^{-6}$
.6	$+.3256 \times 10^{-5}$	3.55690	11.0	$+.3256 \times 10^{-5}$	$.19344 \times 10^{-5}$	$.09672 \times 10^{-5}$
.7	$+.978 \times 10^{-5}$	4.1297	11.0	$+.978 \times 10^{-5}$	$1.3692 \times 10^{-5}$	$.6846 \times 10^{-5}$
.8	$+.2770 \times 10^{-4}$	4.69148	11.0	$+.2770 \times 10^{-4}$	$.4432 \times 10^{-4}$	$.2216 \times 10^{-4}$
.9	$+.787 \times 10^{-4}$	5.2382	11.0	$+.787 \times 10^{-4}$	$1.4166 \times 10^{-4}$	$.7083 \times 10^{-4}$
1.0	$+.2635 \times 10^{-3}$	5.7622	11.0	$+.2635 \times 10^{-3}$	$.5270 \times 10^{-3}$	$.2635 \times 10^{-3}$
1.1	$+.790 \times 10^{-3}$	6.2491	13.5	$+.790 \times 10^{-3}$	$1.738 \times 10^{-3}$	$.869 \times 10^{-3}$
1.2	$+.1860 \times 10^{-3}$	6.731	7.0	$+.1860 \times 10^{-3}$	$.4464 \times 10^{-3}$	$.2232 \times 10^{-3}$
1.2	$-.380 \times 10^{-3}$	6.711	16.0	$-.380 \times 10^{-3}$	$.9120 \times 10^{-3}$	$.4560 \times 10^{-3}$
1.3	$-.2091 \times 10^{-2}$	7.181	12.0	$-.2091$	$.54366 \times 10^{-2}$	$.27188 \times 10^{-2}$
1.4	$-.366 \times 10^{-2}$	7.655	9.5	$-.366 \times 10^{-2}$	$1.0248 \times 10^{-2}$	$.5124 \times 10^{-2}$
1.5	$-.460 \times 10^{-2}$	8.1285	9.0	$-.460 \times 10^{-2}$	$1.380 \times 10^{-2}$	$.690 \times 10^{-2}$
1.6	$-.4761 \times 10^{-2}$	8.6025	10	$-.4761 \times 10^{-2}$	$1.5235 \times 10^{-2}$	$.7618 \times 10^{-2}$
1.7	$-.428 \times 10^{-2}$	9.082	10.5	$-.428 \times 10^{-2}$	$1.4552 \times 10^{-2}$	$.7276 \times 10^{-2}$
1.8	$-.3370 \times 10^{-2}$	9.571	13	$-.337 \times 10^{-2}$	$1.2132 \times 10^{-2}$	$.6061 \times 10^{-2}$
1.9	$-.227 \times 10^{-2}$	10.072	15	$-.227 \times 10^{-2}$	$.8626 \times 10^{-2}$	$.4313 \times 10^{-2}$
1.9	$+.273 \times 10^{-3}$	10.019	4.5	$+.273 \times 10^{-3}$	$1.037 \times 10^{-3}$	$.5185 \times 10^{-3}$
2.0	$+.139 \times 10^{-2}$	10.523	8.0	$+.139 \times 10^{-2}$	$.556 \times 10^{-2}$	$.278 \times 10^{-2}$
2.0	$-.117 \times 10^{-2}$	10.579	17.0	$-.117 \times 10^{-2}$	$.468 \times 10^{-2}$	$.234 \times 10^{-2}$
2.1	$+.272 \times 10^{-2}$	11.027	9.0	$+.272 \times 10^{-2}$	$1.1424 \times 10^{-2}$	$.5712 \times 10^{-2}$
2.1	$-.295 \times 10^{-3}$	11.099	19.5	$-.295 \times 10^{-3}$	$1.239 \times 10^{-3}$	$.6195 \times 10^{-3}$
2.2	$+.411 \times 10^{-2}$	11.547	11.0	$+.411 \times 10^{-2}$	$1.8084 \times 10^{-2}$	$.9042 \times 10^{-2}$
2.3	$+.545 \times 10^{-2}$	12.071	12.0	$+.545 \times 10^{-2}$	$2.5070 \times 10^{-2}$	$1.2535 \times 10^{-2}$
2.4	$+.6675 \times 10^{-2}$	12.595	12.5	$+.6675 \times 10^{-2}$	$3.204 \times 10^{-2}$	$1.602 \times 10^{-2}$
2.5	$+.779 \times 10^{-2}$	13.140	13.5	$+.779 \times 10^{-2}$	$3.895 \times 10^{-2}$	$1.948 \times 10^{-2}$
2.6	$+.882 \times 10^{-2}$	13.67	13.5	$+.882 \times 10^{-2}$	$4.586 \times 10^{-2}$	$2.293 \times 10^{-2}$
2.7	$+.970 \times 10^{-2}$	14.22	13.5	$+.970 \times 10^{-2}$	$5.238 \times 10^{-2}$	$2.619 \times 10^{-2}$
2.8	$+.105 \times 10^{-1}$	14.70	13.5	$+.105 \times 10^{-1}$	$.588 \times 10^{-1}$	$.294 \times 10^{-1}$
2.9	$+.111 \times 10^{-1}$	15.33	13.5	$+.111 \times 10^{-1}$	$.6438 \times 10^{-1}$	$.3219 \times 10^{-1}$
3.0	$+.117 \times 10^{-1}$	15.89	13.5	$+.117 \times 10^{-1}$	$.702 \times 10^{-1}$	$.356 \times 10^{-1}$

THE FRANKLIN INSTITUTE • *Laboratories for Research and Development*

I-A2321-1

APPENDIX F

FREQUENCY OF FREE VIBRATIONS - OUTER RING

APPENDIX F

FREQUENCY OF FREE VIBRATIONS - OUTER RING

(Deep Groove Radial Ball Bearing)

50 MM. Bore	{	Extra Light	110
		Light	210
		Medium	310

In the following, it is assumed that the cross-sectional dimensions of the outer ring are small in comparison with the radius of its center line and that each cross section has an axis of symmetry situated in the plane of the ring.

Vibrations of a Circular Ring

Pure Radial Vibrations:

Center line of the ring forms a circle of periodically varying radius and all cross sections move radially without rotation.

Torsional Vibrations

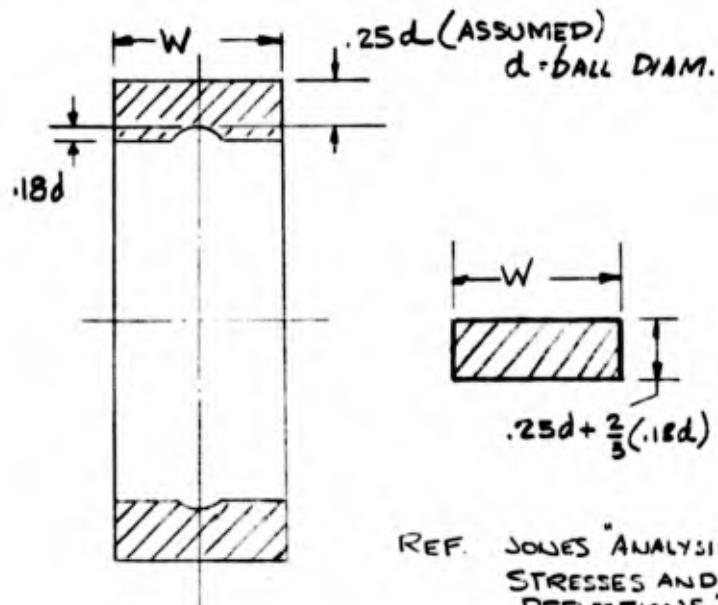
Center line of ring remains undeformed and all cross sections of the ring rotate during vibrations through some angle.

Flexural Vibrations

(1) In Plane of Ring

The exact shape of the mode of vibration consists of a curve which is a sinusoid on the developed circumference of the ring.

(2) Involving both displacements at right angles to the plane of the ring and twist.



REF. JONES "ANALYSIS OF  
STRESSES AND  
DEFLECTIONS"  
PAGES 55-58  
NEW DEPARTURE DIV.  
GENERAL MOTORS CORP.  
1976.

EQUIVALENT SECTION OF OUTER RING

BEARING #110 (DEEP GROOVE RADIAL)

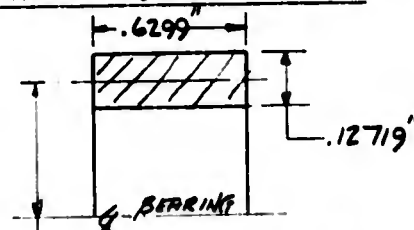
$$d = .34375 \text{ INCHES}$$

$$O.DIA. = 3.1496 \text{ INCHES}$$

$$W = .6299$$

$$.25d + \frac{2}{3}(.18d) = .25(.34375) + .12(.34375) = .12719 \text{ INCHES}$$

EQUIVALENT RECTANGULAR SECTION



$$\text{RADIUS TO CG OF SECTION} = \frac{3.1496 - .12719}{2} = 1.5112"$$

$$\text{AREA OF SECTION} = .6299 \times .12719 = .08 \text{ IN}^2$$

PURE RADIAL VIBRATIONS



TIMOSHENKO "VIBRATION

PROBLEMS IN ENGINEERING"

3RD ED. PAGE 425

VAN NOSTRAND CO, 1954.

FUNDAMENTAL FREQUENCY

$$f = \frac{1}{2\pi} \sqrt{\frac{Eg}{\gamma R^2}}$$

$$f = \frac{1}{2\pi} \sqrt{\frac{30 \times 10^6 \times 386}{.293 \times (1.5112)^2}}$$

$$f = \frac{1}{2\pi} \sqrt{172.5 \times 10^8}$$

$$f = \frac{13.12 \times 10^4}{2\pi} = 20950 \text{ cps}$$



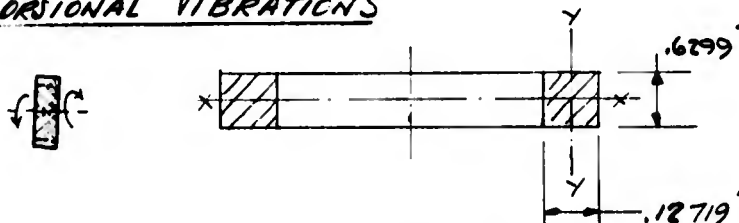
MODES OF VIBRATIONS

#110 BRG

$$f_i = \frac{1}{2\pi} \sqrt{\frac{Eg}{\gamma R^2}} \sqrt{1+i^2}$$

WHERE  $i$  = NO. WAVES PER CIRCUMFERENCE

$$\begin{aligned} i=1 & f_1 = 20950 \sqrt{1+1} = 29600 \text{ cps} \\ i=2 & f_2 = 20950 \sqrt{1+4} = 46900 \text{ cps} \\ i=3 & f_3 = 20950 \sqrt{1+9} = 66200 \text{ cps} \\ i=4 & f_4 = 20950 \sqrt{1+16} = 86000 \text{ cps} \end{aligned}$$

TORSIONAL VIBRATIONS

$$I_x = \frac{bd^3}{12} = \frac{.12719(.6299)^3}{12} = .00265 \text{ IN}^4$$

$$I_y = \frac{bd^3}{12} = \frac{.6299(.12719)^3}{12} = .000108 \text{ IN}^4$$

$$I_p = I_x + I_y = .00265 + .000108 = .002758 \text{ IN}^4$$

$$f = \frac{1}{2\pi} \sqrt{\frac{Eg}{\gamma R^2} \frac{I_x}{I_p}}$$

$$f = 20950 \sqrt{\frac{.00265}{.002758}} = 20550 \text{ cps}$$

TORSIONAL VIBRATIONS

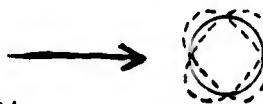
4110 BEG

MODES

$$f_i = \frac{1}{2\pi} \sqrt{\frac{Eg}{\gamma R^2} \frac{I_x}{I_p} \frac{1}{1+i^2}}$$

$$\begin{aligned} i=1 & f_1 = 20550 \sqrt{2} = 29000 \text{ cps} \\ i=2 & f_2 = 20550 \sqrt{5} = 46000 \text{ cps} \\ i=3 & f_3 = 20550 \sqrt{10} = 65000 \text{ cps} \\ i=4 & f_4 = 20550 \sqrt{17} = 84400 \text{ cps} \end{aligned}$$

FLEXURAL VIBRATIONS  
IN PLANE OF RING:



$$f_i = \frac{1}{2\pi} \sqrt{\frac{Eg}{\gamma} \frac{I_y}{AR^4} \frac{i^2(1-i^2)^2}{1+i^2}}$$

$i=1, f=0$ , RING MOVES AS A RIGID BODY

$$i=2 \quad f_2 = \frac{1}{2\pi} \sqrt{\frac{30 \times 10^6 \times 386}{.293} \frac{.0001084}{(.08)(1.512)^4} \frac{4(3)^2}{5}}$$

$$f_2 = \frac{1}{2\pi} \sqrt{10.23 \times 10^6 \times \frac{36}{5}}$$

$$f_2 = \frac{8.58}{2\pi} \times 10^3 = 1365 \text{ CPS (FUNDAMENTAL)}$$

$$i=3 \quad f_3 = \frac{1}{2\pi} \sqrt{10.23 \times 10^6 \frac{9(64)}{10}}$$

$$f_3 = \frac{1}{2\pi} \sqrt{590 \times 10^6} = 3870 \text{ cps}$$

#110 BRG

$$\begin{aligned}
 i=4 \quad f_4 &= \frac{1}{2\pi} \sqrt{10.23 \times 10^6 \frac{16(225)}{17}} \\
 f_4 &= \frac{1}{2\pi} \sqrt{2165 \times 10^6} \\
 f_4 &= 7400 \text{ cps}
 \end{aligned}$$

$$\begin{aligned}
 i=5 \quad f_5 &= \frac{1}{2\pi} \sqrt{10.23 \times 10^6 \frac{25(24)^2}{26}} \\
 f_5 &= \frac{1}{2\pi} \sqrt{5650 \times 10^6} = 12000 \text{ cps}
 \end{aligned}$$

$$\begin{aligned}
 i=6 \quad f_6 &= \frac{1}{2\pi} \sqrt{10.23 \times 10^6 \frac{36(35)^2}{37}} \\
 f_6 &= \frac{1}{2\pi} \sqrt{12200 \times 10^6} = 17600 \text{ cps}
 \end{aligned}$$

$$\begin{aligned}
 i=7 \quad f_7 &= \frac{1}{2\pi} \sqrt{10.23 \times 10^6 \frac{49(48)^2}{50}} \\
 f_7 &= \frac{1}{2\pi} \sqrt{23150 \times 10^6} = 24300 \text{ cps}
 \end{aligned}$$

$$\begin{aligned}
 i=8 \quad f_8 &= \frac{1}{2\pi} \sqrt{10.23 \times 10^6 \frac{64(63)^2}{65}} \\
 f_8 &= \frac{1}{2\pi} \sqrt{40000 \times 10^6} = 31900 \text{ cps}
 \end{aligned}$$

$$\begin{aligned}
 i=9 \quad f_9 &= \frac{1}{2\pi} \sqrt{10.23 \times 10^6 \frac{81(80)^2}{82}} \\
 f_9 &= \frac{1}{2\pi} \sqrt{64700 \times 10^6} = 40500 \text{ cps}
 \end{aligned}$$

FLEXURAL VIBRATIONS

#110 BRG

AT RIGHT ANGLES TO RING PLANE PLUS TWIST.



$$f_i = \frac{1}{2\pi} \sqrt{\frac{E_f}{\gamma} \frac{I_x}{AR^4} \frac{l^2(l^2-1)^2}{(l^2+1+\nu)}}$$

 $\nu$  = POISSON'S RATIO = .33 (STEEL) $l=1, f=0$ , RING MOVES AS RIGID BODY

$$l=2 \quad f_1 = \frac{1}{2\pi} \sqrt{\frac{30 \times 10^6 \times 386}{.293} \frac{.00265}{(.08)(1.5112)^4} \frac{4(3)^2}{5.33}}$$

$$f_2 = \frac{1}{2\pi} \sqrt{250 \times 10^6 \frac{36}{5.33}}$$

$$f_2 = 6560 \text{ cps}$$

$$l=3 \quad f_3 = \frac{1}{2\pi} \sqrt{250 \times 10^6 \frac{1664}{10.33}}$$

$$f_3 = 18790 \text{ cps}$$

$$l=4 \quad f_4 = \frac{1}{2\pi} \sqrt{250 \times 10^6 \frac{16(225)}{17.33}}$$

$$f_4 = 36300 \text{ cps}$$

BEARING #210 (DEEP GROOVE RADIAL)

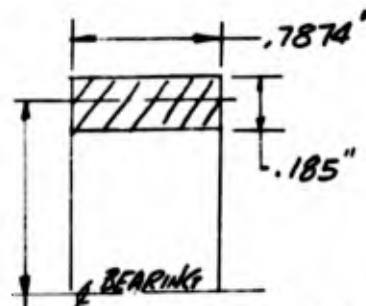
$$d = .500 \text{ INCHES}$$

$$O.D. = 3.5433 \text{ INCHES}$$

$$W = .7874 \text{ INCHES}$$

$$.25d + \frac{2}{3}(.18d) = .25(.5) + .12(.5) = .185 \text{ INCHES}$$

EQUIVALENT RECTANGULAR SECTION



$$\text{RADIUS TO C.G. OF SECTION} = \frac{3.5433 - .185}{2}$$

$$R = 1.6791 \text{ INCHES}$$

$$\text{AREA OF SECTION} = (.7874)(.185) = .146 \text{ IN}^2$$

PURE RADIAL VIBRATIONS

$$f = \frac{1}{2\pi} \sqrt{\frac{Eg}{\gamma R^2}}$$

$$f = \frac{1}{2\pi} \sqrt{\frac{30 \times 10^6 \times 386}{.293 \times (1.6791)^2}}$$

$$f = \frac{1}{2\pi} \sqrt{140.2 \times 10^8} = 18789 \text{ cps}$$

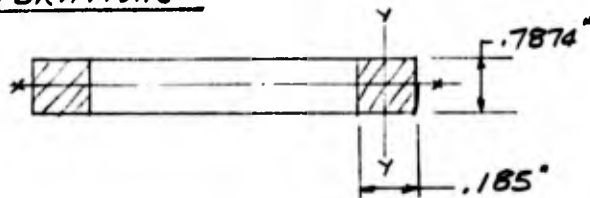
# MODES OF VIBRATIONS

#210 BRG

$$f_i = \frac{1}{2\pi} \sqrt{\frac{Eg}{\gamma R^2}} \sqrt{1 + i^2}$$

$L=1$	$f_1 = 18789 \sqrt{2} = 26800 \text{ cps}$
$L=2$	$f_2 = 18789 \sqrt{5} = 42000 \text{ cps}$
$L=3$	$f_3 = 18789 \sqrt{10} = 59300 \text{ cps}$
$L=4$	$f_4 = 18789 \sqrt{17} = 77500 \text{ cps}$

## TORSIONAL VIBRATIONS



$$I_{xx} = \frac{bd^3}{12} = \frac{.185 (.7874)^3}{12} = .00755 \text{ IN}^4$$

$$I_{yy} = \frac{bd^3}{12} = \frac{.7874 (.185)^3}{12} = .000417 \text{ IN}^4$$

$$I_p = I_{xx} + I_{yy} = .007967 \text{ IN}^4$$

$$f = \frac{1}{2\pi} \sqrt{\frac{Eg}{\gamma R^2} \frac{I_{xx}}{I_p}}$$

$$f = 18789 \sqrt{\frac{.00755}{.007967}}$$

$$f = 17812 \text{ cps}$$

TORSIONAL VIBRATIONS

4210 BRG

MODES

$$f_i = \frac{1}{2\pi} \sqrt{\frac{E_s}{YR^2} \frac{I_x}{I_p}} \sqrt{1+i^2}$$

$$\begin{array}{ll} i=1 & f_1 = 17812 \sqrt{2} = 25186 \text{ cps} \\ i=2 & f_2 = 17812 \sqrt{5} = 39899 \text{ cps} \\ i=3 & f_3 = 17812 \sqrt{10} = 56286 \text{ cps} \\ i=4 & f_4 = 17812 \sqrt{17} = 73364 \text{ cps} \end{array}$$

FLEXURAL VIBRATIONS

IN PLANE OF RING:

$$f_i = \frac{1}{2\pi} \sqrt{\frac{E_s}{Y} \frac{I_y}{AR^4} \frac{i^2(1-i^2)^2}{1+i^2}}$$

 $i=1, f_1 = 0$ . RING MOVES AS A RIGID BODY

$$i=2 \quad f_2 = \frac{1}{2\pi} \sqrt{\frac{30 \times 10^6 \times 386}{.293} \frac{.000417}{(.146)(1.679)^4} \frac{4(3)^2}{5}}$$

$$f_2 = \frac{1}{2\pi} \sqrt{14.1 \times 10^6 \times 7.2}$$

$$f_2 = \frac{10.05 \times 10^3}{2\pi} = 1600 \text{ cps}$$

$$i=3 \quad f_3 = \frac{1}{2\pi} \sqrt{14.1 \times 10^6 \frac{9(64)}{10}}$$

$$f_3 = \frac{28.5 \times 10^3}{2\pi} = 4550 \text{ cps}$$

#210 BRG

$i=4$

$$f_4 = \frac{1}{2\pi} \sqrt{14.1 \times 10^6 \frac{16(25)^2}{17}}$$

$$f_4 = \frac{54.5 \times 10^3}{2\pi} = 8700 \text{ cps}$$

$$L=5 \quad f_5 = \frac{1}{2\pi} \sqrt{14.1 \times 10^6 \frac{25(26)^2}{26}}$$

$$f_5 = \frac{88.3 \times 10^3}{2\pi} = 14050 \text{ cps}$$

$$L=6 \quad f_6 = \frac{1}{2\pi} \sqrt{14.1 \times 10^6 \frac{36(35)^2}{37}}$$

$$f_6 = \frac{130 \times 10^3}{2\pi} = 20700 \text{ cps}$$

$$L=7 \quad f_7 = \frac{1}{2\pi} \sqrt{14.1 \times 10^6 \frac{49(48)^2}{50}}$$

$$f_7 = \frac{177 \times 10^3}{2\pi} = 28400 \text{ cps}$$

$$L=8 \quad f_8 = \frac{1}{2\pi} \sqrt{14.1 \times 10^6 \frac{64(63)^2}{65}}$$

$$f_8 = \frac{235 \times 10^3}{2\pi} = 37500 \text{ cps}$$

$$L=9 \quad f_9 = \frac{1}{2\pi} \sqrt{14.1 \times 10^6 \frac{81(80)^2}{82}}$$

$$f_9 = \frac{299 \times 10^3}{2\pi} = 47700 \text{ cps}$$



FLEXURAL VIBRATIONS

#210 BRG

AT RIGHT ANGLES TO RING PLANE PLUS TWIST.

$$f_i = \frac{1}{2\pi} \sqrt{\frac{Eg}{\gamma} \frac{Ix}{AR^4} \frac{l^2(l^2-1)^2}{(l^2+1)^2}}$$

 $l=1, f_1=0, \text{ RING MOVES AS RIGID BODY}$ 

$$l=2 \quad f_2 = \frac{1}{2\pi} \sqrt{\frac{30 \times 10^6 \times 386}{.293} \frac{.00755}{(.146)(8.02)} \frac{4(3)^2}{5.33}}$$

$$f_2 = \frac{1}{2\pi} \sqrt{255 \times 10^6 \frac{36}{5.33}}$$

$$f_2 = \frac{4.15 \times 10^3}{2\pi} = 6630 \text{ cps}$$

$$l=3 \quad f_3 = \frac{1}{2\pi} \sqrt{255 \times 10^6 \frac{9(64)}{10.33}}$$

$$f_3 = \frac{119 \times 10^3}{2\pi} = 19000 \text{ cps}$$

$$l=4 \quad f_4 = \frac{1}{2\pi} \sqrt{255 \times 10^6 \frac{16(225)}{17.33}}$$

$$f_4 = \frac{230 \times 10^3}{2\pi} = 36700 \text{ cps}$$

BEARING #310 (DEEP GROOVE RADIAL)

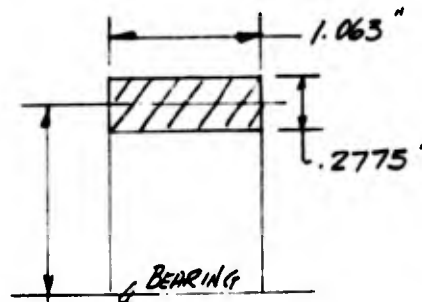
$$d = .7500 \text{ INCHES}$$

$$O.D. = 4.3307 \text{ INCHES}$$

$$W = 1.063 \text{ INCHES}$$

$$.25d + \frac{2}{3}(.18d) = .25(.75) + .12(.75) = .2775 \text{ INCHES}$$

EQUIVALENT RECTANGULAR SECTION



$$\text{RADIUS TO C.G. OF SECTION} = \frac{4.3307 - .2775}{2}$$

$$R = 2.0266 \text{ INCHES}$$

$$\text{AREA OF SECTION} = (1.063)(.2775) = .295 \text{ IN}^2$$

PURE RADIAL VIBRATIONS

$$f = \frac{1}{2\pi} \sqrt{\frac{Eg}{\gamma R^2}}$$

$$f = \frac{1}{2\pi} \sqrt{\frac{30 \times 10^6 \times 386}{.293 \times (2.0266)^2}}$$

$$f = \frac{1}{2\pi} \sqrt{96.3 \times 10^8}$$

$$f = 15650 \text{ cps}$$

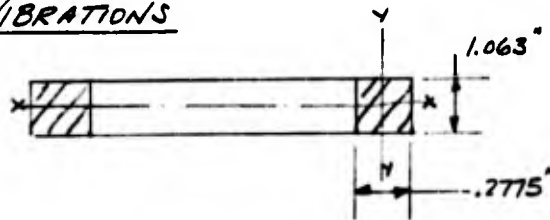
# MODES OF VIBRATIONS

#310 BRG

$$f_i = \frac{1}{2\pi} \sqrt{\frac{Eg}{\gamma R^2}} \sqrt{1+i^2}$$

$$\begin{aligned} L=1 & \quad f_1 = 15650 \sqrt{1} = 22100 \text{ cps} \\ L=2 & \quad f_2 = 15650 \sqrt{5} = 35000 \text{ cps} \\ L=3 & \quad f_3 = 15650 \sqrt{10} = 49400 \text{ cps} \\ L=4 & \quad f_4 = 15650 \sqrt{17} = 64400 \text{ cps} \end{aligned}$$

## TORSIONAL VIBRATIONS



$$I_{xx} = \frac{bd^3}{12} = \frac{.2775(1.063)^3}{12} = .02775 \text{ IN}^4$$

$$I_{yy} = \frac{bd^3}{12} = \frac{1.063(.2775)^3}{12} = .0019 \text{ IN}^4$$

$$I_p = I_{xx} + I_{yy} = .02965 \text{ IN}^4$$

$$f = \frac{1}{2\pi} \sqrt{\frac{Eg}{\gamma R^2} \frac{I_{xx}}{I_p}}$$

$$f = 15650 \sqrt{\frac{.02775}{.02965}}$$

$$f = 15130 \text{ cps}$$

TORSIONAL VIBRATIONS

\*310 BRG

MODES

$$f_i = \frac{1}{2\pi} \sqrt{\frac{Eg}{YR^2} \frac{I_{xx}}{I_p}} \sqrt{1+i^2}$$

$$\begin{aligned} i=1 & \quad f_1 = 15130\sqrt{2} = 21400 \text{ cps} \\ i=2 & \quad f_2 = 15130\sqrt{5} = 33900 \text{ cps} \\ i=3 & \quad f_3 = 15130\sqrt{10} = 47800 \text{ cps} \\ i=4 & \quad f_4 = 15130\sqrt{17} = 62200 \text{ cps} \end{aligned}$$

FLEXURAL VIBRATIONS

IN PLANE OF RING:

$$f_i = \frac{1}{2\pi} \sqrt{\frac{Eg}{Y} \frac{I_{yy}}{AR^4} \frac{i^2(i-1)^2}{14L^2}}$$

$i=1, f_1=0$ , RING MOVES AS A RIGID BODY

$$\begin{aligned} i=2 & \quad f_2 = \frac{1}{2\pi} \sqrt{\frac{30 \times 10^6 \times 386}{.292} \frac{.0019}{(.292 \times 2.046)^4} \frac{4(3)^2}{144}} \\ & \quad f_2 = \frac{1}{2\pi} \sqrt{15.1 \times 10^6 \times 7.2} = 1665 \text{ cps} \end{aligned}$$

$$\begin{aligned} i=3 & \quad f_3 = \frac{1}{2\pi} \sqrt{15.1 \times 10^6 \frac{9(64)}{10}} \\ & \quad f_3 = \frac{1}{2\pi} \sqrt{870 \times 10^6} = 4700 \text{ cps} \end{aligned}$$

#310 Beg

 $l=4$ 

$$f_4 = \frac{1}{2\pi} \sqrt{15.1 \times 10^6 \frac{16(225)}{17}}$$

$$f_4 = \frac{1}{2\pi} \sqrt{3200 \times 10^6} = 9000 \text{ cps}$$

 $l=5$ 

$$f_5 = \frac{1}{2\pi} \sqrt{15.1 \times 10^6 \frac{25(24)^2}{26}}$$

$$f_5 = \frac{1}{2\pi} \sqrt{15.1 \times 10^6 \times 554} = 14550 \text{ cps}$$

 $l=6$ 

$$f_6 = \frac{1}{2\pi} \sqrt{15.1 \times 10^6 \frac{36(35)^2}{37}}$$

$$f_6 = \frac{1}{2\pi} \sqrt{18000 \times 10^6} = 21400 \text{ cps}$$

 $l=7$ 

$$f_7 = \frac{1}{2\pi} \sqrt{15.1 \times 10^6 \frac{49(48)^2}{50}}$$

$$f_7 = \frac{184 \times 10^3}{2\pi} = 29400 \text{ cps}$$

 $l=8$ 

$$f_8 = \frac{1}{2\pi} \sqrt{15.1 \times 10^6 \frac{64(63)^2}{65}}$$

$$f_8 = \frac{244 \times 10^3}{2\pi} = 38800 \text{ cps}$$

 $l=9$ 

$$f_9 = \frac{1}{2\pi} \sqrt{15.1 \times 10^6 \times \frac{81(80)^2}{82}}$$

$$f_9 = \frac{309 \times 10^3}{2\pi} = 49300 \text{ cps}$$

FLEXURAL VIBRATIONS

#310 BRG

AT RIGHT ANGLES TO RING PLANE PLUS TWIST.

$$f_i = \frac{1}{2\pi} \sqrt{\frac{Eg}{\gamma} \frac{I_x}{AR^4} \frac{L(L^2-1)^2}{L^2+12}}$$

$i=1, f=0$ , RING MOVES AS A RIGID BODY

$$i=2 \quad f_2 = \frac{1}{2\pi} \sqrt{\frac{30 \times 10^6 \times 386}{.293} \frac{.02775}{.295 \times 16.8} \frac{4(9)}{5.33}}$$

$$f_2 = \frac{1}{2\pi} \sqrt{221 \times 10^6 \times \frac{36}{5.33}} = 6150 \text{ CPS}$$

$$i=3 \quad f_3 = \frac{1}{2\pi} \sqrt{221 \times 10^6 \times \frac{9(64)}{10.33}} = 17680 \text{ CPS}$$

$$i=4 \quad f_4 = \frac{1}{2\pi} \sqrt{221 \times 10^6 \times \frac{16(325)}{17.33}} = 34100 \text{ CPS}$$

THE FRANKLIN INSTITUTE • Laboratories for Research and Development

1-A2321-1

SUMMARY OF OUTER RING FREE VIBRATIONS (110, 210, 310 BR'GS)

1. Pure Radial Vibrations

$$f_i = \frac{1}{2\pi} \sqrt{\frac{Eg}{\gamma R^2}} \sqrt{1 + i^2}$$

i = No. of waves/circumference

Mode	Frequency of Free Vibration (cps)		
	BR'G Size → 110	210	310
i = 0	20950	18790	15650 ← Fundamental
i = 1	29600	26800	22100
i = 2	46900	42000	35000
i = 3	66200	59300	49400
i = 4	86000	77500	64400

2. Torsional Vibrations

$$f_i = \frac{1}{2\pi} \sqrt{\frac{Eg}{\gamma R^2} - \frac{I_x}{I_p}} \sqrt{1 + i^2}$$

Mode	Frequency of Free Vibration (cps)		
	BR'G Size → 110	210	310
i = 0	20550	17812	15130 ← Fundamental
i = 1	29000	25186	21400
i = 2	46000	39900	33900
i = 3	65000	58290	47800
i = 4	84400	73560	62200

I-A2321-1

3. Flexural Vibrations

A. In plane of ring 
$$f_1 = \frac{1}{2\pi} \sqrt{\frac{Eg I_y}{\gamma AR^4} \times \frac{i^2(1-i^2)^2}{1+i^2}}$$

Frequency of Free Vibrations (c/s)

	BR'G Size → <u>110</u> <u>210</u> <u>310</u>		
<u>Mode</u>			
i = 1	0	0	0
i = 2	1,365	1,600	1,665 ← Funda-
i = 3	3,870	4,550	4,700 mental
i = 4	7,400	8,700	9,000
i = 5	12,000	14,050	14,500
i = 6	17,600	20,700	21,400
i = 7	24,300	28,400	29,400
i = 8	31,900	37,500	35,800
i = 9	40,500	47,700	49,300

B. At right angles to ring plane

$$f_1 = \frac{1}{2\pi} \sqrt{\frac{Eg I_x}{\gamma AR^4} \frac{i^2(i^2-1)^2}{(i^2+1+\nu)}}$$

Frequency of Free Vibrations

	BR'G Size → <u>110</u> <u>210</u> <u>310</u>		
<u>Mode</u>			
i = 1	0	0	0
i = 2	6,560	6,630	6,150 ← Funda-
i = 3	18,790	19,000	17,680 mental
i = 4	36,300	36,700	34,100



THE FRANKLIN INSTITUTE • *Laboratories for Research and Development*

I-A2321-1

APPENDIX G

COMBINED SPRING RATE OF LOADED BALL

APPENDIX G

Combined Spring Rate of Loaded Ball

$\delta_n$  = Normal approach of races

$\delta_o$  = Normal approach of ball to outer race

$\delta_i$  = Normal approach of inner race to ball

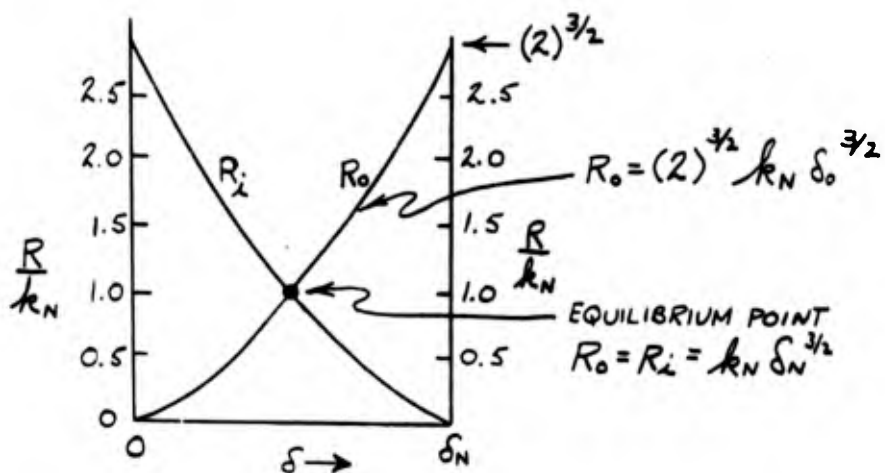
$\delta_n = \delta_o + \delta_i$

Let  $\delta_o = \delta_i = \frac{\delta_n}{2}$  at Equilibrium position

Since  $R$  = Ball load =  $k_N \delta_N^{3/2}$

$$R_i = (2)^{3/2} k_N \delta_i^{3/2}$$

$$R_o = (2)^{3/2} k_N \delta_o^{3/2}$$



THE FRANKLIN INSTITUTE • Laboratories for Research and Development

I-A2321-1

$$(R_o - R_1) = (2)^{3/2} k_N [\delta_o^{3/2} - \delta_1^{3/2}] = (2)^{3/2} k_N [\delta^{3/2} - (\delta_N - \delta)^{3/2}]$$

$$\left. \begin{array}{l} \text{Spring rate} \\ \text{of trapped Ball} \end{array} \right\} = k_b = \frac{d(R_o - R_1)}{d(\delta)} = (2)^{3/2} k_N \left[ \frac{3}{2} \delta^{1/2} - (\delta_N - \delta)^{1/2} \left( \frac{3}{2} \right) (-1) \right]$$

$$k_B = (2)^{1/2} 3k_N [\delta^{1/2} + (\delta_N - \delta)^{1/2}]$$

$$k_B = (2)^{1/2} 3k_N \delta_N^{1/2} \left[ \left( \frac{\delta}{\delta_N} \right)^{1/2} + \left( 1 - \frac{\delta}{\delta_N} \right)^{1/2} \right]$$

$$\text{at } \delta = \frac{\delta_N}{2}$$

$$k_B = 6k_N \delta_N^{1/2} \leftarrow \text{Combined spring rate for ball at equilibrium } (R_o = R_1)$$

I-A2321-1

Examining the linearity of the combined spring rate, we need to evaluate  $\left[\left(\frac{\delta}{\delta_N}\right)^{\frac{1}{2}} + \left(1 - \frac{\delta}{\delta_N}\right)^{\frac{1}{2}}\right]$  from  $\delta=0$  to  $\delta=\delta_N$

$$k_B = (2)^{\frac{1}{2}} 3k_N \delta^{\frac{1}{2}} \left[\left(\frac{\delta}{\delta_N}\right)^{\frac{1}{2}} + \left(1 - \frac{\delta}{\delta_N}\right)^{\frac{1}{2}}\right]$$

$R_L = R_o$  →

$\frac{\delta}{\delta_N}$	$\left(\frac{\delta}{\delta_N}\right)^{\frac{1}{2}}$	$\left(1 - \frac{\delta}{\delta_N}\right)$	$\left(1 - \frac{\delta}{\delta_N}\right)^{\frac{1}{2}}$	$\left[\left(\frac{\delta}{\delta_N}\right)^{\frac{1}{2}} + \left(1 - \frac{\delta}{\delta_N}\right)^{\frac{1}{2}}\right]$	$k_B$
0	0	1.0	1.0	1.0	4.243 $\delta_N^{\frac{1}{2}}$ kN
.1	.3162	0.9	.9487	1.2649	5.367 $\delta_N^{\frac{1}{2}}$ kN
.2	.4472	0.8	.8944	1.3416	5.692 $\delta_N^{\frac{1}{2}}$ kN
.3	.5477	0.7	.8367	1.3844	5.873 $\delta_N^{\frac{1}{2}}$ kN
.4	.6324	0.6	.7746	1.4070	5.969 $\delta_N^{\frac{1}{2}}$ kN
.5	.7071	0.5	.7071	1.4142	6.000 $\delta_N^{\frac{1}{2}}$ kN
.6	.7746	0.4	.6324	1.4070	5.969 $\delta_N^{\frac{1}{2}}$ kN
.7	.8367	0.3	.5477	1.3844	5.873 $\delta_N^{\frac{1}{2}}$ kN
.8	.8944	0.2	.4472	1.3416	5.692 $\delta_N^{\frac{1}{2}}$ kN
.9	.9487	0.1	.3162	1.2649	5.367 $\delta_N^{\frac{1}{2}}$ kN
1.0	1.0	0	0	1.0	4.243 $\delta_N^{\frac{1}{2}}$ kN

Essential-ly Linear

The column for  $k_B$  indicates that the combined spring rate is linear over a wide excursion from equilibrium

$$\therefore k_B \approx 6k_N \delta_N^{\frac{1}{2}}$$

THE FRANKLIN INSTITUTE • *Laboratories for Research and Development*

I-A2321-1

APPENDIX H

ELECTRIC MOTOR MECHANICAL UNBALANCE

APPENDIX H

ELECTRIC MOTOR MECHANICAL UNBALANCE

FROM MIL. SPEC. MIL-M-17060B (SHIPS) 2/25/59

SECTION 3.7.8, pg 36, "DYNAMIC BALANCE"

"THE DEGREE OF [DYNAMIC] BALANCE SHALL BE 'PRECISION' IN ACCORDANCE WITH TABLE VII UNLESS OTHERWISE SPECIFIED IN THE CONTRACT OR ORDER."

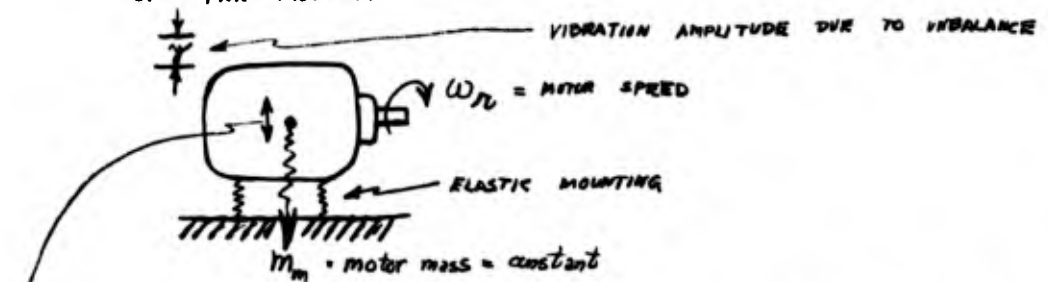
SECTION 3.1.16, pg 11, "MECHANICAL BALANCE"

"TABLE VII - MECHANICAL BALANCE"

WEIGHT OF MOTORS	MAXIMUM ALLOWABLE TOTAL AMPLITUDE		
	STANDARD BALANCE	PRECISION BALANCE	SUPER-PRECISION BALANCE
(POUNDS)	(in.)	(in.)	(in.)
UP TO 350	0.0010	0.0005	0.0002
351 - 800	.0015	.00025	.0003
801 - 2000	.0020	.0010	.0004
2001 AND UP	.0030	.0015	- - - - -

Fig. 72  
SECTION 9.3.4.6, "DYNAMIC BALANCE" [METHOD OF TEST]

"PLACE THE MOTOR ON AN ELASTIC MOUNTING SO PROPORTIONED THAT THE UP AND DOWN NATURAL FREQUENCY SHALL BE AT LEAST AS LOW AS ONE-QUARTER OF THE OPERATING SPEED OF THE MOTOR."



LET  $\omega_n$  = NATURAL FREQUENCY OF ELASTICLY SUPPORTED MOTOR

$$\therefore \omega_m \geq 4 \omega_n$$

$$\text{UNBALANCE FORCE} = P = m_n \delta \omega_m^2 \quad [H-1]$$

$m_n$  = MOTOR ROTOR MASS

$\delta$  = DISTANCE FROM GEOMETRIC CENTER TO MASS CENTER

FOR AN UNDAMPED, SINGLE DEGREE OF FREEDOM, SPRING-MASS SYSTEM, THE AMPLITUDE OF FORCED VIBRATION ( $y$ ) FOR DRIVING FORCE PROPORTIONAL TO SQUARE OF FREQUENCY IS,

$$y = \frac{m_n \cdot \delta}{m_m \left[ \left( \frac{\omega_m}{\omega_n} \right)^2 - 1 \right]}$$

$$\text{FOR } \frac{\omega_m}{\omega_n} \leq \frac{1}{4}$$

$$y \approx \left( \frac{m_n}{m_m} \right) \delta \quad \text{inches} \quad [H-2]$$

$$\therefore \delta = \left( \frac{m_m}{m_n} \right) y \quad \text{inches.} \quad [H-3]$$

COMBINING EQS [H-1] & [H-3] GIVES

$$\text{UNBALANCE FORCE} = P = m_m \gamma \omega_n^2 \quad [H-4]$$

$$\omega_n = \frac{2\pi N}{60} = 0.1045 N$$

$N = \text{RPM OF MOTOR}$

$$\therefore P = m_m \gamma (1.093 \times 10^{-2}) N^2, \text{ lbs}$$

$$m_m = \text{MOTOR MASS} = \frac{W_m}{386}$$

$$W_m = \text{MOTOR WT (lbs)}$$

$$\therefore P = \frac{W_m}{386} \gamma (1.093 \times 10^{-2}) N^2$$

$$P = (0.283 \times 10^{-9}) W_m \gamma \cdot N^2, \text{ lbs} \quad [H-5]$$

MAXIMUM  
INFORMATION ON <sup>MAXIMUM</sup> MOTOR WEIGHTS ( $W_m$ ) IS GIVEN IN TABLE B, FIG. 1, PAGE 3  
OF MIL-M-17060B(SHIPS). THIS INFORM IS PLOTTED ON FIG H-1.

BEARING SIZE INFORMATION IS GIVEN IN SAME TABLE AND SHOWN  
PLOTTED IN FIG NO. H-2. THE "CIRCLED" POINTS IN FIG H-2  
ARE AVERAGE BEARING SIZES.

FIG H-3 COMBINES FIGS H-1 AND H-2 TO OBTAIN MOTOR  
WEIGHT AS A FUNCTION OF BR'G SIZE.

INFORMATION ON ARMATURE WEIGHTS WAS OBTAINED FROM MR.  
RICHARD DORLER OF BUSHIPS AND IS PLOTTED IN FIG H-4



THE UNBALANCE FORCE IS GIVEN BY [H-5] AS

$$P = (0.283 \times 10^{-9}) W_m \cdot \gamma \cdot N^2$$

$W_m$  = MOTOR WT, (lbs)

$\gamma$  = ALLOWABLE AMP. OF VIBRATION, (in)

$N$  = ROTATIONAL SPEED

BRG SIZE	$W_m$ (lbs) FIG. H-3	$\gamma$ (Page 1) (PREC. BAL.)	$0.283 \times 10^{-9} \gamma W_m$	$P$ (lbs)			
				$N=900$	$N=1200$	$N=1800$	$N=3600$
305	105	.0005	$1.49 \times 10^{-5}$	1.21	2.17	4.84	19.36
306	140	↓	1.98	1.60	2.81	6.40	25.6
307	190		2.64	2.18	3.88	8.72	34.9
308	260		3.68	2.98	5.30	11.92	47.7
309	340	.0005	4.81	3.90	6.95	15.60	62.4
310	450	.00075	9.55	7.79	13.8	30.96	124
311	570	↓	12.1	9.8	17.5	39.2	157
312	700	.00075	19.9	12.1	21.7	48.4	194
313	850	.0010	24.0	15.5	24.7	78	312
314	1010	↓	28.6	23.2	41.3	93	372
315	1190		33.7	27.3	48.5	109	436
316	1380		39.1	31.7	56.3	125	500
317	1600	↓	45.3	36.7	65.2	146	584
318	1830	.0010	$51.8 \times 10^{-9}$	41.9	74.5	168	672

PLOTTED IN FIG. H-5

THE FRANKLIN INSTITUTE • Laboratories for Research and Development

I-A2321-1

THE RATIO OF UNBALANCE FORCE TO DEAD WEIGHT FORCE IS  
ON EACH BR'G IS

$$\frac{P/2}{W_N/2} = \frac{P}{W_N}$$

BR'G SIZE	W <sub>N</sub> FIG H-1	P/W <sub>N</sub>			
		N = 900	N = 1200	N = 1800	N = 3600
305	13	.093	.166	.372	1.49
306	19	.084	.150	.347	1.35
307	25	.087	.155	.349	1.39
308	33	.090	.161	.362	1.44
309	43	.091	.162	.363	1.45
310	55	.191	.250	.563	2.25
311	68	.199	.256	.576	2.30
312	82	.198	.264	.592	2.37
313	97	.201	.358	.804	3.22
314	114	.204	.363	.816	3.26
315	132	.207	.369	.828	3.31
316	151	.210	.374	.840	3.36
317	170	.216	.385	.864	3.46
318	190	.220	.392	.880	3.52

THE UNBALANCE "ARM",  $\delta$ , IS FROM [H-3]

$$\delta = \left( \frac{m_m}{m_n} \right) \gamma$$

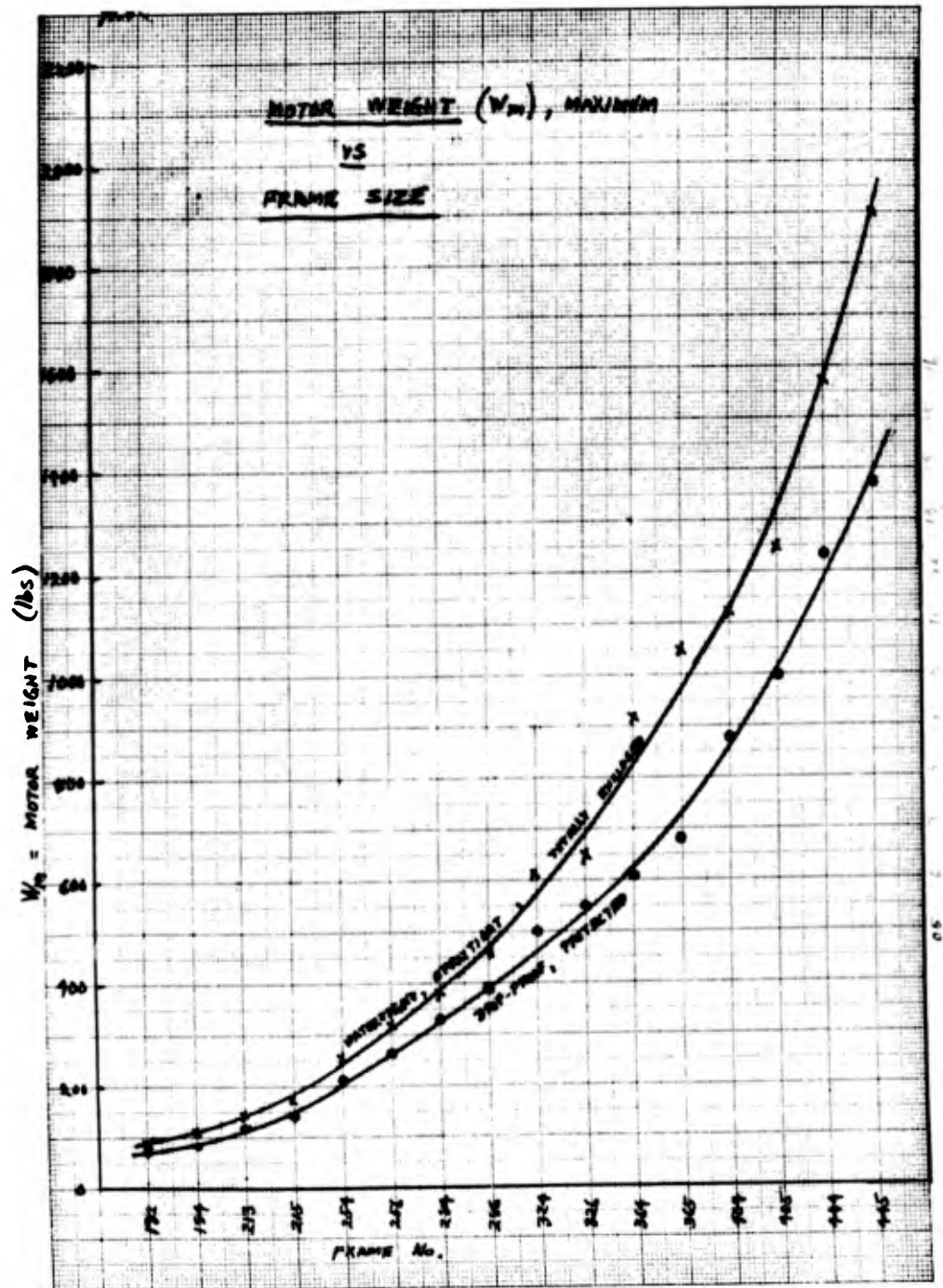
$$\frac{m_m}{m_n} = \frac{W_m/g}{W_n/g} = \frac{W_m}{W_n}$$

$$\delta = \left( \frac{W_m}{W_n} \right) \gamma \quad [H-6]$$

AMOUNT OF UNBALANCE

BRG SIZE	$W_m$ (lbs)	$W_n$ (lbs)	$\gamma$ (in.) Page H-2	$\frac{W_m}{W_n}$	$\delta$ (in.) Eq [H-6]	$W_n \cdot \delta$ (in-lbs)
305	105	13	.0005	8.1	$4.05 \times 10^{-3}$	.053
306	140	19	↓	7.4	3.7	.070
307	190	25	↓	7.6	3.8	.095
308	260	33	↓	7.9	3.95	.131
309	340	43	.0005	7.9	3.95	.170
310	450	55	.00075	8.2	6.10	.335
311	570	68	↓	8.4	6.28	.421
312	700	82	.00075	8.55	6.90	.524
313	850	97	.0010	8.75	8.75	.85
314	1010	114	↓	8.85	8.85	1.01
315	1190	132	↓	9.0	9.0	1.19
316	1380	157	↓	9.15	9.15	1.38
317	1600	170	↓	9.40	9.40	1.60
318	1830	190	.0010	9.60	$9.60 \times 10^{-3}$	1.92

PLOTTED IN FIG H-6 {  $\delta_{avg} \approx 3.0 \times 10^{-3} \times \text{DIA.}$



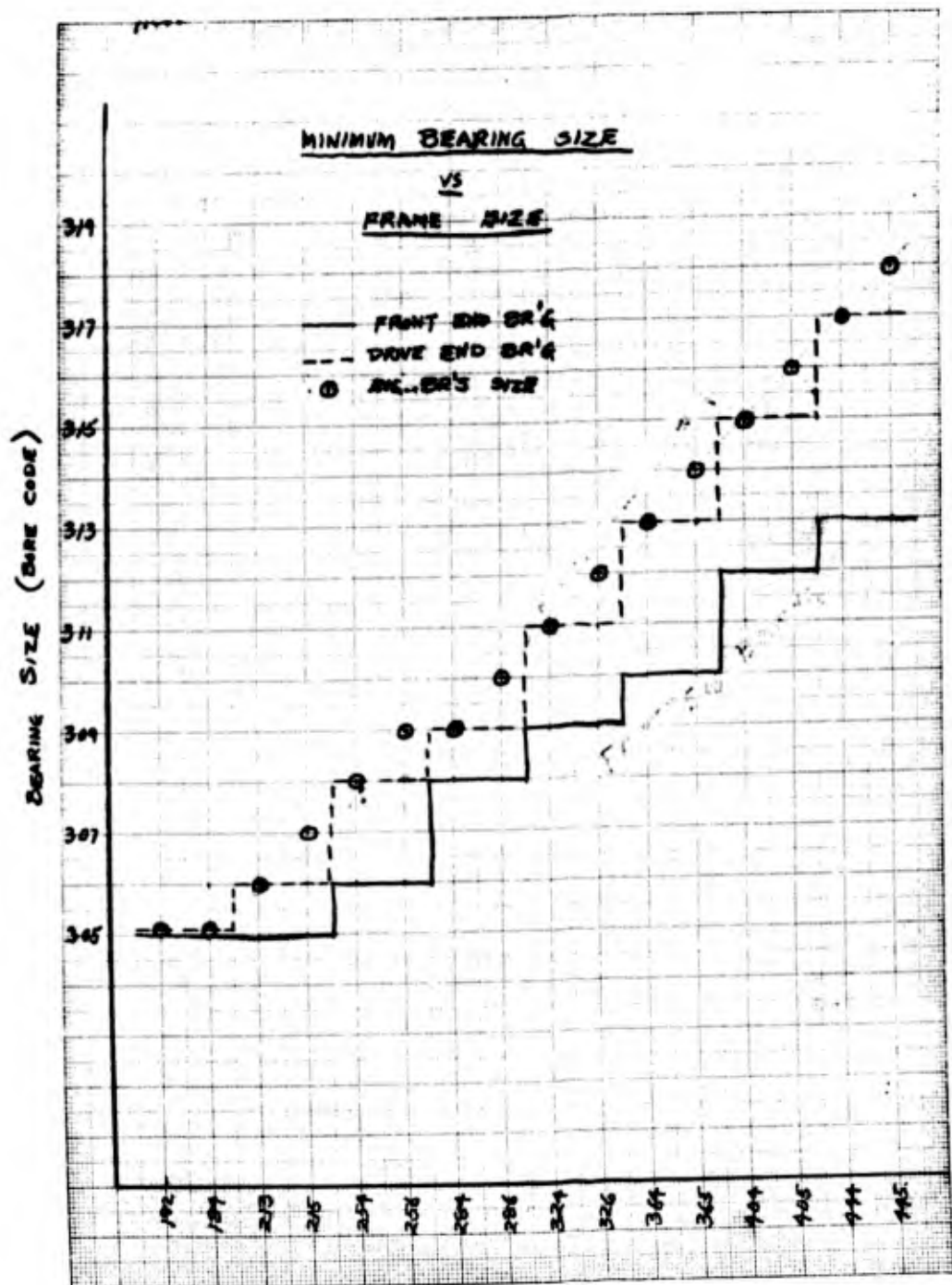


Figure H2

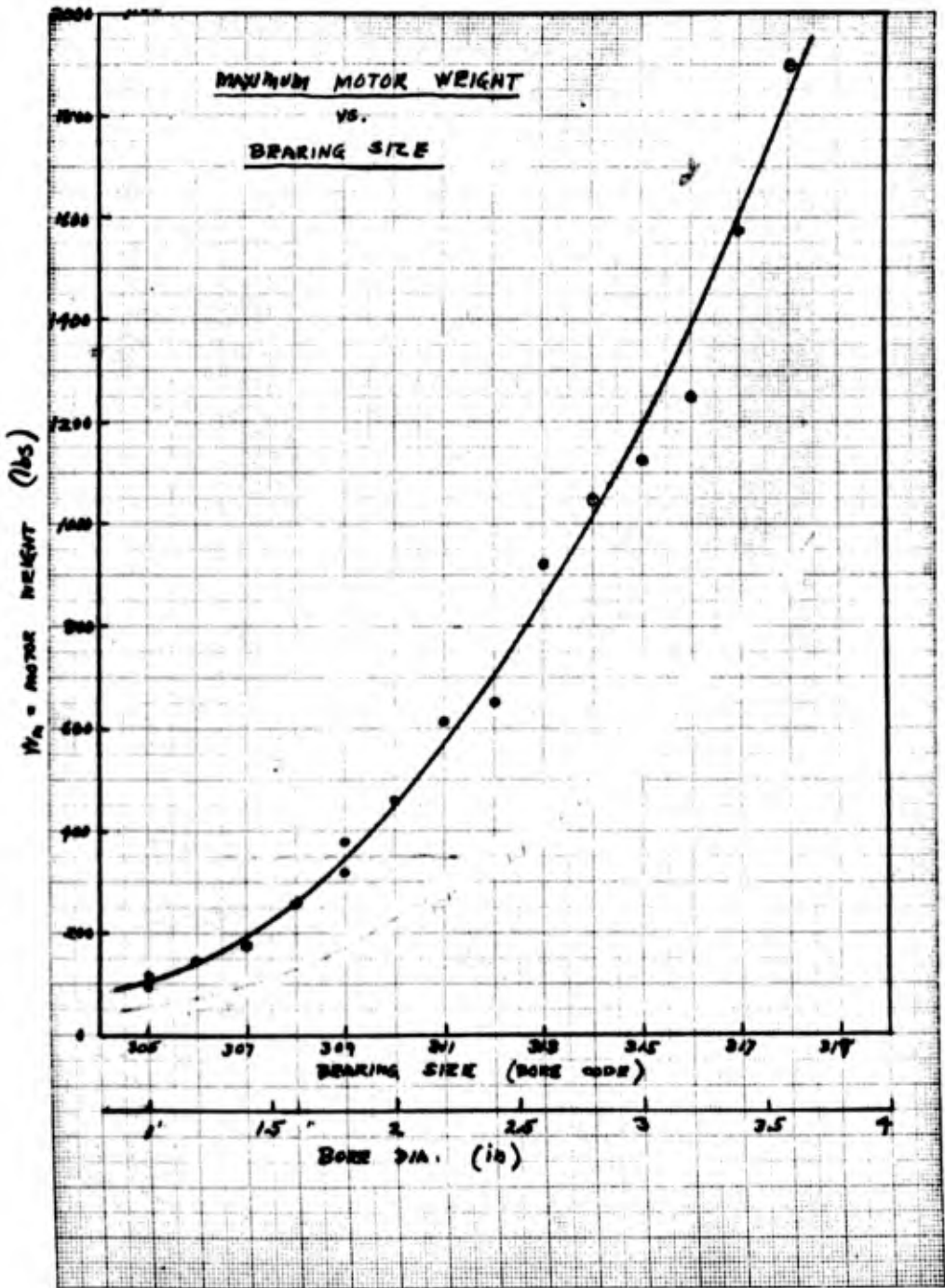


Figure H3

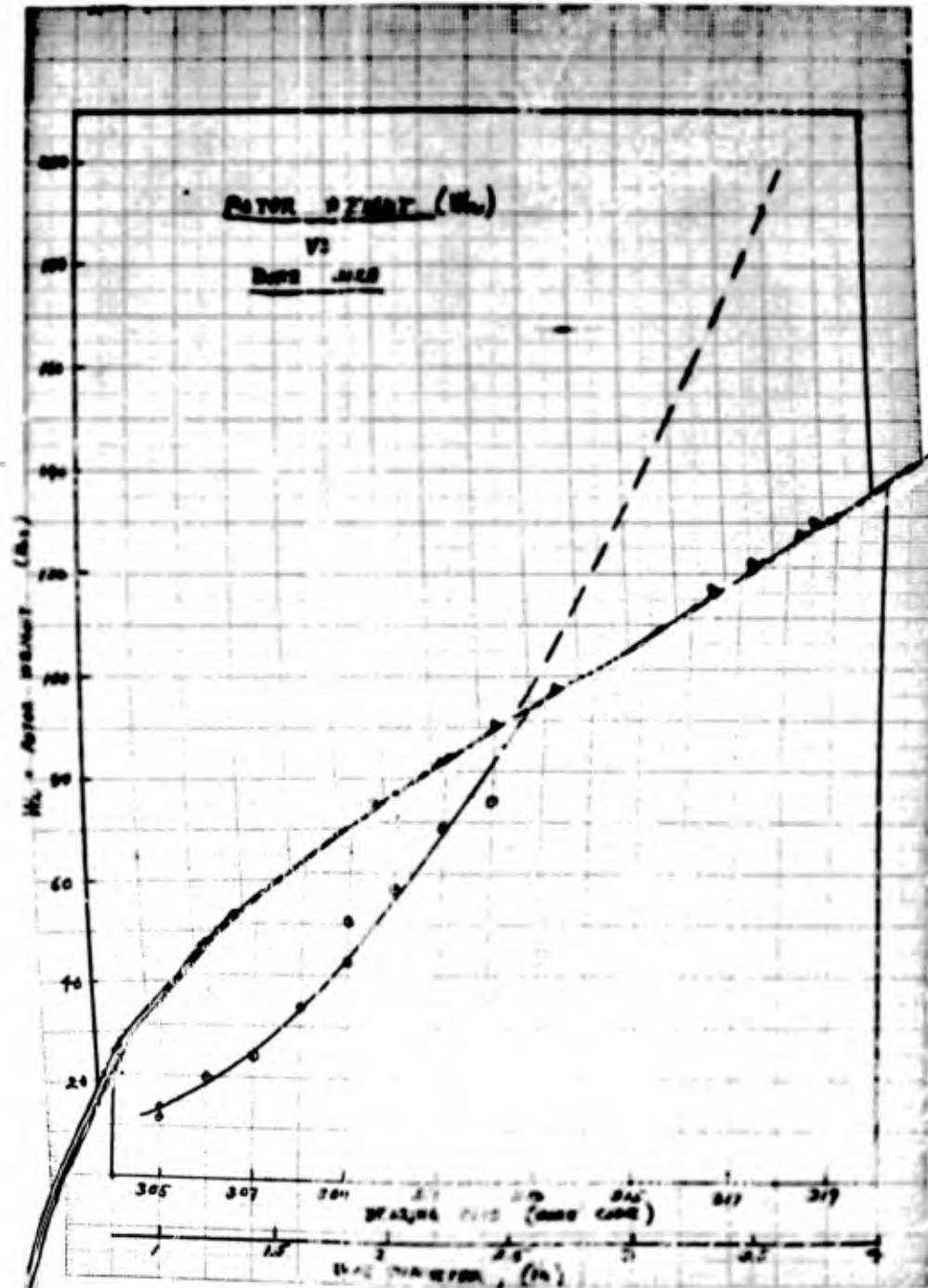


Figure 4C

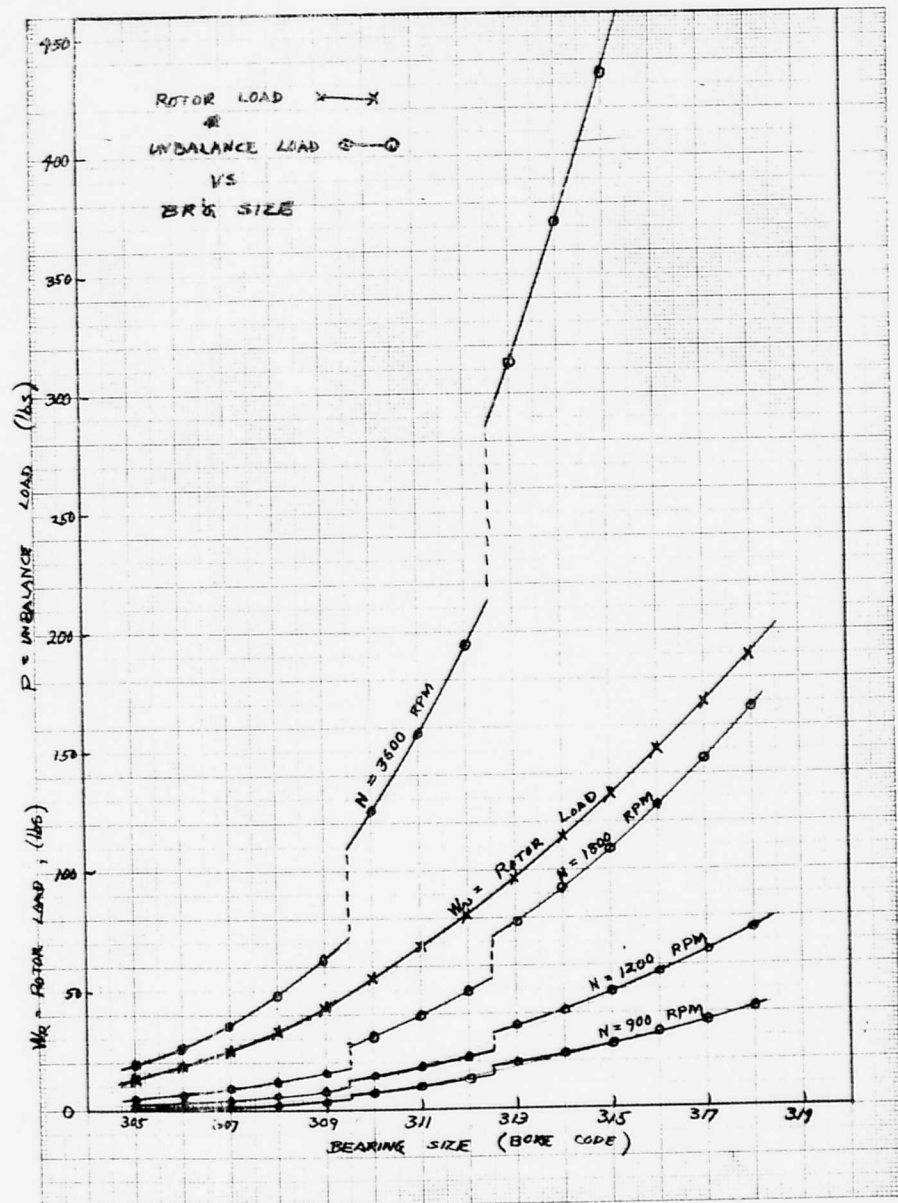


Figure H5



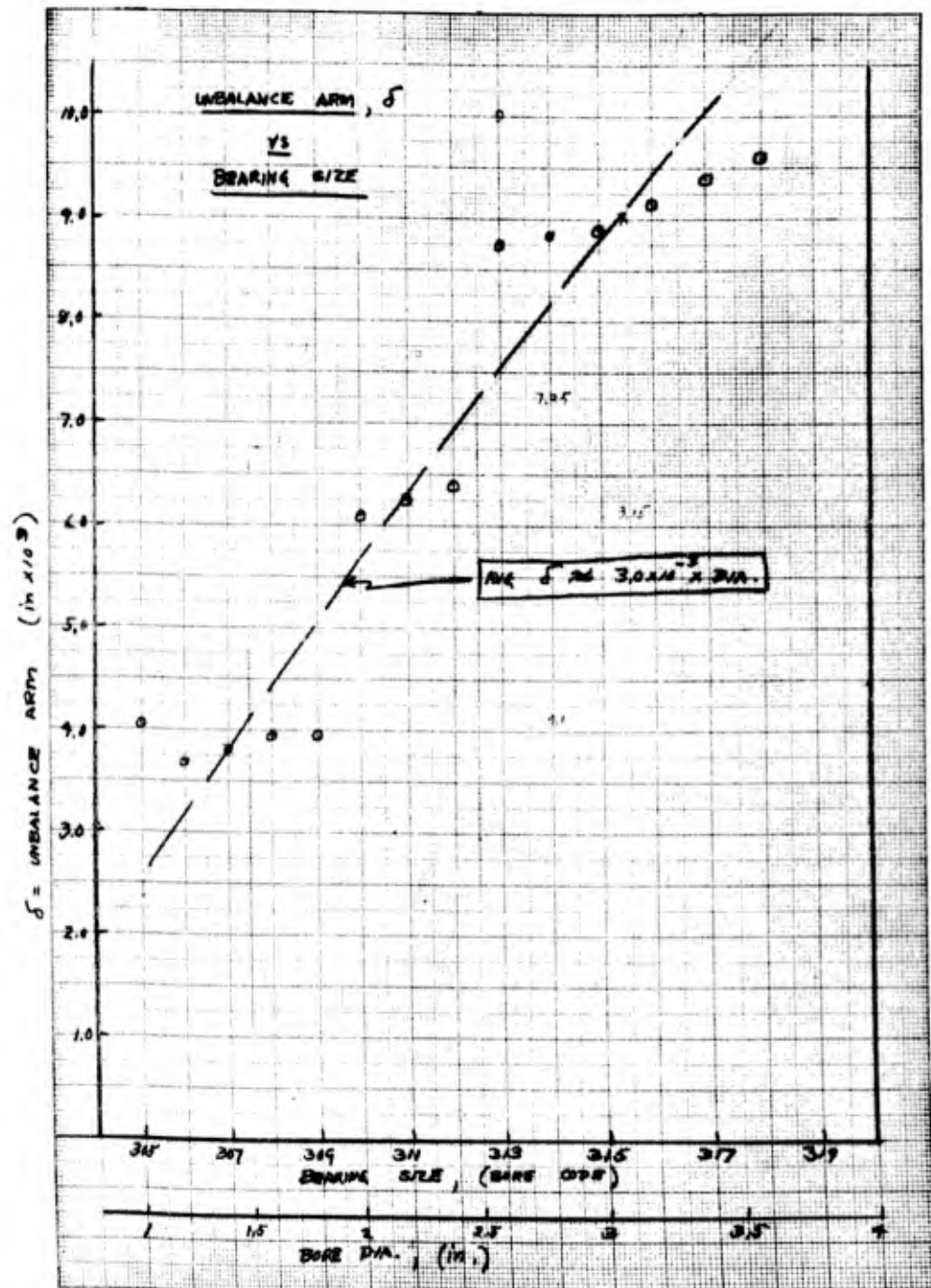


Figure H6

THE FRANKLIN INSTITUTE • *Laboratories for Research and Development*

I-A2321-1

APPENDIX J

FREQUENCY RESPONSE AND TRANSMISSIBILITY CHARACTERISTICS OF A  
JOURNAL BEARING DUE TO PURE UNBALANCE LOAD

APPENDIX J

FREQUENCY RESPONSE AND TRANSMISSIBILITY CHARACTERISTICS OF A JOURNAL BEARING DUE TO PURE UNBALANCE LOAD

The geometry is given in Figure 54, and the force vectors must satisfy equation (96).

$$m\ddot{e} + F = P \quad (96)$$

Taking summation of forces in the x-direction

$$\underline{\Sigma F_x}^+ = 0$$

$$P \cos \beta + m\ddot{e} - F \cos \phi = 0 \quad (J-1)$$

and in the y-direction

$$\underline{\Sigma F_y}^+ = 0$$

$$P \sin \beta - F \sin \phi = 0 \quad (J-2)$$

Squaring (J-1) and (J-2) and adding, yields  $\cos \beta$  as follows,

$$\cos \beta = \frac{+ F^2 - P^2 - (m\ddot{e})^2}{2m\ddot{e}P} \quad (J-3)$$

Substituting (J-3) in (J-1) gives

$$P \left[ \frac{+ F^2 - P^2 - (m\ddot{e})^2}{2m\ddot{e}P} \right] - m\ddot{e} - F \cos \phi = 0$$

which reduces to

$$+ F^2 - P^2 + (m\ddot{e})^2 - 2m\ddot{e}F \cos \phi = 0 \quad (J-4)$$

The radial acceleration,  $\ddot{e}$  is,

$$\ddot{e} = e_0 \omega^2 \quad (J-5)$$

The unbalance force,  $P$  is,

$$P = m\delta \omega^2 \quad (J-6)$$

Sternlicht, Poritsky, and Arwas<sup>3</sup> give the following expression for  $F$ , the fluid film force.

I-A2321-1

$$F = \frac{1}{2\pi} \mu \omega L D \left( \frac{R}{c} \right)^2 f \quad (J-7)$$

where  $\mu$  = absolute viscosity, (lb-sec/in<sup>2</sup>)  
 $\omega$  = rotational velocity, (rad/sec)  
 $L$  = bearing length, (in.)  
 $D$  = bearing diameter, (in.)  
 $R$  = bearing radius, (in.)  
 $c$  = radial clearance, (in.)  
 $f$  = dimensionless force, (dimensionless)

Substituting (J-5), (J-6), and (J-7) in (J-4) gives,

$$+ \left[ \frac{\mu \omega L D}{2\pi} \left( \frac{R}{c} \right)^2 f \right]^2 - [m b \omega^2]^2 + [m e_o \omega^2]^2 - 2 m e_o \omega^2 \left[ \frac{\mu \omega L D}{2\pi} \left( \frac{R}{c} \right)^2 f \right] \cos \phi = 0$$

Cancelling  $\omega^2$  from each term gives,

$$+ \left[ \frac{\mu L D}{2\pi} \left( \frac{R}{c} \right)^2 f \right]^2 - (m b)^2 \omega^2 + (m e_o)^2 \omega^2 - 2 m e_o \left[ \frac{\mu L D}{2\pi} \left( \frac{R}{c} \right)^2 f \right] \omega \cos \phi = 0$$

$$[(m e_o)^2 - (m b)^2] \omega^2 - 2 m e_o \left[ \frac{\mu L D}{2\pi} \left( \frac{R}{c} \right)^2 f \right] \cos \phi \times \omega + \left[ \frac{\mu L D}{2\pi} \left( \frac{R}{c} \right)^2 f \right]^2 = 0$$

$$\omega^2 - \frac{m e_o}{\pi} \frac{\left[ \mu L D \left( \frac{R}{c} \right)^2 f \right]}{[(m e_o)^2 - (m b)^2]} \cos \phi \times \omega + \frac{1}{4\pi^2} \frac{\left[ \mu L D \left( \frac{R}{c} \right)^2 f \right]^2}{[(m e_o)^2 - (m b)^2]} = 0 \quad (J-8)$$

Let  $e_o = \frac{e_o}{c}$ , = eccentricity ratio

$\Delta = \frac{b}{c}$ , = unbalance ratio (J-9)

Substituting in (J-8) and rearranging

$$\omega^2 - \frac{m e_o c}{2\pi m^2} \frac{\left[ \mu L D \left( \frac{R}{c} \right)^2 f \right]}{[e_o^2 - \Delta^2]} \cos \phi \times \omega + \frac{1}{4\pi^2 m^2 c^2} \frac{\left[ \mu L D \left( \frac{R}{c} \right)^2 f \right]^2}{[e_o^2 - \Delta^2]} = 0$$

$$\omega^2 - 2 \left[ \frac{\mu L D \left( \frac{R}{c} \right)^2}{2\pi m c} \right] \frac{f e_o \cos \phi}{[e_o^2 - \Delta^2]} \times \omega + \left[ \frac{\mu L D \left( \frac{R}{c} \right)^2}{2\pi m c} \right] \frac{f^2}{[e_o^2 - \Delta^2]} = 0$$

$$\left\{ \frac{\omega}{\left[ \frac{\mu L D \left( \frac{R}{c} \right)^2}{2\pi m c} \right]} \right\}^2 - 2 \left[ \frac{f e_o \cos \phi}{(e_o^2 - \Delta^2)} \right] \cdot \left\{ \frac{\omega}{\left[ \frac{\mu L D \left( \frac{R}{c} \right)^2}{2\pi m c} \right]} \right\} + \frac{f^2}{(e_o^2 - \Delta^2)} = 0 \quad (J-10)$$

Equation (J-10) is a quadratic equation in the dimensionless frequency  $\left\{ \frac{\omega}{\left[ \frac{\mu LD \left( \frac{R}{c} \right)^2}{2\pi mc} \right]} \right\}$

$$\text{Let } \bar{X} = \left\{ \frac{\omega}{\left[ \frac{\mu LD \left( \frac{R}{c} \right)^2}{2\pi mc} \right]} \right\} \quad (\text{J-11})$$

Notice that  $\bar{X}$  contains all of the bearing parameters of interest (except load) plus the mass being supported rewriting equation (J-11) gives,

$$\bar{X}^2 - 2 \left[ \frac{f \epsilon_0 \cos \phi}{(\epsilon_0^2 - \Delta^2)} \right] \cdot \bar{X} + \frac{f^2}{(\epsilon_0^2 - \Delta^2)} = 0 \quad (\text{J-12})$$

$$\text{Let } k_1 = -2 \left[ \frac{f \epsilon_0 \cos \phi}{(\epsilon_0^2 - \Delta^2)} \right] \text{ and } k_2 = \frac{f^2}{(\epsilon_0^2 - \Delta^2)}$$

Therefore from Equation (J-12)

$$\bar{X}^2 + k_1 \bar{X} + k_2 = 0 \quad (\text{J-13})$$

Solving for the two roots of (J-13) gives

$$\bar{X}_+ = \frac{-k_1 + \sqrt{k_1^2 - 4k_2}}{2} \quad (\text{J-14})$$

and

$$\bar{X}_- = \frac{-k_1 - \sqrt{k_1^2 - 4k_2}}{2} \quad (\text{J-15})$$

The discriminant,  $(k_1^2 - 4k_2)$ , indicates the character of the roots as follows;

I-A2321-1

The Roots of  $\underline{Y}^2 + k_1 \underline{Y} + k_2 = 0$  are

When

Real and Unequal

$$k_1^2 - 4k_2 > 0$$

Real and Equal

$$k_1^2 - 4k_2 = 0$$

Imaginary

$$k_1^2 - 4k_2 < 0$$

Examine  $(k_1^2 - 4k_2)$

$$k_1^2 - 4k_2 = 4 \left[ \frac{f \epsilon_o \cos^2 \phi}{(\epsilon_o^2 - \Delta^2)} \right]^2 - 4 \frac{\epsilon_o^2}{(\epsilon_o^2 - \Delta^2)}$$

$$= 4f^2 \left[ \frac{\epsilon_o^2 \cos^2 \phi}{(\epsilon_o^2 - \Delta^2)^2} - \frac{1}{(\epsilon_o^2 - \Delta^2)} \right] = 4f^2 \left[ \frac{\epsilon_o^2 \cos^2 \phi - \epsilon_o^2 + \Delta^2}{(\epsilon_o^2 - \Delta^2)^2} \right]$$

$$= 4f^2 \left[ \frac{(\cos^2 \phi - 1) + \left(\frac{\Delta}{\epsilon_o}\right)^2}{\left[1 - \left(\frac{\Delta}{\epsilon_o}\right)^2\right]^2} \right]$$

$$\therefore k_1^2 - 4k_2 = \frac{4f^2}{\epsilon_o^2} \left[ \frac{\left(\frac{\Delta}{\epsilon_o}\right)^2 - \sin^2 \phi}{\left[1 - \left(\frac{\Delta}{\epsilon_o}\right)^2\right]^2} \right]$$

$f$ ,  $\Delta$ ,  $\sin \phi$ , and  $\epsilon_o$  are always positive quantities. From above,

$$k_1^2 - 4k_2 > 0 \text{ when } \left(\frac{\Delta}{\epsilon_o}\right) > \sin \phi \text{ } \{ \text{real and unequal roots} \}$$

$$k_1^2 - 4k_2 = 0 \text{ when } \left(\frac{\Delta}{\epsilon_o}\right) = \sin \phi \text{ } \{ \text{real and equal roots} \}$$

$$k_1^2 - 4k_2 < 0 \text{ when } \left(\frac{\Delta}{\epsilon_o}\right) < \sin \phi \text{ } \{ \text{imaginary roots} \}$$

THE FRANKLIN INSTITUTE • *Laboratories for Research and Development*

I-A2321-1

Reference 3 gives some insight into the relationship among  $f$ ,  $\phi$ , and  $\epsilon_0$  for a pure unbalance load. The following numerical data were taken from this reference which applies for an  $L/D = 1$ .

Table J-1

RELATIONSHIP AMONG  $\epsilon$ ,  $f$ , AND  $\phi$

$\epsilon$	$f$	$\phi$ (deg)
0.01	0.075	89.0
0.30	2.56	71.8
0.50	5.58	58.7
0.70	13.3	43.2
0.95	32.3	18.7

Thus for each combination of  $\epsilon_0$  and  $\Delta$ , the coefficients,  $k_1$  and  $k_2$ , of Equation (J-13) are defined, which allows the determination of  $\bar{X}$  for each particular combination of  $\epsilon_0$  and  $\Delta$ . If many combinations of  $\epsilon_0$  and  $\Delta$  are investigated we may obtain the "frequency response" ( $\epsilon_0$  vs  $\bar{X}$ ) for various amounts of unbalance ( $\Delta$ ). Since several hundred combinations of  $\epsilon_0$  and  $\Delta$  would be necessary to provide adequate coverage of both variables, it was decided to use our UNIVAC computer.

The first step in this direction was to obtain more simplified expressions for evaluating the roots of Equation (J-12) than Equations (J-14) and (J-15) so as to minimize computer time. This was done as follows.

$$\bar{X}^2 - 2 \left[ \frac{f \epsilon_0 \cos \phi}{(\epsilon_0^2 - \Delta^2)} \right] \cdot \bar{X} + \frac{f^2}{(\epsilon_0^2 - \Delta^2)} = 0 \quad (J-12)$$

I-A2321-1

$$\begin{aligned}
 (\epsilon_0^2 - \Delta^2) \bar{X}^2 - 2f\epsilon_0 \cos \phi \bar{X} + f^2 &= 0 \\
 f = \epsilon_0 \cos \phi \bar{X} \pm \sqrt{(\epsilon_0 \cos \phi)^2 (\bar{X})^2 - (\epsilon_0^2 - \Delta^2) (\bar{X})^2} \\
 f = \bar{X} \left[ \epsilon_0 \cos \phi \pm \sqrt{\epsilon_0^2 (\cos^2 \phi - 1) + \Delta^2} \right] \\
 \bar{X} = \frac{f}{\epsilon_0 \cos \phi \pm \sqrt{\Delta^2 - \epsilon_0^2 \sin^2 \phi}} \quad (J-16)
 \end{aligned}$$

The transmissibility is from before,

$$\tau = \left| \frac{F}{P} \right|$$

from (J-6) and (J-7)

$$\begin{aligned}
 \frac{F}{P} &= \frac{\frac{1}{2\pi} \mu \omega \Delta D \left( \frac{R}{c} \right)^2 f}{m \omega^2} = \frac{\mu \Delta D \left( \frac{R}{c} \right)^2 f}{2\pi m c \Delta \omega} \\
 \frac{F}{P} &= \frac{f}{\Delta} \left\{ \frac{1}{\frac{\omega}{\left[ \frac{\mu \Delta D \left( \frac{R}{c} \right)^2}{2\pi m c} \right]}} \right\} = \frac{f}{\Delta} \cdot \frac{1}{\bar{X}}
 \end{aligned}$$

Substituting for  $\bar{X}$  from (J-16) gives

$$\tau = \frac{F}{P} = \frac{\left[ \epsilon_0 \cos \phi \pm \sqrt{\Delta^2 - \epsilon_0^2 \sin^2 \phi} \right]}{\Delta} \quad (J-17)$$

In order to obtain more data for the computer, the data of Table J-1 were plotted (Figures J-1 and J-2) and intermediate values determined. The data for the computer are summarized below in Table J-2.



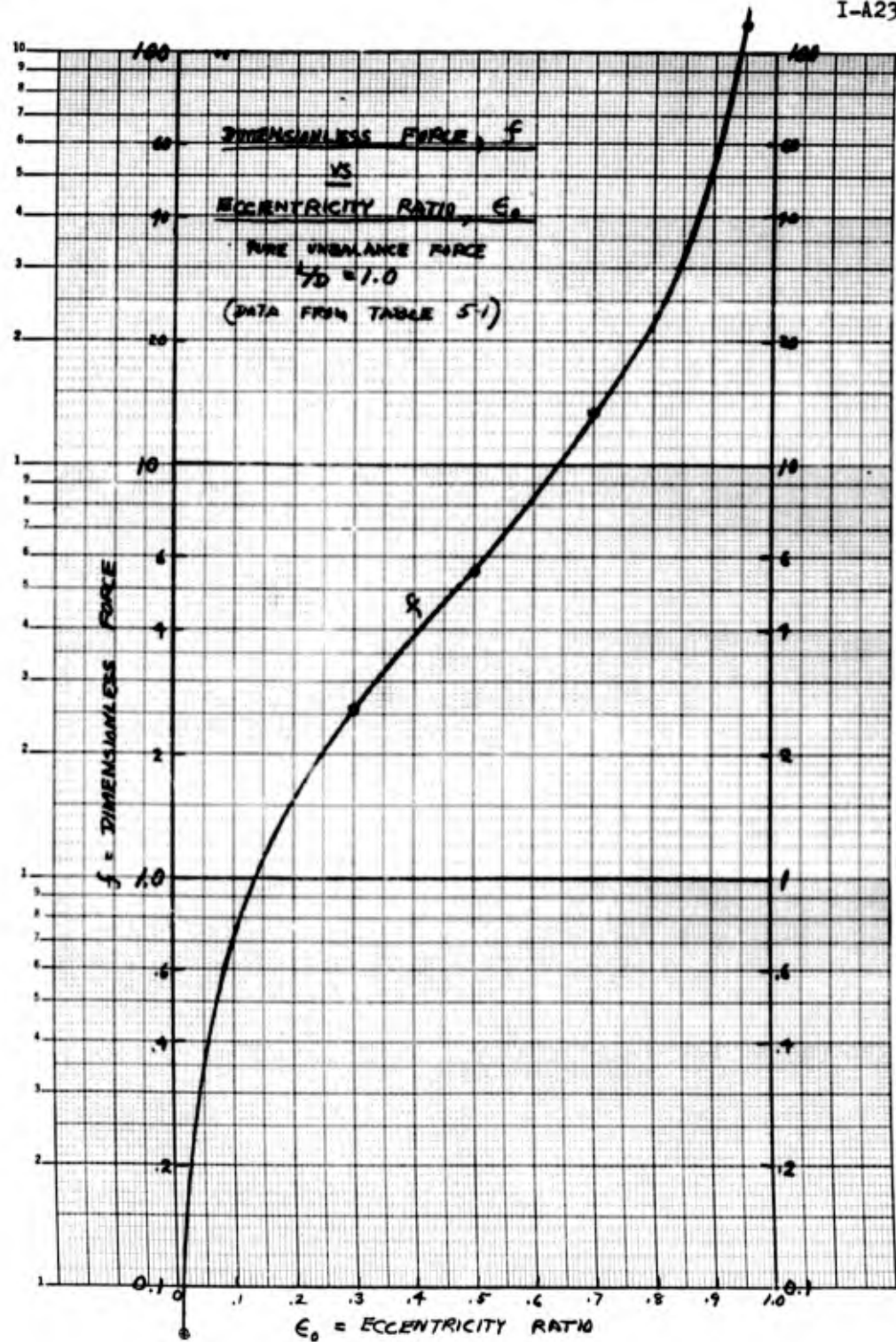


Figure J1

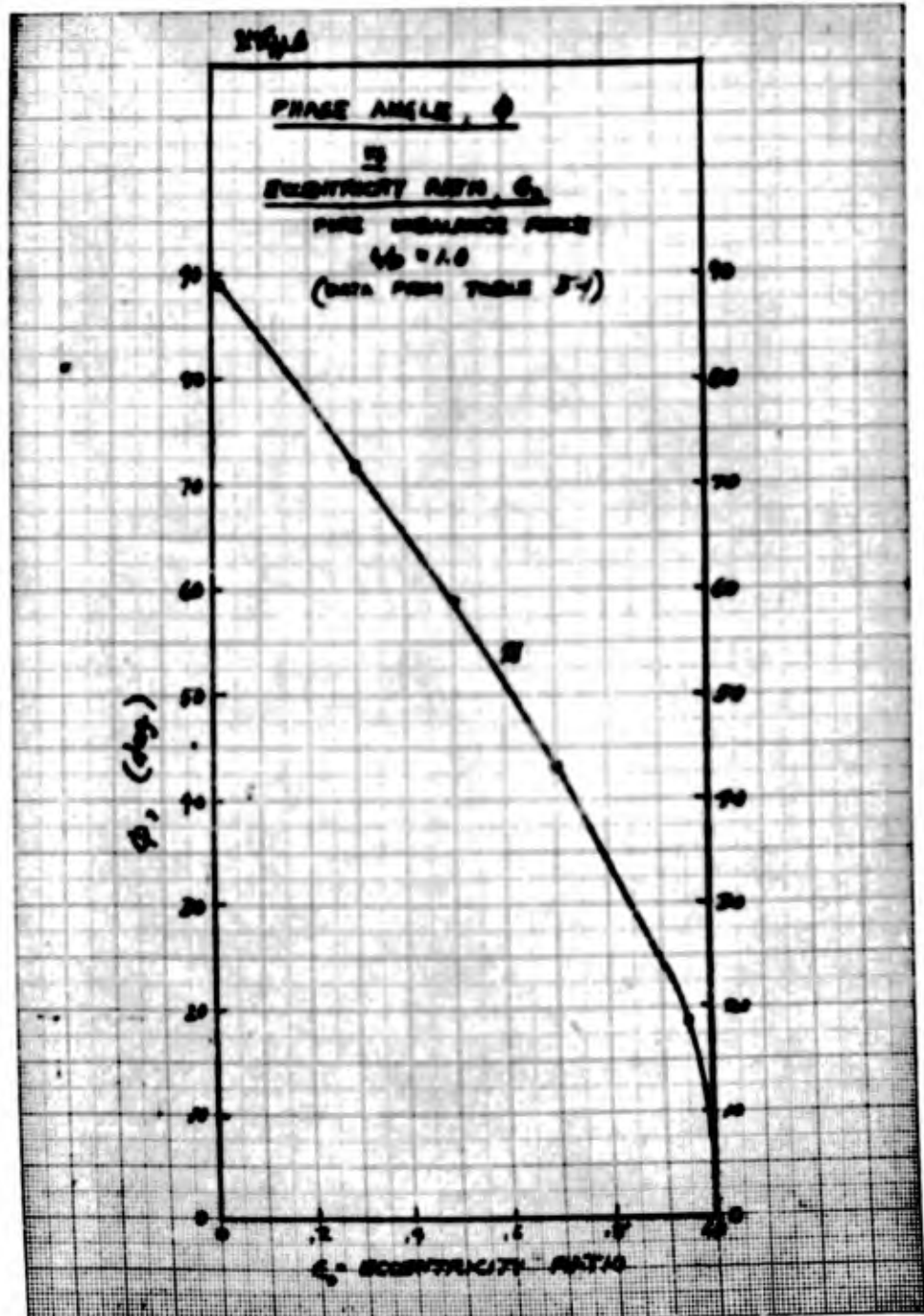


Figure J2

Table J-2

UNBALANCE FORCE COMPUTER DATA  
(From Figures J-1 and J-2)

$\epsilon$	$f$	$\phi$ (deg)
.05	0.35	87.0
.10	0.70	83.9
.15	1.10	80.9
.20	1.55	77.9
.25	2.00	74.9
.30	2.50	71.8
.35	3.20	68.7
.40	3.85	65.5
.45	4.65	62.2
.50	5.58	58.7
.55	6.80	55.1
.60	8.30	51.3
.65	10.30	47.3
.70	13.3	43.2
.75	16.5	39.0
.80	22.0	34.5
.85	32.5	29.5
.90	57.0	24.2
.95	118.0	18.7

Using these data, computer solutions of Equations (J-16) and (J-17) were obtained for  $\Delta=0.1, 0.2, 0.3, 0.4, 0.5, 0.6, 0.7, 0.8, 0.9, 1.0, 2.0, 4.0, 6.0, 8.0, \text{ and } 10.0$ . The frequency response ( $\epsilon_0$  vs  $\bar{X}$ ) is shown plotted in Figure 55, and the transmissibility in Figure 56. For  $\Delta \gg \epsilon_0 \cos \phi$ , (see Equation J-16),

$$\bar{X}_{\Delta > 10} = \frac{f}{\Delta} \quad (\text{J-18})$$

Values of  $f=25, 50, \text{ and } 100$  are also in Figure 55. Likewise from (J-17)

$$\left( r = \frac{F}{P} \right)_{\Delta \gg 10} \approx 1.0$$

THE FRANKLIN INSTITUTE • *Laboratories for Research and Development*

I-A2321-1

APPENDIX K

PRELOADING OF ELECTRIC MOTOR BALL BEARINGS

## APPENDIX K

### PRELOADING OF ELECTRIC MOTOR BALL BEARINGS

Noise generation in deep groove ball bearings is materially improved by axial preloading to stabilize the ball path. The transmission of "noise" from the rotor to the housing will be affected by the amount of preloading since transmission is dependent upon the "spring constant" of the bearing and any damping associated thereto.

Preloading of electric motor ball bearings is achieved by applying an axial load either by

1. The use of preloading springs.
2. Precise dimensional control of bearing fits and amount of axial "squeeze" applied to the bearing.

The first technique is preferred for electric motor use since the desired level of preload is more readily obtained and is not subject to gross change due to slight thermal expansions or contractions of the rotor or motor frame. The second technique produces radial and axial stiffnesses of the same order, whereas the first yields a relatively soft (by an order of magnitude) axial spring rate compared to its radial stiffness.

In order to be effective in suppressing noise generation, the level of preload should be sufficiently high to support the required radial loads without introducing appreciable variation in the individual ball loads, and thereby stabilize the ball path for each ball in the bearing. Radial loads on the bearing are the summation of rotor weight, external loading (applied load), and internal loads (unbalance, magnetic, inertia, gyroscopic). In order to sustain all such radial loads and maintain essentially uniform ball loads around the bearing, prohibitively high axial preloading would be required. Consider the simple case of a well balanced, horizontal motor, the bearings of which are only required

to support the dead weight of the rotor. The radial load carrying capacity of an 8-ball, deep groove bearing (with radial interference) may be written as

$$R \approx 6k_N \delta_o^{3/2} \epsilon \quad (\text{lbs}) \quad [K-1]$$

where  $\epsilon = \frac{\delta}{\delta_o} = \frac{\text{rad. disp. (in.)}}{\text{interference (in.)}}$

If radial interference is obtained by axial preloading, the deformation along the line of contact is,

$$\delta_o^{3/2} = \frac{T}{nk_N \sin \beta_o} \quad [K-2]$$

T = Total axial preload

n = No. of balls

$\beta_o$  = Contact angle

combining Eqs. [K-1] and [K-2], and letting n = 8 balls, we obtain

$$T = \frac{8 \sin \beta_o}{6\epsilon} \cdot R \quad [K-3]$$

In this case,  $R = \frac{1}{2}$  the rotor weight =  $\frac{W_r}{2}$

$$T = \frac{2 \sin \beta_o}{3\epsilon} \cdot W_r \quad \text{lbs} \quad [K-4]$$

It is important to note that the contact angle changes with radial load. For high axial load,  $\epsilon \approx 0$  and the contact angle is the same for all balls which is desirable. When  $\epsilon \approx 1.0$ , one of the balls will be completely unloaded and its contact angle would be zero degrees. Therefore, let  $\epsilon \approx 0.1$

$$\therefore T = 6.67 \sin \beta_o \cdot W_r, \text{ lbs}$$

For a contact angle of  $15^\circ$

$$T = 1.73 W_r, \text{ lbs}$$

Thus for this case, (dead weight load only) a suitable axial preload would be twice the total rotor wt.

$$T \approx 2 W_r \quad \text{lbs.}$$

THE FRANKLIN INSTITUTE • *Laboratories for Research and Development*

I-A2321-1

Preferred axial preloading for cases other than just dead weight may be approximated using Eq [K-3]

$$T = \frac{n \sin \beta_o}{c} \cdot R \quad [K-3]$$

if  $7 < n < 9$  with reasonable results. The 300 series of ball bearings (from 05 to 18) have either 7 or 8 balls with the majority having 8.

$$\therefore T = \frac{1.33 \sin \beta_o}{c} \cdot R$$

$c$  on the order of 0.1 will insure uniform contact angle around the bearing.

$$\therefore T = 13.3 \sin \beta_o \cdot R$$

Practical values of mounted, operating contact angles vary from  $10^\circ$  to  $25^\circ$

$$\therefore 2.3 R < T < 5.6 R$$

$$\therefore T \approx 4R$$

which says that the axial pre-load should be about 4 times the radial load.

THE FRANKLIN INSTITUTE • *Laboratories for Research and Development*

I-A2321-1

APPENDIX L  
LIST OF REFERENCES



APPENDIX L

LIST OF REFERENCES

1. Rippel, H. C., "Cast Bronze Bearing Design Manual," published by the Cast Bronze Bearing Institute, May, 1960.
2. Sternlicht, B., "Elastic and Damping Properties of Cylindrical Journal Bearings," *Journal of Basic Eng., Trans., A.S.M.E.*, June 1959, pp. 101-110.
3. Sternlicht, B., Poritsky, H., E. Arwas, "Dynamic Stability Aspects of Cylindrical Journal Bearings Using Compressible and Incompressible Fluids," General Electric Company Report on Task No. NRO97-348, Contract No. Nonr - 2844(00), 1959.
4. Raimondi, A. A., & J. Boyd, "A Solution for the Finite Journal Bearing and its Application to Design and Analysis - III," *Trans., ASLE*, Vol. 1, No. 1, April, 1958.

**UNCLASSIFIED**

**UNCLASSIFIED**